EFFECT OF ENZYMATIC AND PHYSICAL MODIFICATION OF CASSAVA STARCH ON THE FORMATION OF SLOWLY DIGESTIBLE STARCH AND RESISTANT STARCH AND THEIR PHYSICAL AND FUNCTIONAL PROPERTIES

Sureeporn Boonna

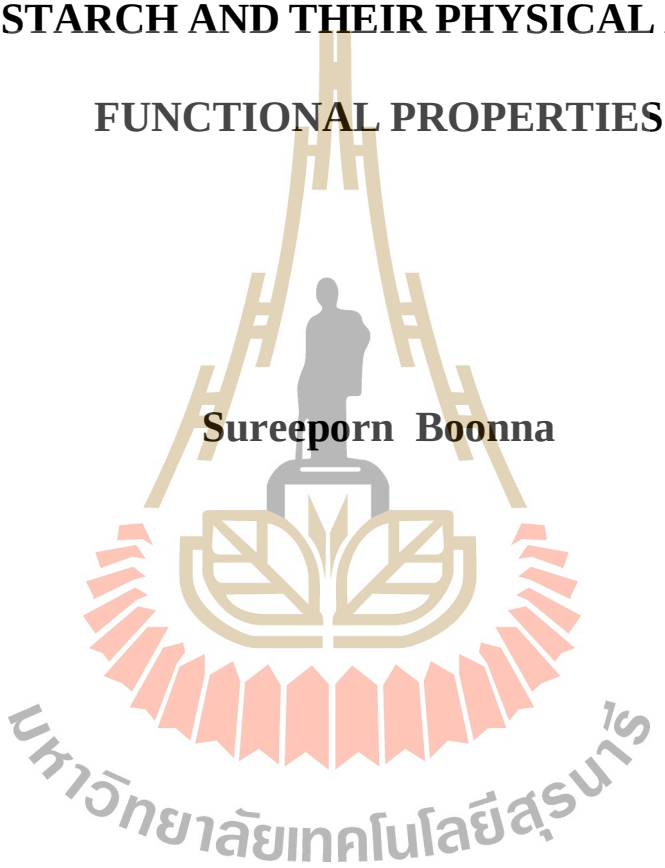

A Thesis Submitted in Partial Fulfillment of the Requirements for the Degree of Doctor of Philosophy in Food Technology

Suranaree University of Technology

Academic Year 2016

ผลของการดัดแปรด้วยเอนไซม์และการดัดแปรทางกายภาพแป้งมันสำปะหลังต่อการเกิดแป้งย่อยช้าและแป้งต้านทาน สมบัติทางกายภาพและสมบัติเชิงหน้าที่

นางสาวสุรีย์พร บุญนา

วิทยานิพนธ์นี้เป็นส่วนหนึ่งของการศึกษาตามหลักสูตรปริญญาวิทยาศาสตรดุษฎีบัณฑิต
สาขาวิชาเทคโนโลยีอาหาร
มหาวิทยาลัยเทคโนโลยีสุรนารี
ปีการศึกษา 2559

EFFECT OF ENZYMATIC AND PHYSICAL MODIFICATION OF CASSAVA STARCH ON THE FORMATION OF SLOWLY DIGESTIBLE STARCH AND RESISTANT STARCH AND THEIR PHYSICAL AND FUNCTIONAL PROPERTIES

Suranaree University of Technology has approved this thesis submitted in partial fulfillment of the requirements for the Degree of Doctor of Philosophy.

Thesis Examining Committee

(Assoc. Prof. Dr. Manote Sutheerawattananonda)
Chairperson

(Asst. Prof. Dr. Sunanta Tongta)
Member (Thesis Advisor)

(Prof. Dr. Denis Lourdin)
Member

(Assoc. Prof. Dr. Klanarong Sriroth)
Member

(Dr. Kuakoon Piyachomkwan)
Member

(Prof. Dr. Sukit Limpijumnong)
Vice Rector for Academic Affairs and Innovation

(Prof. Dr. Neung Teaumroong)
Dean of Institute of Agricultural Technology

สุรีย์พร บุญนา : ผลของการดัดแปรด้วยเอนไซม์และการดัดแปรทางกายภาพแป้งมันสำปะหลังต่อการเกิดแป้งย่อยช้าและแป้งต้านทาน สมบัติทางกายภาพ และสมบัติเชิงหน้าที่ (EFFECT OF ENZYMATIC AND PHYSICAL MODIFICATION OF CASSAVA STARCH ON THE FORMATION OF SLOWLY DIGESTIBLE STARCH AND RESISTANT STARCH AND THEIR PHYSICAL AND FUNCTION PROPERTIES) อาจารย์ที่ปรึกษา : ผู้ช่วยศาสตราจารย์ ดร.สุนันทา ทองทา, 209 หน้า.

การศึกษาผลของการใช้ความร้อนร่วมกับน้ำ (hydrothermal treatment) แบบรอบเดียวและสองรอบของการอบอ่อน (annealing, ANN) และการใช้ความร้อนชื้น (heat-moisture treatment, HMT) ต่อการย่อยของเอนไซม์ สมบัติทางความร้อน และความคงทนต่อการหุงต้มของแป้งมันสำปะหลังตัดกิ่งที่ผ่านการตกผลึก(crystallized debranched cassava starch) พบว่า แป้งที่ผ่านHMT มีปริมาณแป้งต้านทานสูงกว่าเมื่อเทียบกับแป้งที่ผ่าน ANN การใช้ความร้อนร่วมกับน้ำแบบสองรอบของ HMT→ANN สามารถปรับปรุงผลผลิตของแป้งต้านทาน (71%RS) ได้มากกว่าการทำ ANN→HMT (46%RS) อย่างไรก็ตามการทำ ANN→HMT พบว่า มีอุณหภูมิหลอมที่สูงกว่า นอกจากนี้ความคงทนต่อการหุงต้มที่ความชื้น 50 และ 70% ก็ดีขึ้นเมื่อใช้ความร้อนร่วมกับน้ำแบบสองรอบ

การศึกษาการดัดแปรแป้งมันสำปะหลังด้วยเอนไซม์ตัดต่อสายกลูแคน(amylomaltase, AM) พบว่า แป้งที่ดัดแปรด้วย AM มีปริมาณอะไมโลสลดลง การวิเคราะห์โครงสร้างทางโมเลกุลของแป้งที่ดัดแปรด้วย AM นาน 5 นาทีและ 4 ชั่วโมงก่อนและหลังการย่อยด้วยเอนไซม์เบต้าอะมิเลส พบว่า มวลโมเลกุลของแป้งที่ดัดแปรด้วย AM ค่อย ๆ ลดลงตามเวลาการทำปฏิกิริยาที่เพิ่มขึ้น จากการตรวจสอบโดยโปรตอน-นิวเคลียร์แมกเนติกเรโซแนนซ์ พบว่า แป้งที่ดัดแปรด้วย AM นาน 5 นาที มีความยาวสายโซ่โดยเฉลี่ย ความยาวสายโซ่ภายนอกโดยเฉลี่ย และค่าเปอร์เซ็นต์เบต้าอะมิโลไลซิสสูงกว่าแป้งที่ดัดแปรด้วย AM นาน 4 ชั่วโมง สัดส่วนสายโซ่ยาว (DP 25-80) ของแป้งตัดกิ่งดัดแปรด้วย AM ที่มีปริมาณเพิ่มขึ้นแสดงให้เห็นว่าเอนไซม์ AM สามารถเพิ่มความยาวของสายโซ่แป้งมันสำปะหลังได้ เมื่อนำแป้งตัดกิ่งที่ดัดแปรด้วย AM ไปตกผลึกโดยการบ่มแบบอุณหภูมิคงที่และการใช้ความร้อนชื้น พบว่า ปริมาณแป้งต้านทานและการทนต่อความร้อนมีค่าสูงขึ้นเมื่อเทียบกับแป้งที่ไม่ได้ดัดแปรด้วย AM โดยแป้งที่ผ่านการบ่มแบบอุณหภูมิคงที่แสดงปริมาณแป้งต้านทานสูงกว่า (58%RS) ขณะที่แป้งที่ผ่านการให้ความร้อนชื้นมีอุณหภูมิหลอมอยู่ในช่วงสูงกว่า (104-132°ซ) กระบวนการขึ้นรูปด้วยความร้อน (Thermo-molding) ได้ถูกนำมาใช้กับแป้งตัดกิ่งที่ดัดแปรด้วย AM นาน 5 นาที โดยตัวอย่างแม่พิมพ์ที่มีอัตราส่วนพื้นที่ผิวต่อปริมาตรต่ำ (1.93 ต่อมิลลิเมตร) มีปริมาณ

แป้งต้านทานมากกว่า และลักษณะพื้นผิวที่ได้มีความแน่นและเรียบ อย่างไรก็ตามปริมาณผลผลิตแป้งต้านทานของตัวอย่างแม่พิมพ์ขึ้นอยู่กับอัตราส่วนพื้นที่ผิวต่อปริมาตร

การศึกษาความสามารถในการเกิดสารประกอบเชิงซ้อนอะไมโลสกับไขมัน (amylose-lipid complexes, AMLs) โดยกระบวนการเอกซ์ทรูชันแป้งมันสำปะหลังที่เติมกลีเซอรอล กรดลอริค (C12) และกรดสเตียริก (C18) ปริมาณ 5% (โดยน้ำหนัก) พบว่า C12 และ C18 มีดัชนีการสร้างสารประกอบเชิงซ้อนสูงกว่าเมื่อเทียบกับกลีเซอรอล อุณหภูมิการแตกตัวของ AMLs ประเภท I และ II ของตัวอย่างเอกซ์ทรูเดตสูงขึ้นตามความยาวสายโซ่ของกรดไขมัน เอนทัลปีของการแตกตัวของ AMLs ประเภท II มีแนวโน้มลดลงเมื่อปริมาณความชื้นของกระบวนการเอกซ์ทรูชันเพิ่มขึ้น ตัวอย่างเอกซ์ทรูเดตมีลักษณะพื้นผิวที่หยาบ แน่น และมีรูพรุน รูปแบบการดูดกลืนรังสีเอกซ์มุมกว้างแสดงการเกิดโครงสร้างผลึกแบบ V_h ซึ่งแสดงถึงการเกิด AMLs หลังจากนำเอกซ์ทรูเดตมาผ่านการขึ้นรูปด้วยความร้อน พบว่า ตัวอย่างแม่พิมพ์มีลักษณะโครงสร้างพื้นผิวที่แน่นขึ้นและเรียบ จึงมีผลในการเพิ่มปริมาณผลผลิตแป้งย่อยช้า

สาขาวิชาเทคโนโลยีอาหาร ลายมือชื่อนักศึกษา_____

ปีการศึกษา 2559 ลายมือชื่ออาจารย์ที่ปรึกษา_____

SUREEPORN BOONNA : EFFECT OF ENZYMATIC AND PHYSICAL MODIFICATION OF CASSAVA STARCH ON THE FORMATION OF SLOWLY DIGESTIBLE STARCH AND RESISTANT STARCH AND THEIR PHYSICAL AND FUNCTIONAL PROPERTIES. THESIS ADVISOR : ASST. PROF. SUNANTA TONGTA, Ph.D., 209 PP.

HYDROTHERMAL TREATMENTS/AMYLOMALTASE/EXTRUSION/THERMO-MOLDING/SLOWLY DIGESTIBLE STARCH/RESISTANT STARCH

The effects of single and dual hydrothermal treatments of annealing (ANN) and heat-moisture treatment (HMT) on enzyme digestibility, thermal properties and cooking stability of crystallized debranched cassava starch were studied. All HMT-treated starches showed a higher resistant starch (RS) content compared with all ANN-treated starches. Dual hydrothermal treatment of HMT→ANN (71%RS) could improve the RS content more than ANN→HMT (46%RS). Nevertheless, the ANN→HMT treated starch showed a higher melting temperature. In addition, the cooking stability (at 50 and 70% moisture) can be improved by dual hydrothermal treatments.

The modification of cassava starch with amylomaltase (AM) was investigated. The AM-treated starches showed a decreased amylose content. The molecular structure of AM-treated starch for 5 min (AM5min) and 4 h (AM4h) before and after β-amylolysis were characterized. The molar mass of both AM-treated starches gradually decreased with time. The AM5min demonstrated a higher average chain length (CL), external CL, and β-amylolysis than AM4h as determined by H^1-NMR. Both AM-treated starches showed larger proportions of long chain (DP 25-80),

indicating that AM could elongate the starch chain length. After subjected to isothermal incubation and HMT, the crystallized, debranched AM-treated starches showed more RS content and higher thermal stability as compared with the non-AM-treated starch. The isothermal-treated starch showed a higher RS content (58%RS) whereas the HMT-treated starch showed a higher melting temperature (104-132^{o}C). The thermo-molding process was applied with debranched AM5min. The molded sample with a small surface area to volume ratio (1.93 mm^{-1}) showed a higher RS yield (65.1%RS). Its surface morphology was a densely packed structure with a smooth surface. However, the RS yield of the molded sample depends on its surface area to volume ratio.

The ability to form amylose-lipid complexes by extrusion cooking of cassava starch with the addition of glycerol, lauric acid (C12) and stearic acid (C18) at 5% (w/w) was studied. The C12 and C18 showed a higher complexing index as compared with glycerol. The dissociation temperature of amylose-lipid complexes type I and II of extruded samples increased with the longer chain of fatty acid and the dissociation enthalpy of amylose-lipid complexes type II tended to decrease as the extrusion moisture content was increased. The extruded sample had a rough and condensed surface with porosity. Its wide angle X-ray diffraction pattern showed a V_h-type crystalline structure, implying a amylose-lipid complexes formation. After subjected to thermo-molding, the molded samples showed a densely packed or a compact structure with a smooth surface, resulting in the increase of slowly digestible starch yield.

School of Food Technology Student's Signature_____

Academic Year 2016 Advisor's Signature_____

Co-advisor's Signature_____

ACKNOWLEDGEMENTS

I would like to express my sincere gratitude to my advisor Asst. Prof. Dr. SunantaTongta, for her excellent teaching, guidance, patience, encouragement and the continuous support throughout my study course and research. Her guidance helped me in all the time of research and writing of this thesis. Without her contribution, my thesis would not have achieved and completed.

My sincere gratitude also goes to Prof. Denis Lourdin, for kindly accepting me into his laboratory group at BIA-MC2, INRA, Nantes, France and leading me working on a starch modification with the thermo-molding process. I am most grateful for his excellent teaching, guidance, patience and invaluable help during my work at INRA and throughout my study course.

Furthermore, I am grateful to Dr. Agnès Rolland-Sabaté, INRA, France, for good suggestions and invaluable help on the study of structural properties of starches, AM-modified starches, and extruded starches and Prof. AlainBulèon for excellent teaching,guidance and invaluable help on the study of starch structure and crystallization of starch. I am also grateful to the members of my committee for their patience and insightful comments.

Many thanks to Sophie Guilois for kind assistance with chromatography experiments, Bruno Pontoire for the technical support on WAXD experiments, Xavier Falourdfrom INRA for invaluable help and good suggestions on ^{1}H-NMR techniques, Dr. Nicolas Stephant from Jean Rouxel Institute of Materials at University of Nantes for the use of SEM instrument, Marion de Carvalho, Laurent Chaunier,

ChloéChevigny, RoselyneDesirestand Joëlle Davy from BIA lab, INRA, and the staffs of food laboratory from Suranaree University of Technology, for their assistance and supporting. I would also like to thank Dr. Siriwat Soontaranon from BL1.3W beamline (Synchrotron Light Research Institute, Thailand) for his assistance and suggestion on WAXS experiments. Furthermore, I would like to thank the Royal Golden Jubilee (RGJ) Ph.D. program for industry (Grant No. PHD/0090/2552), the Embassy of France in Thailand, and Sanguan Wongse Industries Co., Ltd., Thailand for funding support. I am also thankful for Suranaree University of Technology, Biopolymères Interaction Assemblages (BIA), INRA, Nantes, France and Synchrotron Light Research Institute, Thailand for supporting the laboratory facilities.

Also, I would like to thank Novozymes A/S for providing amylomaltase and SanguanWongse Industries Co., Ltd., Thailand for providing cassava starch.

Thanks to all members of Asst. Prof. Dr. SunantaTongtaand my friends at Suranaree University of Technology, for their friendship, helps, supports and encouragement.

Finally, I most gratefully acknowledge my parents for all of the love, dedication, encouragement and supporting me spiritually throughout my life. Also, I would like to thank my husband and my son for all their love, supports and motivation throughout writing this thesis.

Sureeporn Boonna

CONTENTS

Page

ABSTRACT IN THAI I

ABSTRACT IN ENGLISH III

ACKNOWLEDGEMENTS V

CONTENTS VII

LIST OF TABLES XVI

LIST OF FIGURES XX

CHAPTER

I INTRODUCTION 1

1.1 Introduction 1

1.2 Research objectives 7

1.3 Research hypothesis 8

1.4 Scope of the study 9

1.5 Expected results 10

1.6 References 10

II LITERATURE REVIEW 17

2.1 Starch granular structure 17

2.2 The gelatinization and retrogradation of starch 20

2.3 The nutritional classification of starch 22

2.3.1 Rapidly digestible starch (RDS) 22

CONTENTS (Continued)

Page

2.3.2 Slowly digestible starch (SDS) 23
2.3.3 Resistant starch (RS) 25
2.4 Enzymatic modification of starch with amylomaltase and debranching enzyme 33
2.4.1 Starch modification with amylomaltases enzyme 33
2.4.2 Starch modification with debranching enzyme 38
2.5 Physical modification of starch 39
2.5.1 Hydrothermal treatments 39
2.5.2 Extrusion cooking 42
2.5.3 Thermo-molding process 44
2.6 Location of starch digestion 44
2.7 *In vitro* starch fractions determination 46
2.8 References 48

III IMPROVEMENT OF RESISTANT STARCH AND COOKING STABILITY OF CRYSTALLIZED DEBRANCHED CASSAVA STARCH BY SINGLE AND DUAL HYDROTHERMAL TREATMENTS 63
3.1 Abstract 63
3.2 Introduction 64
3.3 Materials and methods 67
3.3.1 Materials 67

CONTENTS (Continued)

Page

3.3.2 Preparation of recrystallized debranched starch 67
3.3.3 Single hydrothermal treatment 68
3.3.4 Dual hydrothermal treatments 68
3.3.5 Determination of starch fractions..... 69
3.3.6 Thermal properties 70
3.3.7 Crystalline structure 70
3.3.8 Cooking stability 71
3.3.9 Statistical analysis 71
3.4 Results and discussions 72
3.4.1 Single hydrothermal treatment 72
3.4.1.1 Effects of moisture content and heat-moisture treatment (HMT) time on starch fractions and thermal properties 72
3.4.1.2 Impact of annealing and HMT temperature on starch fractions and thermal properties 73
3.4.2 Effect of dual hydrothermal treatment on starch fractions and thermal properties 75
3.4.2 Cooking stability of dual hydrothermal-treated temperature-cycled debranched starch……..……75
3.5 Conclusions 86
3.6 Acknowledgements..... ..87

CONTENTS (Continued)

Page

3.7 References ..... .88

IV EFFECT OF AMYLOMALTASE AND RECRYSTALLIZATION METHOD ON MACRO- MOLECULAR CHARACYERISTICS, STARCH DIGESTIBILITY, THERMAL PROPERTIES AND COOKING STABILITY OF CASSAVA STARCH 93

4.1 Abstract 93

4.2 Introduction 94

4.3 Materials and methods 97

4.3.1 Materials 97

4.3.2 Enzymatic modification 97

4.3.2.1 Preliminary study on cassava starch treated with AM..... 97

4.3.2.2 Cassava starch treated with AM at various reaction times 98

4.3.2.3 Cassava starch treated with AM followed by isoamylase..... 98

4.3.3 Determination of amylose content and wavelength of the maximum absorbance (λmax)..... 99

4.3.4 Structural characteristics analysis of native and AM-treated starch..... 100

CONTENTS (Continued)

Page

4.3.4.1 Chain length distribution determined by high-performance anion exchange chromatography with pulsed amperometric detection (HPAEC-PAD).... ..100

4.3.4.2 The β-limit dextrin preparation…….. ..100

4.3.4.3 Molecular mass and size distribution determined by high-performance size exclusion chromatography coupled with multi-angle laser light scattering and differential refractive index (HPSEC-MALLS-DRI)… . .101

4.3.4.4 Nuclear magnetic resonance spectroscopy (NMR)……. .102

4.3.4.5 Cyclo-structure molecule analysis by MALDI-TOF… . ..103

4.3.5 Recrystallization by hydrothermal treatments……... ….103

4.3.5.1 Isothermal temperature incubation…… . ….103

4.3.5.2 Heat-moisture treatment…… ……104

4.3.6 Chain length distribution of the crystalline residues of debranched native and AM-treated cassava starch by high-performance anion exchange chromatography with pulsed amperometric detection (HPAECPAD)…..... ……104

4.3.7 Starch fractions determination… .... ……..…104

4.3.8 Crystalline properties……... .... ……..…105

4.3.9 Thermal properties…….....……...106

CONTENTS (Continued)

Page

4.3.10 Cooking stability of debranched AM-treated cassava starch (DBSAM5min) and hydrothermal, debranched AM-treated cassava starches……..…..……107

4.3.11 Thermo-molding process modification…… .....……....107

4.3.12 Statistical analysis…….....….110

4.4 Results and discussion 110

4.4.1 Preliminary study on cassava starch treated with AM 110

4.4.2 Structural characteristics of native and AM-treated cassava starches 114

4.4.3 Effect of recrystallization of debranched native and AM-treated cassava starch on starch fractions, crystalline and thermal properties 123

4.4.4 Effect of thermo-molding process on starch fractions, crystallinity, and thermal properties of DAM5min 135

4.4.5 Effect of dimension size and surface area to volume ratio (S/V) of molded DAM5min on SDS and RS content 141

4.4.6 Cooking stability of molded-DAM5min 143

4.5 Conclusions 145

4.6 Acknowledgements..... 146

4.7 References 147

CONTENTS (Continued)

Page

V EXTRUSION COOOKING AND THERMO-MOLDING TO PRODUCE STARCHY PRODUCTS RICH IN SLOWLY DIGESTIBLE STARCH FROM CASSAVA STARCH WITH ADDITION OF FATTY ACID 155

5.1 Abstract 155

5.2 Introduction 156

5.3 Materials and methods 159

5.3.1 Materials 159

5.3.2 Preliminary study: effect of fatty acid concentration on the formation of amylose-lipid complexes 159

5.3.2.1 Complexing index (CI) analysis 159

5.3.3 Extrusion cooking 160

5.3.4 Starch fractions determination 161

5.3.5 Crystalline structure 162

5.3.6 Thermal properties 163

5.3.7 Molecular mass and size distribution determined by high performance size exclusion chromatography coupled with multi-angle laser light scattering and differential refractive index (HPSEC-MALLS-DRI) 164

5.3.8 Thermo-molding process 165

5.3.8.1 Preliminary study on thermo-molding process 165

CONTENTS (Continued)

Page

5.3.8.2 Effect of thermo-molding conditions on starch fractions, crystalline structure and thermal properties of extruded samples 165
5.3.9 The microstructure of extruded and molded-extruded samples monitored by scanning electron microscopy (SEM)..... 165
5.3.10 Cooking stability test of the molded-extruded sample 166
5.3.11 Effect of storage on the SDS and RS content, thermal, and crystalline properties of molded-extruded samples..... 166
5.3.12 Statistical analysis 166
5.4 Results and discussion 167
5.4.1 Preliminary study: effect of fatty acid concentration on the formation of amylose-lipid complexes (AMLs)…… .... …..167
5.4.2 Amylose-lipid complexes formation as induced by extrusion cooking..... 167
5.4.3 Effect of thermo-molding process on the extruded cassava starch with and without adding complexing agents 175
5.4.4 Cooking stability of the molded extruded starch..... 186
5.4.5 Effect of storage condition on SDS content, RS content, crystalline structure and thermal properties of the molded extruded starches..... 187
5.5 Conclusions 191

CONTENTS (Continued)

Page

5.6 Acknowledgements 192

5.7 References 192

VI SUMMARY 197

APPENDICES 200

APPENDIX A 201

APPENDIX B 202

BIOGRAPHY 209

LIST OF TABLES

Page

3.1 Starch fractions and thermal properties of HMT-treated temperature-cycled debranched starch 76

3.2 Starch fractions and thermal properties of single hydrothermal-treated temperature-cycled debranched starch with different annealing and HMT temperature 77

3.3 Physical and crystal properties of single and dual hydrothermal-treated temperature-cycled debranched starch 80

3.4 Effect of dual hydrothermal treatment on starch fractions and thermal properties of temperature-cycled debranched starch 84

3.5 Changing percentages of starch fractions of hydrothermal-treated temperature-cycled debranched starch after cooking at 50% and 70% moisture content 88

4.1 Chain length (CL) distribution of native cassava starch and AM-treated cassava starch after treated with AM at various concentrations and reaction times ... 111

4.2 Amylose content and maximum absorption wavelength value (λ_{max}) of native and AM-treated cassava starch at various reaction times 114

LIST OF TABLES (Continued)

Page

4.3 Macromolecular characteristics of native cassava starch (CS), AM-treated cassava starch (AM5min and AM4h), β-limit dextrins from native cassava starch (B-CS) and AM-treated cassava starches (B-AM5min and B-AM4h) determined by HPSEC-MALLS 120

4.4 Fine structure of native cassava starch, AM-treated cassava starch, determined by HPSEC-MALLS 120

4.5 Starch fractions and crystalline properties of debranched native and AM-treated cassava starch before and after subjected to recrystallization 125

4.6 Thermal properties of debranched native and AM-treated cassava starch with different CL distribution after subjected to recrystallization 126

4.7 Thermal properties of debranched and recrystallized debranched AM-treated cassava starch after cooked at 50% and 70% moisture content..... 133

4.8 Effect of thermo-molding pressure on starch fractions of DAM5min 136

4.9 Effect of thermo-molding pressure on starch fractions, thermal and crystalline properties of molded-DAM5min which were molded at a temperature of 110^{o}C for 8 min 139

4.10 Starch fractions and thermal properties of molded starch samples which were prepared at various thermo-molding conditions..... 140

4.11 The SDS and RS content of molded-DAM5min with different dimension size and surface area to volume ratio 142

LIST OF TABLES (Continued)

Page

5.1 Screw configuration used in extrusion experime 161

5.2 The RS content, complexing index (CI) and crystalline properties of extruded CS as prepared with various water contents and complexing agen 171

5.3 Thermal properties of cassava starch extruded with C12 and C18 at 30 and 50% moisture content 173

5.4 Macromolecular characteristics of extruded cassava starch (CS) and extruded CS as prepared at 30 and 50% moisture content determined by HPSEC-MALLS-DRI 177

5.5 Starch fractions and crystalline properties of molded CS extruded with various complexing agents after molded at 110°C with 2.0 tons pressure for 8 min 178

5.6 Thermal properties of extruded CS* and molded CS extruded with various complexing agents after molded at 110°C with 2.0 tons pressure for 8 min 181

5.7 Starch fractions of molded CS extruded with C12 as prepared at various thermo-molding conditions 184

5.8 Thermal properties of mold, C12 extrudates as prepared at various thermo-molding conditions 185

5.9 The SDS and RS content of molded samples after storage at 80% relative humidity for 15 days 189

LIST OF TABLES (Continued)

Page

5.10 Thermal properties of molded CS and molded CS extruded with C12 and C18 after storage at 80% relative humidity for 15 days 189

LIST OF FIGURES

Page

2.1 Starch granular structure (Reproduced from Mischnick & Momcilovic, 2010) 18

2.2 A- and B-type polymorphs of amylose (Buléon, Colonna, Planchot, & Ball, 1998 19

2.3 X-ray diffractogram of different starches. Labeling refers to (A) A-type from cereal starches, (B) B-type from tuber starch, (C) C-type from seed starches, and (V) V-type from helical amylose complexes (Reproduced from Zobel, 1988) 19

2.4 Conformational changes occurring during retrogradation (Colonna, Leloup, & Buleon, 1992) 21

2.5 Temperature dependence of the nucleation, propagation, and overall crystallization rates according to partially crystalline polymer system (Eerlingen, Crombez, & Delcour, 1993a) 21

2.6 Micelle model (a) and Lamellar model (b) for the formation of resistant starch in amylose solutions (Adapted from Eerlingen et al., 1993b) 21

2.7 Molecular modeling representation of amylose–fatty acid complexes showing the inclusion of the aliphatic part (C12) of the fatty acid inside the hydrophobic cavity of the amylose single helix (Buléon et al., 1998) 21

LIST OF FIGURES (Continued)

FIGURE **Page**

2.8 The generalized mechanism for amylose-lipid complex formation into Type I and Type II complexes (Reproduced from Biliaderis & Galloway, 1989).... 32

2.9 The action mode of AM including, intermolecular transglycosylation reaction catalysis (a), intramolecular transglycosylation reaction catalysis (b), and endo-amylolytic reaction catalysis (c) (Hansen, Blennow, Pedersen, Norgaard, & Engelsen, 2008) 34

2.10 Schematic action for AM on starch. Disproportionation of amylopectin cluster (A), disproportionation of α-glucan chains within amylopectin (B), disproportionation of α-glucan segments from amylose to amylopectin (C) and cyclization of amylopectin (D). Gray bars in B illustrate glucan chains being transferred. Black bars in C illustrate amylose molecules. The linear lines indicate α-1,4-D-glucan segments, whereas vertical arrows within the structure indicate α-1,6-glycosidic linkage. : non-reducing end. The cluster model of amylopectin is adapted from Hizukuri (1986) (Hansen et al., 2008) 37

2.11 Concept of ileal and colonic brake mechanism related to slowly digestible or resistant starches caused by ileal glucose (Glc) release and short-chain fatty acids (SCFA) from fermentation. GLP1 = glucagon-like peptide 1; and PYY = peptide YY (Lee et al., 2013)..... 37

LIST OF FIGURES (Continued)

Page

3.1 PCA score plot describing the variation of starch fractions and melting parameters of TC sample after subjected to various hydrothermal treatment conditions 78

3.2 Cooking stability of the hydrothermal-treated TC sample after cooking at 50% and 70% moisture content compared with Hi-maize 260 and Novelose 330 86

4.1 CL distributions of (a): native cassava starch and AM-treated cassava starches and (b): the different of CL distributions of AM-treated cassava starches at various reaction times as compared to native cassava starch 113

4.2 HPSEC chromatograms of native cassava starch (CS) and AM-treated cassava starch which was treated for 5 min (AM5min) and 4h (AM4h) 116

4.3 Size distributions and molar masses of native cassava starch (CS) and AM-treated cassava starch which was treated for 5 min (AM5min) and 4h (AM4h) obtained by HPSEC-MALL 116

4.4 HPSEC chromatograms of β-limit dextrins from native cassava starch (B-CS) and AM-treated cassava starches (B-AM5min and B-AM4h) after β-amylase hydrolysis 120

4.5 MALDI-TOF analysis to identify cyclo-structure formation, (a): AM5min and (b): AM4h 122

LIST OF FIGURES (Continued)

Page

4.6 HPAEC-PAD analysis of chain length distribution of crystalline residues after 35 days of acid hydrolysis (2.2 N HCl, 35°C) for HMT debranched native cassava starch (HMT_DS), HMT debranched AM-treated cassava starch for 5 min (HMT_DAM5min), and HMT debranched AM-treated cassava starch for 4 h (HMT_DAM4h 131

4.7 Cooking stability of recrystallized debranched AM-treated cassava starches after cooking at 50% and 70% moisture content using steaming for 30 min 133

4.8 SEM micrographs of (a): DAM5min at a magnification of 1,000x and (b): molded-DAM5min at a magnification of 1,000x 137

4.9 Plots of the surface area to volume ratio (S/V) of molded-DAM5min as a function of (a): SDS content and (b): RS content 143

4.10 Cooking stability test of molded-DAM5min with the different surface area to volume ratio (S/V) 144

5.1 Complexing index of cassava starch complexed with C12 and C18 at the concentration of 5% and 10% (w/w) 168

5.2 HPSEC chromatograms of native cassava starch (CS) and extruded CS as prepared at 30 and 50% moisture content 176

5.3 Size distributions and molar masses of native cassava starch (CS) and extruded CS as prepared at 30 and 50% moisture content obtained by HPSEC-MALLS-DRI 176

LIST OF FIGURES (Continued)

Page

5.4 SEM micrographs of sample extruded with C12 as prepared by extrusion cooking at 30% moisture content (a), powder sample extruded with C12 (b), and mold, C12 extrudate which were molded at 110°C with 2 tons pressure for 8 m 182

5.5 Starch fractions of molded extruded cassava starch (Molded_ExtCS), molded CS extruded with C12 (Molded_ExtCS+C12), and molded CS extruded with C18 (Molded_ExtCS+C18) before and after steam cooking at 70% moisture content for 30 min 186

5.6 WAXD patterns of molded cassava starch extrudate (a), mold, C12 extrudate (b), and mold, C18 extrudate (c) before (D00) and after storage at 80% relative humidity for 15 days (D15 190

CHAPTER I

INTRODUCTION

1.1 Introduction

Starch is the largest source of carbohydrates, which serves as energy for human diets. Regarding the nutritional purposes, starch has been classified into rapidly digestible starch (RDS), slowly digestible starch (SDS) and resistant starch (RS) based on the digestion rate (Englyst, Kingman, & Cummings, 1992). Since SDS is completely digested in the small intestine at a lower rate than RDS, it is very important for the prevention of several diseases, such as cardiovascular diseases, type II diabetes, and obesity (Shin et al., 2004; Lehmann & Robin, 2007). RS is the portion of starch that escapes the digestion in the small intestine but it is fermented in the large intestine into short-chain fatty acids, which is beneficial for colon health and protection against colorectal cancer (Lehmann and Robin, 2007). RS has been categorized into 4 or 5 types depending on a mode of resistance (Topping et al., 2010). RS3 seems to be particularly interesting because of its thermal stability and physiological properties. RS3 contains mainly retrograded amylose, which consists of linear segments of α-1, 4-glucans arranged in a crystalline structure in which resistance to enzyme digestion. Therefore, foods containing a high level of SDS and RS can improve the health benefits of foods.

SDS could be produced through chemical, physical, enzymatic, genetic, and combined modifications (Miao, Jiang, & Zhang, 2009; He, Liu, & Zhang, 2008; Shin,

Kim, Ha, Lee, & Moon, 2005). However, the reports on the health benefits of SDS are limited and the relationship between molecular structure and thermal properties of SDS is not fully clear. Thus, the study on factors affecting SDS formation, e.g. type of enzyme, modification methods and modification conditions is very important to understand its molecular structure, thermal and functional properties.

The production of RS3 consists of gelatinization of starches, hydrolysis of amylopectin with debranching enzymes such as pullulanase or isoamylase, followed by controlled retrogradation or recrystallization (Lehmann, Jacobasch, & Schmiedl, 2002; Sajilata, Singhal, & Kulkarni, 2006). The yield and quality of RS3 are affected by various factors such as the amylose/amylopectin ratio, chain length, retrogradation conditions, lipids, and solution compositions. Several crystalline polymorphic structures, termed A, B, C or V-polymorph, are shown to be formed in the RS3 production. A higher retrogradation temperature generally favors the formation of the more stable A-type rather than B-type polymorph (Gidley & Bulpin, 1987). In addition, the crystalline structure polymorphs have influence on thermal and functional properties of RS. Temperature cycling incubation is applied to accelerate starch recrystallization and to increase the yield of RS3 with more thermal stability as compared to isothermal temperature incubation (Zeng et al., 2014). However, some portions of RS are not thermostable and lose their enzymatic resistance during cooking. Therefore, it is necessary to develop clean technologies to produce a high level of thermally stable RS to deliver health benefits to consumers. The effects of annealing and heat-moisture treatment (HMT) on the structural and physicochemical properties of retrograded starch have been studied in various starches (Jacobasch, Dongowski, Schmiedl, & Müller-Schmehl, 2007; Kiatponglarp, Tongta, Rolland-Sabaté, & Buléon, 2015; Mutungi et al., 2011; Mutungi, Rost, Onyango, Jaros, &

Rohm, 2009). The single and dual hydrothermal treatments of annealing and HMT were applied in various native granular starches, for instance normal corn starch (Chung, Hoover, & Liu, 2009), pea, lentil, and navy bean starches (Chung, Liu, & Hoover, 2010), and waxy rice starch (Zeng et al., 2015). The gelatinization temperatures and SDS content of those hydrothermal-treated starches increased for both single and dual treatments, but the RS content decreased. The dual hydrothermal treatments of annealing followed by HMT starch showed a narrower ΔT and a lower ΔH, indicating that crystallite heterogeneity within the granules decreased after HMT of annealed starch. However, the effect of dual hydrothermal treatments on recrystallized starch is limited. A study on the structural transformation and enzyme digestibility during each step of dual hydrothermal treatment is necessary to understand what changes occur during these treatments in order to develop the technology to produce SDS and RS3.

Enzymes have been used to modify starch in order to produce more natural food products due to greater health awareness and avoiding chemical treatments. Recently, 4-α-glucanotranferase namely amylomaltase (AM, EC 2.4.1.25) has been studied to modify the starch structure in many sources, i.e. waxy corn starch, waxy rice starch, corn starch, rice starch, potato starch, high amylose potato starch, pea starch and wheat starch. (Do et al., 2012; Cho et al., 2009; Hansen, Blennow, Pedersen, & Engelsen, 2009; Hansen, Blennow, Pedersen, Norgaard, & Engelsen, 2008; van der Maarel et al., 2005). It catalyzed the disproportionation reaction via intermolecular transglycosylation by transferring segments of amylose to amylopectin branch chains in order to obtain the broad side chain length distribution of amylopectin, which consisted of both shorter and longer chains. The newly formed amylopectin molecules

with longer chain length exhibit an amylose-like behavior in which relation to the formation of thermoreversible starch gels with a high thermal stability. However, the melting temperature of AM-treated starch is dependent on the reaction conditions and enzyme dosage (Lee et al., 2006; van der Maarel, et al., 2005; Kaper et al., 2005). According to Cai & Shi (2010), the crystalline short-chain amylose from debranched waxy potato starch displayed a higher peak melting temperature than those from debranched waxy wheat and maize starch due to its longer average chain length, implying that the longer chains could generate a stronger double helices than shorter chain and becomes more heat resistant. In general, RS yield can be improved by several crystallization methods such as hydrothermal treatments, time-temperature cycling aging, isothermal temperature incubation, and autoclaving-cooling cycles. The local starch molecular density has the major effect on amylase digestion (Zhang, Dhital, & Gidley, 2015). The dense packing of starch chains form under crystallization decreased the enzyme accessibility and improved the yield RS, whereas the dense packing of an amorphous starch polymer may also be an effective structure for slow digestion (Zhang et al., 2015). The combination of high hydrostatic pressure and thermal annealing applied on debranched starch are introduced for improving the quantity of RS due to increasing the rigid density of the crystalline structure formed. (Lertwanawatana, Frazier, & Niranjan, 2015). Moreover, the densely pack matrices can be produced from the thermo-molding process, which is a technique to generate starch biocomposite and biodegradable plastics (Narkchamnan & Sakdaronnarong, 2013; Sun, Song, & Zheng, 2008). This process involves thermal and pressure to form the plastic film. However, there is limited information regarding the combination of AM and debranching enzyme on enzyme digestibility of cassava starch and its thermal properties. The study of the combination of AM and debranching enzyme on the

structural properties, enzyme digestibility, and thermal properties is of interest to understand the relationship between chain length distribution and RS formation. Moreover, the further investigation of various crystallization methods on the enzyme digestibility, thermal properties, and cooking stability of the resulting products is included to provide the optimum method for the development of a novel starch with improving the yield of SDS and RS.

Recently, amylose-lipid complexes (AMLs) was added to the list of RS as RS type V (RS5) which is the inclusion complexes between lipids and starch (Bird & Topping, 2008). These complexes have two major polymorphic forms: an amorphous form (Type I) and a crystalline form (Type II) depending on the melting temperature (Zhang, Huang, Luo, & Fu, 2012). The crystalline structure of AMLs showed V_h-type diffractograms (Godet, Bizot, & Buléon 1995). The formation of two types of AMLs was found to be dependent on the temperatures and durations of the pre-treatment due to an annealing effect. Pre-heating of the complexes leads to the shift of melting temperature of both types (Tufvesson, Wahlgren, & Eliasson, 2003a). The AMLs type I is less rigid and stable than type II, but it could be transformed to type II through annealing at an appropriate temperature (melting temperature of type I < T > melting temperature of type II (Zhang et al., 2015). The formation of AMLs results in the significant changes of glucan properties, including a decrease in amylose solubility and swelling, an increase in gelatinization temperature, retardation of retrogradation during storage, and a decrease in the starch digestibility, leading to increasing the overall amount of RS. There are several factors affecting the formation of AMLs and its properties, e.g. amylose chain length, lipid structure (monoglyceride or free fatty acid), the degree of lipid unsaturation, chain lengths of an aliphatic compound, complexation temperature and duration time, water content, concentration of amylose

and fatty acid, and processing methods. Previous studies revealed that the melting temperature of AMLs was increased with the chain length of the aliphatic chain of lipid and decreased with the degree of unsaturation (Kawai, Takato, Sasaki, & Kajiwara, 2012; Putseys, Derde, Lamberts, Goesaert, & Delcour, 2009; Zabar, Lesmes, Katz, Shimoni, & Bianco-Peled, 2009). Furthermore, AMLs complexes with fatty acids were more heat stable than those with monoglycerides (Tufvesson et al., 2003a; Tufvesson, Wahlgren, & Eliasson, 2003b). Many processing methods can be used to produce AMLs, especially thermal processing, including steam-jet cooking (Fanta, Felker, & Shogren, 2002; Fanta, Kenar, & Felker, 2015), homogenization (Meng, Ma, Cui, & Sun, 2014), and extrusion cooking (De Pilli, Derossi, Talja, Jouppila, & Severini, 2011), which are clean technology. Starch-lipid complex formation during extrusion cooking is an important reaction influencing the structure changes and the properties of extruded products. Thermal treatment, high pressure and shear forces of the extrusion destroyed the granular structure of starch, resulting in the decline of RS content (or increased digestibility) (Vasanthan & Bhatty, 1998). However, if starch polymers are arranged in a dense form (i.e., high local molecular density), they can decrease the digestion rate even through the food matrices are amorphous (Zhang et al., 2015). The enzymatic susceptibility of amylose has been ranked as follows: amorphous amylose > amylose-lipid complex > retrograded amylose (Tufvesson, Skrabanja, Björck, Elmståhl, & Eliasson, 2001). The shearing action of extruder screw at a high barrel temperature may cause degradation of longer amylose chain into small molecular fragments that could be incorporated into a crystalline structure of RS3 (Eerlingen, Deceuninck, & Delcour, 1993; Gidley et al., 1995). An increase in RS content after extrusion was also found from extruded barley which was further freeze-stored (Huth, Dongowski, Gebhardt, & Flamme, 2000).

The extrusion conditions also influence the crystalline structure of the starch, an extreme condition of extrusion (35% moisture, 140°C) resulted in the formation of some crystallinity of single helical V_h-type whereas mild condition of extrusion (50% moisture, 100°C) induced B-type crystalline structure formation (Chanvrier et al., 2007). The study of De Pilli et al. (2011) on the starch-lipid complexes in a model system and real food using extrusion cooking exhibited that the highest formation of starch-lipid complexes was obtained at the highest temperature (128°C) and water feed content (21%), which showed a highest melting enthalpy. Thus, the extrusion parameters and storage conditions are an important factor for producing extruded product with high SDS and RS yield. Nevertheless, the formation of SDS during extrusion cooking has never been reported. Consequently, the study on the formation of SDS and RS from starch with the addition of free fatty acid by extrusion cooking is interested for understanding the mechanism and factors affecting the AMLs formation and its characteristics in terms of enzyme digestibility and thermal properties. The additional step further extrusion cooking for generating the densely packed matrices should be investigated in order to understand the relationship between the enzyme digestibility and structural characteristics such as surface morphology and crystalline structure.

1.2 Research objectives

The objectives of this research were:

1. To study the effect of single and dual hydrothermal treatments on SDS and RS formation and its physicochemical properties from crystallized debranched cassava starch.

2. To characterize the structural properties of modified cassava starch after treating with amylomaltase at various conditions.

3. To investigate the influence of the combined use of amylomaltase and debranching enzyme on chain length distribution, enzyme digestibility, crystalline structure, and thermal properties of the resulting products.

4. To study the effect of chain length distribution, crystallization methods, and thermo-molding process on an improvement of SDS and RS content and its thermal properties.

5. To investigate the formation of amylose-lipid complex by extrusion cooking and thermo-molding on the SDS and RS content, crystalline structure, physical and functional properties of cassava starch with addition of fatty acid.

1.3 Research hypothesis

The hydrothermal treatments with annealing or HMT may improve the SDS and RS content of crystallized debranched cassava starch due to the enhancing glucan chain interaction on double helices formation into a more perfect crystalline structure and high thermal stability. The enzymatic modification of amylomaltase and debranching enzyme may generate longer chain length with the contribution to form double helices and, subsequently, yield a higher SDS and RS content with high thermal stability. The improvement of RS content and thermal stability of debranched starch containing a high proportion of long chain may be achieved from crystallization in which the formation of dense packing of starch chain, which prevents starch digestibility. Extrusion cooking would reduce the molecular size of cassava starch with facilitating the ability to form an inclusion complex with fatty acid, resulting in

the increased SDS and RS content with higher thermal stability as compared to native cassava starch.

1.4 Scope of the study

1.4.1 The effect of single and dual hydrothermal treatments with crystallized debranched cassava starch was studied on SDS and RS3 formation and its physicochemical properties. The debranched cassava starch was prepared by debranching with isoamylase and subsequent recrystallization with time-temperature cycling. The single hydrothermal treatment of annealing or HMT and dual hydrothermal treatments were applied with crystallized debranched cassava starch.

1.4.2 The enzymatic modification of cassava starch with amylomaltase was investigated. The structural properties of amylomaltase-treated cassava starches were characterized. The production of modified cassava starch containing different long chain proportion was studied using amylomaltase and debranching enzyme. Subsequently, the debranched starches with different long chain proportion were subjected to annealing, isothermal temperature incubation, and thermo-molding process. The starch fractions, crystalline structure, thermal properties, and cooking stability of the resulting products were determined.

1.4.3 The formation of amylose-lipid complex by extrusion cooking was investigated from cassava starch with addition of fatty acid. The extrusion cooking was performed using co-rotation twin screw extruder. The starch fractions, crystalline properties, thermal and cooking stability of extruded samples were examined. Then, the extruded samples were subjected to thermo-molding process and storage at high

humidity. The starch fractions, crystalline structure, thermal and cooking stability of the resulting products were examined.

1.5 Expected results

Results from this research will lead to development a fundamental understanding of factors and suitable modification methods where it could be improved the yield of SDS and RS from cassava starch with high thermal stability. Furthermore, it will contribute a better understanding the effect of chain-extended starch on the SDS and RS formation and its thermal properties. In addition, it will lead to more understanding the possibility to produce a starchy product rich in SDS and RS as induced by amylose-lipid complexes formation through extrusion cooking and thermo-molding process for application in many kinds of food and pharmaceutical industries. Regarding this knowledge, it is expected to be applied in the development of a novel starch to improve the health benefit for controlled release of glucose and prevented the colon cancer.

1.6 References

Bird, A. R. & Topping, D. L. (2008). Resistant starch as a prebiotic. In J. Versalovic and Wilson M. (eds.) **Therapectic microbiology: probiotica and related strategies.** ASM Press, Washington, pp. 159-173.

Cai, L. M., & Shi, Y. C. (2010). Structure and digestibility of crystalline short-chain amylose from debranched waxy wheat, waxy maize, and waxy potato starches. **Carbohydrate Polymers,** 79, 1117-1123.

Chanvrier, H., Uthayakumaran, S., Appelqvist, I. A. M., Gidley, M. J., Gilbert, E. P., & Lopez-Rubio, A. (2007). Influence of storage conditions on the structure, thermal behavior, and formation of enzyme-resistant starch in extruded starches. **Journal of Agricultural and Food Chemistry,** 55, 9883-9890.

Cho, K. H., Auh, J. H., Ryu, J. H., Kim, J. H., Park, K. H., Park, C. S., et al. (2009). Structural modification and characterization of rice starch treated by *Thermus aquaticus* 4-α-glucanotransferase. **Food Hydrocolloids,** 23, 2403-2409.

Chung, H. J., Liu, Q., & Hoover, R. (2010). Effect of single and dual hydrothermal treatments on the crystalline structure, thermal properties, and nutritional fractions of pea, lentil, and navy bean starches. **Food Research International,** 43(2), 501-508.

Chung, H. J., Hoover, R., & Liu, Q. (2009). The impact of single and dual hydrothermal modifications on the molecular structure and physicochemical properties of normal corn starch. **International Journal of Biological Macromolecules,** 44(2), 203-210.

De Pilli, T., Derossi, A., Talja, R. A., Jouppila, K., & Severini, C. (2011). Study of starch-lipid complexes on model system and real food produced using extrusion-cooking technology. **Innovative Food Science and Engineering Technologies,** 12, 610-616.

Do, H. V., Lee, E. J., Park, J. H., Park, K. H., Shim, J. Y., Mun. S., et al. (2012). Structural and physicochemical properties of starch gels prepared from partially modified starches using *Thermus aquaticus* 4-α-glucanotransferase. **Carbohydrate Polymers,** 87, 2455-2463.

Eerlingen, R. C., Deceuninck, M., & Delcour, J. A. (1993). Enzyme-resistant starch. II. influence of amylose chain length on resistant starch formation. **Cereal Chemistry,** 70(3), 345-350.

Englyst, H. N., Kingman, S. M. & Cummings, J. H. (1992). Classification and measurement of nutritionally important starch fractions. **European Journal of Clinical Nutrition,** 46, S33-S50.

Fanta, G. F., Felker, F. C., Shogren, R. L. (2002). Formation of crystalline aggregates in slowly-cooled starch solutions prepared by steam jet cooking. **Carbohydrate Polymers,** 48, 161-170.

Fanta, G. F., Kenar, J. A., Felker, F. C. (2015). Nanoparticle formation from amylose-fatty acid inclusion complexes prepared by steam jet cooking. **Industrial Crops and Products,** 74, 36-44.

Gidley, M. J., Bulpin, P. V. (1987). Crystallization of malto-oligosaccharides as models of the crystalline forms of starch: minimum chain-length requirement for the formation of double helices. **Carbohydrate Research,** 161, 291-300.

Gidley, M. J., Cooke, D., Darke, A. H., Hoffman, R. A., Russel, A. L., & Greenwell, P. (1995). Molecular order and structure in enzyme-resistant retrograded starch. **Carbohydrate Polymers,** 28, 23-31.

Godet, M. C., Bizot, H., & Buléon, A. (1995). Crystallization of amylose-fatty acid complexes prepared with different amylose chain lengths. **Carbohydrate Polymers,** 27, 47-52.

Hansen, M. R., Blennow, A., Pedersen, S., &. Engelsen, S. B. (2009). Enzyme modification of starch with amylomaltase results in increasing gel melting point. **Carbohydrate Polymers,** 78, 72-79.

Hansen, M. R., Blennow, A., Pedersen, S., Norgaard, L., & Engelsen, S. B. (2008). Gel texture and chain structure of amylomaltase-modified starches compared to gelatin. **Food Hydrocolloids,** 22, 1551-1566.

He, J., Liu, J., & Zhang, G. (2008). Slowly digestible waxy maize starch prepared by octenyl succinic anhydride esterification and heat-moisture treatment: Glycemic response and mechanism. **Biomacromolecules,** 9, 175-184.

Huth, M., Dongowski, G., Gebhardt, E., & Flamme, W. (2000). Functional properties of dietary fibre enriched extrudates from barley. **Journal of Cereal Science,** 32, 115-128.

Jacobasch, G., Dongowski, G., Schmiedl, D., & Müller-Schmehl, K. (2007). Hydrothermal treatment of Novelose 330 results in high yield of resistant starch type 3 with beneficial prebiotic properties and decreased secondary bile acid formation in rats. **British Journal of Nutrition,** 95(06), 1063-1074.

Kaper, T., Talik, B., Ettema, T. J., Bos, H., Van der Maarel, M.J.E.C., & Dijkhuizen, L. (2005). The amylomaltase of *Pyrobaculum aerophilic* IM2 produces thermo-reversible starch gels. **Applied and Environmental Microbioogy,** 71, 5098-5106.

Kawai, K., Takato, S., Sasaki, T., & Kajiwara, K. (2012). Complex formation, thermal properties, and *in-vitro* digestibility of gelatinized potato starch-fatty acid mixtures. **Food Hydrocolloids,** 27, 228-234.

Kiatponglarp, W., Tongta, S., Rolland-Sabaté, A., & Buléon, A. (2015). Crystallization and chain reorganization of debranched rice starches in relation to resistant starch formation. **Carbohydrate Polymers,** 122, 108-114.

Lehmann, U., Jacobasch, G. & Schmiedl, D. (2002). Characterization of resistant starch typeIII from banana (Musa acuminate). **Journal of Agriculture and Food Chemistry,** 50, 5236-5240.

Lehmann, U., & Robin, F. (2007). Slowly digestible starch-its structure and health implications: A review. **Trends in Food Science and Technology,** 18, 346-355.

Lertwanawatana, P., Frazier, R. A., & Niranjan, K. (2015). High pressure intensification of cassava resistant starch (RS3) yields. **Food Chemistry,** 181, 85-93.

Meng, S., Ma, Y., Cui, J., Sun, D. W. (2014). Preparation of cornstarch-fatty acid complexes by high-pressure homogenization. **Starch/Stärke,** 66, 809-817.

Miao, M., Jiang, B., & Zhang, T. (2009). Effect of pullulanase debranching and recrystallization on structure and digestibility of waxy maize starch. **Carbohydrate Polymers,** 76, 214-221.

Mutungi, C., Onyango, C., Doert, T., Paasch, S., Thiele, S., Machill, S., et al.. (2011). Long- and short-range structural changes of recrystallized cassava starch subjected to in vitro digestion. **Food Hydrocolloids,** 25(3), 477-485.

Mutungi, C., Rost, F., Onyango, C., Jaros, D., & Rohm, H. (2009). Crystallinity, Thermal and Morphological Characteristics of Resistant Starch Type III Produced by Hydrothermal Treatment of Debranched Cassava Starch. **Starch - Stärke,** 61(11), 634-645.

Narkchamnan, S., & Sakdaronnarong, C. (2013). Thermo-molded biocomposite from cassava starch, natural fibers and lignin associated by laccase-mediator system. **Carbohydrate Polymers,** 96, 109-117.

Putseys, J. A., Derde, L. J., Lamberts, L., Goesaert, H., & Delcour, J. A. (2009). Production of tailor made short chain amylose-lipid complexes using varying reaction conditions. **Carbohydrate Polymers,** 78, 854-861.

Sajilata, M. G., Singhal, R. S., & Kulkarni, P. R. (2006). Resistant Starch-A Review. **Comprehensive Reviews in Food Science & Food Safety,** 5, 1-17.

Shin, S. I., Choi, H. J., Chung, K. M., Hamaker, B., Park, K. H., & Moon, T. W. (2004). Slowly digestible starch from debranched waxy sorghum starch: preparation and properties. **Cereal Chemistry,** 81, 404-408.

Shin, S. I., Kim, H. J., Ha, H. J., Lee, H. S., & Moon, T. W. (2005). Effect of hydrothermal treatment on formation and structural characteristics of slowly digestible non-pasted granular sweet potato starch. **Starch/Stärke,** 57, 421-430.

Sun, S., Song,Y., & Zheng, Q. (2008). Thermo-molded wheat gluten plastics plasticized with glycerol: Effect of molding temperature. **Food Hydrocolloids,** 22, 1006-1013.

Topping, D. L., Segal, I., Regina, A., Conlon, M. A., Bajka, B. H., Toden, S. et al. (2010). Resistant starch and human health. In J. Willem van der Kamp, J. Jones, B.McCleary and David T. (eds.) **Dietary fiber: new frontiers for food and health.** Wageningen Academic Publishers, Netherland, pp. 311-322.

Tufvesson, F., Skrabanja, V., Björck, I., Elmståhl, H. L., & Eliasson, A.-C. (2001). Digestibility of starch systems containing amyloseeglycerol monopalmitin complexes. **LWT-Food Science and Technology,** 34, 131-139.

Tufvesson, F., Wahlgren, M., & Eliasson, A. C. (2003a). Formation of amylose-lipid complexes and effects of temperature treatment. Part 1. Monoglycerides. **Starch/Stärke,** 55, 61-71.

Tufvesson, F., Wahlgren, M., & Eliasson, A. C. (2003b). Formation of amylose-lipid complexes and effects of temperature treatment. part 2. Fatty acids. **Starch-Stärke,** 55, 138-149.

van der Maarel, M. J. E. C., Capron, I., Euverink, G. J. W., Bos, T., Kaper, T., Binnema, D. J., et al. (2005). A novel thermoreversible gelling product made by enzymatic modification of starch. **Starch/Stärke,** 57, 465-472.

Vasanthan, T. & Bhatty, R. S. (1998). Enhancement of Resistant Starch (RS3) in Amylomaize, Barley, Field Pea, and Lentil Starches. **Starch/Stärke,** 50, 286-291.

Zabar, S., Lesmes, U., Katz, I., Shimoni, E., & Bianco-Peled, H. (2009). Studying different dimensions of amylose-long chain fatty acid complexes: molecular, nano and micro level characteristics. **Food Hydrocolloids,** 23, 1918-1925.

Zhang, B., Dhital, S., Flanagan, B. M. Luckman, P., Halley, P. J., & Gidley, M. J. (2015). Extrusion induced low-order starch matrices: Enzymic hydrolysis and structure. **Carbohydrate Polymers,** 134, 485-496.

Zhang, B., Huang, Q., Luo, F., & Fu., X. (2012). Structural characterizations and digestibility of debranched high-amylose maize starch complexed with lauric acid. **Food Hydrocolloids,** 28, 174-181.

Zeng, F., Chen, F., Kong, F., Gao, Q., Aadil, R. M., & Yu, S. (2015). Structure and digestibility of debranched and repeatedly crystallized waxy rice starch. **Food Chemistry,** 187, 348-353.

Zeng, F., Ma, F., Gao, Q., Yu, S., Kong, F., & Zhu, S. (2014). Debranching and temperature-cycled crystallization of waxy rice starch and their digestibility. **Carbohydrate Polymers,** 113, 91-96.

CHAPTER I

INTRODUCTION

1.1 Introduction

Starch is the largest source of carbohydrates, which serves as energy for human diets. Regarding the nutritional purposes, starch has been classified into rapidly digestible starch (RDS), slowly digestible starch (SDS) and resistant starch (RS) based on the digestion rate (Englyst, Kingman, & Cummings, 1992). Since SDS is completely digested in the small intestine at a lower rate than RDS, it is very important for the prevention of several diseases, such as cardiovascular diseases, type II diabetes, and obesity (Shin et al., 2004; Lehmann & Robin, 2007). RS is the portion of starch that escapes the digestion in the small intestine but it is fermented in the large intestine into short-chain fatty acids, which is beneficial for colon health and protection against colorectal cancer (Lehmann and Robin, 2007). RS has been categorized into 4 or 5 types depending on a mode of resistance (Topping et al., 2010). RS3 seems to be particularly interesting because of its thermal stability and physiological properties. RS3 contains mainly retrograded amylose, which consists of linear segments of α-1, 4-glucans arranged in a crystalline structure in which resistance to enzyme digestion. Therefore, foods containing a high level of SDS and RS can improve the health benefits of foods.

SDS could be produced through chemical, physical, enzymatic, genetic, and combined modifications (Miao, Jiang, & Zhang, 2009; He, Liu, & Zhang, 2008; Shin,

Kim, Ha, Lee, & Moon, 2005). However, the reports on the health benefits of SDS are limited and the relationship between molecular structure and thermal properties of SDS is not fully clear. Thus, the study on factors affecting SDS formation, e.g. type of enzyme, modification methods and modification conditions is very important to understand its molecular structure, thermal and functional properties.

The production of RS3 consists of gelatinization of starches, hydrolysis of amylopectin with debranching enzymes such as pullulanase or isoamylase, followed by controlled retrogradation or recrystallization (Lehmann, Jacobasch, & Schmiedl, 2002; Sajilata, Singhal, & Kulkarni, 2006). The yield and quality of RS3 are affected by various factors such as the amylose/amylopectin ratio, chain length, retrogradation conditions, lipids, and solution compositions. Several crystalline polymorphic structures, termed A, B, C or V-polymorph, are shown to be formed in the RS3 production. A higher retrogradation temperature generally favors the formation of the more stable A-type rather than B-type polymorph (Gidley & Bulpin, 1987). In addition, the crystalline structure polymorphs have influence on thermal and functional properties of RS. Temperature cycling incubation is applied to accelerate starch recrystallization and to increase the yield of RS3 with more thermal stability as compared to isothermal temperature incubation (Zeng et al., 2014). However, some portions of RS are not thermostable and lose their enzymatic resistance during cooking. Therefore, it is necessary to develop clean technologies to produce a high level of thermally stable RS to deliver health benefits to consumers. The effects of annealing and heat-moisture treatment (HMT) on the structural and physicochemical properties of retrograded starch have been studied in various starches (Jacobasch, Dongowski, Schmiedl, & Müller-Schmehl, 2007; Kiatponglarp, Tongta, Rolland-Sabaté, & Buléon, 2015; Mutungi et al., 2011; Mutungi, Rost, Onyango, Jaros, &

Rohm, 2009). The single and dual hydrothermal treatments of annealing and HMT were applied in various native granular starches, for instance normal corn starch (Chung, Hoover, & Liu, 2009), pea, lentil, and navy bean starches (Chung, Liu, & Hoover, 2010), and waxy rice starch (Zeng et al., 2015). The gelatinization temperatures and SDS content of those hydrothermal-treated starches increased for both single and dual treatments, but the RS content decreased. The dual hydrothermal treatments of annealing followed by HMT starch showed a narrower ΔT and a lower ΔH, indicating that crystallite heterogeneity within the granules decreased after HMT of annealed starch. However, the effect of dual hydrothermal treatments on recrystallized starch is limited. A study on the structural transformation and enzyme digestibility during each step of dual hydrothermal treatment is necessary to understand what changes occur during these treatments in order to develop the technology to produce SDS and RS3.

Enzymes have been used to modify starch in order to produce more natural food products due to greater health awareness and avoiding chemical treatments. Recently, 4-α-glucanotranferase namely amylomaltase (AM, EC 2.4.1.25) has been studied to modify the starch structure in many sources, i.e. waxy corn starch, waxy rice starch, corn starch, rice starch, potato starch, high amylose potato starch, pea starch and wheat starch. (Do et al., 2012; Cho et al., 2009; Hansen, Blennow, Pedersen, & Engelsen, 2009; Hansen, Blennow, Pedersen, Norgaard, & Engelsen, 2008; van der Maarel et al., 2005). It catalyzed the disproportionation reaction via intermolecular transglycosylation by transferring segments of amylose to amylopectin branch chains in order to obtain the broad side chain length distribution of amylopectin, which consisted of both shorter and longer chains. The newly formed amylopectin molecules

with longer chain length exhibit an amylose-like behavior in which relation to the formation of thermoreversible starch gels with a high thermal stability. However, the melting temperature of AM-treated starch is dependent on the reaction conditions and enzyme dosage (Lee et al., 2006; van der Maarel, et al., 2005; Kaper et al., 2005). According to Cai & Shi (2010), the crystalline short-chain amylose from debranched waxy potato starch displayed a higher peak melting temperature than those from debranched waxy wheat and maize starch due to its longer average chain length, implying that the longer chains could generate a stronger double helices than shorter chain and becomes more heat resistant. In general, RS yield can be improved by several crystallization methods such as hydrothermal treatments, time-temperature cycling aging, isothermal temperature incubation, and autoclaving-cooling cycles. The local starch molecular density has the major effect on amylase digestion (Zhang, Dhital, & Gidley, 2015). The dense packing of starch chains form under crystallization decreased the enzyme accessibility and improved the yield RS, whereas the dense packing of an amorphous starch polymer may also be an effective structure for slow digestion (Zhang et al., 2015). The combination of high hydrostatic pressure and thermal annealing applied on debranched starch are introduced for improving the quantity of RS due to increasing the rigid density of the crystalline structure formed. (Lertwanawatana, Frazier, & Niranjan, 2015). Moreover, the densely pack matrices can be produced from the thermo-molding process, which is a technique to generate starch biocomposite and biodegradable plastics (Narkchamnan & Sakdaronnarong, 2013; Sun, Song, & Zheng, 2008). This process involves thermal and pressure to form the plastic film. However, there is limited information regarding the combination of AM and debranching enzyme on enzyme digestibility of cassava starch and its thermal properties. The study of the combination of AM and debranching enzyme on the

structural properties, enzyme digestibility, and thermal properties is of interest to understand the relationship between chain length distribution and RS formation. Moreover, the further investigation of various crystallization methods on the enzyme digestibility, thermal properties, and cooking stability of the resulting products is included to provide the optimum method for the development of a novel starch with improving the yield of SDS and RS.

Recently, amylose-lipid complexes (AMLs) was added to the list of RS as RS type V (RS5) which is the inclusion complexes between lipids and starch (Bird & Topping, 2008). These complexes have two major polymorphic forms: an amorphous form (Type I) and a crystalline form (Type II) depending on the melting temperature (Zhang, Huang, Luo, & Fu, 2012). The crystalline structure of AMLs showed V_h-type diffractograms (Godet, Bizot, & Buléon 1995). The formation of two types of AMLs was found to be dependent on the temperatures and durations of the pre-treatment due to an annealing effect. Pre-heating of the complexes leads to the shift of melting temperature of both types (Tufvesson, Wahlgren, & Eliasson, 2003a). The AMLs type I is less rigid and stable than type II, but it could be transformed to type II through annealing at an appropriate temperature (melting temperature of type I < T > melting temperature of type II (Zhang et al., 2015). The formation of AMLs results in the significant changes of glucan properties, including a decrease in amylose solubility and swelling, an increase in gelatinization temperature, retardation of retrogradation during storage, and a decrease in the starch digestibility, leading to increasing the overall amount of RS. There are several factors affecting the formation of AMLs and its properties, e.g. amylose chain length, lipid structure (monoglyceride or free fatty acid), the degree of lipid unsaturation, chain lengths of an aliphatic compound, complexation temperature and duration time, water content, concentration of amylose

and fatty acid, and processing methods. Previous studies revealed that the melting temperature of AMLs was increased with the chain length of the aliphatic chain of lipid and decreased with the degree of unsaturation (Kawai, Takato, Sasaki, & Kajiwara, 2012; Putseys, Derde, Lamberts, Goesaert, & Delcour, 2009; Zabar, Lesmes, Katz, Shimoni, & Bianco-Peled, 2009). Furthermore, AMLs complexes with fatty acids were more heat stable than those with monoglycerides (Tufvesson et al., 2003a; Tufvesson, Wahlgren, & Eliasson, 2003b). Many processing methods can be used to produce AMLs, especially thermal processing, including steam-jet cooking (Fanta, Felker, & Shogren, 2002; Fanta, Kenar, & Felker, 2015), homogenization (Meng, Ma, Cui, & Sun, 2014), and extrusion cooking (De Pilli, Derossi, Talja, Jouppila, & Severini, 2011), which are clean technology. Starch-lipid complex formation during extrusion cooking is an important reaction influencing the structure changes and the properties of extruded products. Thermal treatment, high pressure and shear forces of the extrusion destroyed the granular structure of starch, resulting in the decline of RS content (or increased digestibility) (Vasanthan & Bhatty, 1998). However, if starch polymers are arranged in a dense form (i.e., high local molecular density), they can decrease the digestion rate even through the food matrices are amorphous (Zhang et al., 2015). The enzymatic susceptibility of amylose has been ranked as follows: amorphous amylose > amylose-lipid complex > retrograded amylose (Tufvesson, Skrabanja, Björck, Elmståhl, & Eliasson, 2001). The shearing action of extruder screw at a high barrel temperature may cause degradation of longer amylose chain into small molecular fragments that could be incorporated into a crystalline structure of RS3 (Eerlingen, Deceuninck, & Delcour, 1993; Gidley et al., 1995). An increase in RS content after extrusion was also found from extruded barley which was further freeze-stored (Huth, Dongowski, Gebhardt, & Flamme, 2000).

The extrusion conditions also influence the crystalline structure of the starch, an extreme condition of extrusion (35% moisture, 140°C) resulted in the formation of some crystallinity of single helical V_h-type whereas mild condition of extrusion (50% moisture, 100°C) induced B-type crystalline structure formation (Chanvrier et al., 2007). The study of De Pilli et al. (2011) on the starch-lipid complexes in a model system and real food using extrusion cooking exhibited that the highest formation of starch-lipid complexes was obtained at the highest temperature (128°C) and water feed content (21%), which showed a highest melting enthalpy. Thus, the extrusion parameters and storage conditions are an important factor for producing extruded product with high SDS and RS yield. Nevertheless, the formation of SDS during extrusion cooking has never been reported. Consequently, the study on the formation of SDS and RS from starch with the addition of free fatty acid by extrusion cooking is interested for understanding the mechanism and factors affecting the AMLs formation and its characteristics in terms of enzyme digestibility and thermal properties. The additional step further extrusion cooking for generating the densely packed matrices should be investigated in order to understand the relationship between the enzyme digestibility and structural characteristics such as surface morphology and crystalline structure.

1.2 Research objectives

The objectives of this research were:

1. To study the effect of single and dual hydrothermal treatments on SDS and RS formation and its physicochemical properties from crystallized debranched cassava starch.

2. To characterize the structural properties of modified cassava starch after treating with amylomaltase at various conditions.

3. To investigate the influence of the combined use of amylomaltase and debranching enzyme on chain length distribution, enzyme digestibility, crystalline structure, and thermal properties of the resulting products.

4. To study the effect of chain length distribution, crystallization methods, and thermo-molding process on an improvement of SDS and RS content and its thermal properties.

5. To investigate the formation of amylose-lipid complex by extrusion cooking and thermo-molding on the SDS and RS content, crystalline structure, physical and functional properties of cassava starch with addition of fatty acid.

1.3 Research hypothesis

The hydrothermal treatments with annealing or HMT may improve the SDS and RS content of crystallized debranched cassava starch due to the enhancing glucan chain interaction on double helices formation into a more perfect crystalline structure and high thermal stability. The enzymatic modification of amylomaltase and debranching enzyme may generate longer chain length with the contribution to form double helices and, subsequently, yield a higher SDS and RS content with high thermal stability. The improvement of RS content and thermal stability of debranched starch containing a high proportion of long chain may be achieved from crystallization in which the formation of dense packing of starch chain, which prevents starch digestibility. Extrusion cooking would reduce the molecular size of cassava starch with facilitating the ability to form an inclusion complex with fatty acid, resulting in

the increased SDS and RS content with higher thermal stability as compared to native cassava starch.

1.4 Scope of the study

1.4.1 The effect of single and dual hydrothermal treatments with crystallized debranched cassava starch was studied on SDS and RS3 formation and its physicochemical properties. The debranched cassava starch was prepared by debranching with isoamylase and subsequent recrystallization with time-temperature cycling. The single hydrothermal treatment of annealing or HMT and dual hydrothermal treatments were applied with crystallized debranched cassava starch.

1.4.2 The enzymatic modification of cassava starch with amylomaltase was investigated. The structural properties of amylomaltase-treated cassava starches were characterized. The production of modified cassava starch containing different long chain proportion was studied using amylomaltase and debranching enzyme. Subsequently, the debranched starches with different long chain proportion were subjected to annealing, isothermal temperature incubation, and thermo-molding process. The starch fractions, crystalline structure, thermal properties, and cooking stability of the resulting products were determined.

1.4.3 The formation of amylose-lipid complex by extrusion cooking was investigated from cassava starch with addition of fatty acid. The extrusion cooking was performed using co-rotation twin screw extruder. The starch fractions, crystalline properties, thermal and cooking stability of extruded samples were examined. Then, the extruded samples were subjected to thermo-molding process and storage at high

humidity. The starch fractions, crystalline structure, thermal and cooking stability of the resulting products were examined.

1.5 Expected results

Results from this research will lead to development a fundamental understanding of factors and suitable modification methods where it could be improved the yield of SDS and RS from cassava starch with high thermal stability. Furthermore, it will contribute a better understanding the effect of chain-extended starch on the SDS and RS formation and its thermal properties. In addition, it will lead to more understanding the possibility to produce a starchy product rich in SDS and RS as induced by amylose-lipid complexes formation through extrusion cooking and thermo-molding process for application in many kinds of food and pharmaceutical industries. Regarding this knowledge, it is expected to be applied in the development of a novel starch to improve the health benefit for controlled release of glucose and prevented the colon cancer.

1.6 References

Bird, A. R. & Topping, D. L. (2008). Resistant starch as a prebiotic. In J. Versalovic and Wilson M. (eds.) **Therapectic microbiology: probiotica and related strategies.** ASM Press, Washington, pp. 159-173.

Cai, L. M., & Shi, Y. C. (2010). Structure and digestibility of crystalline short-chain amylose from debranched waxy wheat, waxy maize, and waxy potato starches. **Carbohydrate Polymers,** 79, 1117-1123.

Chanvrier, H., Uthayakumaran, S., Appelqvist, I. A. M., Gidley, M. J., Gilbert, E. P., & Lopez-Rubio, A. (2007). Influence of storage conditions on the structure, thermal behavior, and formation of enzyme-resistant starch in extruded starches. **Journal of Agricultural and Food Chemistry,** 55, 9883-9890.

Cho, K. H., Auh, J. H., Ryu, J. H., Kim, J. H., Park, K. H., Park, C. S., et al. (2009). Structural modification and characterization of rice starch treated by *Thermus aquaticus* 4-α-glucanotransferase. **Food Hydrocolloids,** 23, 2403-2409.

Chung, H. J., Liu, Q., & Hoover, R. (2010). Effect of single and dual hydrothermal treatments on the crystalline structure, thermal properties, and nutritional fractions of pea, lentil, and navy bean starches. **Food Research International,** 43(2), 501-508.

Chung, H. J., Hoover, R., & Liu, Q. (2009). The impact of single and dual hydrothermal modifications on the molecular structure and physicochemical properties of normal corn starch. **International Journal of Biological Macromolecules,** 44(2), 203-210.

De Pilli, T., Derossi, A., Talja, R. A., Jouppila, K., & Severini, C. (2011). Study of starch-lipid complexes on model system and real food produced using extrusion-cooking technology. **Innovative Food Science and Engineering Technologies,** 12, 610-616.

Do, H. V., Lee, E. J., Park, J. H., Park, K. H., Shim, J. Y., Mun. S., et al. (2012). Structural and physicochemical properties of starch gels prepared from partially modified starches using *Thermus aquaticus* 4-α-glucanotransferase. **Carbohydrate Polymers,** 87, 2455-2463.

Eerlingen, R. C., Deceuninck, M., & Delcour, J. A. (1993). Enzyme-resistant starch. II. influence of amylose chain length on resistant starch formation. **Cereal Chemistry,** 70(3), 345-350.

Englyst, H. N., Kingman, S. M. & Cummings, J. H. (1992). Classification and measurement of nutritionally important starch fractions. **European Journal of Clinical Nutrition,** 46, S33-S50.

Fanta, G. F., Felker, F. C., Shogren, R. L. (2002). Formation of crystalline aggregates in slowly-cooled starch solutions prepared by steam jet cooking. **Carbohydrate Polymers,** 48, 161-170.

Fanta, G. F., Kenar, J. A., Felker, F. C. (2015). Nanoparticle formation from amylose-fatty acid inclusion complexes prepared by steam jet cooking. **Industrial Crops and Products,** 74, 36-44.

Gidley, M. J., Bulpin, P. V. (1987). Crystallization of malto-oligosaccharides as models of the crystalline forms of starch: minimum chain-length requirement for the formation of double helices. **Carbohydrate Research,** 161, 291-300.

Gidley, M. J., Cooke, D., Darke, A. H., Hoffman, R. A., Russel, A. L., & Greenwell, P. (1995). Molecular order and structure in enzyme-resistant retrograded starch. **Carbohydrate Polymers,** 28, 23-31.

Godet, M. C., Bizot, H., & Buléon, A. (1995). Crystallization of amylose-fatty acid complexes prepared with different amylose chain lengths. **Carbohydrate Polymers,** 27, 47-52.

Hansen, M. R., Blennow, A., Pedersen, S., &. Engelsen, S. B. (2009). Enzyme modification of starch with amylomaltase results in increasing gel melting point. **Carbohydrate Polymers,** 78, 72-79.

Hansen, M. R., Blennow, A., Pedersen, S., Norgaard, L., & Engelsen, S. B. (2008). Gel texture and chain structure of amylomaltase-modified starches compared to gelatin. **Food Hydrocolloids,** 22, 1551-1566.

He, J., Liu, J., & Zhang, G. (2008). Slowly digestible waxy maize starch prepared by octenyl succinic anhydride esterification and heat-moisture treatment: Glycemic response and mechanism. **Biomacromolecules,** 9, 175-184.

Huth, M., Dongowski, G., Gebhardt, E., & Flamme, W. (2000). Functional properties of dietary fibre enriched extrudates from barley. **Journal of Cereal Science,** 32, 115-128.

Jacobasch, G., Dongowski, G., Schmiedl, D., & Müller-Schmehl, K. (2007). Hydrothermal treatment of Novelose 330 results in high yield of resistant starch type 3 with beneficial prebiotic properties and decreased secondary bile acid formation in rats. **British Journal of Nutrition,** 95(06), 1063-1074.

Kaper, T., Talik, B., Ettema, T. J., Bos, H., Van der Maarel, M.J.E.C., & Dijkhuizen, L. (2005). The amylomaltase of *Pyrobaculum aerophilic* IM2 produces thermo-reversible starch gels. **Applied and Environmental Microbioogy,** 71, 5098-5106.

Kawai, K., Takato, S., Sasaki, T., & Kajiwara, K. (2012). Complex formation, thermal properties, and *in-vitro* digestibility of gelatinized potato starch-fatty acid mixtures. **Food Hydrocolloids,** 27, 228-234.

Kiatponglarp, W., Tongta, S., Rolland-Sabaté, A., & Buléon, A. (2015). Crystallization and chain reorganization of debranched rice starches in relation to resistant starch formation. **Carbohydrate Polymers,** 122, 108-114.

Lehmann, U., Jacobasch, G. & Schmiedl, D. (2002). Characterization of resistant starch typeIII from banana (Musa acuminate). **Journal of Agriculture and Food Chemistry,** 50, 5236-5240.

Lehmann, U., & Robin, F. (2007). Slowly digestible starch-its structure and health implications: A review. **Trends in Food Science and Technology,** 18, 346-355.

Lertwanawatana, P., Frazier, R. A., & Niranjan, K. (2015). High pressure intensification of cassava resistant starch (RS3) yields. **Food Chemistry,** 181, 85-93.

Meng, S., Ma, Y., Cui, J., Sun, D. W. (2014). Preparation of cornstarch-fatty acid complexes by high-pressure homogenization. **Starch/Stärke,** 66, 809-817.

Miao, M., Jiang, B., & Zhang, T. (2009). Effect of pullulanase debranching and recrystallization on structure and digestibility of waxy maize starch. **Carbohydrate Polymers,** 76, 214-221.

Mutungi, C., Onyango, C., Doert, T., Paasch, S., Thiele, S., Machill, S., et al.. (2011). Long- and short-range structural changes of recrystallized cassava starch subjected to in vitro digestion. **Food Hydrocolloids,** 25(3), 477-485.

Mutungi, C., Rost, F., Onyango, C., Jaros, D., & Rohm, H. (2009). Crystallinity, Thermal and Morphological Characteristics of Resistant Starch Type III Produced by Hydrothermal Treatment of Debranched Cassava Starch. **Starch - Stärke,** 61(11), 634-645.

Narkchamnan, S., & Sakdaronnarong, C. (2013). Thermo-molded biocomposite from cassava starch, natural fibers and lignin associated by laccase-mediator system. **Carbohydrate Polymers,** 96, 109-117.

Putseys, J. A., Derde, L. J., Lamberts, L., Goesaert, H., & Delcour, J. A. (2009). Production of tailor made short chain amylose-lipid complexes using varying reaction conditions. **Carbohydrate Polymers,** 78, 854-861.

Sajilata, M. G., Singhal, R. S., & Kulkarni, P. R. (2006). Resistant Starch-A Review. **Comprehensive Reviews in Food Science & Food Safety,** 5, 1-17.

Shin, S. I., Choi, H. J., Chung, K. M., Hamaker, B., Park, K. H., & Moon, T. W. (2004). Slowly digestible starch from debranched waxy sorghum starch: preparation and properties. **Cereal Chemistry,** 81, 404-408.

Shin, S. I., Kim, H. J., Ha, H. J., Lee, H. S., & Moon, T. W. (2005). Effect of hydrothermal treatment on formation and structural characteristics of slowly digestible non-pasted granular sweet potato starch. **Starch/Stärke,** 57, 421-430.

Sun, S., Song,Y., & Zheng, Q. (2008). Thermo-molded wheat gluten plastics plasticized with glycerol: Effect of molding temperature. **Food Hydrocolloids,** 22, 1006-1013.

Topping, D. L., Segal, I., Regina, A., Conlon, M. A., Bajka, B. H., Toden, S. et al. (2010). Resistant starch and human health. In J. Willem van der Kamp, J. Jones, B.McCleary and David T. (eds.) **Dietary fiber: new frontiers for food and health.** Wageningen Academic Publishers, Netherland, pp. 311-322.

Tufvesson, F., Skrabanja, V., Björck, I., Elmståhl, H. L., & Eliasson, A.-C. (2001). Digestibility of starch systems containing amyloseeglycerol monopalmitin complexes. **LWT-Food Science and Technology,** 34, 131-139.

Tufvesson, F., Wahlgren, M., & Eliasson, A. C. (2003a). Formation of amylose-lipid complexes and effects of temperature treatment. Part 1. Monoglycerides. **Starch/Stärke,** 55, 61-71.

Tufvesson, F., Wahlgren, M., & Eliasson, A. C. (2003b). Formation of amylose-lipid complexes and effects of temperature treatment. part 2. Fatty acids. **Starch-Stärke,** 55, 138-149.

van der Maarel, M. J. E. C., Capron, I., Euverink, G. J. W., Bos, T., Kaper, T., Binnema, D. J., et al. (2005). A novel thermoreversible gelling product made by enzymatic modification of starch. **Starch/Stärke,** 57, 465-472.

Vasanthan, T. & Bhatty, R. S. (1998). Enhancement of Resistant Starch (RS3) in Amylomaize, Barley, Field Pea, and Lentil Starches. **Starch/Stärke,** 50, 286-291.

Zabar, S., Lesmes, U., Katz, I., Shimoni, E., & Bianco-Peled, H. (2009). Studying different dimensions of amylose-long chain fatty acid complexes: molecular, nano and micro level characteristics. **Food Hydrocolloids,** 23, 1918-1925.

Zhang, B., Dhital, S., Flanagan, B. M. Luckman, P., Halley, P. J., & Gidley, M. J. (2015). Extrusion induced low-order starch matrices: Enzymic hydrolysis and structure. **Carbohydrate Polymers,** 134, 485-496.

Zhang, B., Huang, Q., Luo, F., & Fu., X. (2012). Structural characterizations and digestibility of debranched high-amylose maize starch complexed with lauric acid. **Food Hydrocolloids,** 28, 174-181.

Zeng, F., Chen, F., Kong, F., Gao, Q., Aadil, R. M., & Yu, S. (2015). Structure and digestibility of debranched and repeatedly crystallized waxy rice starch. **Food Chemistry,** 187, 348-353.

Zeng, F., Ma, F., Gao, Q., Yu, S., Kong, F., & Zhu, S. (2014). Debranching and temperature-cycled crystallization of waxy rice starch and their digestibility. **Carbohydrate Polymers,** 113, 91-96.

,

CHAPTER II

LITERATURE REVIEWS

2.1 Starch granular structure

Starch granules are composed of two major types of polysaccharides, amylose, and amylopectin but the ratio varies regarding the botanical sources of starch. Amylose comprises primarily linear molecules with α-D-(1→4) glycosidic linkages and some of a few branches, which locates in the amorphous domains. Amylopectin is highly branched molecules with α-D-(1→4) glycosidic-linked short linear chains connected by α-D-(1→6) glycosidic linkages and form the crystalline layers. Amylopectin has a higher molecular weight than amylose (M=10^7-10^8 for amylopectin and 10^4-10^6g.mol^{-1} for amylose) (Mischnick & Momcilovic, 2010). The branch chains of the amylopectin are packed into a semi-crystalline structure of double helices in the starch granules (Jane & Pyun, 1997) (Figure 2.1). The levels of branching points are less dense and ordered (amorphous), whereas crystallinity results from clustered side chains with different lengths (Mischnick & Momcilovic, 2010).

The semi-crystalline structures of starch are separated into A-, B-, polymorphs which differ in their packing of double helices and water content (Figure 2.2). The A-type polymorphic crystallizes in a monoclinic unit cell with 4 water molecules per unit cell, which is closely packed and found in cereal starches. In contrast, the B-type polymorphic crystallizes in a hexagonal unit cell, which is relatively loosely packed with an open channel of 36 water molecules in the unit cell, found in many tuber

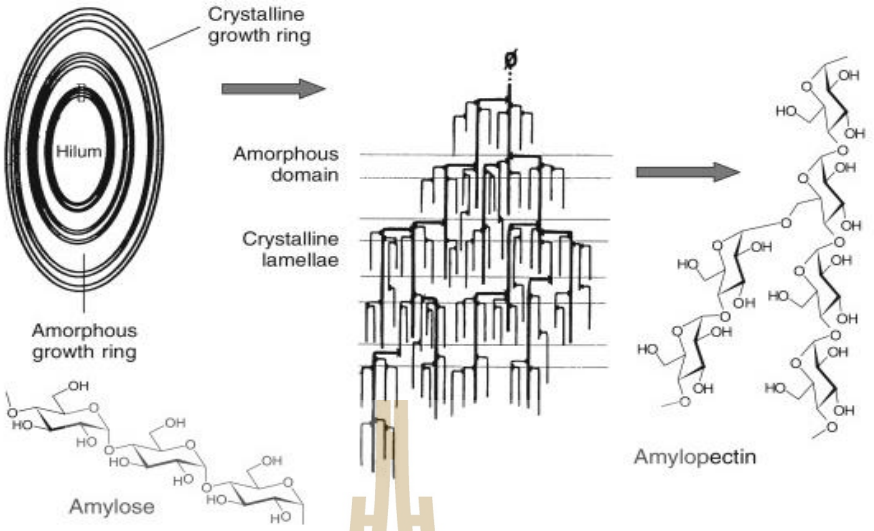

Figure 2.1 Starch granular structure (Reproduced from Mischnick & Momcilovic, 2010).

starches and in high amylose starches (Imberty, Buléon, Tran, & Péréz, 1991). The C-type polymorph is a mixture of A- and B-type polymorphs, which found in legume starches and some tuber starches. In addition, single helices of amylose, which are co-crystallized with other compounds such as iodine, DMSO, alcohol or fatty acid (Sajilata, Singhal, & Kulkarni, 2006), is considered as the V-type polymorph. The different crystalline polymorphs of starch have been identified based on X-ray diffraction patterns and illustrated in Figure 2.3.

The branching points of the B-type polymorphic amylopectin are mostly located in the amorphous regions, whereas the branching points of the A-type counterpart are scattered in both amorphous and crystalline regions (Jane & Pyun, 1997). As a result of the A-type starch granules show more pinholes on the surface and serpentine-like channels inside the granules than the B-type starch granules (Fannon, Hauber, BeMiller, 1992; Huber & BeMiller, 2000), the A-type starch

granules are easily hydrolyzed by enzyme than the B- and some C-type starch granules.

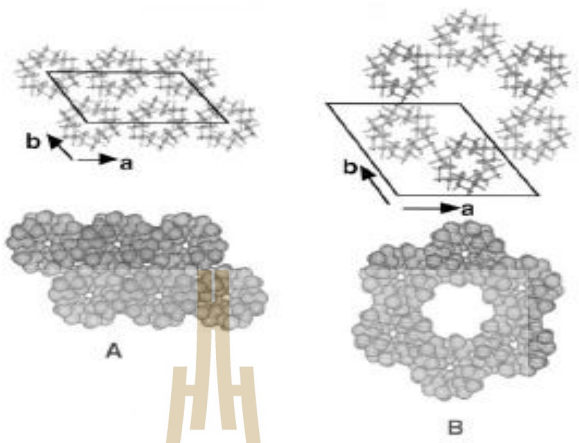

Figure 2.2 A- and B-type polymorphs of amylose (Buléon, Colonna, Planchot, & Ball, 1998).

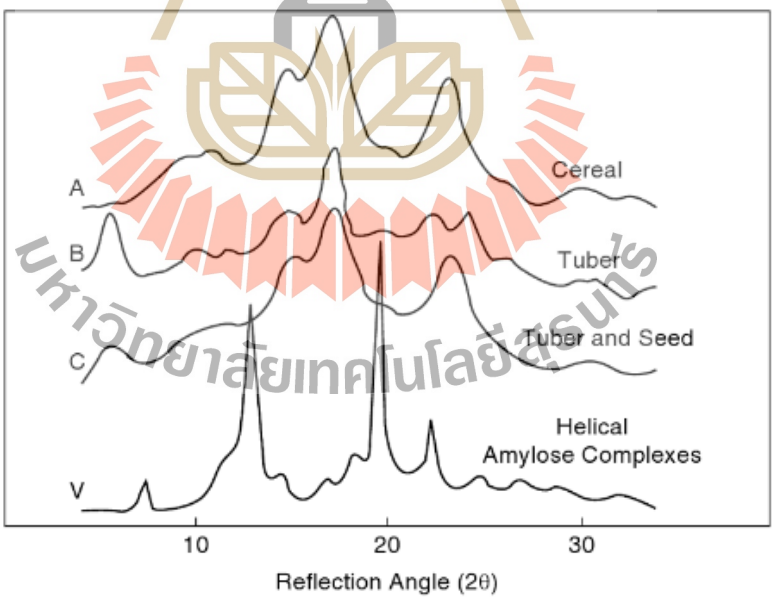

Figure 2.3 X-ray diffractogram of different starches. Labeling refers to (A): A-type from cereal starches, (B): B-type from tuber starch, (C): C-type from seed starches, and (V): V-type from helical amylose complexes (Reproduced from Zobel, 1988).

2.2 The gelatinization and retrogradation of starch

Starch gelatinization is an irreversible process that occurs when starch was heated in a presence of enough water. During heating, the water acts as a plasticizer, is first absorbed in the amorphous regions, leading to granular swelling. This provides sufficient stress connectivity of amorphous regions to tightly bound areas of double helical structures of amylopectin, resulting in the disruption of starch crystallites. The soluble amylose molecules leach into the surrounding water and the granule structure disintegrates, as evidenced by the loss of birefringence under the microscope in polarized light (Jenkins & Donald, 1998). Normally, differential scanning calorimetry technique is used to observe this endothermic gelatinization phenomenon. The gelatinization temperature of starch is generally dependent on the starch source and amylose content.

Starch retrogradation or recrystallization is a physical process that follows starch gelatinization in which starch molecules (both amylose and amylopectin) can re-associate to form ordered structures of double helices and crystallites during cooling and/or storage. The typical conformation changes of amylose during retrogradation are illustrated in Figure 2.4. In general, amylose in aqueous solution exists as a random coil. When cooling and storage, amylose can re-crystallize into either A- or B-type double helices which are a spontaneous process. The metastable state with lower free energy occurs. Then, the double helices are infinitely aggregated to form a three-dimensional network with different microstructure features, i.e. crystallinity and porosity (Zhang et al., 2015). The storage time and temperature are critical factors influencing the formation of retrograded starch in an excess water. Normally, the crystallization of starch which is a partially crystalline polymer system is governed by

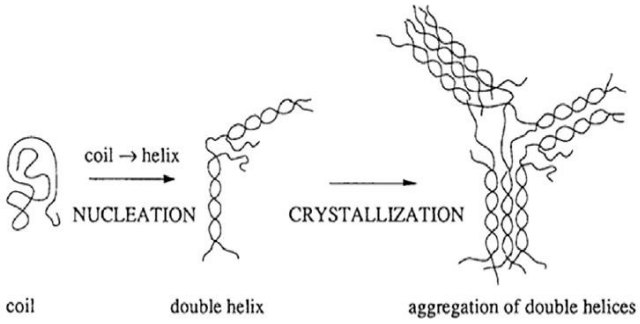

Figure 2.4 Conformational changes occurring during retrogradation (Colonna, Leloup, & Buleon, 1992).

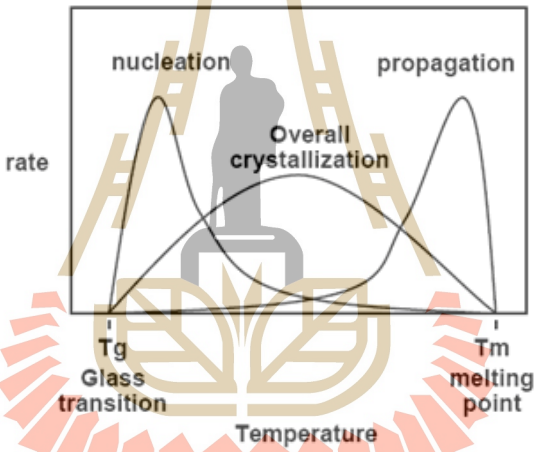

Figure 2.5 Temperature dependence of the nucleation, propagation, and overall crystallization rates according to partially crystalline polymer system (Eerlingen, Crombez, & Delcour, 1993a).

glass transition temperature (T_g) and melting temperature of crystal (T_m). The crystallization comprises three steps, including nucleation, propagation, and maturation. The nucleation rate is favored at a temperature near the T_g whereas a higher temperature closed to T_m favored the propagation rate. The maturation rate is

dependent on temperature similar to that of propagation rate. The overall recrystallization rate depends mainly on the nucleation and propagation rates (Figure 2.5). For partially crystalline polymer system, crystallization occurred only at a temperature between glass transition temperature (T_g) and melting temperature of crystal (T_m) (Levine & Slade, 1998).

2.3 The nutritional classification of starch

For nutritional characteristics, starch is classified into rapidly digestible starch (RDS), slowly digestible starch (SDS) and resistant starch (RS), according to the rate of glucose release and its absorption in the gastrointestinal tract (Englyst, Kingman, & Cummings, 1992). In a recent physiological classification, the fractions RDS and SDS are grouped as glycemic or available carbohydrates, whereas RS is regarded as a non-glycemic carbohydrate (Cummings & Stephen, 2007; Englyst, Liu, & Emglyst, 2007).

2.3.1 Rapidly digestible starch (RDS)

RDS is the fraction of starch that causes a sudden increase in blood glucose level after ingestion (Cummings, Beatty, Kingman, Bingham, & Englyst, 1996). Normally, it consists mainly of amorphous and dispersed starch. *In vitro* experiment of Englyst et al. (1992), it is converted to the glucose molecules in 20 min of enzyme digestion. RDS is found in freshly cooked starchy foods such as mashed potatoes and bread. In this case, starch granules are gelatinized and are more accessible to enzymatic digestion. The rapid increases in blood glucose and insulin levels caused by RDS contribute to several health complications, such as diabetes and cardiovascular disease (Brennan, 2005).

2.3.2 Slowly digestible starch (SDS)

SDS is a starch fraction that is completely digested in the small intestine at a lower rate as compared to RDS. Therefore, the potential health benefits of SDS are linked to a stable glucose metabolism, diabetes management, mental performance, and satiety (Lehmann & Robin, 2007). The benefit of products rich in SDS is their moderate impact on the glycemic index (GI). Normally, GI is often used as a measurement of the level postprandial glucose in the food, which can assess the effects of certain food or glucose.

2.3.2.1 The structure and formation of SDS

As mentioned that starch granules have a complex and highly ordered semi-crystalline structure. At the molecular level, the crystalline structure and the packing of the amorphous phase influence the enzymatic susceptibility. The A-type starch with shorter double helices are more readily digestible and show a high amount of RDS and SDS compared to B-type starches, which often contain a high amount of RS (Jane & Pyun, 1997). Generally, tuber starches are more resistant to enzymatic hydrolysis than cereal starches due to a higher granule surface, their surface properties, the channel in cereal starches and the supramolecular arrangement (Letmann et al., 2007). Guraya, James, & Champagne et al. (2001) reported that the SDS fraction of debranched waxy rice starch might result from the formation of imperfect B-type crystallites with lower density, which are more prone to digestion. Moreover, the study of Shin, Kim, Ha, Lee, & Moon (2005) also confirmed that the SDS fraction of debranched waxy sorghum starch might consist of less perfect crystallites and amorphous components. Chung, Lim, & Lim. (2006) described that the proportion of SDS depends mainly on the rigidity of the amorphous regions in the

retrograded starch gel. Zhang, Ao, & Hamaker (2006) studied on the slow digestion property of native cereal starches and proposed that the densely packed of amorphous regions and arranged tightly to the crystalline regions may inhibit a susceptible of an enzyme to hydrolysis.

The formation of SDS involves the step of gelatinization, debranching and retrogradation process similar to the RS formation. More recently, the production of SDS based on physical, chemical, and enzymatic treatments has been reported. According to Guraya et al. (2001), SDS formation was most favored with partial debranching of starch. In 2003, Shi, Cui, Birkett, & Thatcher patented the technology to produce SDS by using enzymatically debranching amylose-containing starches and followed by recrystallization to a highly crystalline form. In addition, Shin et al. (2004) observed an increase in SDS up to 22% in cooked waxy sorghum starch after debranched with isoamylase. Moreover, SDS was also efficiently generated by hydrolysis of starches with α-amylase and followed by partial crystallization of the resulting linear chains (Hamaker & Han, 2004). Hydrothermal treatment has been used to enhance the formation of SDS. According to Niba (2003), the SDS yield of cocoyam, maize, potato and rice flour was increased after heat treatment as compared to the raw flour. The storage at room temperature significantly decreased SDS content, whereas frozen storage increased the SDS yield for maize, potato and yam flours. The heat-moisture treated rice starch showed a slower digestion pattern than that for the native starch (Anderson, Guraya, James, & Salvaggio, 2002). Furthermore, Shin et al. (2005) reported that hydrothermal treatment could be increased the SDS content as compared to the raw starch.

2.3.3 Resistant starch (RS)

RS is defined as the sum of starch and products of starch degradation not absorbed in the small intestine of healthy individuals (EURESTA, 1992). Since it is escapes digestion in the small intestine. A number of physiological effects have been attributed to RS, which are the prevention of colonic cancer, hypoglycemic effects, hypocholestrolemic effects, prebiotic, inhibition of fat accumulation, and mineral absorption (Ashwar, Gani, Shah, Wani, & Masoodi, 2016). The product of the fermentation by human colonic bacteria is short-chain fatty acids (SCFA) such as acetate, butyrate, propionate and gasses, CO_2, H_2 and CH_4 (Topping et al., 2008). However, butyrate plays an important role in suppressing tumor cells and decreasing the proliferation of colonic mucosal cells.

2.3.3.1 The classification of RS

According to the mechanism that prevents the enzymatic digestion, RS can be categorized into four types (Englyst et al., 1992). RS type I represent physically inaccessible to pancreatic α-amylase, which is entrapped within whole or partly milled grains or seeds. RS type II is a native granular starch found in food containing uncooked starch (i.e. green banana starch, potato starch, and high amylose maize starch). RS type III (RS3) comprises of retrograded starch formed during processing. RS type IV (RS4) is a group of chemically modified starches such as oxidized starch and cross-linking starch. However, in recent year, amylose-lipid complexes was added to the list of RS as RS type V (RS5), which is the inclusion complexes form between starch and lipids (Topping et al., 2010).

2.3.3.2 The structure and formation of RS3

RS3 is considered as a retrograded starch, which precipitated

from starch pastes or gels after gelatinization and cooling/storage. Some parts of RS3 undergo enzymatic hydrolysis. However, the major part typically behaves resistance to the hydrolysis of amylolytic enzymes. Eerlingen, Deceuninck, & Delcour, (1993b) proposed two possible models of RS3 formation in aqueous amylose solutions, which were micelle form and lamellar structure (Figure 2.6). For the micelle form, it was formed by aggregation of a number of different molecules over a particular region of the chain in an ordered structure interspersed with an amorphous region. In the case of retrograded amylose, the micelles must be composed of double helices in a hexagonal structure to show a B-type of X-ray diffraction pattern. The folding of the polymer chain led to two-dimensional structures or lamellar shapes. The regions of the folding were amorphous whereas the center of the lamella was crystalline. It demonstrated that hydrolysis with amylolytic enzymes could remove these folding regions, and the molecules with short chain were obtained.

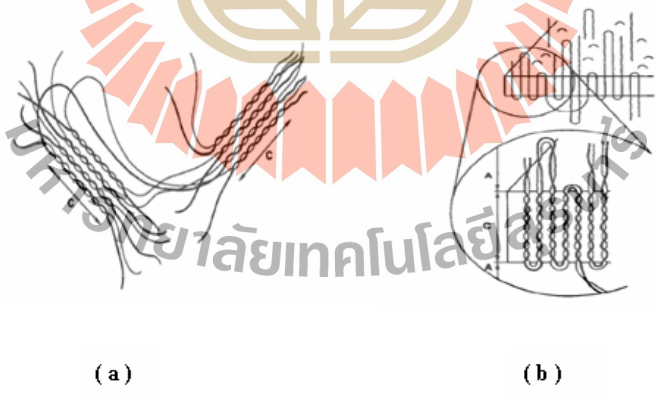

Figure 2.6 Micelle model (a) and Lamellar model (b) for the formation of resistant starch in amylose solutions (Adapted from Eerlingen et al., 1993b).

RS3 is formed when the linear glucans of gelatinized starch retrogrades by realigning into double helical strands, and then aggregation thereafter

(Eerlingen & Delcour, 1995). It is known that amylose content was correlated to RS3 yield (Sievert & Pomeranz, 1989). The long-branch chains of amylopectin have properties similar to amylose, which increase the apparent amylose content of the starch. On the contrary, the short-branch chains of amylopectin form double helices that are not long enough to produce stable crystallites.

RS3 contains mainly retrograded amylose (Eerlingen et al., 1993a) which consists of short linear segments of α-1,4-glucans arranged in a crystalline structure. Thus, starch with large amounts of amylose and/or long branch chains of amylopectin, such as legume and high-amylose starches (high amylose maize starch), has been widely used as a starting material to produce RS3 over the last decades (Sievert & Pomeranz 1989; Vasanthan & Bhatty 1998), which is expensive. Many technologies have been developed to produce RS3 from a group of amylose-containing starches, including repeated cycles of autoclaving and heating together with complete debranching. Due to the interference of amylopectin during amylose retrogradation, debranching enzymes, such as isoamylase and pullulanase was applied to hydrolyze α-D-(1→6) glycosidic branching of amylopectin in order to produce linear molecules that can re-associate, leading to decreasing the susceptible to hydrolysis with amylolytic enzymes. The mild acid hydrolysis of starch is another method to increase the linear chains as well. It hydrolyzes the amorphous regions of the starch granules where the branching points of amylopectin are mostly located, then promoting amylose retrogradation (Vasanthan & Bhatty, 1998; Guraya et al., 2001). According to Mutungi et al. (2011), the acid treatment of cassava starch before debranching process increased the fraction of linear glucan comprising DP 13-30, resulting in the improvement of RS3 content. Schmiedl, Báuerlein, Bengs, &

Jacobasch. (2000) reported that DP of chain length about 20-35 was optimal for the formation of RS3 with a high yield and enhanced thermal stability.

The retrogradation or recrystallization conditions also affected the RS3 formation. An increase in starch concentration could increase the RS3 content (Lehmann, Jacobasch, & Schmiedl, 2002; Schmiedel, Konig, & Jacobasch, 2003). With respect to storage temperature, Eerlingen et al. (1993a) found that isothermal formation of RS3 is favored at 100°C while Eerlingen (1994) reported that incubation at a lower temperature and extended periods of time also produced a higher RS3 yield. A higher temperature generally favored the formation of the more stable A-type rather than B-type starch polymorph (Gidley & Bulpin, 1987). Temperature cycle aging is another method was applied to accelerate the retrogradation and to improve the thermal properties of starch. This method involves a series of temperature and time to induce retrogradation. Haynes et al. (2000) demonstrated that the production of particularly thermostable RS3 with peak temperature above 140^{o}C was induced by temperature cycling. The nucleation temperature was 60^{o}C and the propagation was 120^{o}C and was produced RS3 with 35% total dietary fiber (TDF). In 2007, Leong et al. demonstrated that the debranched sago starch subjected to temperature cycling and incubation at a series of temperature and time could induce the yield of RS3. Besides, Park, Baik, & Lim. (2009) found that storage of gelatinized waxy maize starch at the cycled temperatures of 4^{o}C and 30^{o}C induced a greater amount of RS3 and reduced the *in vitro* glycemic index more effectively than the isothermal storage condition at 4^{o}C. Furthermore, the starch crystal formed under temperature-cycled storage melted at a higher onset temperature (T_o) than those formed at isothermal storage.

The crystalline polymorphic structures of starch are distinguished from each other by a number of characteristics and properties such as crystallization temperature, molecular structure and amount of bound water where the diversity of polymorph has more influence on thermal and functional properties of RS3. The physical modification by hydrothermal treatments, namely annealing and heat-moisture treatment (HMT) is used to modify the structure of starch because it is consistent with society trends toward natural products and offers the potential to change starch functionality at a low cost and environmental friendly way. Moreover, it also showed an impact on the RS3 formation. According to Jacobasch, Dongowski, Schmiedl, & Müller-Schmehl, (2006) studied the effect of hydrothermal treatment of novelose 330 (commercial RS3) on the yield and prebiotic properties, They found an increase in the yield of RS3 after subjecting to annealing and HMT up to 75% (as measured by *in vitro* method of Englyst et al., 1992) with peak temperature above 120^{o}C. HMT provides a method for the economical production of a high-quality RS3 with dominated prebiotic properties in the distal colon for the health-promoting application. Furthermore, the study of Muntungi, Rose, Onyango, Jaros, & Rohm (2009) showed that time-temperature cycling aging at a temperature of 120/60^{o}C of debranched cassava starch further subjected to HMT increased RS3 content up to 88% and its melting temperature was also improved.

2.3.3.3 The structure and formation of RS5 (amylose-lipid complexes)

Generally, amylose-lipid complexes occur during HMT, especially during gelatinization of starch with naturally containing lipids or when lipids such as certain emulsifiers, are added to defatted starch or pure amylose free of

natural lipids. Both naturally occurring and heat formed complexes results in the significant changes of glucan properties, including a decrease in amylose solubility and swelling, higher gelatinization temperature, and retardation of retrogradation during storage.

The complexes formation started with amylose change from the coil to single left-handed helices structure and lipid molecules enter the central cavities of amylose helices, resulting in partially crystalline amylose structure or V-amylose. The polar head of lipid is located at the outer surface of the helix, whereas its aliphatic chain situated in the helix cavity with the methyl end groups facing each other (Figure 2.7). The amylose helix is hydrophilic on the outside while the internal cavity is lined with methylene groups and glucosidic oxygen, favoring the formation of hydrophobic interaction. The numerous intra-and interhelical such as van der Waals forces and hydrogen bonds stabilized consecutive turns of helices. However, van der Waals forces are possible only between methylene groups of lipid and hydrogen of carbon five in glucose (Karkala, Ma, Morrison, & Pethrick, 1995). The investigation of Godet, Tran, Delage, & Buléon, (1993) by computer modeling and solid state ^{13}C NMR exhibited that the polar carboxyl group of fatty acid and the glycerol group of monoacylglycerols do not enter the hydrophobic cavity due to the steric and electrostatic repulsions. This limits helical segment lengths to two fatty acids or monoacylglycerol molecules situated with their terminal methyl groups end-to-end. Moreover, Godet et al. (1995b) proposed that the acyl chains of fatty acid are included in crystalline areas and the carboxylic groups in amorphous areas. The aliphatic molecules with small head groups are spatially less demanding than -COOH groups fit smoothly into V-channels. The inner diameter of amylose helix is controlled by the

size of the complexing agent. For lipids, it forms complexes with six glucose residues per turn with an inner diameter of 0.48 nm (Putseys, Derde, Lamberts, Goesaert, & Delcour, 2010).

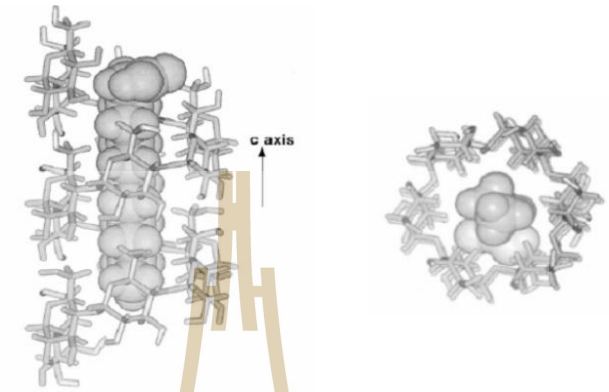

Figure 2.7 Molecular modeling representation of amylose-fatty acid complexes showing the inclusion of the aliphatic part (C12) of the fatty acid inside the hydrophobic cavity of the amylose single helix (Buléon et al., 1998).

The amylose-lipid complexes exist in two polymorphic forms, types I and II depend on the complexing and dissociation temperature (Zhang, Huang, Luo, & Fu, 2012) (Figure 2.8). The formation and characteristics of amylose complexes with various lipids have been studied extensively in a function of complexation temperature and duration of complexation time. Several studies revealed that the dissociation temperature of amylose-lipid complexes was increased with the complexation temperature (Karkalas et al., 1995; Tufvesson, Wahlgren, & Eliasson, 2003a and 2003b; Zabar, Lesmes, Katz, Shimoni, & Bianco-Peled, 2009). At lower temperature ($\leq 60^{o}$C), type I complexes is formed, whereas type II complexes are obtained at a higher temperature ($\geq 90^{o}$C). Type I polymorphs is considered to be amorphous structure and dissociates at lower temperatures ($<100^{o}$C). Since it occurs at

low complexation temperatures (≤60°C), the nucleation rate is very high and amylose helices 'freeze' rapidly in a structure with a little crystallographic order (Biliaderis & Galloway, 1989). In contrast, Type II polymorphs are believed to have a lamellar-like organization of amylose complexes to form a semi-crystalline structure and yield at higher complexation temperatures (≥90°C). At this temperature, the nucleation rate is slow and followed by crystal growth (Biliaderis & Galloway, 1989). Type II polymorphs are divided into type II_a and II_b based on the degree of crystallinity and/or perfection of the ordered domains. Type II_b complexes have a slightly higher melting temperature than type II_a complexes but both are above 100°C (Seneviratne & Biliaderis, 1991). In order to produce type II, type I is partial melting at the appropriate temperature, which appears to promote crystalline formation and thickening by chain diffusion (Tufvesson et al., 2003a).

Figure 2.8 The generalized mechanism for amylose-lipid complex formation into Type I and Type II complexes (Reproduced from Biliaderis & Galloway, 1989).

2.4. Enzymatic modification of starch with amylomaltase and debranching enzyme

2.4.1 Starch modification with amylomaltases enzyme

Amylomaltases (AM, EC 2.4.1.25) are an intracellular enzyme of 4-α-glucanotransferases (4αGtase) family, which belongs to α-amylase super-family based on the catalytic, substrate specificity, and sequence homology. It shows multiple action modes which are disproportionation, cyclization, coupling, and hydrolysis reaction (Fujii et al., 2005). However, the unique action modes of AM depends on the species of microorganisms. AM catalyzes the reversible intermolecular transglycosylation reaction in which one α-1,4-glucan is transferred to another or to glucose, which called a "disproportionation reaction" as shown in Figure 2.9a. This intermolecular transglycosylation is readily reversible. In addition, most of AM also catalyzes an intramolecular transglycosylation reaction which called a "cyclization reaction". This reaction, a single linear glucan (amylose) were used as substrates, resulting in a production of cyclic glucan termed cycloamylose (CA). Furthermore, AM also catalyzes the reverse reaction of cyclization, in which cycloamylose is opened by the enzyme and a linearized fragment is transferred to an acceptor. This reaction called "coupling reaction" (Figure 2.9b). Besides transglycosylation activity, this enzyme also shows a minor hydrolytic activity as presented in Figure 2.9c. However, the hydrolytic activity of AM is not significant (van der Maarel et al., 2005). The ratio of hydrolytic to transglycosylation activities differs among enzymes. Nevertheless, the disproportionation reaction is by far the dominating for the AM from *Thermus thermophillus* (Van der Maarel et al., 2005; Kaper, et al., 2005).

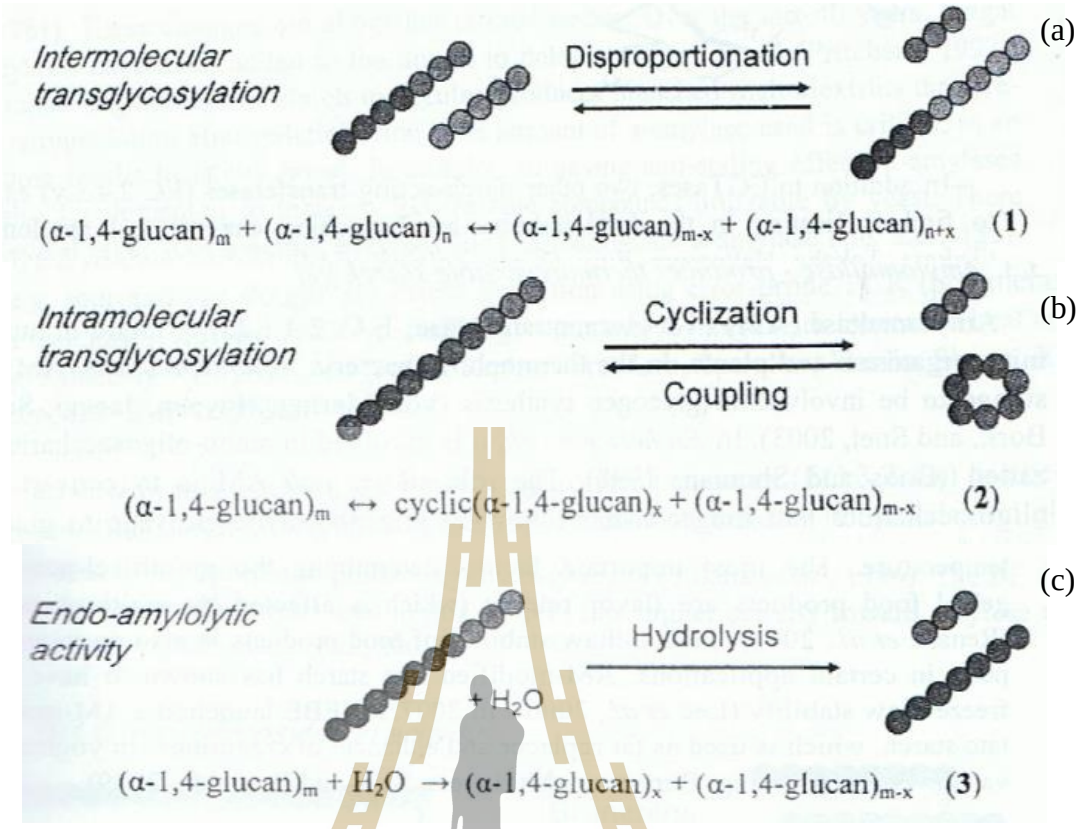

Figure 2.9 The action mode of AM including, intermolecular transglycosylation reaction catalysis (a), intramolecular transglycosylation reaction catalysis (b), and endo-amylolytic reaction catalysis (c) (Hansen, Blennow, Pedersen, Norgaard, & Engelsen, 2008).

This enzyme has been found in many hyperthermophilic organisms, with varying degree of substrate specificities, and is also known as the disproportionating enzyme (D-enzymes) in plants. In microorganisms, they are either involved in maltose metabolism or in the synthesis/degradation of glycogen but, in plants, D-enzymes have a function in starch metabolism. However, the exact function is less clear (Critchley, Zeeman, Takaha, Smith, & Smith, 2001). Most of the work on AM and D-enzyme has been carried out with maltooligosaccharides (Terada, Fujii, Takaha, &

Okada, 1999) due to they are effective donors. The major units transferred from the donor molecule were glucosyl or maltosyl groups (Przylas et al., 2000). The products formed by the action of AM are various and heterogeneous due to the reversibility of the enzymatic reactions. Furthermore, AM originating from various species have more or less unique activities of disproportionation and cyclization (Cho et al., 2009)

For the application in the food industry, AM can be used for the production of thermoreversible starch gels with gelatin-like properties (Lee, Kim, Park, & Lee, 2006; van der Maarel, 2005; Kaper et al., 2005) and cycloamylose (CA) (Bhuiyan, Kitaoka, & Hayashi, 2003; Terada et al., 1999), which are both of commercial interest. The thermoreversible gelling derivative, which is marketed under the trade name Etenia™ by AVEBE of The Netherlands (Euverink & Binnema, 1998) are produced from *thermals thermophilus*. For the CA production, the different size of CA can be generated, depending on the species of microorganisms. For example, AM from *Aquifex aeolicus* produced the smallest CA with DP 16 whereas AM from *Thermus aquaticus* produced the smallest CA with DP 22 (Bhuiyan et al., 2003). Terada et al. (1999) reported that the CA structure with DP26 consists of two short, left-handed amylose helices in an anti-parallel arrangement. Along the axis of the helices runs a hydrophobic channel which can form complexes with hydrophobic guest molecules. As a result, cycloamylose is used as artificial chaperones that help with the proper folding of heterologously produced proteins/enzymes (Machida et al., 2000). Another application of AM is the production of resistant starch (RS) by the sequential use of AM and a debranching enzyme such as pullulanase that claimed in some patents (Harris, 2008; Richmond et al., 2008; Norman, Pedersen, Stanley, Stanley, & Richmond, 2007). The debranched products consist of linear

maltooligosaccharides of such a degree of polymerization in that they form crystallites. These crystallites are inaccessible by salivary and pancreatic α-amylases and thus end up in the large intestine. The AM of hyperthermophilic organisms have an intrinsic stability, which allows for its use above 70°C, a temperature necessary to dissolve the starch completely.

The activity of AM on starch was investigated on various starches (waxy corn starch, waxy rice starch, corn starch, rice starch, potato starch, high amylose potato starch, pea starch and wheat starch) as a substrate (Do et al., 2012; Cho et al., 2009; Hansen, Blennow, Pedersen, &. Engelsen, 2009; Hansen et al., 2008; van der Maarel et al., 2005). After AM treatment, the hydrolyzed products consisted of amylose fragments, cycloamylose, and small amylopectin clusters, including the association of the modified amylopectin cluster reorganized by hydrolysis and disproportionation (Park et al., 2007; Lee et al., 2006; Takaha, Yanase, Takaha, Okada, & Smith, 1998). Hansen et al. (2008) proposed the action of AM on starch as illustrated in Figure 2.10. Such structures can be formed through disproportionation of entire amylopectin cluster units or reorganization of clusters (Figure 2.10A) and/or transfer of long chains on the same molecule (Figure 2.10B) as proposed by Takaha et al. (1998). Moreover, linear amylose is cleaved and then the cleaved fragment is transferred to amylopectin resulted in the increasing of longer chains (Figure 2.10C). In addition, as proposed by Takaha et al. (1998), AM also is capable of catalyzing intramolecular transglycosylation, and the formation of cyclo-amylopectin clusters could also occur as shown in Figure 2.10D.

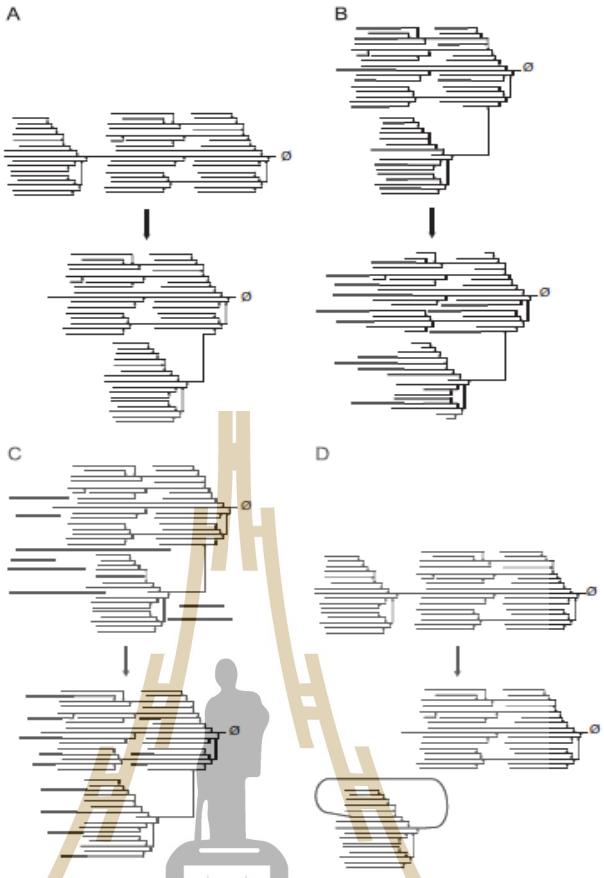

Figure 2.10 Schematic action for AM on starch. Disproportionation of amylopectin cluster (A), disproportionation of α-glucan chains within amylopectin (B), disproportionation of α-glucan segments from amylose to amylopectin (C) and cyclization of amylopectin (D). Gray bars in B illustrate glucan chains being transferred. Black bars in C illustrate amylose molecules. The linear lines indicate α-1,4-D-glucan segments, whereas vertical arrows within the structure indicate α-1,6-glycosidic linkage. ø: non-reducing end. The cluster model of amylopectin is adapted from Hizukuri (1986) (Hansen et al., 2008).

After modification with AM, the side chain length distribution of amylopectin was broadened, which consisted of both shorter and longer chains (van der Maarel et al., 2005), resulting from the action of AM to catalyze the disproportionation reaction via intermolecular transglycosylation. In addition, AM has been noted for its action of degrading starch components into smaller molecules with a range of polymodal distributions (Cho et al., 2009; Lee, Oh, & Yoo, 2009; Park et al., 2007). AM-modified starch showed thermoreversible gelation property with gelatin-like properties which increasing T_p and ΔH as compared to their parent samples (Hansen, Blennow, Pedersen, &. Engelsen, 2009). The most reasonable explanation for the increasing T_p during AM-treatment is that the newly formed longer chains in amylopectin molecules exhibit an amylose-like behavior. The increase of longer chains results in a higher content of longer double helices formation becoming more heat resistant. Therefore, AM could be used to modify the starch structure to obtain the desired products. However, the products and their properties depend on the source of AM, the substrate, and the treatment conditions.

2.4.2 Starch modification with debranching enzyme

Debranching enzymes belong to the group of α-amylase which are categorized into direct debranching enzymes and indirect debranching enzymes. Isoamylase and pullulanase are a group of direct debranching enzymes, which widely used to cleave the branching points, or α-1,6-linkages of starch both amylose-containing starch and waxy starch (Hizukuri, Abe, & Hanashiro, 2006; Manners, 1989). Isoamylase attack more readily the large molecular size polymer, in contrast, pullulanase show preferential activity against α-limit dextrin, and its activity is retarded against large molecular weight glucans (Mutungi et al., 2009). After

debranching, the resulting products contain a mixture of long and short linear chains or short linear side chains, depending on starting materials. For an amylose-containing starch, the debranching produce a mixture of long and short linear chains, whereas short linear side chains from amylopectin were released after debranching of waxy starch (Shi, Capitani, Trzasko, & Jeffcoat, 1998). From these result, many patents have applied the debranching techniques to produce resistant starch (RS) (Chiu, Henley, & Altieri, 1994; Gross & Haralampu, 1999; Haralampu & Gross, 1998; Kettlitz, Coppin, Roper, & Bornet, 2000; Shi, Cui, Birkett, & Thatcher, 2006) and slowly digestible starch (SDS) (Shi, Cui, Birkett, & Thatcher, 2005a; Shi, Cui, Birkett, & Thatcher, 2005b). There are several factors affecting the properties of debranched starch, e.g. amylose content and MW distribution of starting starch, the degree of debranching, type of debranching enzyme used, and crystallization conditions such as solids content, temperature, time, and type. According to Berry (1986) reported that after debranching of starch with pullulanase, the linear fragments liberated contributed to a high RS3 yield formation. Furthermore, Guraya et al. (2001) revealed that a high debranching enzyme concentration and longer time accelerated the production of RS3 of rice starch. In the study of Cai & Shi (2010) demonstrated that debranched waxy potato starch, which contained a higher average chain length, resulted in a higher yield of crystallized product with stronger crystalline structure, higher peak melting temperature, and higher RS3 content.

2.5. Physical modification of starch

2.5.1 Hydrothermal treatments

Hydrothermal treatments, namely annealing and heat-moisture treatment

(HMT) which are widely used to modify the physicochemical properties of starch, while maintaining its granular structure and birefringence. Annealing is treatment which is conducted in the presence of excess water (>60% w/w) or at intermediate water content (40-45% w/w) for a certain time period at a temperature above the T_g but below the onset (T_o) temperature of gelatinization (Tester & Debon, 2000). The conformation changes during annealing have been proposed by Perry & Donald (2000) and Waigh, Jenkins, & Donald (1996) in which the double helices of the unhydrated form of starch are intact, but are not arranged regularly side by side, which is called a nematic, collapsed or a withered state. During annealing, the amorphous regions of the granular starch are hydrated, leading to increasing the mobility of the amorphous regions. This hydration of the granule limited but reversible granule swelling, allowing mobility of crystalline domains. This dynamic nature allows limited side by side movement of the double helices (Perry & Donald, 2000; Waigh et al., 2000), resulting in the formation of a smectic-type structure. Additionally, Jayakody & Hoover (2008) proposed the two models of annealing process in semi-crystalline polymers as "sliding diffusion" and "complete or partial fusion". The sliding diffusion relates to the moving of complete molecular sequences within a crystalline lattice, whereas complete or partial fusion relates to the crystal and subsequence re-crystallisation of the melted materials at the annealing temperature. The initially weaker or imperfect crystallites gradually decreased with the progress of annealing due to fusion and re-crystallization, leading to the formation of more perfect crystallites (Jayakody & Hoover, 2008) with higher melting temperature. The crystalline perfection on annealing may suggest by: (1) larger crystal formation from smaller crystals, (2) a change of crystal shape, (3) a change in direction of crystal

growth, (4) orientation of crystallites, (5) interactions between crystallites, and (6) changes within the amorphous regions (Stute, 1992). After annealing, the physicochemical properties of starch are changed, e.g. improving its crystalline perfection, increased granule stability, facilitating interaction between starch chains within the amorphous and crystalline domains of the granule, formation of double helices, increased gelatinization temperatures, narrowing of the gelatinization temperature range, decreased granular swelling, decreased amylose leaching, and decreased formation of RS. However, the crystallinity, amylose-lipid interactions, and susceptibility towards acid and enzyme hydrolysis are shown to increase, decrease or remain unchanged upon annealing depending on the starch source (Jacobs & Delcour, 1998; Tester & Debon, 2000).

HMT is one of the physical modification in which starch granules are subjected to lower moisture levels than that required for gelatinization (usually in a restricted range of 10-30% at a temperature above T_g but below gelatinization temperature for several times (Jacobs & Delcour, 1998). HMT enhanced the disruption the crystalline structure and dissociating the double helical structure in the amorphous regions, leading to promotes the interaction of polymer chains and the rearrangement of the disrupted crystalline (Gunaratne & Hoover, 2002). Therefore, it changes the starch structure and its properties but depends on the starch source, amylose content and treatment conditions. For instance, HMT improved the crystalline perfection of potato starch by changes the crystalline pattern from B- to A-type (Gunaratne & Hoover, 2002). Moreover, The raising of onset (T_o), peak (T_p), and conclusion gelatinization temperature (T_c) of starch was found in potato, cassava, and true yam starches after increased heat and moisture content during HMT. It was

attributed to the structural changes within starch granules, involving the interaction between amylose-amylose and amylose-lipid (Hoover & Vasanthan, 1994). As a result of the crystalline disruption and dissociating the double helical structure in the amorphous regions after HMT, the accessibility of α-amylase within the granules are facilitated. Therefore, the enzymatic susceptibility of starch increased with HMT. However, the increase in SDS and RS content were reported in previous studies (Niba, 2003; Chung, Liu, & Hoover, 2009). They suggested that some interactions formed during HMT restricted the enzyme accessibility to hydrolysis.

2.5.2 Extrusion cooking

Extrusion cooking is a common processing for producing many kinds of food such as breakfast cereals, snack food, and pasta products. Since the extrusion of cereal based products has low cost, short time, high productivity, versatility, unique product shapes, and energy savings, it has advantages over other usual processing methods (Faraj, Vasanthan, & Hoover, 2004). Extrusion involves the application of high heat, high pressure, and shear forces to an uncooked mass, promoting the structural changes of starch such as gelatinization, melting, degradation and fragmentation (Lai & Kokini, 1991). During extrusion, molecular, supramolecular and granular structures of starch are disrupted by various parameters such as thermal (barrel temperature), humidity (plasticizer content) and energy input (e.g., screw speed, feeding rate, die size and screw configuration), leading to increasing the accessibility of degrading enzymes to starch polymers in extruded products (Zhang et al., 2015). The ordered structures of starch and double helices are damaged by high shearing within the extruder. Moreover, the larger molecules of amylopectin especially, outer branches are also degraded (Liu, Halley, & Gilbert, 2010). The

previous studies reported a decrease in the RS content (or increased digestibility) after extrusion which resulted from the destruction of a granular structure due to thermal treatment, high pressure and shear forces of the process (Vasanthan & Bhatty, 1998; Wolf, 2010). However, an increase in RS content after extrusion was also found. According to Huth, Dongowski, Gebhardt, & Flamme, (2000), an increase in RS up to 6% was found in barley extrudates which further freeze-stored after extrusion. A number of extrusion parameters e.g. feed moisture, feed rate, barrel temperature, screw speed, a diameter of the die nozzle and storage conditions are known to affect the RS content of extrudates. Desirable properties of the extruded product are obtained by varying the processing conditions as well as the composition of raw material. According to Kim, Tanhehco, & Ng, (2006), increasing extrusion feed moisture and storage periods resulted in the significant increase of RS contents because moisture acts as a plasticizer for the retrogradation of starch. With respect to the barrel temperature of extrusion, the study of González-Soto et al. (2006) revealed that at 100ºC and the specified moisture contents induced starch fragmentation, leading to the formation of amylose chains (with reduced degree of polymerization) that could be incorporated into the crystalline structure of RS3. Moreover, the shearing action of extruder screw at a high barrel temperature may have caused degradation of longer amylose chain into small molecular fragments that could be incorporated into a crystalline structure of RS3 (Eerlingen et al., 1993b; Gidley et al., 1995). Extrusion cooking also affects the crystalline structure of the starch. For example, an extreme condition of extrusion (35% moisture, 140°C, $750s^{-1}$) resulted in some crystallinity of single helical V-type whereas mild condition of extrusion (50% moisture, 100°C, $150s^{-1}$) gave B-type crystalline structure which was determined by XRD (Chanvrier et

al., 2007). Moreover, the study of De Pilli, Derossi, Talja, Jouppila, & Severini, (2011) on the starch-lipid complexes in a model system and real food using extrusion cooking showed that the highest formation of starch-lipid complexes for both model system and real food was obtained at the highest value of temperature (128°C) and water feed content (21%), which showed a highest melting enthalpy.

2.5.3 Thermo-molding process

The thermo-molding process is a thermal treatment, which is applied to produce many kinds of non-food and food packaging such as bioplastic, starch-based composite (Sun, Song, & Zheng, 2008; Narkchamnan & Sakdaronnarong, 2013). This process involves the thermal and pressure to form the sheet and film. For the processing of plant protein-based products, heating plays an important role (Cuq, Boutrot, Redl, & Lullien-Pellerin, 2000; Mo, Sun, & Wang, 1999) due to it effect on the molecular conformations of proteins, their polymeric state and their molecular interaction (Domenek, Morel, Bonicel, & Guilbert, 2002). Sun et al. (2008), studied the production of the biodegradable wheat gluten plastics plasticized with glycerol at various molding temperature and found that crosslinking density of the three-dimensional protein network through disulfide bonding was improved as molding temperature increased. Thermal treatment at temperatures above 70 and 85°C improves water barrier properties for glutenin- and gliadin-rich films and improves resistance to disintegration in water for gliadin-rich films (Hernandez-Munoz et al., 2004).

2.6 Location of starch digestion

Starch digestion in the human body begins in the mouth by salivary α-amylase,

which hydrolyzes amylose to maltose, maltotriose and maltotetraose, and amylopectin to the same product plus two α-limit dextrin (Robyt, 1984). Then, food starch enters to the stomach with salivary α-amylase but it was inactivated due to the pH in the stomach is about 2. The partially hydrolyzed starch passes into the small intestine lumen, where it is neutralized. At this location, the starch is mainly hydrolyzed by α-amylase secreted from the pancreatic duct to obtain maltose, maltotriose, and other fragments containing α-1,6 bonds, which are the α-limit dextrins. For converting the α-amylase hydrolysates into glucose, two enzymes are the brush border glucogenic enzyme maltase-glucoamylase and sucrose-isoamylase are necessary (Nochols et al., 2003). Maltase-glucoamylase hydrolyses to maltose, maltotriose, and maltotetraose from non-reducing end into D-glucose (Robyt, 1984), whereas sucrose-isoamylase hydrolyses the α-1, 6-linkages. The D-glucose products can be transported across the luminal membrane of the small intestine into the blood and served as an energy source. The indigestible starch or RS pass into the colon and it is fermented by the colonic microbiota (Englyst et al., 1992; Englyst & Hudson 1996), generating the short-chain fatty acids (SCFAs; e.g., acetate, propionate, and butyrate) and gases (e.g., hydrogen, carbon dioxide, and methane). The caloric value from colonic fermentation of RS less than one-half of the caloric value of direct digestion of starch and absorption of glucose in the small intestine (Lee, Bello-Pérez, Lin, Kim, & Hamaker, 2013). The SCFAs production shows many benefits including supplying energy to colonocytes, regulating of lipogenesis, cholesterol biogenesis in the liver, and triggering secretion of glucagon-like peptide 1 (GLP-1) and peptide YY (PYY) hormones, which decrease gastric emptying rate related to satiety and food intake (Maljaars, Peters, Mela, & Masclee, 2008). Furthermore, SDS can also decrease

gastric emptying due to the slow digestion in the intestine. The released glucose in the ileum has been revealed to promote the ileal brake effects (Siegle, Schmid, & Ehrlei, 1990; Maljaars et al., 2008) by stimulating the release of hormones (e.g., GLP-1 and PYY). Regarding to gastric emptying, the stomach plays an important role to regulate gastric emptying (Delzenne et al. 2010) through sensing of nutrients throughout the progress of the small intestine (≈15-20 inch in length) and a feedback control system involving hormonal and nervous systems (Maljaars et al., 2008) (Figure 2.11).

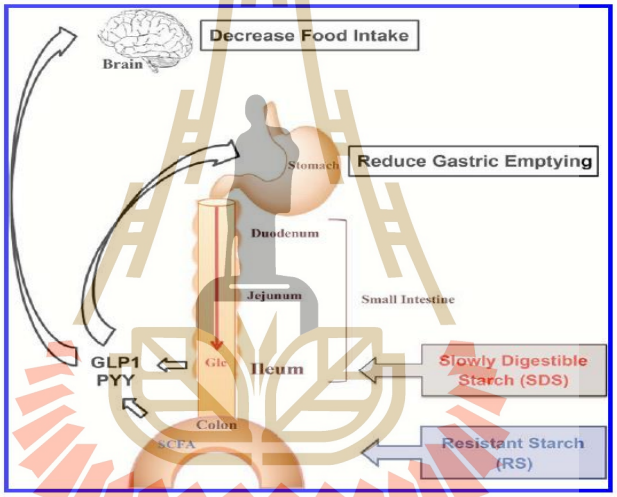

Figure 2.11 Concept of ileal and colonic brake mechanism related to slowly digestible or resistant starches caused by ileal glucose (Glc) release and short-chain fatty acids (SCFA) from fermentation. GLP1 = glucagon-like peptide 1; and PYY = peptide YY (Lee et al., 2013).

2.7 *In vitro* starch fractions determination

Starch fractions of RDS, SDS, and RS was originally quantified based on the in vitro Englyst method (Englyst et al., 1992). This procedure includes the measurement of free glucose (FG) and total glucose (TG) in order to accurately calculate each

fraction. The glucose released after digestion for 20 min (G20) and 120 min (G120) are used to calculate the RDS and SDS. The starch fraction can be calculated as follows: (where 0.9 is the conversion fraction from glucose to starch).

$$TS = (TG - FG) \times 0.9 \quad (1)$$

$$RDS = (G20 - FG) \times 0.9 \quad (2)$$

$$SDS = (G120 - G20) \times 0.9 \quad (3)$$

$$RS = TS - RDS - SDS \quad (4)$$

Another method for determination starch fraction is Goni's method in which only a low concentration of porcine pancreatic α-amylase are used. This method is simpler than Englyst method, but the sample needs pretreatment to remove lipids and protein. Moreover, the additional analysis to measure the RS content is also needed (Zhang & Hamaker, 2009). After α-amylase digestion, amyloglucosidase is used to convert starch degradation products to glucose. However, the concept for calculation RDS and SDS similar to Englyst method. The RDS is digested starch at 30 min and SDS is the digested portion between 30 and 120 min (Rosin, Lajolo, & Menezes, 2002).

The Guraya's method is the simplest method to determine RDS, SDS, and RS. This procedure based on the measurement of the maltose products obtained from porcine pancreatic α-amylase digestion. The maltose concentration is measured using the 3,5-dinitrosalicylic acid (DNS) assay. The total starch needs to analysis for calculating each fraction. The RDS is digested starch at 60 min and SDS is the digested portion at the maximum digestion minus the digestion at 60 min (Rosin et al., 2002), whereas the RS is derived from total starch minus the maltose released at the maximum digestion.

For the determination of RS, the Megazyme assay kit is widely used in analytical laboratories. It determined based on the method of AACC Method 32–40 and AOAC method 2002.02 (Megazyme, 2008). The raw or processed food samples was hydrolyzed in a mixture of α-amylase and amyloglucosidase at 37°C for 16 h. Then, the indigested starch was recovered and hydrolyzed with amyloglucosidase at 50°C for 30 min. The glucose oxidase–peroxidase colorimetric assay was used to determine glucose concentration in the final hydrolysate. This protocol is not applicable to the determination of SDS and RDS (Ashwar et al., 2016).

2.8 References

Anderson, A.K., Guraya, H.S., James, C., & Salvaggio, L. (2002). Digestibility and pasting properties of rice starch heat-moisture treated at the melting temperature (T_m). **Starch/Stärke,** 54, 401-409.

Ashwar, B. A., Gani, A., Shah, A., Wani, I. A., & Masoodi, F. A. (2016). Preparation, health benefits, and applications of resistant starch-a review. **Starch/Stärke,** 68, 287-301.

Berry, C. S. (1986). Resistant starch: formation and measurement of starch that survives exhaustive digestion with amylolytic enzymes during the determination of dietary fiber. **Journal of Cereal Science,** 4, 301-314.

Bhuiyan, S. H., Kitaoka, M., & Hayashi, K. (2003). A cycloamylose-forming hyperthermostable 4-α-glucanotransferase of *Aquifex aeolicus* expressed in *Escherichia coli*. **Journal of Molecular Catalysis B: Enzymatic,** 22, 45-53.

Biliaderis, C. G., & Galloway, G. (1989). Crystallization behavior of amylose-V complexes: structure property relationships. **Carbohydrate Research,** 189, 31-48.

Brennan, C. S. (2005). Dietary fibre, glycaemic response, and diabetes. **Molecular Nutrition & Food Research,** 49, 560-570.

Buléon, A., Colonna, P., Planchot, V., & Ball, S. (1998). Starch granules: structure and biosynthesis. **International Journal of Biological Macromolecules,** 23, 85-112.

Cai, L. M., & Shi, Y. C. (2010). Structure and digestibility of crystalline short-chain amylose from debranched waxy wheat, waxy maize, and waxy potato starches. **Carbohydrate Polymers,** 79, 1117-1123.

Chiu, C-W., Henley, M., & Altieri, P. (1994). Process for making amylase resistant starch from high amylose starch. **US Patent Office,** Pat. No. 5 281 276.

Cho, K. H., Auh, J. H., Ryu, J. H., Kim, J. H., Park, K. H., Park, C. S., et al. (2009). Structural modification and characterization of rice starch treated by *Thermus aquaticus* 4-α-glucanotransferase. **Food Hydrocolloids,** 23, 2403-2409.

Chung, H.-J., Lim, H. S., Lim, S. T. (2006). Effect of partial gelatinization and retrogradation on the enzymatic digestion of waxy rice starch. **Journal of Cereal Science,** 43, 353-359.

Chung, H.-J., Liu, Q., & Hoover, R. (2009). Impact of annealing and heat-moisture treatment on rapidly digestible, slowly digestible and resistant starch levels in native and gelatinized corn, pea and lentil starches. **Carbohydrate Polymers,** 75, 436-447.

Colonna, P., Leloup, V., & Buléon, A. (1992). Limiting factors of starch hydrolysis. **European Journal of Clinical Nutrition,** 46, S17-S32.

Critchley, J. H., Zeeman, S. C., Takaha, T., Smith, A. M., & Smith, S. M. (2001). A critical role for disproportionating enzyme in starch breakdown is revealed by a knock-out mutation in Arabidopsis. **The Plant Journal,** 26, 89-100.

Cummings, J. H., Beatty, E. R., Kingman, S. M., Bingham, S. A., & Englyst, H. N. (1996). Digestion and physiological properties of resistant starch in the human large bowel. **British Journal of Nutrition,** 75, 733-747.

Cummings, J. H. & Stephen, A. M. (2007). Carbohydrate terminology and classification. **European Journal of Clinical Nutrition,** 61, S5-S18.

Cuq, B., Boutrot, F., Redl, A., & Lullien-Pellerin, V. (2000). Study of the temperature effect on the formation of wheat gluten network: Influence on mechanical properties and protein solubility. **Journal of Agricultural and Food Chemistry,** 48, 2954-2959.

De Pilli, T., Derossi, A., Talja, R. A., Jouppila, K., & Severini, C. (2011). Study of starch-lipid complexes on model system and real food produced using extrusion-cooking technology. **Innovative Food Science and Engineering Technologies,** 12, 610-616.

Delzenne, N., Blundell, J., Brouns, F., Cunningham, K., De Graaf, K., Erkner, A., Lluch, A., Mars, M., Peters, H. P. F., & Westerterp-Plantenga, M. 2010. Gastrointestinal targets of appetite regulation in humans. **Obesity Reviews,** 11, 234-250.

Do, H. V., Lee, E. J., Park, J. H., Park, K. H., Shim, J. Y., Mun. S., et al. (2012). Structural and physicochemical properties of starch gels prepared from partially modified starches using *Thermus aquaticus* 4-α-glucanotransferase. **Carbohydrate Polymers,** 87, 2455-2463.

Domenek, S., Morel, M. H., Bonicel, J., & Guilbert, S. (2002). Polymerization kinetics of wheat gluten upon thermosetting. A mechanical model. **Journal of Agricultural and Food Chemistry,** 50,5947-5954.

Eerlingen, R. (1994). **Formation, structure, and properties of enzyme resistant starch.** Doctoraatsproefschritf Nr. 248 aan de Faculteit Landbouwkendige en Toegepaste Biologische Wetenschappen van de K.U. Leuven.

Eerlingen, R. C., and Delcour, J. A. (1995). Formation, analysis, structure and properties of type III enzyme resistant starch. **Journal of Cereal Science,** 22, 129-138.

Eerlingen, R. C., Crombez, M., & Delcour, J. A. (1993a). Enzyme-resistant starch. I. Quantitative and qualitative influence of incubation time and temperature of autoclaved starch on resistant starch formation. **Cereal Chemistry,** 70(3), 339-344.

Eerlingen, R. C., Deceuninck, M., & Delcour, J. A. (1993b). Enzyme-resistant starch. II. influence of amylose chain length on resistant starch formation. **Cereal Chemistry,** 70(3), 345-350.

Englyst, H. N., & Hudson, G. J. (1996). The classification and measurement of dietary carbohydrates. **Food Chemistry,** 57, 15-21.

Englyst, H. N., Kingman, S. M. & Cummings, J. H. (1992). Classification and measurement of nutritionally important starch fractions. **European Journal of Clinical Nutrition,** 46, S33-S50.

Englyst, K. N., Liu, S. & Englyst, H. N. (2007). Nutritional characterization and measurement of dietary carbohydrates. **European Journal of Clinical Nutrition,** 61, S19-S39.

EURESTA (European Flair Action Concerted on Resistant Starch). **Newsletter ZZZ** (1992). 7. Department of Human Nutrition. Wageningen Agricultural University.

Euverink, G. J. W., & Binnema, D. J. (1998). Use of modified starch as an agent for forming a thermoreversible gel. **WO Patent,** Pat. No. 9 815 347.

Fannon, J. E., Hauber, R. J. & BeMiller, J. N. (1992). Surface pores of starch granules. **Cereal Chemistry,** 69, 284-288.

Faraj, A. Vasanthan, T, & Hoover, R. (2004). The effect of extrusion cooking on resistant starch formation in waxy and regular barley flours. **Food Research International,** 37, 517-525.

Fujii, K., Minagawa, H., Terada, Y., Takaha, T., Kuriki, T., Shimada, J., et al. (2005). Protein engineering of amylomaltase from Thermus aquaticus with random and saturation mutagenesis. **Biologia,** 60, 97-102.

Gidley, M. J., Bulpin, P. V. (1987). Crystallisation of malto-oligosaccharides as models of the crystalline forms of starch: minimum chain-length requirement for the formation of double helices. **Carbohydrate Research,** 161, 291-300.

Gidley, M. J., Cooke, D., Darke, A. H., Hoffman, R. A., Russel, A. L., & Greenwell, P. (1995). Molecular order and structure in enzyme-resistant retrograded starch. **Carbohydrate Polymers,** 28, 23-31.

Godet, M. C., Tran, V., Delage, M. M., & Buléon, A. (1993). Molecular modeling of the specific interactions involved in the amylose complexation by fatty acids. **International Journal of Biological Macromolecules,** 15, 11-16.

González-Soto, R. A., Sánchez-Hernández, L., Solorza-Feria, J., Núñez-Santiago, C., Flores-Huicochea1, E., & Bello-Pérez1, L. A. (2006). Resistant Starch Production from Non-conventional Starch Sources by Extrusion. **Food Science and Technology International,** 12(1), 5-11.

Gross, A., & Haralampu, S. G. (1999). Microcrystalline starch-based product and use in foods. **US Patent Office,** Pat. No. 5 962 047.

Gunaratne, A., & Hoover, R. (2002). Effect of heat-moisture treatment on the structure and physicochemical properties of tuber and root starches. **Carbohydrate Polymers,** 49, 425-437.

Guraya, H. S., James, C., & Champagne, E. T. (2001). Effect of enzyme concentration and storage temperature on the formation of slowly digestible starch digestibility from cooked debranched rice starch. **Starch/Stärke,** 53, 131-139.

Hansen, M. R., Blennow, A., Pedersen, S., &. Engelsen, S. B. (2009). Enzyme modification of starch with amylomaltase results in increasing gel melting point. **Carbohydrate Polymers,** 78, 72-79.

Hansen, M. R., Blennow, A., Pedersen, S., Norgaard, L., & Engelsen, S. B. (2008). Gel texture and chain structure of amylomaltase-modified starches compared to gelatin. **Food Hydrocolloids,** 22, 1551-1566.

Hamaker, B., & Han, X. Z. (2004). Slowly digestible starch. Purdue Research Foundation. **WO Patent,** Pat. No. 066 955 A2.

Haralampu, S. G., & Gross, A. (1998). Granular resistant starch and method of making. **US Patent Office,** Pat. No. 5 849 090.

Harris, D. W. (2008). Production of resistant starch product having tailored of degree of polymerization. **US Patent Office,** Pat. No. 0 280 332 A1.

Haynes, L., Gimmler, N., Locke, J. P., Kweon, M.-R., Slade, L. & Levine, H. (2000). Process for making enzyme-resistant starch for reduced. calorie flour replacer. **US Patent Office,** Pat. No. 6 013 299.

Hernandez-Munoz, P., Villalobos, R., & Chiralt, A. (2004). Effect of thermal treatments on functional properties of edible films made from wheat gluten fractions. **Food Hydrocolloids,** 18, 647-654.

Hizukuri, S., Abe, J., & Hanashiro, I. (2006). Starch: Analytical aspects. In A.-C. Eliasson (ed). **Carbohydrates in food**. Boca Raton, FL: Taylor & Francis Group., pp. 305-391.

Hoover, R., & Vasanthan, T. (1994). The effect of annealing on the physicochemical properties of wheat, oat, potato and lentil starches. **Journal of Food Biochemistry,** 17, 303-325.

Huber, K. C. & BeMiller, J. N. (2000). Channels of maize and sorghum starch granules. **Carbohydrate Polymer,** 41, 269-276.

Huth, M., Dongowski, G., Gebhardt, E., & Flamme, W. (2000). Functional properties of dietary fibre enriched extrudates from barley. **Journal of Cereal Science,** 32, 115-128.

Imberty, A., Buléon, A., Tran, V., & Perez, S., (1991). Recent advances in knowledge of starch structure. **Starch/Stärke,** 43, 375-384.

Jacobasch, G., Dongowski, G., Schmiedl, D., & Müller-Schmehl, K. (2006). Hydrothermal treatment of Novelose 330 results in high yield of resistant starch type 3 with beneficial prebiotic properties and decreased secondary bile acid formation in rats. **British Journal of Nutrition,** 95, 1063-1074.

Jacobs, H., & Delcour, J. (1998). Hydrothermal modifications of granular starch with retention of the granular structure: A review. **Journal of Agricultural and Food Chemistry,** 46, 2895-2905.

Jang, J. K. & Pyun, Y. R. (1997). Effect of moisture level on the crystallinity of wheat starch aged at different temperatures. **Starch/Stärke,** 49, 272-277.

Jayakody, L., & Hoover, R. (2008). Effect of annealing on the molecular structure and physicochemical properties of starches from different botanical origins: A review. **Carbohydrate Polymers,** 74, 691-703.

Jenkins, P. J., & Donald, A. M. (1998). Gelatinization of starch: a combined SAX/WAXS/DSC and SANS study. **Carbohydrate Research,** 308(1), 133-147.

Karkalas, J., Ma, S., Morrison, W. R., & Pethrick, R. A. (1995). Some factors determining the thermal-properties of amylose inclusion complexes with fatty-acids. **Carbohydrate Research,** 268, 233-247.

Kaper, T., Talik, B., Ettema, T. J., Bos, H., Van der Maarel, M. J. E. C., & Dijkhuizen, L. (2005). The amylomaltase of *Pyrobaculum aerophilum* IM2 produces thermo-reversible starch gels. **Applied and Environmental Microbiology,** 71, 5098-5106.

Kettlitz, B. W., Coppin, J. V. J.-M., Roper, H. W. W., & Bornet, F. (2000). Highly fermentable resistant starch. **US Patent Office,** Pat. No. 6 043 229.

Kim, J. H., Tanhehco, E. J., & Ng, P. K. W. (2006). Effect of extrusion conditions on resistant starch formation from pastry wheat flour. **Food Chemistry,** 99, 718-723.

Lai, L. S., & Kokini, J. L. (1991). Physicochemical changes and rheological properties of starch during extrusion. **Biotechnology Progress,** 7(3), 251-266.

Lee, B-O., Bello-Pérez, L. A., Lin, A. H-M., Kim, C. Y., & Hamaker, H. R. (2013). Importance of location of digestion and colonic fermentation of starch related to its quality. **Cereal Chemistry,** 90(4), 335-343.

Lee, K. Y., Kim, Y. R., Park, K. H., & Lee, H. G. (2006). Effects of alphaglucanotransferase treatment on the thermo-reversibility and freeze-thaw stability of a rice starch gel. **Carbohydrate Polymers,** 63, 347-354.

Lee, B. H., Oh, D. K., & Yoo, S. H. (2009). Characterization of 4-α-glucanotransferase from Synechocystis sp. PCC 6803 and its application to various corn starches. **New Biotechnology,** 26, 29-36.

Lehmann, U., Jacobasch, G. & Schmiedl, D. (2002). Characterization of resistant starch type III from banana (Musa acuminate). **Journal of Agriculture and Food Chemistry,** 50, 5236-5240.

Lehmann, U., & Robin, F. (2007). Slowly digestible starch-its structure and health implications: A review. **Trends in Food Science and Technology,** 18, 346-355.

Levine, H. & Slade, I. (1988). Water as plasticizer: Physico-chemical aspects of low-moisture polymer system. In F. Frank (eds). **Water Science Reviews,** Vol.3, Water Dynamics. Cambridge University Press: Cambridge, U.K., pp. 79-185.

Liu, W. C., Halley, P. J., & Gilbert, R. G. (2010). Mechanism of degradation of starch, a highly branched polymer, during extrusion. **Macromolecules,** 43(6), 2855-2864.

Machida, S., Ogawa, S., Xiaohua, S., Takaha, T., Fujii, K., & Hayashi, K. (2000). Cycloamylose as an efficient artificial chaperone for protein refolding. **FEBS Letters,** 486, 131-135.

Maljaars, P. W. J., Peters, H. P. F., Mela, D. J., and Masclee, A. A. M. (2008). Ileal brake: Asensible food target for appetite control. A review. **Physiology & Behavior,** 95, 271-281.

Manners, D. J. (1989). Recent developments in our understanding of amylopectin structure. **Carbohydrate Polymer,** 11, 87-112.

Megazyme (2008). Resistant starch assay procedure. [On-line]. Available: http://secure.megazyme.com/ downloads/en/data/KRSTAR.pdf

Mischnick, P., & Momcilovic, D. (2010). Chemical Structure Analysis of Starch and Cellulose Derivatives. **Advances in Carbohydrate Chemistry and Biochemistry,** 64, 117-210.

Mo, X. Q., Sun, X. S., & Wang, Y. Q. (1999). Effects of molding temperature and pressure on properties of soy protein polymers. **Journal of Applied Polymer Science,** 73, 2595-2602.

Mutungi, C., Onyango, C., Doert, T., Paasch, S., Thiele, S., Machill, S. et al. (2011). Long-and short-range structural changes of recrystallized cassava starch subjected to in vitro digestion. **Food Hydrocolloids,** 25, 477-485.

Mutungi, C., Rost, F., Onyango, C., Jaros, D., & Rohm, H. (2009). Crystallinity, thermal and morphological characteristics of resistant starch type III produced by hydrothermal treatment of debranched cassava starch. **Starch/Stärke,** 61(11), 634-645.

Narkchamnan, S., & Sakdaronnarong, C. (2013). Thermo-molded biocomposite from cassava starch, natural fibers and lignin associated by laccase-mediator system. **Carbohydrate Polymers,** 96, 109-117.

Niba, L. L. (2003). Processing effects on susceptibility of starch to digestion in some dietary starch sources. **International Journal of Food Sciences and Nutrition,** 54, 97-109.

Nichols, B. L., Avery, S. E., Sen, P., Swallow, D. M., Hanh, D.,Sterchi, E. E. (2003). The matase-glocoamylase gene: common ancestry to sucrose-isomaltase with complementary starch digestion activities. **Proceeding of the National Acadamy of Sciences in the United States of America,** 100, 1432-1437.

Norman, B., Pedersen, S., Stanley, K., Stanley, E., & Richmond, P. (2007). Production of crystalline short chain amylase. **US Patent Office,** Pat. No. 0 059 432.

Park, E. Y., Baik, B.-K., Lim, S.-T., (2009). Influences of temperature-cycled storage on retrogradation and in vitro digestibility of waxy maize starch gel. **Journal of Cereal Science,** 50, 43-48.

Park, J. H., Kim, H. J., Kim, Y. H., Cha, H. J., Kim, Y. W., Kim, T. J., et al. (2007). The action mode of *Thermus aquaticus* YT-1,4-α-glucanotransferase and its chimeric enzymes introduced with starch-binding domain on amylose and amylopectin. **Carbohydrate Polymers,** 67, 164-173.

Perry, P. A., & Donald, A. M. (2000). SANS study of the distribution of water within starch granules. **International Journal of Biological Macromolecules,** 28, 31-39.

Przylas, I., Tomoo, K., Terada, Y., Takaha, T., Fujii, K., Saenger, W., Strater, N. (2000) Crystal structure of amylomaltase from thermus aquaticus, α-glycosyltransferase catalysing the production of large cyclic glucans. **Journal of Molecular Biology,** 296, 873-886.

Putseys, J. A., Derde, L. J., Lamberts, L., Goesaert, H., & Delcour, J. A. (2009). Production of tailor made short chain amylose-lipid complexes using varying reaction conditions. **Carbohydrate Polymers,** 78, 854-861.

Richmond, P. A., Marion, E. A., Eilers, T. A., Evan, A., Zhang, H.X., Shakeel, A., et al. (2008). Production of resistant starch product. **WO Patent,** Pat. No. 109 206.

Robyt, J. F. (1998). Enzymes in the hydrolysis and synthesis of starch. In: Whistler, R.L., BeMiller, J.N., Paschall, E.F. (eds). **Starch: Chemistry and Technology,** New York, Academic Press, Inc., pp 87-118.

Rosin, P. M., Lajolo, F. M., & Menezes, E. W. (2002). Measurement and characterization of dietary starches. **Journal of Food Composition Analytical,** 15, 367-377.

Sajilata, M. G., Singhal, R. S., & Kulkarni, P. R. (2006). Resistant Starch-A Review. **Comprehensive Reviews in Food Science & Food Safety,** 5, 1-17

Schmiedl, D., Báuerlein, M., Bengs, H., & Jacobasch, G. (2000). Production of heat-stable, butyrogenic resistant starch. **Carbohydrate Polymer,** 43, 183-193.

Schmiedel, D, Konig, B.J, & Jacobasch, G. (2003) Processing for preparing resistant starch. **US Patent Office,** Pat. No. 6 623 943.

Seneviratne, H. D., & Biliaderis, C. G. (1991). Action of a-amylases on amylose-lipid complex superstructures. **Journal of Cereal Science,** 13, 129-143.

Shi, Y. C., Cui, X., Birkett, A., & Thatcher, M. G. (2003). Slowly digestible starch product. National Starch and Chemical Investment Holding Corporation. **EP Patent,** Pat. No. 1 362 919 A1.

Shi, Y-C., Capitani, T., Trzasko, P., & Jeffcoat, R. (1998). Molecular structure of a low amylopectin starch and other high-amylose maize starches. **Journal of Cereal Science,** 27, 289-299.

Shi, Y-C., Cui, X. M., Birkett, A. G., & Thatcher, M. (2005a). Slowly digestible starch product. **US Patent Office,** Pat. No. 6 890 571.

Shi, Y-C., Cui, X. M., Birkett, A. G., & Thatcher, M. (2005b). Slowly digestible starch product. **US Patent Office,** Pat. No. 6 929 817.

Shi, Y-C., Cui, X. M., Birkett, A. G., & Thatcher, M. (2006). Resistant starch prepared by isoamylase debranching of low amylose starch. **US Patent Office,** Pat. No. 7081 261.

Shin, S. I., Choi, H. J., Chung, K. M., Hamaker, B., Park, K. H., & Moon, T. W. (2004). Slowly digestible starch from debranched waxy sorghum starch: preparation and properties. **Cereal Chemistry,** 81, 404-408.

Shin, S. I., Kim, H. J., Ha, H. J., Lee, H. S., & Moon, T. W. (2005). Effect of hydrothermal treatment on formation and structural characteristics of slowly digestible non-pasted granular sweet potato starch. **Starch/Stärke,** 57, 421-430.

Siegle, M. L., Schmid, H. R., and Ehrlein, H. J. 1990. Effects of ileal infusions of nutrients on motor patterns of canine small intestine. **American Journal of Physiology,** 259, G78-G85.

Sievert, F., & Pomeranz, Y. (1989). Enzyme-resistant starch I: Characterization and Evaluation by Enzyme, Thermoanalytical Microscopic Method. **Cereal Chemistry,** 66, 342-347.

Stute, R. (1992). Hydrothermal modification of starches. The differences between annealing and heat–moisture treatment. **Starch/Stärke,** 44, 205-214.

Sun, S., Song, Y., & Zheng, Q. (2008). Thermo-molded wheat gluten plastics plasticized with glycerol: Effect of molding temperature. **Food Hydrocolloids,** 22, 1006-1013.

Takaha, T., Yanase, M., Takaha, H., Okada, S., & Smith, S. M. (1998). Cyclic glucans produced by the intramolecular transglycosylation activity of potato D-enzyme on amylopectin. **Biochemical and Biophysical Research Communications,** 247, 493-497.

Terada, Y., Fujii, K., Takaha, T., & Okada, S. (1999). Thermus aquaticus ATCC 33923 amylomaltase gene cloning and expression and enzyme

characterization: Production of cycloamylose. **Applied and Environment Microbiology,** 65, 910-915.

Tester, R. F., & Debon, S. J. J. (2000). Annealing of starch-A review. *International* **Journal of Biological Macromolecules,** 27, 1-12

Topping, D. L., Bajka, B. H., Bird, A. R., Clarke, J. M., Cobiac, L., Conlon, M. A. et al. (2008). Resistant starches as a vehicle for delivering health benefits to the human large bowel. **Microbial Ecology in Health and Disease,** 20, 103-108.

Topping, D. L., Segal, I., Regina, A., Conlon, M. A., Bajka, B. H., Toden, S. et al. (2010). Resistant starch and human health. In J. Willem van der Kamp, J. Jones, B.McCleary and David T. (eds.) **Dietary fiber: new frontiers for food and health.** Wageningen Academic Publishers, Netherland, pp. 311-322.

Tufvesson, F., Wahlgren, M., & Eliasson, A. C. (2003a). Formation of amylose-lipid complexes and effects of temperature treatment. Part 1. Monoglycerides. **Starch/Stärke,** 55, 61-71.

Tufvesson, F., Wahlgren, M., & Eliasson, A. C. (2003b). Formation of amylose-lipid complexes and effects of temperature treatment. Part 2. Fatty acids. ***Starch-Stärke,*** 55, 138-149.

van der Maarel, M. J. E. C., Capron, I., Euverink, G. J. W., Bos, T., Kaper, T., Binnema, D. J., et al. (2005). A novel thermoreversible gelling product made by enzymatic modification of starch. **Starch/Stärke,** 57, 465-472.

Vasanthan, T. & Bhatty, R. S. (1998). Enhancement of Resistant Starch (RS3) in Amylomaize, Barley, Field Pea, and Lentil Starches. **Starch/Stärke,** 50, 286-291.

Waigh, T. A., Jenkins, P. J., & Donald, A. M. (1996). Quantification of water in carbohydrate lamellae using SANX. **Faraday Discussion,** 103, 325-337.

Wolf, B. (2010). Polysaccharide functionality through extrusion cooking. **Current Opinion in Colloid and Interface Science,** 15, 50-54.

Zabar, S., Lesmes, U., Katz, I., Shimoni, E., & Bianco-Peled, H. (2009). Studying different dimensions of amylose-long chain fatty acid complexes: molecular, nano and micro level characteristics. **Food Hydrocolloids,** 23, 1918-1925.

Zhang, G.; Ao, Z.; Hamaker, B. R. (2006). Slow digestion property of native cereal starches. **Biomacromolecules,** 7, 3252-3258.

Zhang, B., Dhital, S., Flanagan, B. M. Luckman, P., Halley, P. J., & Gidley, M. J. (2015). Extrusion induced low-order starch matrices: Enzymic hydrolysis and structure. **Carbohydrate Polymers,** 134, 485-496.

Zhang, G., & Hamaker, B. R. R. (2009). Slowly digestible starch: Concept, mechanism, and proposed extended glycemic index. **Critical Reviews in Food Science and Nutrition,** 49, 852-867.

Zhang, B., Huang, Q., Luo, F., & Fu., X. (2012). Structural characterizations and digestibility of debranched high-amylose maize starch complexed with lauric acid. **Food Hydrocolloids,** 28, 174-181.

Zobel, H. F. (1988). Molecules to granules: A comprehensive starch review. **Starch/Stärke,** 40(2), 44-50.

CHAPTER III

IMPROVEMENT OF RESISTANT STARCH AND COOKING STABILITY OF CRYSTALLIZED DEBRANCHED CASSAVA STARCH BY SINGLE AND DUAL HYDROTHERMAL TREATMENTS

3.1 Abstract

Annealing (ANN) and heat-moisture treatment (HMT) are two types of hydrothermal treatments which are widely used to modify the physicochemical properties and digestibility of starch. Effects of single (ANN or HMT) and dual hydrothermal treatments on enzyme digestibility, thermal properties and cooking stability of crystallized debranched cassava starch were investigated. Crystallized debranched cassava starch was prepared by temperature cycling at 30/80^{o}C and used as the starting material (TC sample). An increase in moisture content from 20 to 30% and time from 1 to 3 h during HMT resulted in an increment in resistant starch (RS) content. All HMT-treated starches showed a higher RS content compared with all ANN-treated starches. Annealing the TC sample at 8^{o}C below peak temperature demonstrated a higher melting temperature. HMT at a temperature of 100-140^{o}C tended to increase the RS formation and the melting temperature. Dual hydrothermal treatment with HMT at 130^{o}C followed by ANN at 100^{o}C (HMT→ANN) was more efficient and improved the yield of RS (71% RS) than that of ANN followed by HMT

(ANN→HMT) (46% RS). Although ANN→HMT exhibited a lower RS content, it showed a higher melting temperature (105-127°C and 135-142°C). The cooking stability of the samples with 50 and 70% moisture using steaming for 30 min was investigated. Cooking at 50% moisture of ANN→HMT treated starch improved RS content whereas a decreased RS content of less than 6% was observed at 70% moisture for cooking. These results indicate that RS content and cooking stability can be improved by both single and dual hydrothermal treatments.

Keywords: resistant starch, single hydrothermal treatment, dual hydrothermal treatments, cooking stability

3.2 Introduction

The consumption of food containing high carbohydrate content such as starch may induce many diseases, for example, obesity, type II-diabetes and hyperlipidemia which correlate with glucose release in the blood. Regarding the rate of glucose release and absorption in the intestinal tract, starch is classified into three fractions including rapidly digestible starch (RDS), slowly digestible starch (SDS), and resistant starch (RS) (Englyst, Kingman, & Cummings, 1992). RDS is a fraction of starch which is digested in 20 min whereas SDS is slowly but completely digested in the small intestine. Several reports reveal that SDS benefits human health and correlate with a low glycemic index which is very important for the treatment and prevention of several diseases, such as cardiovascular diseases, type II-diabetes, and obesity (Shin et al., 2004; Lehmann & Robin, 2007). RS cannot be digested and absorbed in the small intestine. It shows prebiotic properties and associated health benefits for the colon (Topping & Clifton, 2001). RS has been categorized into 4 or 5 types (Topping et al.,

2010) depending on the mode of resistance. RS3 seems to be of interest because of its physical and physiological properties. RS3 contains mainly retrograded amylose which consists of linear segments of α-1, 4-glucans arranged in a crystalline structure which results in resistance to enzyme digestion. Therefore, foods containing a high level of SDS and RS can improve the health benefits of foods. Studies on methods to increase the amount of SDS and RS have attracted considerable interest. SDS can be produced through chemical, physical, enzymatic, genetic, and combined modifications (He, Liu, & Zhang, 2008; Miao, Jiang, & Zhang, 2009; Shin, Kim, Ha, Lee, & Moon, 2005).

The production of RS3 consists of gelatinisation of starches, hydrolysis of amylopectin with debranching enzymes such as pullulanase or isoamylase, followed by controlled retrogradation or recrystallization (Lehmann, Jacobasch, & Schmiedl, 2002; Sajilata, Singhal, & Kulkarni, 2006). The yield and quality of RS3 are affected by various factors such as the amylose/amylopectin ratio, chain length, retrogradation conditions, lipids, and solution compositions. Some crystalline polymorphs, A, B, C or V-polymorphs, were formed in the RS3 production. A higher retrogradation temperature generally favors the formation of more stable A-type rather than B-type starch polymorphs (Gidley & Bulpin, 1987). In addition, the crystalline starch polymorphs had an influence on the thermal properties of RS. Temperature cycling incubation is applied to accelerate starch recrystallization and to increase the yield of RS3 with more thermal stability as compared to isothermal temperature incubation (Zeng et al., 2014). However, some portions of RS are not thermostable and lose their enzyme resistance during cooking. Therefore, it is necessary to develop cleaner technologies to produce a high level of thermally stable RS to deliver health benefits

to consumers. The effects of annealing (ANN) and heat-moisture treatment (HMT) on the structural and physicochemical properties of retrograded starch were studied (Jacobasch, Dongowski, Schmiedl, & Müller-Schmehl, 2007; Kiatponglarp, Tongta, Rolland-Sabaté, & Buléon, 2015; Mutungi et al., 2011; Mutungi, Rost, Onyango, Jaros, & Rohm, 2009). Niba (2003) points out that SDS levels of cocoyam, maize, potato and rice flour increase after heat treatment and storage. Furthermore, hydrothermal treatment can increase the SDS content as compared to raw starch (Shin et al., 2005). Single hydrothermal treatment of ANN and HMT can improve RS content and thermal properties of retrograded starch by inducing structural changes which decrease its enzyme digestibility. Moreover, the effects of single and dual hydrothermal treatments on enzyme digestibility and thermal properties of normal corn starch (Chung, Hoover, & Liu, 2009), pea, lentil, and navy bean starches (Chung, Liu, & Hoover, 2010), and waxy rice starch (Zeng et al., 2015) were investigated. The gelatinization temperatures and SDS content of all hydrothermally treated starches increased for both single and dual treatments, but the RS content decreased. Dual hydrothermal treatment of ANN followed by HMT (ANN→HMT) of waxy rice starch showed a higher *To*, *Tp*, and *Tc* than single hydrothermal treatment of ANN but ΔT and ΔH of ANN→HMT starch were narrower and lower, indicating that crystallite heterogeneity within the granules decreased after HMT of annealed starch. These studies focus on the effect of dual hydrothermal treatments on enzyme digestibility and the thermal properties of native granular starches. However, the effect of dual hydrothermal treatments on recrystallized starch is limited. A study on the structural transformation and enzyme digestibility during each step of dual hydrothermal treatment is necessary to understand how what changes occur during these treatments.

Therefore, the objective of this study was to investigate the effects of the combination of recrystallization processes, temperature cycling incubation, and hydrothermal treatments (ANN or HMT) on starch fractions, thermal properties, and the cooking stability of debranched cassava starch.

3.3 Materials and Methods

3.3.1 Materials

Cassava starch was provided by Sanguan Wongse Industries Co., Ltd. (Nakhon Ratchasima, Thailand). The commercial debranching enzyme, pullulanase (Promozyme D2, 458 PUN/ml) from *Bacillus deramificans*, was purchased from Novozymes A/S (Bagsvaerd, Denmark). Pancreatic α-amylase (EC 3.2.1.1, type VI-B from porcine pancrease, A3176, 25 U/mg), amyloglucosidase (EC 3.2.1.3 from *Aspergillus niger*, A7095, 300 U/mL), PGO enzyme kits (P1179) and o-dianisidine (D3252) were purchased from Sigma Chemical Co. Other chemicals were of analytical grade.

3.3.2 Preparation of crystallized debranched starch

Cassava starch suspension (8% (w/v) in 0.05 M acetate buffer, pH 4.5) was gelatinized using a shaking water bath at 60°C for 15 min followed by heating at 80°C for 20 min and at 100°C for 30 min with continuous shaking. After cooling to 50°C, pullulanase (65 PUN/g of starch) was added and the suspension was incubated for 24 h with constant shaking; then it was heated at 85°C for 30 min to inactivate enzyme activity. The debranched starch was recrystallized by temperature cycling incubation for three cycles at a temperature of 30°C for 5 h and 80°C for 5 h. The products were air-dried to obtain 12% moisture. Then, they were milled using mortar

and pestle and sieved through a 120 mesh screen and named as the temperature-cycled debranched starch (TC sample)

3.3.3 Single hydrothermal treatment

3.3.3.1 Effect of moisture content and heat-moisture treatment (HMT) time

The TC sample was adjusted to a moisture content of 20 to 30% by using deionized water. The samples in a closed container were heated in a hot air oven at a temperature of 120°C for 1, 2, and 3h, respectively. The HMT-treated starch was air-dried to obtain 12% moisture content, then ground and sieved.

3.3.3.2 Impact of annealing and HMT temperature

The first TC sample was adjusted to a moisture content of 90% by using deionized water and annealed at 8°C and 28°C below the peak temperature (*Tp*) of the TC sample for 48h. The second TC sample was adjusted to a moisture content of 20% by using deionized water and heated at temperatures of 100, 120, 130, and 140°C for 2h. Next, the samples were air-dried to obtain 12% moisture content, then ground and sieved.

3.3.4 Dual hydrothermal treatment

Dual hydrothermal treatments were ANN followed by HMT (ANN→HMT) or HMT followed by ANN (HMT→ANN). The ANN was conducted at 8°C below the peak temperature (*Tp*) of the TC sample for 48 h. The HMT was performed at 130°C for 2h. Finally, the sample was air-dried to obtain 12% moisture content, then ground, and sieved.

3.3.5 Determination of starch fractions

The starch fractions (RDS, SDS and RS) of samples were measured according to the method of official AOAC method 2002.02 and Englyst et al. (1992) with slight modifications. A sample (100 mg) was weighed in a screw cap tube and 4 ml of sodium maleate buffer (pH 6.0) containing pancreatic α-amylase (10 $mg.mL^{-1}$) and amyloglucosidase (3 $U.mL^{-1}$) was added, the cap tightened and the content were mixed. The sample was incubated in a shaking water bath with continuous shaking at 37°C for 16 h. After 20 min and 16 h of reaction time, 4 mL of 99% ethanol was added, mixed well and centrifuged at 1,500x*g* for 10 min. The supernatant was carefully decanted and collected. Then, the residue at 16 h was rinsed twice with 8 ml of 50% ethanol, followed by being centrifuged at 1500x*g* for 10 min. The residue was re-suspended in 2 mL of 2 M potassium hydroxide and stirred in an ice bath for 20 min. The 1.2 M sodium acetate buffer pH 3.8 (8 mL) was added, and followed by 0.1 mL of amyloglucosidase (3,300 U/mL). The sample was mixed and incubated at 50°C in a shaking water bath with continuous shaking for 30 min. The collected supernatant was diluted with deionized water at 20 min and 16 h and the hydrolyzed sample at 16 h .The liberated glucose of all the samples was determined using PGO enzyme reagent (Sigma, P1179 and D3252). The PGO enzyme reagent (5 ml) was added to the 0.5 mL diluted sample, then incubated at 37°C for 30 min. The absorbance was measured against a reagent blank at 440 nm. The percentages of RDS, SDS, and RS were calculated as follows:

RDS (%) = glucose released at 20 min x 162/180 x 100

SDS (%) = glucose released at 16 h - glucose released at 20 min x 162/180 x 100

RS (%) = glucose released in undigestible starch at 16 h x 162/180 x 100

3.3.6 Thermal properties

The thermal properties of the samples were monitored using differential scanning calorimetry (DSC). The DSC1 instrument (Mettler Toledo, Switzerland) was calibrated with indium using an empty stainless steel pan as a reference. Approximately ten mg of the sample were weighed in a 60 µl stainless steel pan and deionized water was added to obtain a starch-water suspension ratio of 1:3. A DSC pan was hermetically sealed and heated in the DSC from 25°C to 200°C at a heating rate of 3°C/ min. The onset temperature (*To*), peak temperature (*Tp*), conclusion temperature (*Tc*) and enthalpy (ΔH) were calculated by mettle software and defined as the thermal transition of the sample.

3.3.7 Crysalline structure

The crystalline structure and relative crystallinity of samples were investigated by using wide-angle X-ray scattering (WAXS). The experiments were carried out at BL1.3W: SAXS (Small/Wide Angle X-ray Scattering), Synchrotron Light Research Institute (SLRI), Nakhon Ratchasima, Thailand. The sample was prepared by adjustment of the moisture content to 90% relative humidity for 10 days under partial vacuum in the presence of a saturated barium chloride solution. Approximately twenty mg of the sample were placed between two aluminum foil sheets on a sample holder. The eight keV synchrotron X-ray beam was monochromatized by a double multilayer monochromator. The exposure time for each data collection was 10 sec. The sample to detector distance was determined to be 276 mm using titanium dioxide as a standard. The scattering patterns were recorded with a MAR-CCD (SX165) detector. The program called SAXSIT (Small Angle X-ray Scattering Image Tool) was used to analyze the relative crystallinity and the

crystalline pattern. The lateral crystal size was established from peak half width of 100 reflection (2θ ~5.6°) using the Scherre equation: $D_{hkl} = k\lambda/\beta\cos\theta$, when D_{hkl} is the average length of the diffraction domain normal to the family plane (*hkl*), k is a constant as 0.9 for cellulose, λ is the wavelength used and β is the peak half width (Cairns, Bogracheva, Ring, Hedley & Morris, 1997).

3.3.8 Cooking stability

The TC, TC→ANN→HMT and TC→HMT→ANN samples were selected to test cooking stability as a food model system at 50% and 70% moisture content. Deionized water was added to the powder samples to obtain a moisture content of 50 and 70%. The starch suspension was sealed in a closed container and heated in a steaming bath (99°C) for 30 min. After cooling to room temperature (27-30°C), they were analyzed for starch fractions as described previously.

3.3.9 Statistical analysis

Analysis of variance was carried out using SPSS software for window version 13.0 (SPSS Inc., Cary, NC, USA). The differences between mean values were established using Duncan's multiple-range test. Principal component analysis (PCA) was performed using SPSS software. All measurements and analyses were conducted in three replications.

3.4 Results and discussion

3.4.1 Single hydrothermal treatment

3.4.1.1 Effects of moisture content and heat-moisture treatment (HMT) time on starch fractions and thermal properties

The debranched starch was recrystallized by temperature-cycled treatment and was used as the starting material (temperature-cycled debranched starch, TC sample). Starch fractions (RDS, SDS and RS content) and thermal properties or melting parameters (*To*, *Tp*, *Tc* and *ΔH*) of TC sample and all TC→HMT starches are presented in Table 3.1. The TC sample shows the RDS, SDS, and RS content of 18.7%, 44.6%, and 36.7%, respectively. The TC sample melted at *To* of 100°C was slightly higher than that of the debranched starch (98°C). Thus, the crystalline structure of TC sample was more perfect. This indicated that the temperature-cycled treatment promoted the growth of the crystalline regions and crystalline perfection by accelerating the starch crystallization which was a stepwise nucleation and propagation (Silvero, Fredriksson, Andersson, Eliasson, & Aman, 2000). As expected, after HMT with 20-30% moisture content at 120°C for 1 to 3 h, the RS contents increased to a range of 44-52% ($p<0.05$). Moreover, the melting temperatures (*To*, *Tp* and *Tc*) shifted to higher temperatures. An increase in moisture content during HMT from 20 to 30% decreased the RS content ($p < 0.05$). Although water acts as an effective plasticizer for starchy materials (Fahart, Blanshard, & Mitchell, 2000) and facilitates molecular mobility, in this case, the lower RS content is probably due to excess plasticization that lead to weak intra-helical linkages between coupling glucans (Mutungi et al., 2009). Similar results were found by Jacobasch et al. (2007) who found that RS yield decreased with higher moisture content during HMT

of Novelose 330. In addition, the reduction of melting enthalpy (*ΔH*) was noticed after HMT at 30% moisture content, suggesting that some double helices and the crystalline order were disrupted during heating at a higher moisture content which was consistent with the lower RS content. An increase in HMT time from 1 to 3 h tended to increase the RS content and *To*. However, the RS content, *To*, *Tp* and *Tc* of TC→HMT starches between 2 and 3 h were not different, implying that the formation of RS with thermally stable crystallites required an optimal heating time to induce the rearrangement of linear glucans to form double helices and then crystalline domain. The highest RS content of 52% was obtained from HMT at 20% moisture content for 2 and 3 h. The reduction of SDS content was observed in all samples after HMT, which showed a range of 31-39% while the RDS contents were no different from those of the TC sample. These results suggest that some fraction of SDS, which contained a small proportion of imperfect crystallites (Shin et al., 2004), transformed into a crystalline structure of RS during HMT, consequently improving RS content with higher melting temperatures. Regarding the RDS content, some conditions of HMT induced the reduction of the RDS content. This can be explained by the HMT induced conversion of the amorphous fraction of RDS into the imperfect crystallites of SDS; subsequently that SDS was transformed into the crystalline form of RS.

3.4.1.2 Impact of annealing and HMT temperature on starch fractions and thermal properties

Table 3.2 presents the starch fractions, *To*, *Tp*, *Tc* and *ΔH* of all TC samples after single hydrothermal treatments at various ANN and HMT temperatures. ANN increased RS content of TC sample from 37 to 43%. However, a higher ANN temperature for this study did not improve SDS and RS content.

Annealing at 8°C and 28°C below *Tp* of the TC sample (*Tp*-8C and *Tp*-28C respectively) enhanced the formation of RS at the same content of 42-43%. The initial crystalline perfection and packing density of A- or B-type crystalline structure influenced the ability to induce RS formation during annealing. The RS content of the recrystallized debranched waxy rice starch with more perfect structure of A-type increased after annealing at *Tp*-7°C, whereas annealing at *Tp*-15°C improved the RS content of recrystallized debranched waxy rice starch with a less perfect structure of B-type (Kiatponglarp et al., 2015). ANN at *Tp*-8C shifted melting temperatures to a higher temperature in the range of 108-122°C. However, the ΔH was lower (5.5 $J.g^{-1}$), suggesting that some double helices were lost. The ΔH reflects the amount of double helices and the crystalline order (Gunaratne & Hoover, 2002; Shi, Chen, Yu, & Gao, 2013). This demonstrated that ANN at a higher temperature enhanced the rearrangement of debranched starch molecules to improve its crystalline perfection. Increasing HMT temperature from 100°C to 140°C resulted in more RS formation from 52% to 55%. The melting temperatures also increased from 100-117°C to 104-124°C. This was probably due to the fact that HMT at a high temperature promotes the formation of crystalline perfection in two steps, including the disruption of the imperfect crystalline structure and dissociation of the double helical structure in the amorphous region followed by the re-crystallization process (Gunaratne & Hoover, 2002) to generate perfect crystallites. However, HMT at 130°C and 140°C showed similar RS content and thermal stability, suggesting that hydrothermal treatment of the TC sample, which had a perfect crystalline structure, required higher energy to unravel the weak helical glucans followed by rearrangement into the crystalline domain. Overall, the optimum condition for annealing was at *Tp*-8C for 48 h due to its

higher melting temperature range whereas the optimum condition for HMT was 20% moisture content at temperatures of 130°C and 140°C for 2 h because this generated the highest RS content.

Figure 3.1 shows the PCA score plot of all hydrothermal-treated TC samples. The total variation of 81.5% in the two principal components (PCs) of the PCA score plot clearly exhibits the contribution of melting parameters and starch fractions for all samples. The PC1 well described the variation of melting temperatures including *To*, *Tp*, and *Tc*. The TC→ANN starch at *Tp*-28C, TC→HMT starch at 100°C for 2 h, TC→HMT starch at 120°C for 1 h and TC sample were categorized into the group of lower *To*, *Tp*, and *Tc* in accordance with the results in Table 3.1 and 3.2 whereas the other samples located to the right of the vertical middle line were categorized into the higher *To*, *Tp*, and *Tc*. In addition, all of the TC→HMT starches with 20% moisture content which were located in the upper part of the horizontal middle line were categorized into the higher RS content and *ΔH*, which were separated from the TC sample, all TC→ANN samples, and TC→HMT samples with 30% moisture content, as partially described by PC2.

3.4.2 Effect of dual hydrothermal treatments on starch fractions and thermal properties

The combination of ANN at *Tp*-8C for 48 h and HMT with 20% moisture content at 130°C for 2 h was used in order to improve the RS content and the thermal properties of the TC sample. The percentages of increased RS, thermal and crystalline properties of single and dual hydrothermal-treated TC samples are summarized in Table 3.3. The TC→ANN sample showed an increased RS content of 16% compared to the TC sample which resulted from the enhancement of the glucan

Table 3.1 Starch fractions and thermal properties of HMT-treated temperature-cycled debranched starch

Sample	RDS (%)	SDS (%)	RS (%)	*To* (^{o}C)	*Tp* (^{o}C)	*Tc* (^{o}C)	*ΔH* (J.g^{-1})
TC	18.7 ± 1.3^{ab}	44.6 ± 1.1^{a}	36.7 ± 0.3^{e}	100.1 ± 0.1^{b}	108.6 ± 1.7^{c}	115.2 ± 1.0^{c}	7.3 ± 1.1^{ab}
TC→HMT 20mc120C 1h	16.0 ± 0.9^{c}	36.0 ± 0.4^{c}	48.0 ± 0.5^{b}	101.1 ± 0.4^{b}	110.7 ± 2.9^{bc}	118.2 ± 1.0^{b}	8.2 ± 1.1^{ab}
TC→HMT 20mc120C 2h	16.9 ± 0.6^{bc}	31.0 ± 1.0^{e}	52.1 ± 0.7^{a}	102.4 ± 0.0^{a}	113.9 ± 1.4^{ab}	120.1 ± 0.9^{ab}	11.0 ± 1.2^{a}
TC→HMT 20mc120C 3h	16.3 ± 0.5^{c}	31.8 ± 0.2^{e}	51.9 ± 0.7^{a}	102.7 ± 0.1^{a}	114.0 ± 1.7^{ab}	120.1 ± 1.8^{ab}	10.2 ± 0.5^{a}
TC→HMT 30mc120C 1h	18.1 ± 1.5^{abc}	38.0 ± 1.5^{b}	43.9 ± 0.0^{d}	101.4 ± 0.2^{b}	114.0 ± 0.4^{ab}	120.3 ± 0.5^{ab}	5.9 ± 2.3^{b}
TC→HMT 30mc120C 2h	16.1 ± 1.1^{c}	39.1 ± 0.9^{b}	44.8 ± 0.1^{c}	102.5 ± 0.3^{a}	115.8 ± 0.7^{a}	121.0 ± 0.6^{ab}	6.5 ± 2.4^{b}
TC→HMT 30mc120C 3h	17.1 ± 0.7^{bc}	33.8 ± 0.3^{d}	49.1 ± 0.7^{b}	102.7 ± 0.4^{a}	116.7 ± 1.4^{a}	121.5 ± 0.1^{a}	6.2 ± 1.9^{b}

Mean values with different superscripts within each column are significantly different ($p < 0.05$). RDS = rapidly digestible starch, SDS = slowly digestible starch, RS = resistant starch, *To* = onset melting temperature, *Tp* = peak melting temperature, *Tc* = conclusion melting temperature, *ΔH* = melting enthalpy, TC = temperature-cycled debranched starch, HMT = heat-moisture treatment, 20mc = 20% moisture content, 30mc = 30% moisture content, 120C = HMT at 120^{o}C, 1h = HMT for 1 h, 2h = HMT for 2 h, and 3h = HMT for 3 h.

Table 3.2 Starch fractions and thermal properties of single hydrothermal-treated temperature-cycled debranched starch with different annealing and HMT temperature

Sample	RDS (%)	SDS (%)	RS (%)	*To* (^{o}C)	*Tp* (^{o}C)	*Tc* (^{o}C)	*ΔH* (J.g^{-1})
TC	18.7 ± 1.3^{bc}	44.6 ± 1.1^{a}	36.7 ± 0.3^{d}	100.1 ± 0.1^{e}	108.6 ± 1.7^{c}	115.2 ± 1.0^{d}	7.3 ± 1.1^{cd}
TC→ANN : *Tp*-28C	20.8 ± 0.7^{a}	37.0 ± 0.6^{b}	42.2 ± 0.1^{c}	100.8 ± 0.0^{d}	109.0 ± 0.3^{c}	116.4 ± 0.3^{d}	8.1 ± 1.2^{c}
TC→ANN : *Tp*-8	19.4 ± 0.5^{b}	37.9 ± 0.8^{b}	42.7 ± 0.1^{c}	108.3 ± 0.1^{a}	115.7 ± 0.1^{a}	122.4 ± 0.1^{b}	5.5 ± 1.2^{d}
TC→HMT : 100C	15.8 ± 0.9^{d}	32.2 ± 0.1^{c}	52.0 ± 1.0^{b}	100.6 ± 0.4^{de}	108.3 ± 1.2^{c}	117.4 ± 2.7^{cd}	8.9 ± 2.1^{bcd}
TC→HMT : 120C	16.9 ± 0.6^{cd}	31.0 ± 1.3^{cd}	52.1 ± 0.7^{b}	102.4 ± 0.0^{c}	113.9 ± 1.4^{b}	120.1 ± 0.9^{c}	10.9 ± 1.4^{a}
TC→HMT : 130C	16.0 ± 0.4^{d}	29.4 ± 1.0^{d}	54.6 ± 0.9^{a}	103.9 ± 0.1^{b}	115.7 ± 0.0^{a}	124.6 ± 1.7^{a}	13.0 ± 1.3^{a}
TC→HMT : 140C	17.1 ± 0.3^{c}	30.7 ± 0.7^{cd}	54.2 ± 0.4^{a}	104.4 ± 0.4^{b}	115.4 ± 0.1^{a}	124.4 ± 0.4^{a}	8.6 ± 0.6^{bc}

Mean values with different superscripts within each column are significantly different ($p < 0.05$). RDS = rapidly digestible starch, SDS = slowly digestible starch, RS = resistant starch, *To* = onset melting temperature, *Tp* = peak melting temperature, *Tc* = conclusion melting temperature, *ΔH* = melting enthalpy, TC = temperature-cycled debranched starch, ANN = annealing, *Tp*-28C = annealed at a temperature 28^{o}C below *Tp* of TC sample for 48 h, *Tp*-8C = annealed at a temperature 8^{o}C below *Tp* of TC sample for 48 h, HMT = heat-moisture treatment at 20% moisture content for 2 h, 100C = HMT at 100^{o}C, 120C = HMT at 120^{o}C, 130C = HMT at 130^{o}C, and 140=HMT at140^{o}C.

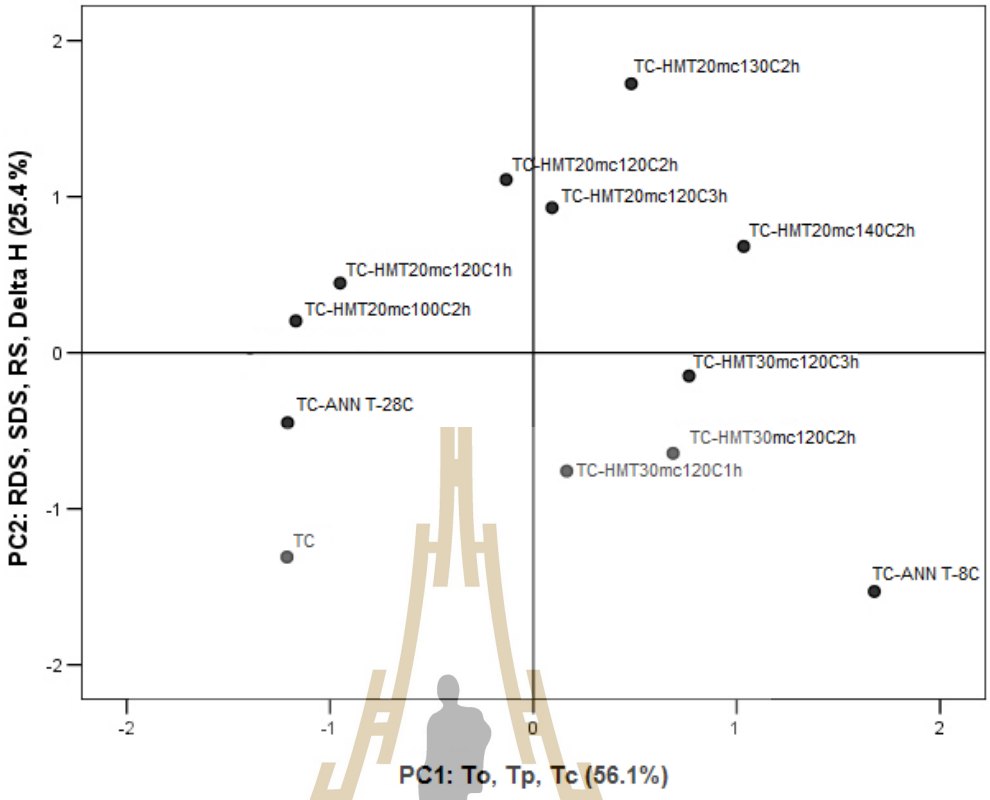

Figure 3.1 PCA score plot describing the variation of starch fractions and melting parameters of TC sample after subjected to various hydrothermal treatment conditions.

chain interaction within the crystalline and non-crystalline regions during ANN (Chung et al., 2010). As stated previously, the starch crystals of the TC sample were relatively perfect (*To*~100^{o}C). After ANN, some unstable crystallites of the TC sample were more susceptible to crystallite perfection which corresponded to a narrower peak width at half-height and a larger lateral crystal size. The TC→ANN sample showed a narrower *Tc-To*, suggesting that ANN induced molecular reorganization with more crystallite homogeneity. In addition, the relative crystallinity of TC→ANN sample increased from 40% (TC sample) to 49%. In contrast to the TC→ANN sample

a higher percentage of increased RS of the TC→HMT sample was obtained (49%). HMT probably induced a more perfect crystalline formation in two steps, as described previously, which decreased the enzyme digestibility. A larger *Tc-To* of the TC→HMT sample from 15.1°C to 20.7°C was observed, corresponding to a slightly decreased peak width at half-height and a larger lateral crystal size. This implies that HMT induced further formation of the double helical structure and induced the association of glucan chains in the amorphous and crystalline regions (Huang, Zhou, Jin, Xu, & Chen, 2015) to form more crystallite heterogeneity which was correlated with an increase in ΔH from 7.3 $J.g^{-1}$ to 13.0 $J.g^{-1}$ (Table 3.2). A similar result was also observed by Mutungi et al. (2009). The relative crystallinity of TC→HMT increased to 50%. Furthermore, HMT induced the transformation of the crystalline pattern from B-type to C-type. This was caused by dehydration of water during HMT as well as the movement of a pair of double helices of a less thermodynamically stable B-type structure with hexagonal packing of double helices into the central channel, resulting in changing the crystalline orientation to a more stable A-type structure (Gunaratne & Hoover, 2002).

Table 3.3 Physical and crystal properties of single and dual hydrothermal-treated temperature-cycled debranched starch

Properties	**TC**	**TC→ANN**	**TC→ANN→HMT**	**TC→HMT**	**TC→HMT→ANN**
Percentage of increased RS (%)	0	16.3	26.2	48.8	93.2
Tc-*To* (°C)	15.1	14.0	22.3	20.7	13.9
Crystalline pattern	B-type	B-type	C-type	C-type	B-type
Relative crystallinity (%)	40.2 ± 0.1	49.2 ± 0.8	51.0 ± 2.8	49.5 ± 1.8	53.1 ± 1.7
(100) peak width at half-height (°)	1.12 ± 0.02	0.98 ± 0.07	1.05 ± 0.03	1.02 ± 0.01	0.94 ± 0.04
Lateral crystal size (nm)	7.1 ± 0.1	8.2 ± 0.7	7.6 ± 0.2	7.8 ± 0.1	8.5 ± 0.3

To = onset melting temperature, *Tc* = conclusion melting temperature, TC = temperature-cycled debranched starch, TC→ANN = temperature-cycled debranched starch subjected to annealing at 8°C below *Tp* of TC sample for 48 h, TC→HMT = temperature-cycled debranched starch subjected to heat-moisture treatment with 20% moisture content at 120°C for 2 h, TC→ANN→HMT = temperature-cycled debranched starch subjected to annealing followed by heat-moisture treatment, and TC→HMT→ANN = temperature-cycled debranched starch subjected to heat-moisture treatment followed by annealing.

Regarding the dual hydrothermal treatment, TC→HMT→ANN showed an increased percentage of RS up to 93% as compared with the TC sample which exhibited the highest RS content (70.9%, Table 3.4). This result can be explained by the principle of the initial crystalline structure. As the crystallite form of the TC→HMT sample was relatively perfect and displayed more heterogeneity, after being subjected to HMT, the higher temperature could have melted the unstable crystalline part followed by a rearrangement to a new perfect crystalline structure. The additional step of ANN could have induced chain mobility within the amorphous and crystalline regions, subsequently rearranging a double helical aggregation to form a more perfect crystalline structure (Jagakody & Hoover, 2008) which showed a larger lateral crystal size (8.5 nm, Table 3.3). The larger lateral crystal size may have reduced the accessibility of enzymes because it had a lower surface area to volume ratio. This surface area to volume ratio is a more definitive parameter to describe particle aggregation (Lowell, Shields, Thomas, & Thommes, 2004). Mutungi et al. (2010) reported that the recrystallized starch accompanied by a bigger particle size and lower surface area to volume ratio showed a higher RS content. Moreover, the structure of RDS and SDS, which were amorphous and imperfect crystalline structures respectively, could have been transformed and/or re-arranged to the perfectly crystalline structure of RS during ANN corresponding to the reduction of RDS and SDS content to 11.2% and 17.9% respectively (Table 3.4). On the contrary, the TC→ANN→HMT showed a lower SDS content (25.4% SDS, Table 3.4) as compared with the TC→ANN sample (37.9% SDS, Table 3.2), suggesting that HMT at 130^{o}C could have destroyed some imperfect crystalline structures of SDS to become an amorphous structure of RDS which corresponded to the increased RDS content from 19.4% (TC→ANN) to 28.3% (Table 3.4). Simultaneously, HMT may also have

induced the realignment of some melted structures within the crystalline regions into a more perfect crystalline structure of RS. Thus, the RDS and SDS were transformed to RS as implied by the increased RS content from 42.7% to 46.3%. Obviously, the TC→ANN→HMT showed a lower percentage of increased RS than the TC→HMT→ANN (Table 3.3). Since the crystalline structure of the TC→ANN sample was improved to a more perfect structure (*To*~108^{o}C) and homogeneity (*Tc*-*To*= 14^{o}C), its partially unstable crystalline could have melted during HMT in order to form a more newly ordered structure. Moreover, the high temperature of HMT may have destroyed some crystalline regions (Zavareze & Dias, 2011). The last step of ANN in the TC→HMT→ANN could have reduced the variation in crystalline stability of the TC→HMT sample, resulting in a narrower *Tc*-*To*, associated with a smaller peak width at half-height as shown in Table 3.3. Furthermore, ANN enabled water hydration in the central channel of A-type crystallites and then rearranged the orientation of double helix to the B-type (Katopo, Song, & Jane, 2002), resulting in the transformation of the crystalline pattern from C+Vh type (TC→HMT) to B+Vh type but *Tp* of TC→HMT→ANN sample was similar to that of TC→HMT (115^{o}C). While the HMT of the TC→ANN→HMT induced the transformation of a crystalline pattern from B-type (TC→ANN) to C-type which had a more stable A-type structure, correlating to the slight shift of *Tp* from 116^{o}C (Table 3.2) to 118^{o}C (Table 3.4). Additionally, the *Tc*-*To* of the TC→ANN→HMT sample was broader, indicating that HMT facilitated the formation of inter and intra double helices by hydrogen bonding to form heterogeneous crystallites with a different stability. This result was relevant to a larger peak width at half-height and the smaller lateral crystal size of the TC→ANN→HMT.

For thermal properties, both dual hydrothermal treatments exhibited two melting temperature ranges of 106-128°C and 127-143°C respectively, as shown in Table 3.4. The first melting temperature range corresponded to the melting of RS formed by intermediate and longer chain glucans or by an amylose-lipid complex (Zaidual et al., 2008). The second melting temperature range was a characteristic of the dissociation of a recrystallized amylose (Onyango, Bley, Jacob, Henle, & Rohm, 2006) where it was reported in RS3 from other starchy sources (Sievert & Würsch, 1993; Shamai, Bianco-Peled, & Shimoni, 2003; Onyango et al., 2006). When compared with the TC→HMT→ANN, the TC→ANN→HMT showed a higher *Tp* (118°C) and *Tc* (128°C) for the first melting temperature. Moreover, the higher *To*, *Tp*, and *Tc* (135, 138, and 143°C) were also observed in the second melting temperature. This result indicates that the extreme condition of HMT may destroy the unstable crystalline aggregates and starch chains interaction in amorphous regions of the TC→ANN followed by the formation of the crystalline perfection to form more heat-stable crystalline structures (Mutungi et al., 2009). Therefore, the dual hydrothermal treatment of the TC→ANN→HMT can improve the stability of the crystallites. On the other hand, the *To* of the TC→HMT→ANN sample was shifted from 104°C to 108°C, indicating that the weakest crystallites of the TC→HMT were improved to crystallite perfection on ANN. However, when compared with dual hydrothermal treatment, the single hydrothermal treatment of ANN or HMT may not be sufficient to induce the formation of an amylose-amylose interaction in the TC sample. Thus, they showed only single melting temperature in the range of 104-125°C (Table 3.2).

Table 3.4 Effect of dual hydrothermal treatment on starch fractions and thermal properties of temperature-cycled debranched starch

Hydrothermal treatments	**TC→ANN→HMT**	**TC→HMT→ANN**
Starch fractions		
RDS (%)	28.3 ± 0.6[a]	11.2 ± 0.1[b]
SDS (%)	25.4 ± 0.3[a]	17.9 ± 0.9[b]
RS (%)	46.3 ± 0.3[b]	70.9 ± 2.7[a]
Thermal properties		
First endothermic transition		
To (°C)	105.5 ± 0.1[b]	108.8 ± 0.2[a]
Tp (°C)	118.4 ± 0.0[a]	115.4 ± 0.1[b]
Tc (°C)	127.6 ± 0.4[a]	122.7 ± 0.4[b]
ΔH ($J.g^{-1}$)	9.0 ± 0.1[a]	8.7 ± 0.5[a]
Second endothermic transition		
To (°C)	134.7 ± 0.3[a]	127.4 ± 1.3[b]
Tp (°C)	138.2 ± 0.0[a]	132.2 ± 0.9[b]
Tc (°C)	142.8 ± 0.1[a]	142.8 ± 0.1[a]
ΔH ($J.g^{-1}$)	0.9 ± 0.1[a]	1.2 ± 0.4[a]

Means values with different superscripts within each row are significantly different ($p < 0.05$). RDS = rapidly digestible starch, SDS = slowly digestible starch, RS = resistant starch, *To* = onset melting temperature, *Tp* = peak melting temperature, *Tc* = conclusion melting temperature, *ΔH* = melting enthalpy, TC→ANN→HMT = temperature-cycled debranched starch subjected to annealing followed by heat-moisture treatment, and TC→HMT→ANN = temperature-cycled debranched starch subjected to heat-moisture treatment followed by annealing.

3.4.3 Cooking stability of dual hydrothermal-treated temperature-cycled debranched starch

The cooking stability of dual hydrothermal-treated TC samples is illustrated in Figure 3.2. Interestingly, the RS content of all samples with 50% moisture cooking increased while that of 70% moisture cooking decreased. The extent of RS increment after cooking was related to the initial RS content. After cooking at intermediate moisture content (50%), the TC→HMT→ANN sample with a higher initial RS content (70.9%) showed an increase in RS content less than the TC→ANN→HMT sample with a lower initial RS content (46.3%). The lowest initial RS content of the TC sample (36.7%) showed an increase of RS and RDS. However, the 50% moisture cooked TC and the TC→ANN→HMT sample demonstrated a higher RS increment as compared with commercial RS2 (Hi-maize) and commercial RS3 (Novelose). Furthermore, the crystalline perfection also affects the amount of the RS increment after cooking. For instance, the crystalline structure of the TC→ANN→HMT sample was more perfect and had more thermal stability than the TC→HMT→ANN and TC samples, consequently cooking at 50% moisture content for 30 minutes promoted the rearrangement of linear glucan chains and induced the transformation of SDS to RS which was greater than for the other samples.

At high moisture content (70%), the reduction of RS content was observed in all cooked samples, whereas RDS was increased. The increasing of SDS content was detected for the 70% moisture cooked TC→HMT→ANN, Hi-maize, and Novelose. This indicates that heating of these starches at a higher moisture content can disrupt some imperfect crystallites in the RS structure and convert the unstable RS to SDS as well as the unstable SDS to RDS (Wandee, Puttanlek, Rungsardthong,

Puncha-arnon, & Uttapap, 2012). In addition, the reduction of RS content in the TC→ANN→HMT sample was the lowest which is associated with its higher thermal stability (Table 3.4). This implies that the TC and TC→ANN→HMT samples had a higher cooking stability.

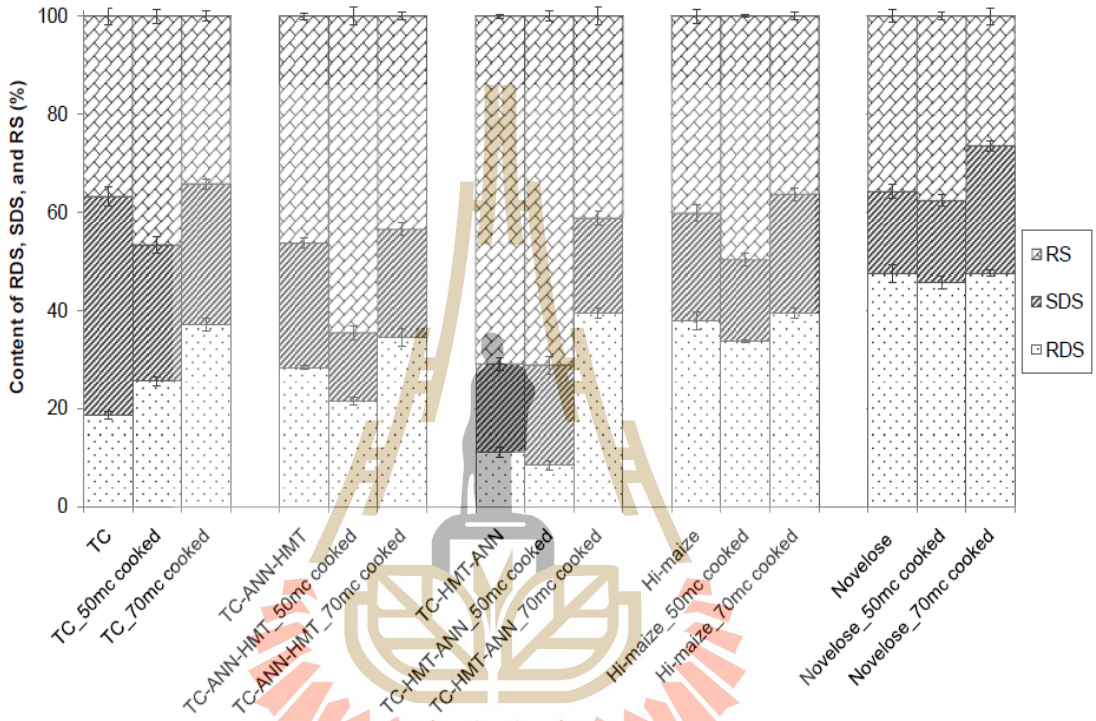

Figure 3.2 Cooking stability of the hydrothermal-treated TC sample after cooking at 50% and 70% moisture content compared with Hi-maize 260 and Novelose 330.

3.5 Conclusions

Single hydrothermal treatment with annealing or HMT can increase RS content and thermal stability of the TC sample due to the fact that both annealing and HMT can induce the interaction of glucan chains on double helical formation and a more perfect crystalline structure of RS. However, HMT showed a higher increment of RS

content than annealing because it melted some imperfect crystallites and facilitated the formation of double helices by hydrogen bonding to form crystallites with different stability. Applying the dual hydrothermal treatments of annealing and HMT improved the amount of RS and thermal stability more than a single hydrothermal treatment. The sequence of ANN or HMT had an influence on both structural and thermal properties. The HMT→ANN treatment showed the highest RS content whereas the ANN→HMT treatment showed higher thermal stability by inducing the transformation of the crystalline structure to a more crystalline perfection. The initial RS content and crystalline perfection of products had an impact on the starch fractions after cooking. After cooking at 50% moisture, the sample with a lower initial RS content and more crystalline perfection (TC→ANN→HMT) showed an improvement of RS content greater than the TC→HMT→ANN sample with a higher initial RS content and less crystalline perfection. Cooking at 70% moisture induced the transformation of RS into SDS and SDS into RDS. Therefore, the combination of temperature cycled treatment together with hydrothermal treatment have the potential to improve the RS content, thermal stability and cooking stability of debranched cassava starch.

3.6 Acknowledgements

This research was financially supported by the Thailand Research Fund (TRF) through the Royal Golden Jubilee (RGJ) Ph.D. Program (Grant No. PHD/0090/2552) and Suranaree University of Technology. The authors are grateful to A. Buléon, L. Chaunier and S. Soontaranon for their interpretation and technical support.

3.7 References

AOAC. (2002). **Official methods of analysis of AOAC international 17th ed.,** AOAC International, Gairhersburg, MD, USA.

Cairns, P., Bogracheva, T, Y., Ring, S. G., Hedley, C. L., & Morris, V. J. (1997). Determination of the polymorphic composition of smooth pea starch. **Carbohydrate Polymers,** 32, 275-282.

Chung, H.-J., Liu, Q., & Hoover, R. (2010). Effect of single and dual hydrothermal treatments on the crystalline structure, thermal properties, and nutritional fractions of pea, lentil, and navy bean starches. **Food Research International,** 43(2), 501-508.

Chung, H.-J., Hoover, R., & Liu, Q. (2009). The impact of single and dual hydrothermal modifications on the molecular structure and physicochemical properties of normal corn starch. **International Journal of Biological Macromolecules,** 44(2), 203-210.

Englyst, H. N., Kingman, S. M., & Cummings, J. H. (1992). Classification and measurement of nutritionally important starch fractions. **European Journal of Clinical Nutrition,** 46, S33-S50.

Farhat, I. A., Blanshard, J. M. V. & Mitchell, J. R. (2000). The retrogradation of waxy maize starch extrudates: effects of storage temperature and water content. **Biopolymers**, 53(5), 411-422.

Gidley, M. J., & Bulpin, P. V., (1987). Crystallisation of malto-oligosaccharides as models of the crystalline forms of starch: minimum chain-length requirement for the formation of double helices. **Carbohydrate Research,** 161, 291-300.

Gunaratne, A., & Hoover, R. (2002). Effect of heat-moisture treatment on the structure and physicochemical properties of tuber and root starches. **Carbohydrate Polymers,** 49, 425-437.

He, J., Liu, J., & Zhang, G. (2008). Slowly digestible waxy maize starch prepared by octenyl succinic anhydride esterification and heat-moisture treatment: Glycemic response and mechanism. **Biomacromolecules,** 9, 175-184.

Huang, T.-T., Zhou, D.-N., Jin, Z.-Y., Xu, X.-M., & Chen, H.-Q. (2015). Effect of debranching and heat-moisture treatments on structural characteristics and digestibility of sweet potato starch. **Food Chemistry,** 187, 218-224.

Jacobasch, G., Dongowski, G., Schmiedl, D., & Müller-Schmehl, K. (2007). Hydrothermal treatment of Novelose 330 results in high yield of resistant starch type 3 with beneficial prebiotic properties and decreased secondary bile acid formation in rats. **British Journal of Nutrition,** 95(06), 1063-1074.

Jayakody, L., & Hoover, R. (2008). Effect of annealing on the molecular structure and physicochemical properties of starches from different botanical origins-A review. **Carbohydrate Polymers,** 74, 691-703.

Katopo, H., Song, Y., & Jane, J.-I. (2012). Effect and mechanism of ultrahigh hydrostatic pressure on the structure and properties of starches. **Carbohydrate Polymers,** 47(3), 233-244.

Kiatponglarp, W., Tongta, S., Rolland-Sabaté, A., & Buléon, A. (2015). Crystallization and chain reorganization of debranched rice starches in relation to resistant starch formation. **Carbohydrate Polymers,** 122, 108-114.

Lehmann, U., Jacobasch, G., & Schmiedl, D. (2002). Characterization of resistant starch typeIII from banana (Musa acuminate). **Journal of Agriculture and Food Chemistry,** 50, 5236-5240.

Lowell, S., Shields, J. E., Thomas, M. A., & Thommes, M. (2004). **Characterization of porous solids and powders: Surface area, pore size and density.** Dordrecht: Kluwer Academic Publishers.

Miao, M., Jiang, B., & Zhang, T. (2009). Effect of pullulanase debranching and recrystallization on structure and digestibility of waxy maize starch. **Carbohydrate Polymers,** 76, 214-221.

Mutungi, C., Onyango, C., Doert, T., Paasch, S., Thiele, S., Machill, S., et al.. (2011). Long- and short-range structural changes of recrystallised cassava starch subjected to in vitro digestion. **Food Hydrocolloids,** 25(3), 477-485.

Mutungi, C., Onyango, C., Rost, F., Doert, T., Jaros, D., & Rohm, H. (2010). Structural and physicochemical properties and in vitro digestibility of recrystallized linear α-D-(1→4) glucans derived from mild-acid-modified cassava starch. **Food Research International,** 43(4), 1144-1154.

Mutungi, C., Rost, F., Onyango, C., Jaros, D., & Rohm, H. (2009). Crystallinity, Thermal and Morphological Characteristics of Resistant Starch Type III Produced by Hydrothermal Treatment of Debranched Cassava Starch. **Starch-Stärke,** 61 (11), 634-645.

Niba, L. L. (2003). Processing effects on susceptibility of starch to digestion in some dietary starch sources. **International Journal of Food Sciences and Nutrition,** 54, 97-109.

Onyango, C., Bley, T., Jacob, A., Henle, T., & Rohm, H. (2006). Influence of incubation temperature and time on resistant starch type III formation from autoclaved and acid-hydrolysed cassava starch. **Carbohydrate Polymers,** 66,494-499.

Sajilata, M. G., Singhal, R. S., & Kulkarni, P. R. (2006). Resistant Starch- A Review. **Comprehensive Reviews in Food Science & Food Safety,** 5, 1-17.

Shamai, K., Bianco-Peled, H., & Shimoni, E. (2003). Polymorphism of resistant starch type III. **Carbohydrate Polymers,** 54, 363-369.

Shi, M., Chen, Y., Yu, S., & Gao, Q. (2013). Preparation and properties of RS III from waxy maize starch with pullulanase. **Food Hydrocolloid,** 33, 19-25.

Shin, S. I., Choi, H. J., Chung, K. M., Hamaker, B., Park, K. H., & Moon, T. W. (2004). Slowly digestible starch from debranched waxy sorghum starch: preparation and properties. **Cereal Chemistry,** 81, 404-408.

Shin, S. I., Kim, H. J., Ha, H. J., Lee, H. S., & Moon, T. W. (2005). Effect of hydrothermal treatment on formation and structural characteristics of slowly digestible non-pasted granular sweet potato starch. **Starch/Stärke,** 57, 421-430.

Sievert, D., & Würsch, P. (1993). Thermal behaviour of potato amylose and enzyme-resistant starch from maize. **Cereal Chemistry,** 70, 333-350.

Silverio, J., Fredriksson, H., Andersson, R., Eliasson, A.-C., & Aman, P. (2000). The effect of temperature cycling on the amylopectin retrogradation of starches with different amylopectin unit-chain length distribution. **Carbohydrate Polymers,** 42, 175-184.

Topping, D. L., & Clifton, P. M. (2001). Short-chain fatty acid and human colonic function: Roles of resistant starch and nonstarch polysaccharides. **Physiological Reviews,** 81(3), 1031-1064.

Topping, D. L., Segal, I., Regina, A., Conlon, M. A., Bajka, B. H., Toden, S. et al. (2010). Resistant starch and human health. In J. Willem van der Kamp, J. Jones, B.McCleary and David T. (eds.) **Dietary fiber: new frontiers for food and health.** Wageningen Academic Publishers, Natherland, pp. 311-322.

Wandee, Y., Puttanlek, C., Rungsardthong V., Puncha-arnon, S., & Uttapap, D. (2012). Effects of gelatinization and gel storage conditions on the formation of canna resistant starch. **Food Bioprocess Technology,** 5, 2665-2673.

Zaidul, I. S. M., Absar, N., Kim, S-J., Suzuki, T., Karim, A. A., Yamauchi, H. et al. (2008). DSC study of mixtures of wheat flour and potato, sweet potato, cassava, and yam starches. **Journal of Food Engineering,** 86, 68-73.

Zavareze, E. . R., & Dias, A. R. G. (2011). Impact of heat-moisture treatment and annealing in starches: A review. **Carbohydrate Polymers,** 83(2), 317-328.

Zeng, F., Chen, F., Kong, F., Gao, Q., Aadil, R. M., & Yu, S. (2015). Structure and digestibility of debranched and repeatedly crystallized waxy rice starch. **Food Chemistry,** 187, 348-353.

Zeng, F., Ma, F., Gao, Q., Yu, S., Kong, F., & Zhu, S. (2014). Debranching and temperature-cycled crystallization of waxy rice starch and their digestibility. **Carbohydrate Polymers,** 113, 91-96.

CHAPTER IV

EFFECT OF AMYLOMALTASE AND RECRYSTALLIZATION METHOD ON MACRO-MOLECULAR CHARACTERISTICS, STARCH DIGESTIBILITY, THERMAL PROPERTIES AND COOKING STABILITY OF CASSAVA STARCH

4.1 Abstract

The modification of cassava starch with amylomaltase (AM) was investigated. The AM-treated starches showed a decreased amylose content. The proportion of long chain (DP 25-80) increased with longer reaction time up to 24 h. The molecular structure of AM-treated starch for 5 min (AM5min) and 4 h (AM4h) before and after β-amylolysis were characterized. The results showed that molar mass of both AM-treated starches gradually decreased with the reaction time. The AM5min demonstrated a higher average chain length (CL), external CL, and β-amylolysis than AM4h as determined by H^1-NMR. Both AM-treated starches showed larger proportions of long chain (DP 25-80) as compared with non-AM-treated starch, indicating that AM could elongate the starch chain length. After recrystallized by isothermal incubation and HMT, the crystallized, debranched AM-treated starches showed more RS content and higher thermal stability as compared with the non-AM-treated starch, which resulted from its crystallized residues after acid hydrolysis had a

higher proportion of DP >25. The isothermal-treated starch had a higher RS content (58% RS) but the HMT-treated starch showed the higher melting temperature (104-132^{o}C). The thermo-molding process was applied with debranched AM-treated starch for 5 min. The molded sample with a small surface area to volume ratio (1.93 mm^{-1}) showed an improvement of RS yield (65.1% RS). Its surface morphology was a densely packed structure with a smooth surface as monitored by SEM. Nevertheless, the slowly digestible starch and RS yield of the molded sample depends on its surface area to volume ratio. The cooking stability of molded sample with different surface area to volume ratio was improved at 70% moisture cooking. All cooked, molded samples showed an increase in RS content. Overall, the combination of enzymatic modification, hydrothermal treatments, and thermo-molding could be improved RS content, thermal properties and cooking stability of cassava starch.

Keywords: amylomaltase, recrystallization, thermo-molding process, slowly digestible starch, resistant starch, thermal stability

4.2 Introduction

Starch is one of the major components of food products and serves as energy for human diets. For the nutritional starch, it was classified into three major fractions, including rapidly digestible starch (RDS), slowly digestible starch (SDS) and resistant starch (RS), regarding the rate of glucose release and absorption in the intestinal tract (Englyst, Kingman, & Cummings, 1992). Since SDS is completely digested in the small intestine at a lower rate than RDS, SDS may help control and prevent hyperglycemia. RS is the portion of starch that escapes the digestion in the small intestine, but it is fermented in the large intestine into short-chain fatty acids, which is

beneficial for colon health and protection against colorectal cancer (Lehmann and Robin, 2007). Therefore, the methods for improvement of SDS and RS content of starchy food have been widely studied in recent years. RS has been categorized into 4 or 5 types (Topping et al., 2010) depending on the mode of resistance. However, RS3 seems to be of interest because of its physical and physiological properties.

It is well recognized that RS3 contains mainly retrograded amylose (Eerlingen et al., 1993) which consists of short linear segments of α-1,4-glucans arranged in a crystalline structure. Thus, starch with large amounts of amylose and/or long branch chains of amylopectin, such as legume and high-amylose starches (high amylose maize starch), has been widely used as a starting material to produce RS3 over the last decades (Sievert & Pomeranz 1989; Vasanthan & Bhatty 1998), which is expensive. Many technologies have been developed to produce RS3 from a group of amylose-containing starches, including repeated cycles of autoclaving and heating together with complete debranching. Because of the interference of amylopectin during amylose retrogradation, debranching enzymes, such as isoamylase and pullulanase was applied to hydrolyze α-D-(1→6) glycosidic branching of amylopectin in order to produce linear molecules that can re-associate, leading to decreasing the susceptibility to hydrolysis with amylolytic enzymes. The long-branch chains of amylopectin have properties similar to amylose, which increase the apparent amylose content of the starch. On the contrary, the short-branch chains of amylopectin form double helices that are not long enough to produce stable crystallites. The longer chains of debranched starch could generate stronger double helices than shorter chain and becomes more heat resistant (Cai & Shi, 2010).

Recently, 4-α-glucanotranferase namely amylomaltase (AM, EC 2.4.1.25) has

been studied to modify the starch structure in many sources, i.e. waxy corn starch, waxy rice starch, corn starch, rice starch, potato starch, high amylose potato starch, pea starch and wheat starch. (Do et al., 2012; Cho et al., 2009; Hansen, Blennow, Pedersen, & Engelsen, 2009; Hansen, Blennow, Pedersen, Norgaard, & Engelsen, 2008; van der Maarel et al., 2005). It catalyzed the disproportionation reaction of starch gel via intermolecular transglycosylation by transferring segments of amylose to amylopectin branch chains in order to obtain the broadening of the side chain length distribution of amylopectin, which consisted of both shorter and longer chains. The newly formed of amylopectin molecules with longer chains length exhibits an amylose-like behavior in relation to the formation of thermoreversible starch gels with a high thermal stability as compared to its corresponding parent starch gels but the melting temperature is dependent on the reaction conditions and enzyme dosage (Lee, Kim, Park, & Lee, 2006; van der Maarel, et al., 2005; Kaper et al., 2005). Moreover, AM can be used for the production of cycloamylose (CA) by an intermolecular transglycosylation (Bhuiyan, Kitaoka, & Hayashi, 2003; Terada, Fujii, Takaha, & Okada, 1999). There is limited information regarding the combination used of AM and debranching enzyme on enzyme digestibility of cassava starch and its thermal properties. The study of the combination of AM and debranching enzyme on the enzyme digestibility and thermal properties is of interesting to understand the relationship among chain length distribution, RS3 formation, and thermal properties. Moreover, the further investigation of recrystallization methods on the enzyme digestibility, thermal properties, and cooking stability of the resulting products will be included to provide the optimum method for the development of a starchy product with improving the yield of RS and its thermal properties.

4.3 Materials and Methods

4.3.1 Materials

Cassava starch was a gift from SanguanWongse Industries Co., Ltd. (Nakhon Ratchasima, Thailand). Amylomaltase (AM) from *Thermus aquaticus* was provided by Novozymes (Bagsvaerd, Denmark) (4,967.14 $U.mL^{-1}$). One unit of AM activity is defined as the amount of enzyme that produces 1 μmol of glucose per minute at pH 6.5, 70°C with maltotriose as substrate. Isoamylase (EC 3.2.1.68, E-ISAMY, specific activity 210 $U.mL^{-1}$), a resistant starch assay kits, and β-amylase (2,484 U mg^{-1}) from *Bacillus cereus* were purchased from Megazyme International (Ireland). The β-amylase was desalted against 40 mM phosphate buffer, pH 7.2, by using dialysis tubing cellulose membranes (MW 10233) purchased from Sigma (Saint Quentin Fallavier, France). The PGO enzyme kits (P1179), o-dianisidine (D3252), glucose, maltose, maltotriose, maltotetraose, maltopentaose, maltohexaose, and maltoheptaose were purchased from Sigma Chemical Co. (St. Louis, MO., USA). Other chemicals were of analytical grade.

4.3.2 Enzymatic modification

4.3.2.1 Preliminary study on cassava starch treated with AM

A preliminary study was carried out by varying AM concentration at 5 and 8 U.g $starch^{-1}$. The AM-treated cassava starch was prepared according to the procedure of van der Marrel et al. (2005) with slight modification. The 8% (w/v in 50 mM phosphate buffer, pH 6.0) cassava starch suspension was gelatinized using a shaking water bath with a heating at 70°C for 30 min followed by heating at 100°C for 30 min. After cooling to 70°C, AM (5 and 8 U.g $starch^{-1}$) was added and then incubated for 3 h and 24 h with glass bead shaking. At each time of

reaction, the enzyme reaction was terminated by boiling at 100°C for 30 min. Then, the products were freeze-dried using liquid N_2 and a freeze dryer (GEA, GT2-S, Germany), milled using mortar and pestle and sieved through a 120 mesh screen. The chain length (CL) distribution of samples was analyzed as a procedure following section 4.3.4.1.

4.3.2.2 Cassava starch treated with AM at various reaction times

The gelatinized cassava starch (8%) was prepared by the procedure described above. After cooling to 70°C, AM (8 U g starch^{-1}) was added and then incubated for 5 min, 30 min, 2 h, 3 h, 4 h, and 24 h with glass bead shaking. At each time of reaction, the enzyme reaction was terminated by boiling at 100°C for 30 min. Then, the products were freeze-dried using liquid N_2 and a freeze dryer (GEA, GT2-S, Germany), milled using mortar and pestle and sieved through a 120 mesh screen. The sample powders were analyzed amylose content and wavelength of the maximum absorbance as procedure following section 4.3.3, CL distribution as procedure following section 4.3.4.1 respectively.

4.3.2.3 Cassava starch treated with AM followed by isoamylase

The cassava starch was treated with AM (8 U g starch^{-1}) for 0 min, 5 min and 4 h as the procedure described in section 4.3.2.2. At each time of reaction, the enzyme reaction was terminated by boiling at 100°C for 30 min. The pH was adjusted to 4.5 using 0.5 M phosphoric acid solution. After that, isoamylase 5 U g starch^{-1} (unit was defined as the supplier) was added and the reaction mixture was incubated at 50°C for 24h with glass bead shaking. At the end of hydrolysis, the enzyme activity was stopped by heating at 85°C for 30 min. Then, the products were freeze-dried using liquid N_2 and a freeze dryer (GEA, GT2-S, Germany), milled using

mortar and pestle and sieved through a 120 mesh screen. The debranched AM-treated cassava starch for 0 min was referred to debranched native cassava starch (DS) whereas debranched AM-treated cassava starches for 5 min and 4 h were labeled to DAM5min and DAM4h respectively.

4.3.3 Determination of amylose content and wavelength of the maximum absorbance (λmax)

Amylose content of native and AM-treated cassava starch was determined using the method of Juliano (1971) with a slight modification. Sample (100 mg) was wet with 1 mL of ethyl alcohol. After that, 10 mL of 1 N sodium hydroxide solution was added and swirled to disperse the sample. The mixture was heated in a boiling water bath for 10 min. Then, it was diluted to 100 mL with distilled water. An aliquot (0.5 mL) was pipetted into a separate tube. Distilled water (5 mL) was added, followed by adding 0.1 mL of acetic acid and 0.2 mL of iodine solution. Finally, distilled water was added in order to make volume to 10 mL, mixed immediately on a vortex and stored for 30 min to fully develop color. The absorbance at 600 nm of developed color has measured against the blank (for amylose content determination) and wavelength was scanned from 400 to 800 nm (for λmax determination). The amylose content was calculated from calibration curves of a standard mixture between amylose and amylopectin from potato starch.

4.3.4 Structural characteristics analysis of native and AM-treated starch

4.3.4.1 Chain length distribution determined by high-performance anion exchange chromatography with pulsed amperometric detection (HPAEC-PAD)

Chain length (CL) distribution of starches was analyzed after isoamylase debranching as the procedure of Rolland-Sabaté et al. (2012) with slight modification. The debranched sample (25 mg) was solubilized in 0.5 mL of 1 M potassium hydroxide at 4ºC for 3 days under gentle magnetic stirring. Then, the deionized (DI) water (2 mL) and 0.1 M hydrochloric acid (2.5 mL) were added. The resulting solution (5 g L^{-1}) was filtered through 0.2 μm filter. CL distribution was analyzed by HPAEC-PAD (Model ICS-5000 DC, Dionex, Sunnyvale, CA, USA). Samples of 20 μL (100 μg of linear α- glucan) were injected on a CarboPac PA-200 column (3 mm x 250 mm). The separation was carried out at 30°C, the eluent was 500 mM sodium hydroxide (eluent A), 1 M sodium acetate (eluent B), and DI water (eluent C) with a flow rate of 0.3 mL·min^{-1}. The elution was an isocratic 30% eluent A, 70% eluent C and the following eluent B gradient profile: 0-5 min: 0-12.5%, 5-50 min: 12.5-30.5%, 50-110 min: 30.5-50%, and 110-142.5 min: 50-0%. Single peaks were integrated and corrected for the detector response. The linear glucans of DP 2-7 were used as a standard.

4.3.4.2 The β-limit dextrin preparation

The β-limit dextrins of native and AM-treated cassava starches were prepared following the method of Rolland-Sabaté et al. (2014) with slight modification. The starch samples were dissolved in 90% dimethyl sulfoxide (50 mg.mL^{-1}) for 3 days with agitation at room temperature. The starch solution was

diluted five times in phosphate buffer (40 mM, pH 7.2). The diluted solution was incubated with *B. cereus* β-amylase (15 $U.mg^{-1}$) at 40 °C for 24 h with agitation. Then, the reaction medium was heated in a boiling water bath for 10 min and centrifuged at 10,000x*g* for 10 min at 4°C. The supernatant was dialyzed against water for 24 h and then against 40 mM phosphate buffer at pH 7.2. Thereafter, the β-limit dextrins were incubated with *B. cereus* β-amylase (15 $U.mg^{-1}$) at 40 °C for a further 24 h with agitation in order to complete enzymatic hydrolysis. At the end of hydrolysis, the β-amylase activity was terminated by heating in a boiling water bath for 10 min. The final β-limit dextrins were dialyzed against water for 24 h and precipitated with 10 volumes of 96% ethanol. The precipitate was collected by centrifugation (10 min, 10,000x*g*) and washed three times with 1 volume of absolute ethanol at 4 °C. The resulting precipitate was resuspended in milliQ water and freeze-dried. The β-limit dextrins were injected in the HPSEC-MALL-DRI system and also determined the amount of branching degree and percentage of β-amylolysis by ^{1}H NMR.

4.3.4.3 Molecular mass and size distribution determined by high-performance size exclusion chromatography coupled with multi-angle laser light scattering and differential refractive index (HPSEC-MALLS-DRI)

Native and AM-treated cassava starches and their β-limit dextrins samples were prepared by the method of Rolland-Sabaté et al. (2012) with a slight modification. The samples were dissolved in 95% dimethyl sulfoxide (50 mg mL^{-1}) for 3 days with agitation at room temperature. Then, the solution was precipitated with 95% ethanol at 4^{o}C overnight. The precipitates were recovered by centrifugation at 27,000x*g* for 10 min at 25°C. The sediments were rinsed with 99% ethanol followed by acetone and then air-dried. The sample powder (10 mg) was

dissolved in 20 mL of Millipore water followed by carefully degassed with nitrogen gas. After that, the solution was heated in microwave 900 W for 40 sec followed by cooled down in ice batch. The resulting solution was filtered through 0.5 µm syringe filter and diluted before injected into SEC-MALLS-DRI system. The system was operated with Shodex KW-802.5 column (8 mm ID x 30 cm) from Showa Denko K.K. (Tokyo, Japan) together with KW-G guard column (6 mm ID x 5 cm) from Showa Denko K.K. The column and guard column were maintained at 30^{o}C using a Crococil temperature control system from Cluzeau (Bordeaux, France). The eluant (Millipore water containing 0.02 g.L^{-1} sodium azide) was carefully degassed and filtered through Durapore GV (0.2 µm) membrane from Millipore before used and eluted at the flow rate 0.5 ml/min. The two online detectors consisted of a MALLS instrument (Wyatt Technology Corporation, Santa Barbara, CA) and an ERC-7515A refractometer (Erma, Tokyo, Japan).

4.3.4.4 Nuclear magnetic resonance spectroscopy (NMR)

Native and AM-treated cassava starches and their β-limit dextrins were determined branching degree (%BD) and average CL using ^{1}H NMR. The samples were prepared according to the method of Nilsson, Nilsson, and Lund. (1996) with slight modification. Dried samples were exchanged in 99.9 % atom deuterium oxide (8.33 mg mL^{-1}) and heated at 95^{o}C for 25 min followed by lyophilized. This process was repeated twice. Before measurement, the dried, deuterated samples were prepared immediately by dissolved in 99.9% atom deuterium oxide and never cooled below 70^{o}C. The ^{1}H NMR measurements were performed with Bruker Avance III (NB) 400 MHz spectrometer using a 5 mm BBO H/X probe at 70^{o}C. In order to estimate the areas of interested, a spectral decomposition with a

mixture of Gaussian and Lorentzian curves was carried out using Peakfit® software. The percentages of α (1,4) and α (1,6) linkages in all samples were calculated by integrating the corresponding anomeric proton signals. The %BD and average CL were calculated according to Nilsson et al. (1996), average external chain length (ECL), internal chain length (ICL), and β-amylolysis (%) were calculated according to Yan & Matheson, 1993 and Rolland-Sabaté et al. (2014) as follows:

$$\text{Branching degree (BD, \%)} = \frac{\text{integral (H1}-\text{Glc } \alpha 1\rightarrow 6)}{\text{integral(H1}-\text{Glc } \alpha\ 1\rightarrow 4)+\text{integral (H1}-\text{Glc } \alpha 1\rightarrow 6)} \times 100 \quad (1)$$

$$\text{Average chain length (CL)} = \text{integral(H1} - \text{Glc } \alpha\ 1\rightarrow 4) + \text{integral (H1} - \text{Glc } \alpha 1\rightarrow 6) \quad (2)$$

$$\text{Average external chain length(ECL)} = \text{CL of sample} - \text{CL of } \beta - \text{limit dextrin} + 2 \quad (3)$$

$$\text{Internal chain length (ICL)} = \text{CL} - \text{ECL} - 1 \quad (4)$$

$$\beta - \text{amylolysis (\%)} = \frac{(\text{ECL}-2)}{\text{CL}} \text{x } 100 \quad (5)$$

4.3.4.5 Cyclo-structure molecule analysis by MALDI-TOF

The AM-treated cassava starches (AM5min and AM4h) were hydrolyzed with amyloglucosidase at a concentration of 20 U g^{-1} sample at 37°C for 24 h. Then, the hydrolyzed products were precipitated with 70% ethanol. The precipitates were air-dried and ground for characterization of the cyclo-structure molecule using MALDI-TOF (Bruker, microflex) based on the method of Sorndech et al. (2015) compared to a standard protein with Mw 800-17000 Dalton and using cycloamylose from Ezaki Glico as a reference sample.

4.3.5 Recrystallization method

4.3.5.1 Isothermal temperature incubation

The debranched native and AM-treated cassava starches prepared from section 4.3.2.3 (1 g, db) were adjusted the moisture content to 90% by DI water in tightly closed tubes and incubated at 50°C for 3 days in a hot air oven.

After 3 days of reaction, the products were filtered and the precipitates were air-dried to obtain 12% moisture content, milled as mentioned previously.

4.3.5.2 Heat-moisture treatment

The debranched native and AM-treated cassava starches as prepared following section 4.3.2.3 (1 g, db) were mixed with DI water in tightly closed tubes to obtain 30% moisture content. It was placed in a hot air oven at 130°C for 3h. The HMT-treated starches were air-dried to obtain 12% moisture content, milled as mentioned previously.

4.3.6 Chain length distribution of the crystalline residues of debranched native and AM-treated cassava starch by high-performance anion exchange chromatography with pulsed amperometric detection (HPAEC-PAD)

The crystalline residues of debranched native and AM-treated cassava starches were prepared according to the method of Gérard, Colonna, Buléon, & Planchot, (2002) with slight modification. Samples (3 g) were hydrolyzed with 2.2 N hydrochloric acid (10 mL) at 35ºC for 35 days to remove the amorphous regions of samples. The obtained crystalline residues of all debranched starches were rinsed with DI water until the pH closer to 7 and centrifuged at 2,000x*g* for 10 min followed by air drying. Then, the dried samples were prepared to analyze CL distribution according to the method as described previously.

4.3.7 Starch fractions determination

The starch fractions (RDS, SDS, and RS) of samples were measured according to the method of official AOAC method 2002.02 and Englyst et al. (1992) with slight modification. A sample (100 mg) was incubated with 4 mL of sodium maleate buffer (pH 6.0) containing pancreatic α-amylase (10 $mg.mL^{-1}$) and

amyloglucosidase (3 $U.mL^{-1}$) in a shaking water bath with continuous shaking at 37°C for 16 h. During 20 min of incubation, an aliquot (0.4 mL) was taken and mixed well with an equal volume of absolute ethanol, followed by adding two volumes of 50% ethanol (v/v). The volume was adjusted to 10 mL and the D-glucose content was measured using glucose oxidase/peroxidase reagent (GOPOD reagent) for used to calculate the SDS content. After 16 h of incubation, the reaction is terminated by the addition of an equal volume of absolute ethanol and the RS is recovered as a pellet on centrifugation. Then, the pellet was washed twice by suspension in 4 mL of 50% ethanol (v/v), followed by centrifugation. The supernatant was carefully decanted and collected. Then, the volume was adjusted to 10 mL and the D-glucose content was measured using GOPOD reagent for used to calculate the SDS content. The RS in the pellet was dissolved in 2 mL of 2 M potassium hydroxide and stirred in an ice bath for 20 min. The 1.2 M sodium acetate buffer pH 3.8 (8 mL) was added and followed by 0.1 mL of amyloglucosidase (3,300 U/mL). After that, it was incubated at 50°C in a shaking water bath for 30 min. The hydrolyzed sample was diluted with deionized water. The D-glucose content was determined using GOPOD reagent. The GOPOD enzyme reagent (3 ml) was added to 0. 1 mL of diluted sample, then it was incubated at 50°C for 20 min. The absorbance at 510 nm was measured against a reagent blank. The percentages of RDS, SDS, and RS were calculated as follows:

RDS (%) = glucose released at 20 min x 162/180 x 100 (6)

SDS (%) = glucose released at 16 h - glucose released at 20 min x 162/180 x 100 (7)

RS (%) = glucose content in the indigested starch at 16 h x 162/180 x 100 (8)

4.3.8 Crystalline properties

The crystalline properties were monitored using wide-angle X-ray diffraction

(WAXD). The samples were prepared by adjustment the moisture content at 90% relative humidity for 10 days in desiccators under partial vacuum in the presence of a saturated barium chloride solution. Approximately twenty mg sample was placed between two tape foils during the experiment. The diffractograms were recorded on a BRUKER^{TM} (Karlsruhe, Germany) D8 Discover diffractometer with Cu $K_{\alpha 1}$ radiation (λ=1.54Å). A two-dimension GADDS detector was used to collect the diffracted beam. The recording time for each data collection was 600 s. The sample to detector distance was 100 mm. X-ray spectral data were visualized and normalized using KaleidaGraph software. The Origin Pro 8 (OriginLab Corporation, Northampton, USA) was used to calculate the relative crystallinity of the sample as the ratio of the area of the crystalline sharp peak over the total diffractograms area (Frost, Karninski, Kirwan, Lascaris, & Shanks, 2009). The lateral crystal size was established from peak half width of 100 reflections (2θ ~5.6°) using the Scherre equation: $D_{hkl} = k\lambda/\beta\cos\theta$, when D_{hkl} is the average length of the diffraction domain normal to the family plane (*hkl*), k is a constant as 0.9 for cellulose, λ is the wavelength used and β is the peak half width (Cairns, Bogracheva, Ring, Hedley & Morris, 1997).

4.3.9 Thermal properties

Thermal properties were monitored using differential scanning calorimetry (DSC, a DSC Q100, TA Instruments Inc., Eschborn, Germany). The samples (10 mg) were weighed into a hermetic stainless steel pan and DI water (30 mg) was added. The sealed pan was operated by heating from 0 to 160°C at a rate of 3°Cmin^{-1}. Indium was used for the standard and empty stainless steel pan was used as a reference. The onset temperature (*To*), peak temperature (*Tp*), conclusion temperature (*Tc*) and enthalpy (ΔH) were used to define as the thermal transition of

starch and calculated automatically by Universal Analysis 2000 V4.4 software (TA Instruments-Waters LLC**).**

4.3.10 Cooking stability of debranched AM-treated cassava starch (DBSAM5min) and hydrothermal, debranched AM-treated cassava starches

The cooking stability was studied in a model system at 50% and 70% moisture content which represented intermediate and high moisture food products respectively. Debranched AM-treated cassava starch (DAM5min) and hydrothermal, debranched AM-treated cassava starches were selected to determine the cooking stability. The DI water was added to the powder samples to obtain a moisture content of 50% and 70%. The starch suspension was mixed and sealed in a closed container and then heated in a steaming bath (99^{o}C) for 30 min. After cooling to room temperature (27-30°C), some portions were withdrawn for starch fractions determination as described previously. The remaining portions were air-dried for thermal properties measurement using the DSC1 instrument (Mettler Toledo, Switzerland) with the preparation method as described previously. The thermal transition of starch was calculated by Mettler software.

4.3.11 Thermo-molding process modification

4.3.11.1 Preliminary study on debranched AM-treated cassava starch modified by thermo-molding process

The DAM5min powder (10% moisture content, 700 mg) was weighed into a rectangular stainless steel mold with the size of 0.15 cm in thickness, 3 cm in length and 1cm in width. Then, it was placed in the molding machine (Carver Press, Model 1835 CB, Carver Inc., USA) and the temperature was programmed to 110^{o}C during a 15 min ramp. Afterward, the 2 tons pressure was

applied for 8 and 60 min and then the temperature was cooled down to 20°C in 10 min by cold water recirculation. The molded products were about 1.5 mm thickness. Some portions of samples were then cut into the dimension size of 1.5 mm in thickness, 10 mm in length and 5 mm in width and another portion was ground into powder by cryo-grinding and was used for starch fractions analysis and thermal property measurement according to the method described previously.

4.3.11.2 The microstructure of surface of DBSAM5min and molded-DBSAM5min monitored by scanning electron microscopy (SEM)

A thin layer of dried sample was placed on aluminum stubs with conductive carbon tape and sputter coated with gold-palladium by using a JEOL JFC-110 Fine Coater Ion Sputter coater (Tokyo, Japan). The microstructure at the surface of the sample was monitored using a JEOL JSM-5800LV scanning electron microscope (Tokyo, Japan) and operated at an accelerating voltage of 2 kV.

4.3.11.3 Effect of thermo-molding pressure on starch fractions, crystalline structure and thermal properties of DAM5min

The molded sample was prepared as mentioned above. After heating to 110°C during a 15 min ramp, the pressure was varied from 0, 1, 2, and 3 tons for 8 min and then the temperature were cooled down to 20°C in 10 min by cold water recirculation. The molded products were then cut into the same dimension size as section 4.3.12.1 and were used for starch fractions analysis, relative crystallinity, and thermal properties measurement according to the method described previously.

4.3.11.4 Effect of thermo-molding conditions on starch fractions, crystalline structure and thermal properties of DBSAM5min.

The molded sample was prepared at various conditions which were molding temperature of 90°C, 110°C, and 130°C and the pressure of 2 and 3 tons for 8 min. After molding, the molded products were cut into the same dimension size as section 4.3.12.1 and were used for starch fractions analysis, relative crystallinity, and thermal property measurement according to the method described previously.

4.3.11.5 Effect of surface area to volume ratio on starch fractions

The molded sample prepared from the conditions of 130°C and the pressure of 3 tons for 8 min was transformed into 6 dimension sizes including 5 x 10 x 1.5, 2.5 x 5 x 1.5, 5 x 10 x 0.75, 1.25 x 2.5 x 1.5, 1.5 x 1.5 x 1.5, and 1 x 1 x 1.5 (width x length x thickness, mm, respectively). The dimension size of molded sample was used to calculate surface area to volume ratio (S/V) as follows: $\frac{S}{V} =$ [(2 x width x thickness) + (2 x width x length) + (2 x length x thickness)]/ (width x length x thickness). Then, the starch fractions were analyzed according to the method described previously.

4.3.11.6 Cooking stability test of molded sample with different S/V

The cooking stability was studied in a model system at 70% moisture content which represented high moisture food products. The molded sample preparing from the conditions of 130°C and the pressure of 3 tons for 8 min with different S/V (1.93, 3.73, and 5.33 mm^{-1}) were adjusted moisture content to 70% by DI water in a closed container and then heated in a steaming bath (99°C) for 30 min.

After cooling to room temperature (27-30°C), the starch fractions were analyzed according to the method described previously.

4.3.12 Statistical analysis

All the experiments were conducted in two replications. Analysis of variance (ANOVA) was analyzed using SPSS version 13.0 (SPSS Institute Inc., Cary, NC, USA). The differences between mean values were established using Duncan's multiple-range test.

4.4 Results and discussion

4.4.1 Preliminary study on cassava starch treated with AM

The cassava starch modification with AM on structural properties was preliminary studied in order to optimize the enzyme concentration. The chain length (CL) distribution of AM-treated starches were analyzed by HPAEC-PAD and summarized in Table 4.1. Cassava starch treated with AM at a concentration of 8 U g starch^{-1} showed a larger proportion of intermediate and long chain with DP 25-80 and a smaller proportion of short chain with DP 6-24 when compared with cassava starch treated with AM at a concentration of 5 U g starch^{-1}. Nevertheless, the reaction time of 3 h and 24 h did not show the difference in the proportion of DP 6-24 and DP 25-80. All AM-treated cassava starches also showed a larger proportion of DP 25-80 and a smaller proportion of DP 6-24 as compared to native cassava starch. Therefore, the modification of cassava starch with AM can increase the chain length of starch. The enzyme concentration of 8 U g starch^{-1} was selected for further study on the structural modification of cassava starch by varying reaction time.

Table 4.1 Chain length (CL) distribution of native cassava starch and AM-treated cassava starch after treated with AM at various concentrations and reaction times

Sample	CL distribution (%)				
	DP 6-12	DP 13-24	DP 25-36	DP 37-59	DP 60-80
CS	23.64	44.67	16.50	14.22	0.98
AM_5U3h	21.14	37.85	21.14	18.17	1.71
AM_8U3h	17.27	29.83	25.48	24.22	3.20
AM_5U24h	20.15	36.57	22.14	19.38	1.76
AM_8U24h	16.98	29.51	26.13	24.12	3.26

In order to study the optimum conditions to elongate the CL of cassava starch with a higher proportion of intermediate and long chains, cassava starch gel was treated with AM at various reaction times and its CL distribution was determined using HPAEC-PAD. Figure 4.1a shows the CL distribution of native cassava starch and AM-treated cassava starches at various reaction times and the difference of CL distribution among native cassava starch and AM-treated cassava starches are illustrated in Figure 4.1b. Generally, the CL of native starches was classified into 3 types: short chain (SC, DP < 9), intermediate chain (IC, 9 ≤ DP ≤ 24), and long chain (LC, DP > 24) (Bertoft, 1991; Bertoft, Laohaphatanalert, Piyachomkwan, & Sriroth, 2010; Hizukuri, 1986). All AM-treated cassava starches showed the higher proportion of LC with DP 25-80 and SC with DP < 8, while those of IC with DP 8-24 was lower as compared to native cassava starch. An increase in its LC might be due to a combined effect of amylose to amylopectin chain transfer and the transfering of glucan chain within the amylopectin molecules by disproportionation reaction while a higher of SC can be a result of shorten longer chains which were residual segments from the donor chains (Do et al.,

2012). The similar results was reported on potato starch (van der Maarel et al., 2005; Kaper et al., 2005), rice starch (Park et al., 2007; Cho et al., 2009), and cassava starch (Sorndech et al., 2015). A longer reaction time from 5 min to 24 h tended the increased proportion of DP 25-80. This was possible that the disproportional reaction by the action of AM was enhanced at a longer reaction time. However, the proportion of DP 25-80 seemed to decrease at the prolonged reaction time of 24 h, presumably due to the minor hydrolysis reaction as catalyzed by AM (Fujii et al., 2005; Kuriki et al., 2006). The modification of cassava starch by AM resulted in the consumption of amylose as the evidence of the reduction of amylose content from 17-18% (native cassava starch) to 4-7% (AM-treated cassava starches) as demonstrated in Table 4.2. The amylose content rapidly decreased with reaction time of 5 min (7.3%) and showed a slight lower with increasing reaction time. This was supposedly described by several AM actions on amylose and amylopectin (Park et al., 2007; Kaper et al., 2004; Takaha et al., 1996): (a) segments of amylose chains could be cleaved and then transferred to amylopectin branch chains by intermolecular transglycosylation, (b) cyclic glucans could form by intramolecular transglycosylation, and (c) smaller linear chains could remain through (a) and (b). In addition, the AM-treated cassava starches demonstrated the shift of λmax from 597 nm (native cassava starch) to 551-564 nm (AM-treated cassava starches) which is close to λmax of potato amylopectin (567 nm) (Do et al., 2012), indicating that AM catalyzed the disproportionation reaction by disassembled long chain amylose into a large amount of shorter helical glucans (Do et al., 2012). Regarding the preliminary result, three samples of AM treated cassava starches were selected for further study. The AM-treated cassava starch for 4h (AM4h), representing to the modified starch with a larger proportion of longer CL (DP 25-80) whereas the

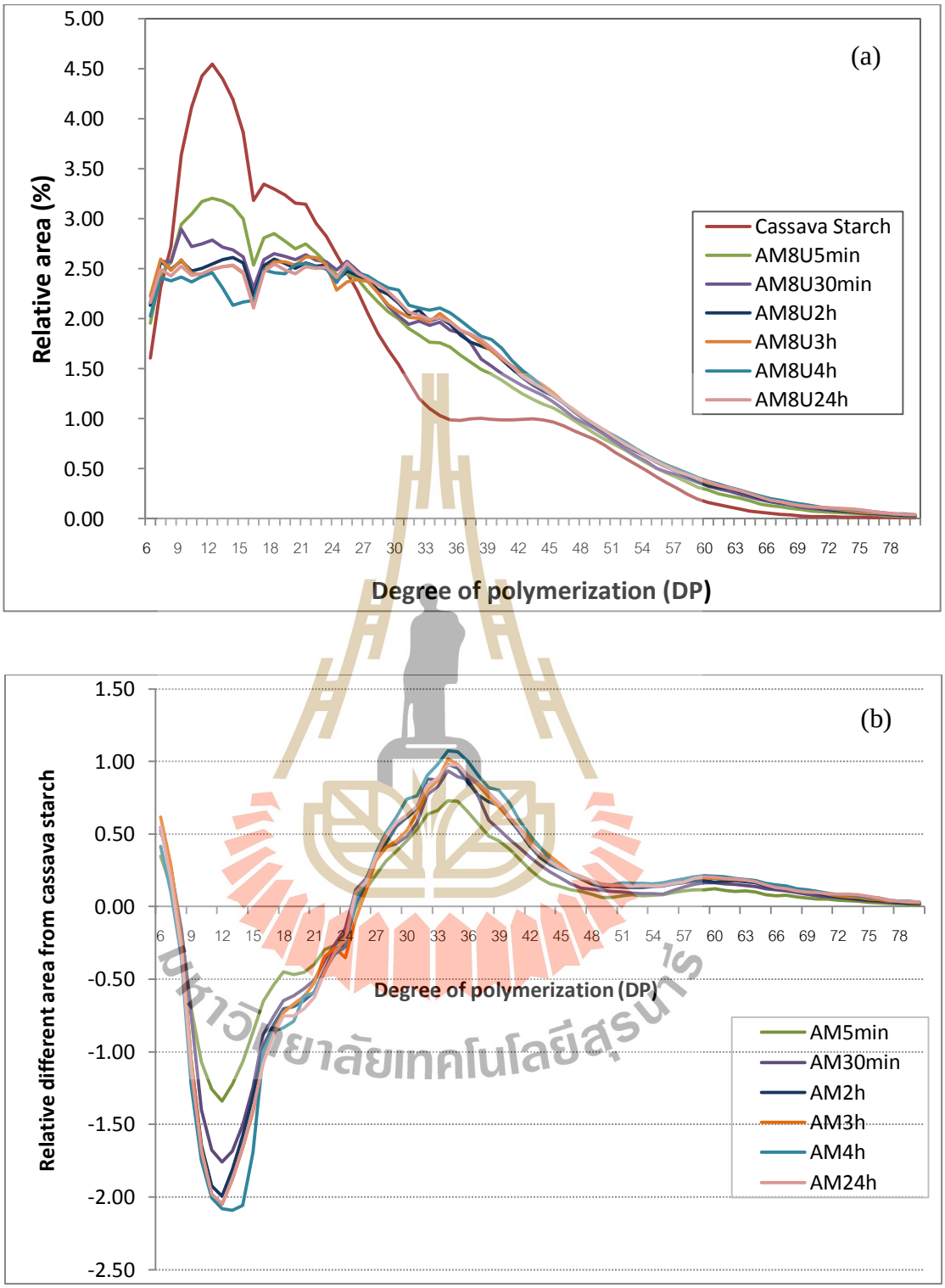

Figure 4.1 CL distributions of (a): native cassava starch and AM-treated cassava starches and (b): the different of CL distributions of AM-treated cassava starches at various reaction times as compared to native cassava starch.

Table 4.2 Amylose content and maximum absorption wavelength value (λ_{max}) of native and AM-treated cassava starch at various reaction times

Sample	Amylose content (%)	λ_{max} (nm)
CS	17.8 ± 0.2	597
AM5min	7.3 ± 0.9	564
AM30min	6.1 ± 0.2	549
AM2h	6.3 ± 0.1	541
AM3h	6.6 ± 0.7	557
AM4h	6.5 ± 0.3	554
AM24h	4.5 ± 0.3	551

native cassava starch was referred to the starch with a larger proportion of a shorter CL (DP 6-24) and AM-treated cassava starch for 5 min (AM5min) was referred to the modified starch with showing the median CL distribution between the short and long CL.

4.4.2 Structural characteristics of native and AM-treated cassava starches

4.4.2.1 Macromolecular characteristics determined by HPSEC-MALLS and HPAEC-PAD

The HPSEC chromatograms of native cassava starch (CS), AM5min, and AM4h illustrate in Figure 4.2. The CS showed a bimodal distribution whereas a monomodal distribution was observed from AM5min and AM4h. For CS, amylopectin was eluted at the elution volume between 5.5-6.7 mL. In addition, a shoulder between the elution volumes of 6.2-6.7 mL was detected which corresponded to smaller molecular sizes of amylose. For AM5min, amylopectin eluted at the same elution volume as CS, indicating that the molecular size of amylopectin was not modified. In case of AM4h, the sample peak eluted at higher elution volume compared

to CS and AM5min, suggesting that the amylopectin was mostly modified by the action of AM. The peak of both AM5min and AM4h were broadened and no distinction of amylose fraction appeared (Figure.4.2). This implied that two actions may occur on amylose: (i) amylose was not depolymerized or (ii) if amylose was depolymerized, the chains produced were used to be grafted on amylopectin residues. Hansen et al. (2008) proposed the action of AM on amylose molecule that linear amylose is cleaved and then the cleaved fragment was transferred to amylopectin resulting in the increasing of longer chains.

To analyze the size distributions, HPSEC chromatograms were transformed to size distributions using hydrodynamic radius (R_H) versus elution volume curves (Rolland-Sabaté, Guilois, Jaillais, & Colonna, 2011). The size distributions of CS displayed two populations of amylopectin and amylose fraction. The amylopectin (corresponding to the major fraction) was eluted at R_H ~156 nm and amylose fraction was eluted at R_H ~71 nm (Figure 4.3). They are in agreement with previous results (Rolland-Sabaté et al., 2012) in that the R_H of amylopectin fraction from novel nonwaxy cassava starches was ~120-176 nm but the R_H obtained from amylose fraction was slightly differed. This could be due to the difference in cassava cultivars. The size distributions of AM5min showed a single broad peak at R_H ~155 nm whereas the AM4h demonstrated the sharp single peak at R_H ~85 nm, indicating that the molecular size of CS substantially reduced after AM treatment at a longer reaction time. This may imply that newly structures can be formed through disproportionation of entire amylopectin cluster units or reorganization of clusters (Hansen et al., 2008) during longer reaction time.

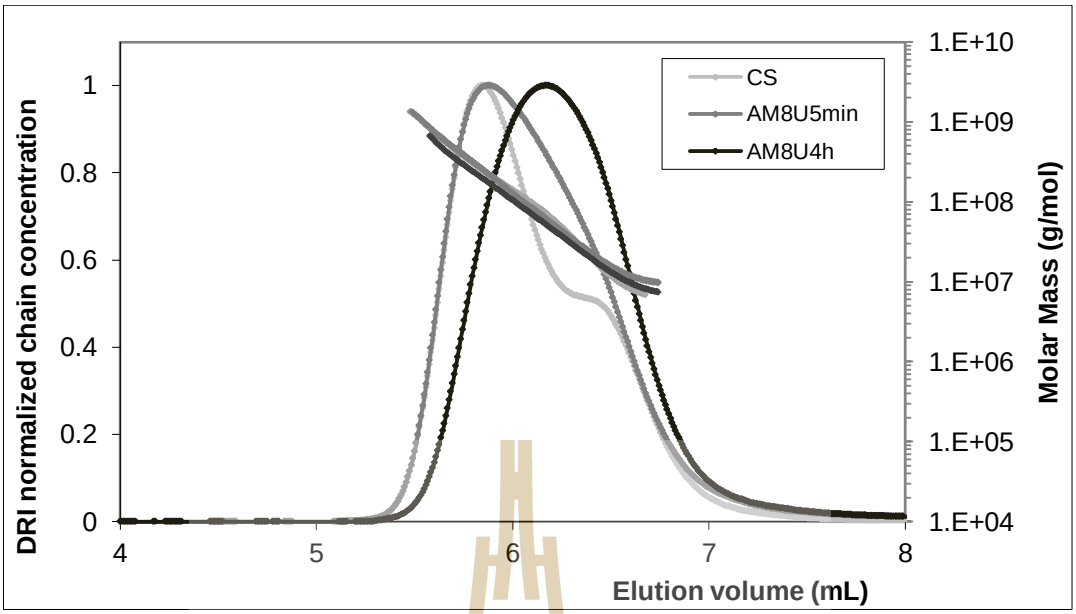

Figure 4.2 HPSEC chromatograms of native cassava starch (CS) and AM-treated cassava starch which was treated for 5 min (AM5min) and 4h (AM4h).

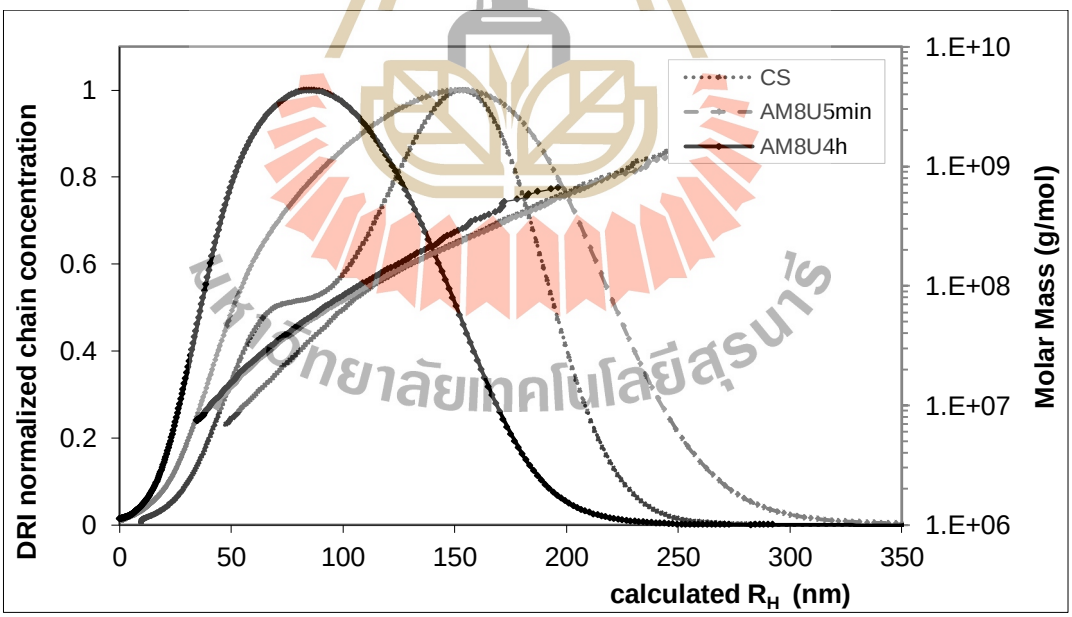

Figure 4.3 Size distributions and molar masses of native cassava starch (CS) and AM-treated cassava starch which was treated for 5 min (AM5min) and 4h (AM4h) obtained by HPSEC-MALL.

The molar mass and radius values of amylopectin from CS were 2.16 x 10^8 g.mol^{-1}, 270.5 nm for $R_{g,}$ and 176.4 for R_h, respectively (Table 4.3). After AM treatment, the molar mass of AM-treated starches gradually decreased (1.91 x 10^8 g.mol^{-1} for AM5min and 8.6 x 10^7 g.mol^{-1} for AM4h). This implied that AM degraded amylopectin molecules, leading to produce a smaller amylopectin cluster associated with the reduction of R_H as mentioned previously. The reduction of amylopectin molecular size during AM treatment has been reported elsewhere (van der Maarel et al., 2005; Park et al., 2007; Hansen et al., 2008). In addition, the dispersity index (M_w/M_n) of AM-treated cassava starches tended to decrease, especially for AM4h, indicating that the molecular rearrangement occurred. The molecular density of CS was 7.7 g. mol^{-1}.nm^{-3} and it gradually increased to 8.3 g.mol^{-}.nm^{-3} for AM5min and thereafter 10.6 g.mol^{-1}.nm-^{3} for AM4h. This parameter could describe the conformation of the molecule and give then additional indication on branching (Rolland-Sabaté et al., 2012). As the molecular density increased with longer reaction time (4 h), suggesting that the dense structure was formed. This was possible only due to the generation of small amylopectin clusters with shortened branch chain by the action of AM to cleave the inner chains of amylopectin (Park et al., 2007).

Table 4.3 Macromolecular characteristics of native cassava starch (CS), AM-treated cassava starch (AM5min and AM4h), β-limit dextrins from native cassava starch (B-CS) and AM-treated cassava starches (B-AM5min and B-AM4h) determined by HPSEC-MALLS

Sample	$\overline{M}_w$ x10^6 (g.mol^{-1})	$\overline{M}_n$ x10^6 (g.mol^{-1})	$\overline{R}_g$ (nm)	$\overline{R}_h$ (nm)	$\overline{M}_w/\overline{M}_n$	D_{gapp} (g.mol^{-1} .nm^{-3})
CS	216.0	43.8	270.5	176.4	4.93	7.7
AM5min	191.0	44.8	266.5	173.5	4.26	8.3
AM4h	85.6	27.1	184.5	126.0	3.16	10.6
B-CS	4.1	8.5	130.0	132.1	4.31	12.8
B-AM5min	2.1	3.8	88.5	96.9	5.50	30.3
B-AM4h	6.9	6.7	120.0	129.0	10.62	49.7

$\overline{M}_w$ = weight average molar mass, $\overline{M}_n$ = number average molar mass, $\overline{R}_g$ = z-average radius of gyration, $\overline{R}_h$ = z-average hydrodynamic radius, $\overline{M}_w/\overline{M}_n$ = dispersity index, and D_{gapp} = molecular density ($\overline{M}_w/4\pi/3)\ \overline{R}_g^3$) for the amylopectin population.

4.4.2.2 Fine structure analysis of native and AM-treated starch

For the determination of the internal structure of AM5min and AM4h, β-amylase was used to hydrolyze their external chains. The β-limit dextrins obtained from CS (B-CS), AM-treated cassava starch for 5 min (B-AM5min), and AM-treated cassava starch for 4 h (B-AM4h) were determined for the molar mass distributions by HESEC-MALLS. The HPSEC peak of B-AM4h was eluted before that of B-AM5min (Figure 4.4), indicating that the molar mass and size were higher for the B-AM4h which were 6.9 x 10^6 g.mol^{-1} whereas the molar mass of B-AM5min was 2.1 x 10^6 g.mol^{-1} (Table 4.3). The radius values (120.0 nm for R_g,and 129.0 for R_h, Table 4.3) of B-AM4h were higher than those from B-AM5min. This result might explain that at a longer reaction time of 4 h enhance the formation of cyclo-structure by the action of AM on catalysis the cyclization reaction which is in agreement with the previous

reports in that smaller amylopectin clusters and cyclic glucans were formed after AM modification (Park et al., 2007; Takaha et al., 1996). Moreover, the molecular density of β-limit dextrins of AM4h was higher than AM5min, probably due to the high dense internal structure would be generated at a longer reaction time.

The in-depth analysis of structural characteristics of the internal layer structure, the average chain length (CL), the external chain length (ECL), and the internal chain length (ICL) of AM-treated cassava starches and their β-limit dextrins were examined by H^1-NMR (Rolland-Sabaté et al., 2014) and showed in Table 4.4. The AM5min demonstrated the higher CL and ECL and lower BD than those of AM4h. Therefore, it is the less dense, branch particle. In addition, the external layer of AM5min seemed to be less dense than AM4h as confirmed by the longer ECL. However, the ICL and BD of their β-limit dextrins were very close, meaning that they have a similar internal density. As compared to CS, the β-limit dextrins of AM-treated cassava starches showed a higher BD, suggesting that the internal structure was more dense branching. The higher CL and ECL of AM-treated cassava starches were detected compared to CS, confirming the hypothesis that AM can elongate the starch chain length. The percentage of β-amylolysis was also evaluated by H^1-NMR and showed in Table 4.4. The β-amylolysis of CS was 49.7% which was in accordance with data obtained for cassava starch in the literature (Laohaphatanaleart, Piyachomkwan, Sriroth, Santisopasri, & Bertoft, 2009). For AM-treated cassava starches, the β-amylolysis of AM5min (62.6%) was higher than that of AM4h (57.9%). This could be due to either more numerous ECL or longer ECL for AM5min. Another reason was probably due to the rearrangements in the AM4h structure, leading to the formation of cyclo-structure in which β-amylase was unable to hydrolyze.

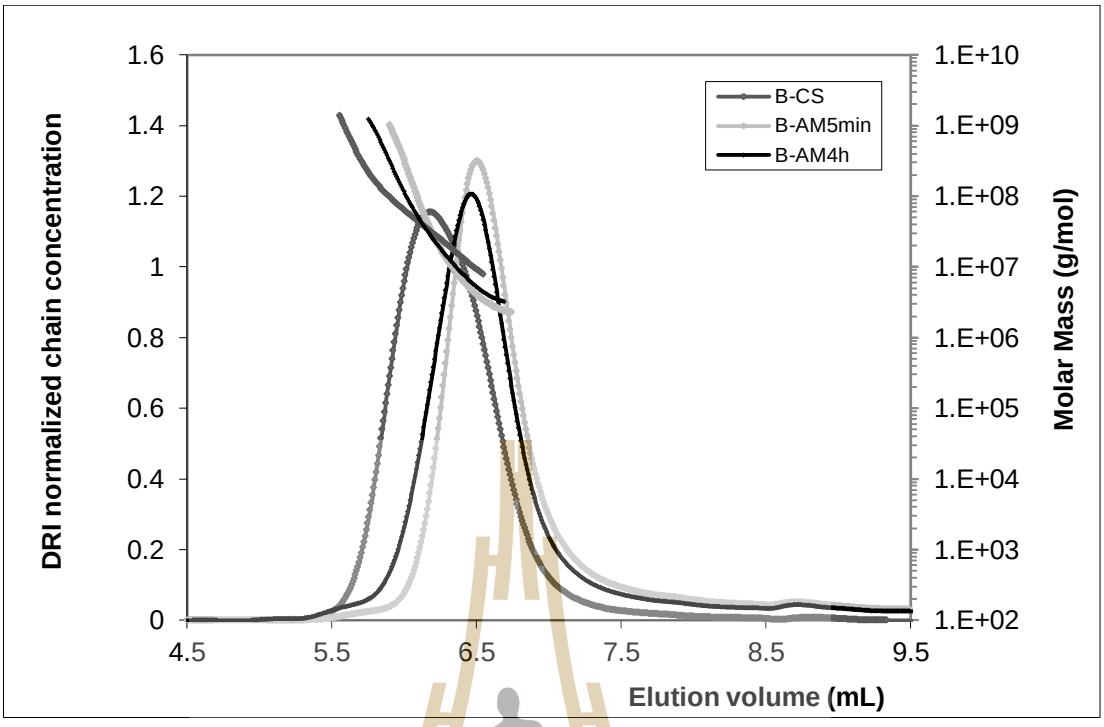

Figure 4.4 HPSEC chromatograms of β-limit dextrins from native cassava starch (B-CS) and AM-treated cassava starches (B-AM5min and B-AM4h) after β-amylase hydrolysis.

Table 4.4 Fine structure of native cassava starch, AM-treated cassava starch, and their β-limit dextrins determined by H^1-NMR

Sample	BD (%)	CL	ECL	ICL	β-amylolysis (%)
CS	3.6	22.8	13.3	8.5	49.7
AM5min	3.4	27.3	19.1	7.2	62.6
AM4h	3.7	25.3	16.6	7.6	57.9
B-CS	8.7	11.5	2	8.5	-
B-AM5min	9.8	10.2	2	7.2	-
B-AM4h	9.4	10.6	2	7.6	-

BD = branching degree, CL = average chain length, ECL = external chain length, ICL = internal chain length.

4.4.2.3 Cyclo-structure analysis of AM-treated cassava starches

In order to confirm that cyclo-structure was formed in AM-treated cassava starches, AM5min and AM4h was treated with glucoamylase because cyclo-structure is resistant to this enzyme. The cyclic nature of the glucoamylase-resistant glucans formed was monitored by MALDI-TOF. The smallest cyclic α-glucan found was DP8 (m/z 1,320) and it was detected in both AM-treated starches (Figure 4.5) in which consistent with the previous results (Sorndech et al., 2015). However, the larger cyclo-structure was detected in AM4h (Figure 4.5b). The largest size of cyclo-structure obtained from AM4h was DP32 (m/z 5,207). This suggested that a longer reaction time for 4 h enhanced the formation of cyclization reaction that catalyzed by the action of AM in order to produce the cyclo-structure with different size. This was in accordance with the lower susceptibility to β-amylase and smaller ECL in AM4h.

The structural characteristics obtained from HPSEC-MALL, HPAEC-PAD, H^1-NMR, and MALDI-TOF, the structural change following AM treatment could explain in that AM can elongate the CL of cassava starch. AM treatment for 5 min catalyzed the disproportionation reaction or inter-transglycosylation by transferring α-glucan segments from amylose to amylopectin molecule, resulting in the reduction of amylose content and molar mass of amylopectin whereas the CL and ECL were increased. Meanwhile, the minor cyclization reaction or intra-transglycosylation also occurred by the formation of cyclo-structure with DP 8. For a longer AM treatment of 4 h, the native amylopectin was mostly modified by the action of AM. It catalyzed the disproportionation reaction and molecular reorganization by cyclization reaction in line with the decrease of the

molar mass of amylopectin and the formation of cyclo-structure with several sizes. Thus, it showed a lower susceptibility to β-amylase. Moreover, AM also catalyzed the minor hydrolysis reaction of the linear chain consistent with the reduction of ECL. The structure of AM-treated cassava starches exhibited a more branched structure with a denser core (smaller ICL) but the AM4h had more dense branched structure as compared with cassava starch and AM5min.

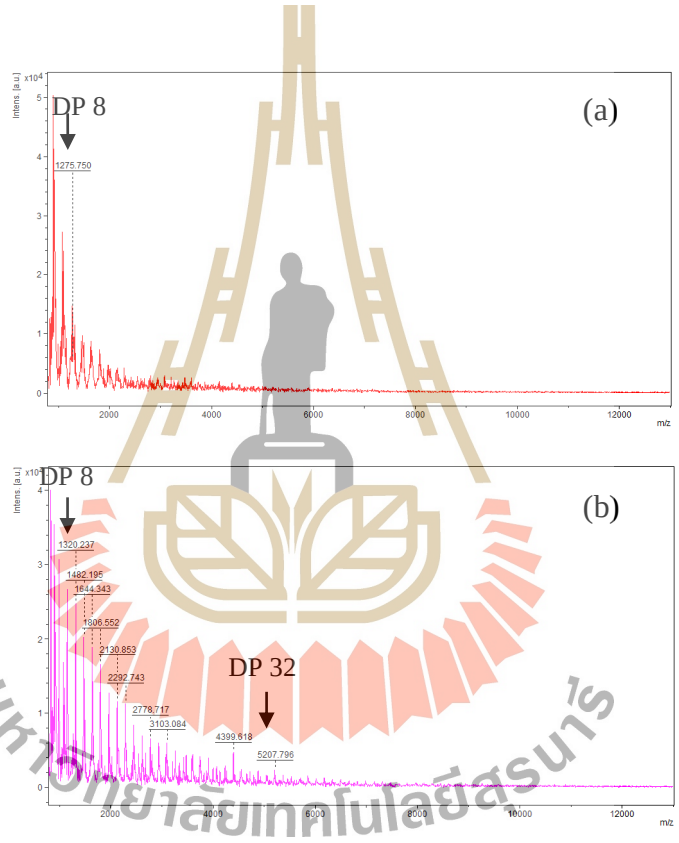

Figure 4.5 MALDI-TOF analysis to identify cyclo-structure formation, (a): AM5min and (b): AM4h.

4.4.3 Effect of recrystallization of debranched native and AM-treated cassava starch on starch fractions, crystalline and thermal properties

4.4.3.1 Starch fractions, crystalline and thermal properties of debranched native and AM-treated cassava starch

Starch fractions and crystalline properties of all debranched native and AM-treated cassava starches are shown in Table 4.5. As the AM reaction time increased from 5 min to 4 h, a higher RS formation in debranched starch was observed and the reduction of RDS and SDS content appeared. It suggested that the linear fragments with longer chain length, which were liberated during debranching can be formed double helices and preferred to recrystallize into an ordered structure. As mentioned previously, the DBSAM4h had a higher proportion of LC with DP>24 rather than the DAM5min, resulting in the promotion of more ordered structure of RS. For debranched cassava starch (control sample, DS), the higher proportion of IC with DP 8-24 leads to induce more formation of the non-ordered structure of RDS and SDS (Table 4.5) which are more susceptible to enzyme hydrolysis. Leloup, Colonna, Ring, Roberts, & Well, 1992) proposed the structure of amorphous fraction or non-ordered structure in which consist of dangling chains ($6 < DP < 30$) linking to double helices in the macroporous network and proposed to be mainly responsible for the hydrodynamic behavior and the network porosity. Starch surface with less porosity and a smoother area can resist the enzyme digestion, leading to the increased RS content (Lertwanawatana, Frazier, & Niranjan, 2015).

The crystal structure obtained from all debranched starches were B-type crystallites (Table 4.5), indicating that crystallization during debranching occurred. Similar results were reported on debranched native rice starch (Kiatponglarp, Tongta, Rolland-Sabaté, & Buléon, 2015). However, an increase in the

relative crystallinity about 5% was observed for both DAM5min and DAM4h compared to DS, indicating that the higher proportion of LC may promote the formation of localized molecular density of ordered structure.

Regarding the thermal properties (Table 4.6), the melting temperature range of both debranched AM-treated starches was shifted to a higher temperature (from 94-119^{o}C to 96-125^{o}C) compared with DS which was consistent with the CL distribution. An increase in the proportion of LC with DP 37-80 showed a positive correlation to the *Tp* of starch (Hansen et al., 2009). The longer glucan chains could generate stronger double helices than shorter chains and becomes more heat tolerance. According to Cai & Shi (2010), the crystalline short-chain amylose from debranched waxy potato starch displayed a higher peak melting temperature than that from debranched waxy wheat and maize starch due to its longer average CL. Furthermore, the greater *ΔH* was detected as the reaction time increased from 5 min to 4 h. This suggested that the higher proportion of LC might enhance the more formation of double helices, leading to a higher RS content of the DAM4h. However, the crystals formed during the debranching may have a non-well organized structure; thus, the melting temperature ranges of DAM5min and DAM4h were similar.

Table 4.5 Starch fractions and crystalline properties of debranched native and AM-treated cassava starch before and after subjected to recrystallization

Sample	RDS (%)	SDS (%)	RS (%)	Crystalline structure	Relative crystallinity (%)	(100) peak width at half-height (°)	Lateral crystal size (nm)
DS	42.5 ± 0.7[a]	35.9 ± 0.3[a]	21.6 ± 1.4[f]	B-type	30	1.25 ± 0.03	6.4 ± 0.1
DAM5min	31.9 ± 0.7[c]	34.2 ± 0.1[b]	33.9 ± 0.4[e]	B-type	35	1.17 ± 0.00	6.8 ± 0.0
DAM4h	29.3 ± 0.8[d]	29.4 ± 0.7[c]	41.3 ± 1.3[c]	B-type	35	1.18 ± 0.00	6.7 ± 0.0
Iso_DS	42.9 ± 0.1[a]	15.0 ± 0.9[g]	42.1 ± 0.0[c]	B-type	62	1.06 ± 0.00	7.5 ± 0.0
Iso_ DAM5min	27.7 ± 1.0[d]	14.0 ± 0.0[g]	58.3 ± 0.7[a]	B-type	62	0.97 ± 0.00	8.2 ± 0.0
Iso_DAM4h	22.0 ± 0.6[e]	19.5 ± 0.0[f]	58.5 ± 1.2[a]	B-type	64	0.96 ± 0.00	8.2 ± 0.0
HMT_DS	37.8 ± 0.2[b]	24.0 ± 0.5[e]	38.2 ± 1.1[d]	C_A-type	62	1.35 ± 0.06	5.9 ± 0.2
HMT_ DAM5min	20.2 ± 0.1[f]	30.7 ± 1.2[c]	49.1 ± 0.2[b]	C_A-type	53	1.23 ± 0.03	6.5 ± 0.1
HMT_DAM4h	21.8 ± 0.8[e]	28.6 ± 0.2[d]	49.6 ± 0.4[b]	C_A-type	53	1.25 ± 0.02	6.4 ± 0.1

Means values with different superscripts within each column are significantly different ($p < 0.05$). DS = debranched native cassava starch, DAM5min = debranched AM-treated cassava starch for 5 min, DAM4h = debranched AM-treated cassava starch for 4 h, Iso = isothermal temperature incubation with 90%mc at 50°C for 3 days, and HMT = heat- moisture treatment with 30%mc at 130°C for 3h.

Table 4.6 Thermal properties of debranched native and AM-treated cassava starch with different CL distribution after subjected to recrystallization

Sample	Peak 1				Peak 2			
	To (^oC)	*Tp* (^oC)	*Tc* (^oC)	*ΔH* (Jg^{-1})	*To* (^oC)	*Tp* (^oC)	*Tc* (^oC)	*ΔH* ($J.g^{-1}$)
DS	N.D.	N.D.	N.D.	N.D.	94.3^{d}	105.6^{d}	119.4^{e}	1.9^{f}
DAM5min	N.D.	N.D.	N.D.	N.D.	95.9^{d}	109.4^{c}	124.8^{c}	4.8^{d}
DAM4h	N.D.	N.D.	N.D.	N.D.	96.3^{d}	109.9^{c}	124.8^{c}	6.5^{bc}
Iso_DS	74.7^{a}	85.8^{a}	102.9^{a}	4.6^{a}	111.3^{a}	115.6^{b}	119.8^{e}	0.6^{f}
Iso_ DAM5min	75.5^{a}	85.1^{a}	93.4^{b}	0.9^{b}	99.1^{c}	110.2^{c}	122.5^{d}	3.2^{de}
Iso_DAM4h	77.3^{b}	85.1^{a}	93.2^{b}	0.5^{b}	99.6^{c}	109.5^{c}	121.6^{d}	4.3^{d}
HMT_DS	N.D.	N.D.	N.D.	N.D.	106.6^{b}	115.9^{b}	129.1^{b}	4.8^{d}
HMT_ DAM5min	N.D.	N.D.	N.D.	N.D.	104.2^{b}	118.7^{a}	131.7^{a}	10.6^{a}
HMT_DAM4h	N.D.	N.D.	N.D.	N.D.	106.9^{b}	117.8^{a}	131.1^{a}	8.7^{b}

Means values with different superscripts within each column are significantly different ($p < 0.05$). DS = debranched native cassava starch, DAM5min = debranched AM-treated cassava starch for 5 min, DAM4h = debranched AM-treated cassava starch for 4 h, Iso = isothermal temperature incubation with 90%mc at 50^{o}C for 3 days, HMT = heat- moisture treatment with 30%mc at 130^{o}C for 3h, and N.D. = Not detected.

4.4.3.2 Effect of recrystallization method on starch fractions, crystalline and thermal properties of debranched native and AM-treated starch

Isothermal temperature incubation (Iso) and heat-moisture treatment (HMT) were applied with debranched native and AM-treated cassava starches, aiming to recrystallize and improve SDS and RS content and thermal stability. Isothermal temperature incubation was conducted at 50°C for 3 days and HMT was carried out with 30%mc at 130°C for 3h. The starch fractions and crystalline properties of recrystallized starch are given in Table 4.5. Both DAM5min and DAM4h after subjected to recrystallization showed a higher RS content than that of DS which in correlated to the increase of LC proportions (Figure 4.1). However, the RS content between recrystallized DAM5min and DAM4h was similar ($p>0.05$). This indicated that the crystallization processes induced the crystals propagation and/or maturation further from the former nucleation step during debranching and it may be independent of the proportion of LC. According to Eerlingen, Deceuninck, and Delcour (1993) who studied the enzyme RS formation from amylose with different average DP ranging from 40 to 610 and reported that the yield of enzyme RS was correlated with the DP of amylose. However, the isolated RS comprised the short chains of average DP 19-26 and were independent of the CL of the starting amylose used. Crystallization processes could improve the RS content of all debranched starches by transformation a non-ordered structure of RDS and SDS fractions to ordered structure of RS as suggested by the reduction of those fractions. However, the reduction of SDS content was observed from isothermal incubation. It was probably because this process may induce chain mobility within the non-ordered structure, subsequently rearranging to form a tightly packed structure and increased localized molecular density. On the other hand, HMT was conducted in the limit of water at a

higher temperature and shorter time. This may restrict the mobility of starch chain in both non-ordered and ordered structure to form a densely packed ordered structure of RS.

The crystalline structure of isothermal treated starches showed B-type structure similar to its starting material which was in accordance with the other reports (Mutungi, Rose, Onyango, Jaros, & Rohm, 2009; Mutungi et al, 2011; Kiatponglarp et al., 2015) in that the crystalline type of debranched starch after incubation at isothermal temperature did not change. In this study, isothermal incubation was conducted in excess water (90% moisture content) at 50^{o}C for 3 days which was comparable to annealing treatment. Thus, it promoted the realignment of starch chains, consequently improving its crystalline perfection and/or crystalline size (Tester, Debon, & Karkalas, 1998) by forming a densely packed crystalline structure, resulting in the high localized molecular density of ordered structure which was related to a larger lateral crystal size (Table 4.5). The more RS formation for isothermal treated starches may be resulted from a larger lateral crystal size. For HMT-treated starches, the intensity of a peak at 2θ of 5.6° tended to decrease. In addition, the peak at 2θ of 17° became split into two peaks and peak at 2θ of 22°and 24° merged to one board peak at 2θ of 23° (data not shown), which were the typical A-type characteristics. Therefore, HMT induced the transformation of crystalline type from preferential B-type crystal during the debranching to the C_A-type. It was attributed to be the helical rearrangement without extensive molecular mobility and chain flexibility within the crystalline domain due to the limit of water content resulting in the loss of intra-helical moisture (Le Bail, Bizot, & Buleon, 1993).

Regarding thermal properties, isothermal treated starches showed two melting temperature ranges in low melting temperatures of 75-103^{o}C and high melting temperatures of 99-122^{o}C respectively shown in Table 4.6. This results

may be probably due to the broad of CL distribution in starting material. Melting at low temperature could occur from the short chain crystallites whereas that of high temperature participated with the crystalline structure formed by the long linear chain (Gidley et al., 1995). In contrast to isothermal treated starches, HMT-treated starches demonstrated only single melting temperature range at a high temperature of 104-132^{o}C. This might be caused by HMT facilitating the disruption of less perfect crystallites (B-type) from the short linear chains, followed by chain realignment to form the more perfect crystalline structure of C_A-type with more thermal stability. This result was in agreement with the crystalline properties in Table 4.5 in which C_A-type crystallites displayed a higher melting temperature than B-type crystallites. Consequently, HMT improved thermal properties of all debranched starches greater than isothermal incubation. Moreover, AM-treated cassava starch prior debranching could increase thermal stability of debranched starches due to its higher melting temperature. This was a result of the AM action on CL elongation of debranched cassava starch.

4.4.3.3 Chain length distribution of acid hydrolyzed treated starch

It has been demonstrated previously that the proportion of longer chain of debranched AM-treated starches was higher than that from debranched native starch. In addition, the melting temperature of debranched AM-treated starches before and after recrystallization by HMT was improved (Table 4.7). It could be a result of the extent of the amylopectin CL by the action of AM. To confirm this result, the CL distributions of all HMT debranched starches were analyzed after acid hydrolysis for 35 days under the assumption that the amorphous parts of starch were eliminated and the crystalline parts remained. The HPAEC-PAD analysis in the crystalline residues of all HMT debranched starches are shown in Figure 4.6. The

HMT debranched native starch showed a distribution with a maximum peak area at DP 15 and a slight shoulder at DP 27 and DP 43 respectively. The similar results were obtained from HMT debranched AM-treated starches but the first shoulder was detected at DP 31 instead of DP 27. The relative areas (%) under each maximum peak were calculated. For HMT debranched native starch, the relative area under DP 12-19 (32%) was higher than that from HMT debranched AM-treated starches (27-28%) whereas the relative area under DP 25-32 was lower (17% for HMT-treated debranched native starch and 21% for HMT-treated debranched AM-treated starches) and the relative area under DP 40-47 was similar (6%). This indicated that the higher proportions of DP 25-32 in the crystalline residues of both HMT debranched AM-treated starches could increase its melting temperature. However, the relative area under each maximum peak between 5 min and 4 h HMT debranched AM-treated starch was not difference, relevant to their similar melting temperature ranges (Table 4.6). The higher melting temperature was an indication of more perfect crystals or a higher co-operative unit i.e. longer chains in the crystal or a larger crystal size (Miao, Jiang, Zhang, Jin, & Mu, 2011). These results suggested that the CL of glucan involving in crystalline residues of all HMT debranched starches was DP 15-43 in which can form a densely packed crystalline structure. However, the DP 25-32 were the major proportions to improve thermal stability of debranched starches. It was consistent with the report by Schmiedi, Báuerlein, Bengs, & Jacobasch. (2000) in that the CL of linear glucan with DP 20-35 was an ideal for RS3 production with high thermal stability.

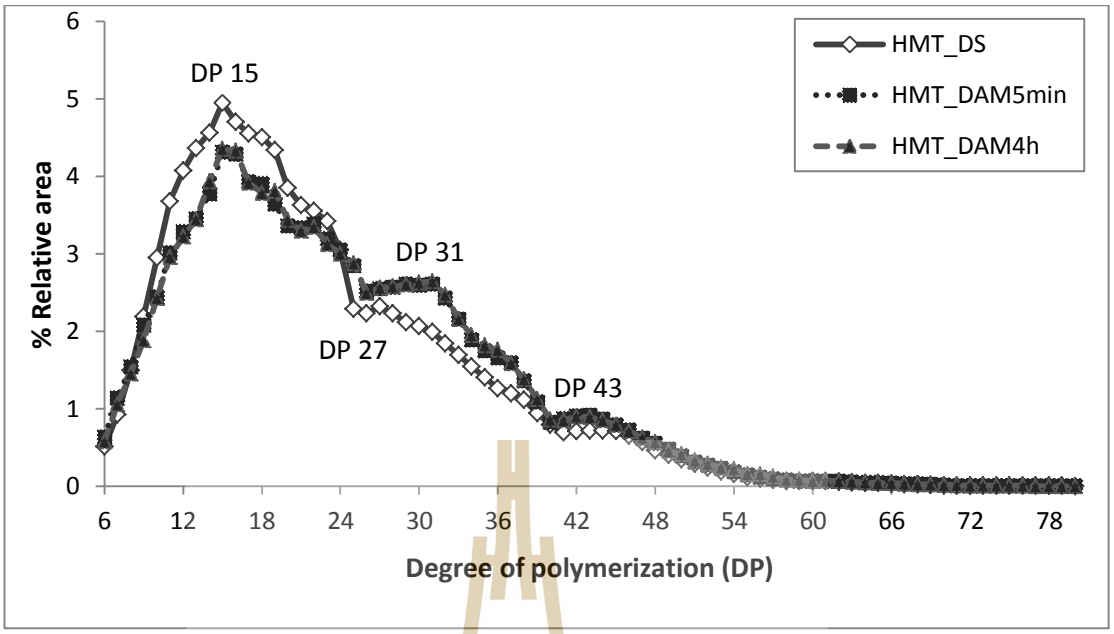

Figure 4.6 HPAEC-PAD analysis of chain length distribution of crystalline residues after 35 days of acid hydrolysis (2.2 N HCl, 35°C) for HMT debranched native cassava starch (HMT_DS), HMT debranched AM-treated cassava starch for 5 min (HMT_DAM5min), and HMT debranched AM-treated cassava starch for 4 h (HMT_DAM4h).

4.4.3.4 Cooking stability of recrystallized debranched starches

The recrystallized debranched AM-treated starches (Iso_DAM5min, and HMT_DAM5min) were selected for the cooking stability test to compare with debranched AM-treated cassava starch (DAM5min). After cooking at intermediate (50%) and higher (70%) moisture content, Iso_DAM5min sample was the group of the higher RS content sample followed by HMT_DAM5min and DAM5min respectively (Figure 4.7). The SDS and RS content of all recrystallized samples with 50% moisture cooking were increased while RS content of 70% moisture cooking was slightly decreased. The results indicated that recrystallized samples could

be tolerated with this cooking condition. Cooking of all recrystallized samples at 50% and 70% moisture content could induce the rearrangement of glucan chain, the amorphous structure of RDS is likely converted to SDS and then the imperfect crystalline structure SDS was further transformed to be ordered structure of RS. The initial crystalline perfection of starch has an influence on thermal stability. HMT_DAM5min sample showed higher melting temperature and more perfect crystallites than Iso_DAM5min sample (Table 4.6), the rearrangement of its structure to form the ordered structure of RS during cooking was less occurred. Thus, RS content of 50% moisture cooked HMT_DAM5min was slightly improved whereas that of 50% moisture cooked Iso_DAM5min was more increased. Furthermore, the highest increment of RS content was obtained from 50% moisture cooked DAM5min sample (Figure 4.7). It implied that the structure of DAM5min which contained less perfect crystals and RS content than recrystallized sample could be able to rearrange to form the ordered structure of RS during cooking. Kiatponglarp et al. (2015) reported that the initial RS content and hydrothermal treatment conditions influenced the extensive RS improvement and the low initial RS content sample yielded higher RS content than the high initial RS content sample after hydrothermal treatments. Thermal properties of cooked recrystallized debranched AM-treated cassava starches in Table 4.7 showed that this cooking treatments shifted the melting temperature to a higher temperature especially for 70% moisture content, implying that the ordered structure and/or crystalline structure was rearranged to more perfect crystallites during cooking which is considered to be a repeating step of hydrothermal treatments. Thermal and moisture content during cooking could destroy less perfect crystallites, then the melted crystalline structure rearrangement to form more perfect crystallites occurred as it was

evidence from the disappearance of the first peak and the slightly increase of melting temperature of the second peak for cooked Iso_DAM5min samples.

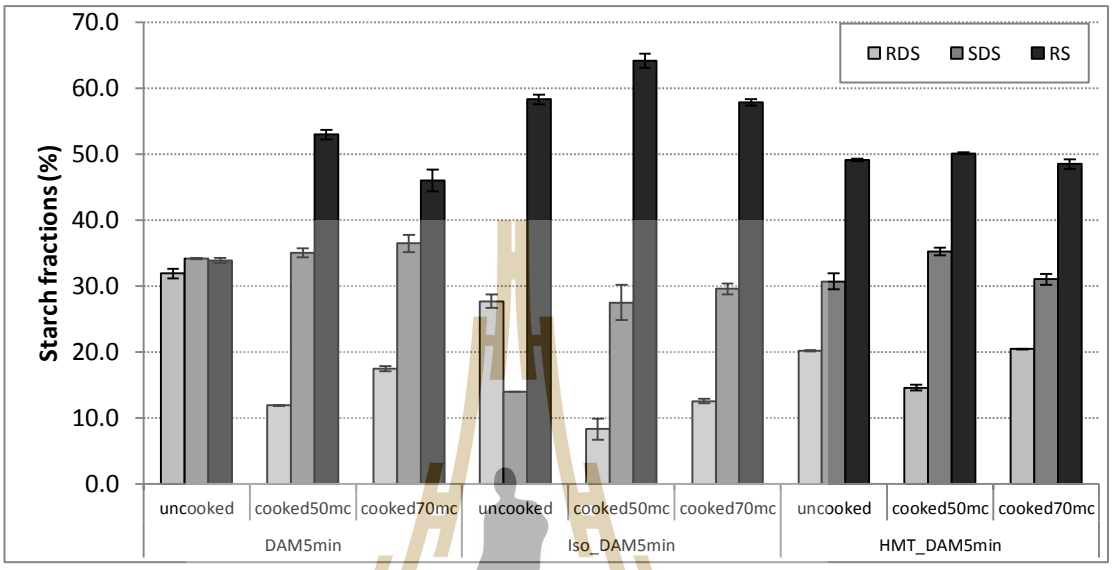

Figure 4.7 Cooking stability of recrystallized debranched AM-treated cassava starches after cooking at 50% and 70% moisture content using steaming for 30 min.

Table 4.7 Thermal properties of debranched and recrystallized debranched AM-treated cassava starch after cooked at 50% and 70% moisture content

Sample	Peak 1				Peak 2			
	To (^{o}C)	*Tp* (^{o}C)	*Tc* (^{o}C)	*ΔH* (Jg^{-1})	*To* (^{o}C)	*Tp* (^{o}C)	*Tc* (^{o}C)	*ΔH* (J.g^{-1})
DAM5min	N.D.	N.D.	N.D.	N.D.	96.1	108.2	117.6	4.5
Cooked50mc_DAM5min	N.D.	N.D.	N.D.	N.D.	98.2	109.0	117.5	5.3
Cooked70mc_DAM5min	N.D.	N.D.	N.D.	N.D.	103.9	112.1	119.5	4.8
Iso_ DAM5min	72.2	81.7	91.9	0.5	97.8	108.5	116.8	4.8
Cooked50mc_Iso_DAM5min	N.D.	N.D.	N.D.	N.D.	98.5	109.0	118.2	7.5
Cooked70mc_Iso_ DAM5min	N.D.	N.D.	N.D.	N.D.	104.5	112.6	119.4	5.5
HMT_ DAM5min	N.D.	N.D.	N.D.	N.D.	92.7	107.1	118.2	8.5
Cooked50mc_HMT_ DAM5min	N.D.	N.D.	N.D.	N.D.	95.3	108.4	119.4	8.9
Cooked70mc_HMT_ DAM5min	N.D.	N.D.	N.D.	N.D.	100.4	110.7	121.1	8.8

Means values with different superscripts within each column are significantly different ($p < 0.05$). DAM5min = debranched AM-treated cassava starch for 5 min, Iso = isothermal temperature incubation with 90%mc at 50^{o}C for 3 days, HMT = heat- moisture treatment with 30%mc at 130^{o}C for 3h, and N.D. = Not detected.

4.4.4 Effect of thermo-molding process on starch fractions, crystallinity, and thermal properties of DAM5min

4.4.4.1 Preliminary study on thermo-molding process

The thermo-molding process was applied with the DAM5min base on assumption that this process can improve their SDS and RS content. The preliminary study was carried out by molding DAM5min with 10% moisture content at a temperature of 110°C for 8 and 60 min with a pressure of 2 tons. After cutting to obtain a dimension size of 5 x 10 x 1.5 mm (width x length x thickness), the rectangular molded-DAM5min samples showed an improvement of RS content (from 33.9% to 65.05% RS) as compared to control sample (Table 4.8). Nevertheless, the reduction of RS content was detected after grinding to a powder (13.3% RS). The major starch fraction of powder of molded-DAM5min was RDS (50.8% RDS) followed by 35.7% SDS. This could explain that thermo-molding process enhanced the formation of densely packed ordered and non-ordered structure that reduces the accessibility of α-amylase. However, these structures were destroyed by the grinding process. It might be due to an increase in the surface area and the macromolecular destruction after grinding (Silva, Couturier, Berrin, Buléon, & Rouau, 2012). The higher surface area favored the ability of amylase to bind to the substrate. A longer molding time for 60 min did not improve the SDS and RS content compared to a shorter molding time for 5 min, suggesting that the molding time of 8 min was enough to induce the formation of a densely packed ordered and non-ordered structure. Thus, the optimum molding time for this study was 8 min.

Table 4.8 Effect of thermo-molding pressure on starch fractions of DAM5min

Sample	RDS (%)	SDS (%)	RS (%)
Powder_AM5min (control)	31.9 ± 0.7^{b}	34.2 ± 0.4^{a}	33.9 ± 0.6^{b}
Molded_DAM5min_110c8m	2.9 ± 0.4^{d}	31.1 ± 0.8^{b}	65.1 ± 1.5^{a}
Powder_Molded-DAM5min_110c8m	50.8 ± 0.3^{a}	35.7 ± 0.2^{a}	13.3 ± 0.6^{c}
Molded_DAM5min_110c60m	5.7 ± 0.9^{c}	28.8 ± 1.4^{b}	65.2 ± 0.5^{a}

Means values with different superscripts within each column are significantly different ($p < 0.05$). DAM5min = debranched AM-treated cassava starch for 5 min, 110c8min = thermo-molding at 110°C with 2 tons pressure for 8 min, and 110c60min = thermo-molding at 110°C with 2 tons pressure for 60 min.

The microstructure at the surface of DAM5min and molded-DAM5min were monitored using scanning electron microscopy (SEM). The SEM micrograph in Figure 4.8a showed that the surface of DAM5min is more spongy and fluffy structure which indicates that the glucan polymers re-associate loosely during debranching (Lertwanawatana et al., 2015). After thermo-molding, the molded-DAM5min showed densely packed surface regions with a smooth surface (Figure 4.8b). It implies that the higher RS content after thermo-molding process should be related to the surface structure. Starch surface with less porosity and a smoother area can resist the enzyme digestion, leading to the increased RS content (Lertwanawatana et al., 2015).

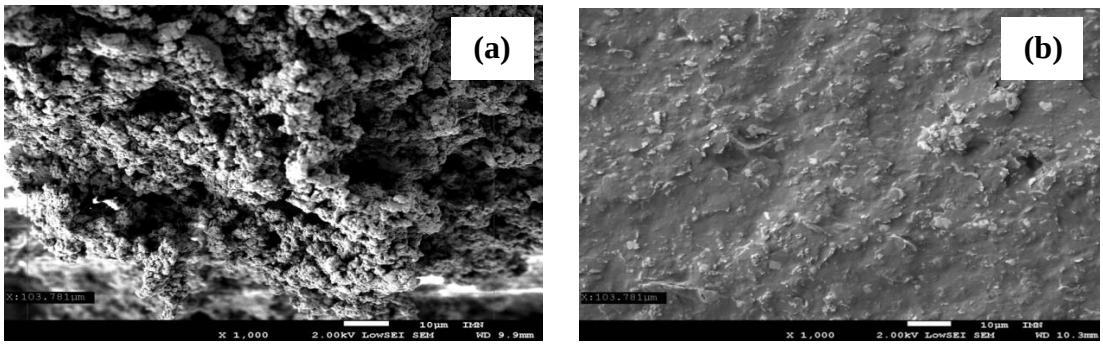

Figure 4.8 SEM micrographs of (a): DAM5min at a magnification of 1,000x and (b)**:** molded-DAM5min at a magnification of 1,000x.

4.4.4.2 Effect of thermo-molding conditions on starch fractions, crystallinity, and thermal properties of DAM5min

4.4.4.2.1 Effect of thermo-molding pressure on starch fractions, crystallinity, and thermal properties of DAM5min

Applying pressure from 0 to 3 tons during the thermo-molding process at 110^{o}C for 8 min was studied on the SDS and RS formation. Increasing molding pressure to 2 tons resulted in the improvement of RS formation, then it decreased. Contrastingly, the SDS content tended to decrease as pressure increased until 2 tons (Table 4.9). It was probably because the increased pressure resulted in the reduction volume of the system, promoting the starch molecules closer together and generating more densly packed ordered structure (Lertwanawatana et al., 2015). The decrease of RS content at 3 tons (from 61.1% to 50.3% RS) could be due to some weak crystalline structure of DAM5min were partial melting during compression at very high pressure. However, thermal properties of all molded-DAM5min samples (T_o, T_p, and T_c) slightly increased as the pressure increased. It might be due to the rigid dense crystalline structure was induced at high pressure.

4.4.4.2.2 Effect of thermo-molding conditions on starch fractions crystallinity and thermal properties of DAM5min

For further study on thermo-molding conditions, three molding temperatures, 90°C, 110°C, and 130°C were varied whereas the molding pressure was conducted at 2 tons and 3 tons due to they showed a higher SDS and RS content and improvement of thermal properties (Table 4.9). Increasing molding temperature from 90 to 130°C induced an improvement in SDS content. However, the RS content declined when increasing molding temperature (Table 4.10). It should be described that at high molding temperatures in this study (130°C) combined with high pressure (2 and 3 tons) may melt some weak crystalline structure of DAM5min, subsequently induce the formation of more densely packed structure of SDS. In contrast, at low molding temperatures may enhance more seed nuclei formation in order to form more ordered structure which resists enzyme digestion and increasing RS content. In general, polymer crystallization process comprises of three steps: nucleation, propagation, and maturation (Eerling et al., 1993). The nucleation rate is slow at a temperature close to melting temperature of crystal whereas the propagation rate is slow at a temperature close to glass transition temperature. For the semi-crystalline structure, the crystallization or the amount of RS can occur only at a temperature between those temperatures. Another reason to explain the different amount of SDS and RS after molding at various conditions might be the effect of interaction between molding temperature and pressure. Molding temperature at 90 to 130°C cooperated with a pressure of 2 and 3 tons in this study did not change the crystal structure of DAM5min. All molded samples showed B-type crystalline structure (data not shown). Therefore, the thermo-molding process in this study is a potential method to improve the yield of SDS and RS. However, particle or dimension

Table 4.9 Effect of thermo-molding pressure on starch fractions, thermal and crystalline properties of molded-DAM5min which were molded at a temperature of 110°C for 8 min

Sample	RDS (%)	SDS (%)	RS (%)	T_o (°C)	T_p (°C)	T_c (°C)	ΔH ($J.g^{-1}$)	Crystallinity (%)
Powder_DAM5min (control)	31.9 ± 0.7^{a}	34.2 ± 0.4^{c}	33.9 ± 0.6^{e}	95.9^{b}	109.4^{c}	124.8^{b}	4.8^{b}	35
Molded_DAM5min_0t	28.6 ± 0.8^{b}	36.2 ± 0.3^{b}	35.3 ± 0.5^{d}	94.9^{b}	111.9^{c}	126.7^{b}	3.7^{c}	30
Molded_DAM5min_1t	9.0 ± 0.1^{c}	33.9 ± 1.0^{c}	57.0 ± 1.0^{b}	93.1^{c}	111.3^{c}	130.7^{a}	6.6^{a}	25
Molded_DAM5min_2t	7.9 ± 0.1^{d}	31.0 ± 1.0^{d}	61.1 ± 0.9^{a}	97.0^{b}	113.7^{b}	130.5^{a}	2.7^{d}	26
Molded_DAM5min_3t	9.5 ± 0.1^{c}	40.2 ± 1.1^{a}	50.3 ± 1.0^{c}	102.7^{a}	115.9^{a}	131.1^{a}	2.8^{d}	27

Means values with different superscripts within each column are significantly different ($p < 0.05$). DAM5min = debranched AM-treated cassava starch for 5 min, Molded_DAM5min = DAM5min after molded at 110°C for 8 min, 0t = no pressure, 1t = one ton pressure , 2t = two tons pressure, and 3t = three tons pressure.

Table 4.10 Starch fractions and thermal properties of molded starch samples which were prepared at various thermo-molding conditions

Sample	RDS (%)	SDS (%)	RS (%)	T_o (^oC)	T_p (^oC)	T_c (^oC)	ΔH ($J.g^{-1}$)
Molded_DAM5min_90c2t8m	7.7 ± 0.5^b	32.1 ± 0.0^b	60.2 ± 1.4^a	101.4^a	114.9^b	132.3^a	1.9^{bc}
Molded_DAM5min_90c3t8m	9.6 ± 0.3^a	28.7 ± 0.1^c	61.7 ± 0.2^a	101.8^a	113.3^c	132.4^a	2.4^b
Molded_DAM5min_110c2t8m	7.9 ± 0.1^b	31.0 ± 1.0^b	61.1 ± 0.9^a	97.0^b	113.7^c	130.5^b	2.7^{ab}
Molded_DAM5min_110c3t8m	9.5 ± 0.1^a	40.2 ± 1.1^a	50.3 ± 1.0^d	101.8^a	116.8^a	131.2^a	3.3^a
Molded_DAM5min_130c2t8m	4.7 ± 0.3^c	42.2 ± 1.2^a	53.1 ± 1.0^c	100.8^a	117.0^a	133.3^a	2.7^{ab}
Molded_DAM5min_130c3t8m	5.0 ± 0.4^c	39.4 ± 0.7^a	55.6 ± 0.9^b	99.1^a	114.1^{bc}	131.6^a	2.5^{ab}

Means values with different superscripts within each column are significantly different ($p < 0.05$). Molded_DAM5min = debranched AM-treated cassava starch for 5 min after molded at various conditions, 90c = molded at 90°C, 110c = molded at 110°C, 130c = molded at 130°C, 2t = two tons pressure, 3t = three tons pressure, and 8min = molded for 8 min.

sizes of the molded product had an influence on the yield. The optimum condition of thermo-molding in this study for enhancing the highest formation of SDS and RS and improved thermal stability of DAM5min was the molding temperature of 130^{o}C with 2 tons pressure for 8 min.

4.4.5 Effect of dimension size and surface area to volume ratio (S/V) of molded DAM5min on SDS and RS content

As mentioned previously, grinding process could reduce SDS and RS content of molded-DAM5min. Therefore, the effects of dimension size and surface area to volume ratio (S/V) of molded-DAM5min on their SDS and RS content were examined in order to optimize the minimum size which still retained the high level of SDS and RS for application in some food products, for instance cereal bar, cookie and cornflake. The S/V of molded-DAM5min was varied from 1.93 to 5.33 mm^{-1} by manual cutting. A larger S/V or smaller dimension size of molded-DAM5min showed higher enzyme accessibility, leading to lower RS content but the SDS content was improved as compared to a smaller S/V or larger size (Table 4.11). The S/V was plotted as a function of SDS or RS content and illustrated in Figure 4.9. The linear relationship between SDS content, RS content and the S/V of molded-DAM5min were detected. The negative correlation between RS content and the S/V (R^2 = 0.9404) suggests that the reduction of RS content in the powder molded-DAM5min as increasing S/V. It was in agreement with the results previously (Mutungi et al., 2010). Thus, larger S/V enhanced the accessibility between enzymes and substrates by inducing the diffusion of enzymes to the starch surface. According to Mahasukhonthachat, Sopade, and Gidley. (2010), the more digested starch was detected in the smaller particle size of sorghum starch. The digestion of starch is dependent on several factors i.e. granule size, crystalline pattern, the degree of

crystallinity, and surface pore or channels (Noda et al., 2008). The positive relationship between SDS content and the S/V (R^2 = 0.8952) were observed. Since SDS is the fraction of imperfect crystallizes and the densely packed non-crystalline structure, the larger S/V may promote its enzyme digestion. Thus, the suggested equation for prediction the RS content of molded-DAM5min at different S/V is y = -6.3034x + 67.041 where x and y are the S/V and RS content with a high R^2 (0.9404). Furthermore, to predict the SDS content of molded-DAM5min with different S/V, the suggested equation is y = 2.955x + 35.674 (R^2 = 0.8952) where x is the S/V and y is SDS content respectively.

Table 4.11 The SDS and RS content of molded-DAM5min with different dimension size and surface area to volume ratio

Dimension size (width x length x thickness, mm)	Surface area to volume ratio (mm^{-1})	SDS (%)	RS (%)
5 x 10 x 1.5	1.93	42.2 ± 0.2^{e}	53.1 ± 1.1^{a}
2.5 x 5 x 1.5	2.53	44.0 ± 0.3^{d}	50.9 ± 0.8^{b}
5 x 10 x 0.75	3.26	44.8 ± 0.5^{cd}	49.1 ± 0.2^{b}
1.25 x 2.5 x 1.5	3.73	45.2 ± 0.2^{c}	45.6 ± 0.9^{c}
1.5 x 1.5 x 1.5	4.00	46.4 ± 0.4^{b}	40.2 ± 0.2^{d}
1 x 1 x 1.5	5.33	52.9 ± 0.9^{a}	32.4 ± 0.6^{e}

Means values with different superscripts within each column are significantly different (p < 0.05). The molded-DAM5min was molded at 130^{o}C with pressure of 2 tons for 8 min followed by cutting to different dimension sizes.

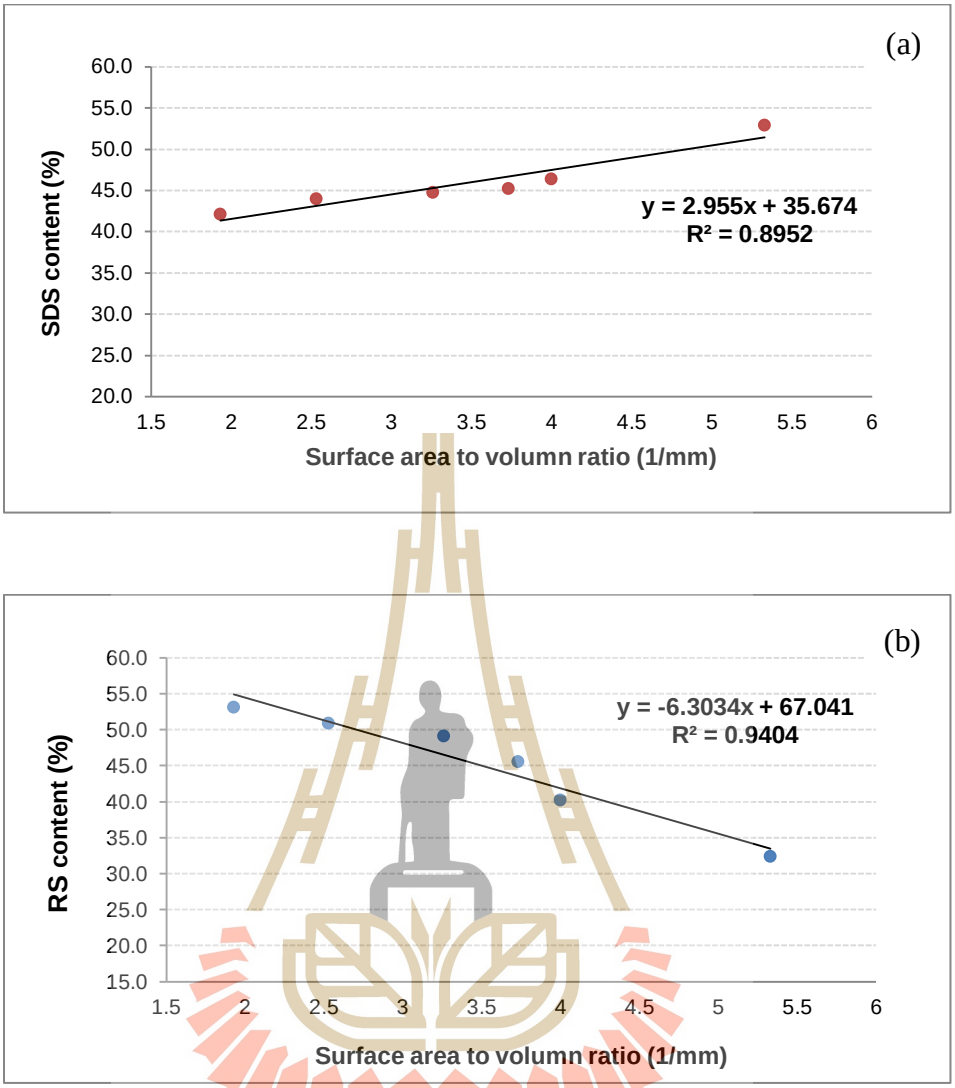

Figure 4.9 Plots of the surface area to volume ratio (S/V) of molded-DAM5min as a function of (a): SDS content and (b): RS content.

4.4.6 Cooking stability of molded-DAM5min

The cooking stability test of molded-DAM5min was studied at three differences S/V which were 1.93, 3.73, and 5.33 as referred to the large, median, and small dimension size, respectively. After cooking at 70% moisture content, the RS content of all dimension sizes was increased whereas SDS content was declined as compared to non-cooked sample (Figure 4.10). It indicated that cooking process in this

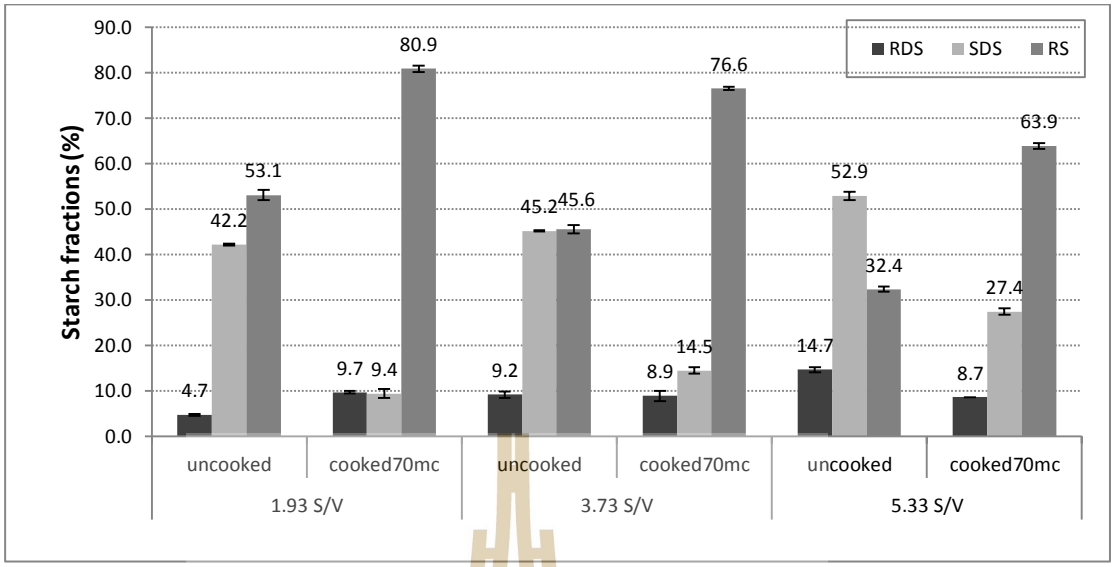

Figure 4.10 Cooking stability test of molded-DAM5min with the different surface area to volume ratio (S/V).

this study (with excess water, 70% moisture content) induced the structural transformation of some imperfect crystallizes and/or the densely packed non-ordered structure of SDS to more ordered structure of RS (both in form of densely packed non-ordered and ordered structure). An increase in the local density of the densely packed non-ordered structure and the densely packed ordered structure is a potential method to achieve the higher RS yield (Zhang et al., 2015). Considering the S/V, the lower RS content was observed with a higer the S/V of molded-sample (Figure 4.10). This may be explained by the different solubilisation of molded sample during cooking. According to Mahasukhonthachat et al. (2010), the water solubility index of the cryo-milled sorghum starch decreased with the larger particle size, which resulted from the reduced surface area for solubilisation. In this case, the larger dimension size of molded sample which has a smaller S/V (1.93 S/V) increases the distance for mass transfer, thus the solubilisation and the structural transformation of order structure of

RS to the non-ordered structure of SDS was lower as compared with the smaller dimension size.

4.5 Conclusions

The structure of cassava starch could be modified by action modes of AM depending on the reaction time. At the short reaction time, AM catalyzed the major disproportionation reaction and the minor cyclization reaction as a result of the reduction of amylose content and the formation of cyclo-structure with DP 8. With longer reaction time, the amylopectin was mostly modified by the disproportionation reaction and molecular reorganization by cyclization reaction resulted in the decrease of molar mass of amylopectin and the formation of cyclo-structure with several sizes. Moreover, AM also catalyzed the minor hydrolysis reaction of the linear chain. The structure of AM-treated cassava starch with longer reaction time had more densely branch structure as compared with AM-treated cassava starch for shorter reaction time. The AM-treated cassava starches also exhibited a higher proportions of long chain with DP 25-80.

CL distribution of starch influenced the enzyme digestibility and thermal properties of debranched starch. Using AM treated with cassava starch prior to debranching could improve the RS content and thermal properties of debranched starch due to the elongation action of AM on starch chains. The debranched AM-treated starch contained higher proportions of long chain which resulted in the higher melting temperature ranges. After isothermal temperature incubation and HMT, with these starches, the RS content and thermal properties could be improved, depending on treatment conditions. The isothermal temperature incubation yielded the highest

RS content but HMT treatment showed a higher thermal stability as a resulted from the transformation of crystalline structure to more perfect structure. Cooking stability of the sample depended on the initial structure and RS content of starting starch. Cooked debranched AM-treated starch increased RS content at a higher level as compared to cooked crystallized, debranched AM-treated cassava starch because it had a lower initial RS content and less crystalline perfection. Cooking at 50 and 70% moisture could be induced the transformation of RDS into SDS and/or SDS into RS.

Thermo-molding process is an alternative method to improve the yield of SDS and RS of debranched AM-treated starch because it enhanced the formation of densely packed surface regions with a smooth surface. However, it depends on the thermo-molding conditions and its dimension size. The molding temperature and pressure play an important factor influencing on the SDS and RS formation and thermal properties. The highest SDS and RS yield with showing higher thermal stability was produced at high molding temperature and pressure. The molded sample with larger dimension size showed a highest RS yield as a result of the lower accessibility of starch-acting enzymes. These results suggested the enzymatic modification of cassava starch using AM combined with debranching enzyme could be improved RS yield, thermal properties and cooking stability of cassava starch. Furthermore, the physical modification of isothermal incubation, HMT, and the thermo-molding process can be further applied in order to achieve the starch product with higher SDS and RS content and cooking stability.

4.6 Acknowledgements

This work was financially supported by the Thailand Research Fund (The Royal

Golden Jubilee (RGJ) Ph.D. Program for industry, Grant No. PHD/0090/2552) and the Embassy of France in Thailand. The author is grateful to A. Rolland-Sabaté, S. Guilois, B. Pontoire, M. de Carvalho, X. Falourd, Joëlle Davy, and N. Stephant for the technical support.

4.7 References

AOAC. (2002). **Official methods of analysis of AOAC international 17th ed.,** AOAC International, Gairhersburg, MD, USA.

Bertoft, E. (1991). Chains of intermediate lengths in waxy-maize amylopectin. **Carbohydrate Research,** 212, 245-251.

Bertoft, E., Laohaphatanalert, K., Piyachomkwan, K., & Sriroth, K. (2010). The fine structure of cassava starch amylopectin. Part 2. Building block structure of clusters. **International Journal of Biological Macromolecules,** 47, 325-335.

Bhuiyan, S. H., Kitaoka, M., & Hayashi, K. (2003). A cycloamylose-forming hyperthermostable 4-α-glucanotransferase of *Aquifex aeolicus* expressed in *Escherichia coli*. **Journal of Molecular Catalysis B: Enzymatic,** 22, 45-53.

Burchard, W. (1999). Solution properties of branched macromolecules. In: Branched Polymers II, vol 143, **Advances in Polymer Science.** Springer, Berlin, pp.113-194.

Cai, L. M., & Shi, Y. C. (2010). Structure and digestibility of crystalline short-chain amylose from debranched waxy wheat, waxy maize, and waxy potato starches. **Carbohydrate Polymers,** 79, 1117-1123.

Cairns, P., Bogracheva, T, Y., Ring, S. G., Hedley, C. L., & Morris, V. J. (1997). Determination of the polymorphic composition of smooth pea starch. **Carbohydrate Polymers,** 32, 275-282.

Cho, K. H., Auh, J. H., Ryu, J. H., Kim, J. H., Park, K. H., Park, C. S., et al. (2009). Structural modification and characterization of rice starch treated by *Thermus aquaticus* 4-α-glucanotransferase. **Food Hydrocolloids,** 23, 2403-2409.

Do, H. V., Lee, E. J., Park, J. H., Park, K. H., Shim, J. Y., Mun. S., et al. (2012). Structural and physicochemical properties of starch gels prepared from partially modified starches using *Thermus aquaticus* 4-α-glucanotransferase. **Carbohydrate Polymers,** 87, 2455-2463.

Eerlingen, R. C., Deceuninck, M., & Delcour, J. A. (1993). Enzyme-resistant starch. II. influence of amylose chain length on resistant starch formation. **Cereal Chemistry,** 70(3), 345-350.

Englyst, H. N., Kingman, S. M. & Cummings, J. H. (1992). Classification and measurement of nutritionally important starch fractions. **European Journal of Clinical Nutrition,** 46, S33-S50.

Euverrink, G. J. W., & Binnema, D. J. (2003). Use of modified starches as an agent for forming a thermoreversible gel. **US Patent Application,** Pat. No 20 030 007 984.

Frost, K., Kaminski, D., Kirwan, G., Lascaris, E., & Shanks, R. (2009). Crystallinity and structure of starch using wide angle X-ray scattering. **Carbohydrate Polymers,** 78(3), 543-548.

Fujii, K., Minagawa, H., Terada, Y., Takaha, T., Kuriki, T., Shimada, J., et al. (2005). Protein engineering of amylomaltase from Thermus aquaticus with random and saturation mutagenesis. **Biologia,** 60, 97-102.

Gérard, C., Colonna, P., Buléon, A., & Planchot, V. (2002). Order in maize mutant starches revealed by mild acid hydrolysis. **Carbohydrate Polymers,** 48(2), 131-141.

Gidley, M. J., & Bulpin, P. V., (1987). Crystallisation of malto-oligosaccharides as models of the crystalline forms of starch: minimum chain-length requirement for the formation of double helices. **Carbohydrate Research,** 161, 291-300.

Gldley. J., Cooke, D., Darke, A. H., Hoffmann, R. A., Russel, A. L. & Greenwell, P. (1995). Molecular order and structure in enzyme-resistant retrograded starch. **Carbohydrate Polymers,** 28, 23-31.

Hansen, M. R., Blennow, A., Pedersen, S., &. Engelsen, S. B. (2009). Enzyme modification of starch with amylomaltase results in increasing gel melting point. **Carbohydrate Polymers,** 78, 72-79.

Hansen, M. R., Blennow, A., Pedersen, S., Norgaard, L., & Engelsen, S. B. (2008). Gel texture and chain structure of amylomaltase-modified starches compared to gelatin. **Food Hydrocolloids,** 22, 1551-1566.

Hizukuri, S. (1986). Polymodal distribution of the chain lengths of amylopectins, and its significance. **Carbohydrate Research,** 147, 342-347.

Juliano, B. O. (1971). A simplified assay for milled rice amylose. **Cereal Science Today,** 16, 334-340.

Kaper, T., van der Maarel, M. J. E. C., Euverink, G. J., & Dijkhuizen, L. (2004). Exploring and exploiting starch-modifying amylomaltases from thermophiles. **Biochemical Society Transactions,** 32, 279-282.

Kaper, T., Talik, B., Ettema, T. J., Bos, H., Van der Maarel, M. J. E. C., & Dijkhuizen, L. (2005). The amylomaltase of *Pyrobaculum aerophilum* IM2

produces thermo-reversible starch gels. **Applied and Environmental Microbiology,** 71, 5098-5106.

Kiatponglarp, W., Tongta, S., Rolland-Sabaté, A., & Buléon, A. (2015). Crystallization and chain reorganization of debranched rice starches in relation to resistant starch formation. **Carbohydrate Polymers,** 122, 108-114.

Kuriki, T., Takata, H., Yanase, M., Ohdan, K., Fujii, K., Terada, Y., et al. (2006). The concept of the α-amylase family: A rational tool for interconverting glucanohydrolases/ glucanotransferases, and their specificities. **Journal of Applied Glycoscience,** 53, 155-161.

Laohaphatanaleart, K., Piyachomkwan, K., Sriroth, K., Santisopasri, V., & Bertoft, E. (2009). A Study of the Internal Structure in Cassava and Rice Amylopectin. **Starch/Stärke,** 61(10), 557-569.

Libail. P., Bizot, H., & Buleon, A. (1993.). B-type to A-type phase-transition in short amylose chains. **Carbohydrate Polymers,** 21, 99-104.

Lee, K. Y., Kim, Y. R., Park, K. H., & Lee, H. G. (2006). Effects of alphaglucanotransferase treatment on the thermo-reversibility and freeze-thaw stability of a rice starch gel. **Carbohydrate Polymers,** 63, 347-354.

Lehmann, U., & Robin, F. (2007). Slowly digestible starch-its structure and health implications: A review. **Trends in Food Science and Technology,** 18, 346-355.

Leloup, V. M., Colonna, P., Ring, S. G., Roberts, K., & Wells, B. (1992). Microstructure of amylose gels. **Carbohydrate Polymers,** 18, 189-197.

Lertwanawatana, P., Frazier, R. A., & Niranjan, K. (2015). High pressure intensification of cassava resistant starch (RS3) yields. **Food Chemistry,** 181, 85-93.

Mahasukhonthachat, K., Sopade, P. A., & Gidley, M. J. (2010). Kinetic of starch digestion in sorghum as affected by particle size. **Journal of Food Engineering,** 96, 18-28.

Miao, M., Jiang, B., Zhang, T., Jin, Z., & Mu, W. (2011). Impact of mild acid hydrolysis on structure and digestion properties of waxy maize starch. **Food Chemistry,** 126(2), 506-513.

Mutungi, C., Rost, F., Onyango, C., Jaros, D., & Rohm, H. (2009). Crystallinity, thermal and morphological characteristics of resistant starch type III produced by hydrothermal treatment of debranched cassava starch. **Starch/Stärke,** 61(11), 634-645.

Mutungi, C., Onyango, C., Doert, T., Paasch, S., Thiele, S., Machill, S., et al.. (2011). Long- and short-range structural changes of recrystallized cassava starch subjected to in vitro digestion. **Food Hydrocolloids,** 25(3), 477-485.

Mutungi, C., Onyango, C., Rost, F., Doert, T., Jaros, D., & Rohm, H. (2010). Structural and physicochemical properties and in vitro digestibility of recrystallized linear α-D-(1→4) glucans derived from mild-acid-modified cassava starch. **Food Research International,** 43(4), 1144-1154.

Narkchamnan, S., & Sakdaronnarong, C. (2013). Thermo-molded biocomposite from cassava starch, natural fibers and lignin associated by laccase-mediator system. **Carbohydrate Polymers,** 96(1), 109-117.

Nilsson, G. S., Bergquist, K-E, Nilsson, U., & Lund, L. G. (1996). Determination of the degree of branching in normal and amylopectin type potato starch with ^{1}H-NMR spectroscopy. **Starch/Stärke,** 48,352-357.

Noda, T., Takigawa, S., Matsuura-Endo, C., Suzuki, T., Hashimoto, N., Kottearachchi, N. S., et al. (2008). Factors affecting the digestibility of raw and gelatinized potato starches. **Food Chemistry,** 110, 465-470.

Norman, B., Pedersen, S., Stanley, K., Stanley, E., & Richmond, P. (2007). Production of crystalline short chain amylase. **US Patent Application,** Pat. No. 2 007 059 432.

Park, J. H., Kim, H. J., Kim, Y. H., Cha, H. J., Kim, Y. W., Kim, T. J., et al. (2007). The action mode of *Thermus aquaticus* YT-1,4-α-glucanotransferase and its chimeric enzymes introduced with starch-binding domain on amylose and amylopectin. **Carbohydrate Polymers,** 67, 164-173.

Richmond, P. A., Marion, E. A., Eilers, T. A., Evan, A., Zhang, H.X., Shakeel, A., et al. (2008). Production of resistant starch product. **WO Patent,** Pat. No. 109 206

Roger, P., Bello-Perez, L. A., & Colonna, P. (1999). Contribution of amylose and amylopectin to the light scattering behavior of starches in aqueous solution. **Carbohydrate Polymer,** 40(25), 6897-6909.

Rolland-Sabaté, A., Guilois, S., Grimaud, F., Lancelon-Pin, C., Roussel, X., Laguerre, S., et al. (2014). Characterization of hyperbranched glycopolymers produced in vitro using enzymes. **Analytical and Bioanalytical Chemistry,** 406, 1607-1617.

Rolland-Sabaté, A., Guilois, S., Jaillais, B., & Colonna, P. (2011). Molecular size and mass distributions of native starches using complementary separation methods: asymmetrical flow field flow fractionation (A4F) and hydrodynamic and size-exclusion chromatography (HDC-SEC). **Analytical and Bioanalytical Chemistry,** 399(4), 1493-1505.

Rolland-Sabaté, A., Sánchez, T., Buléon, A., Colonna, P., Jaillais, B., Ceballos, H., & Dufour, D. (2012). Structural characterization of novel cassava starches with low and high-amylose contents in comparison with other commercial sources. **Food Hydrocolloids,** 27(1), 161-174.

Schmiedl, D., Báuerlein, M., Bengs, H., & Jacobasch, G. (2000). Production of heat-stable, butyrogenic resistant starch. **Carbohydrate Polymer,** 43, 183-193.

Sievert, F., & Pomeranz, Y. (1989). Enzyme-resistant starch I: Characterization and evaluation by enzyme, thermoanalytical microscopic method. **Cereal Chemistry,** 66, 342-347.

Silva, G. G. D., Couturier, M., Berrin, J.-G., Buléon, A., & Rouau, X. (2012). Effects of grinding processes on enzymatic degradation of wheat straw. **Bioresource Technology,** 103(1), 192-200.

Sorndech, W., Meier, S., Jansson, A. M., Sagnelli, D., Hindgaul, O., Tongta, S., & Blennow, A. (2015). Synergistic amylomaltase and branching enzyme catalysis to suppress cassava starch digestibility. **Carbohydrate Polymers,** 132, 409-418.

Sun, S., Song, Y., & Zheng, Q. (2008). Thermo-molded wheat gluten plastics plasticized with glycerol: Effect of molding temperature. **Food Hydrocolloids,** 22(6), 1006-1013.

Takaha, T., Yanase, M., Takaha, H., Okada, S., & Smith, S. M. (1996). Potato D-enzyme catalyzes the cyclization of amylose to produce cycloamylose, a novel cyclic glucan. **Journal of Biological Chemistry,** 271, 2902-2908.

Terada, Y., Fujii, K., Takaha, T., & Okada, S. (1999). Thermus aquaticus ATCC 33923 amylomaltase gene cloning and expression and enzyme

characterization: Production of cycloamylose. **Applied and Environment Microbiology,** 65, 910-915.

Tester, R. F., Debon, S. J. J., & Karkalas, J. (1998). Annealing of wheat starch. **Journal of Cereal Science,** 28(3), 259-272.

van der Maarel, M. J. E. C., Capron, I., Euverink, G. J. W., Bos, T., Kaper, T., Binnema, D. J., et al. (2005). A novel thermoreversible gelling product made by enzymatic modification of starch. **Starch/Stärke,** 57, 465-472.

Vasanthan, T. & Bhatty, R. S. (1998). Enhancement of Resistant Starch (RS3) in Amylomaize, Barley, Field Pea, and Lentil Starches. **Starch/Stärke,** 50, 286-291.

Yan, S-H, & Matheson, N. K. (1993). Structures of the amylopectins of waxy, normal, amylose-extender, and wx : ae genotypes and of the phytoglycogen of maize. **Carbohydrate Research,** 243, 307-321.

Zhang, B., Dhital, S., & Gidley, M. J. (2015). Densely packed matrices as rate determining features in starch hydrolysis. **Trends in Food Science & Technology,** 43(1), 18-31.

CHAPTER V

EXTRUSION COOOKING AND THERMO-MOLDING TO PRODUCE STARCHY PRODUCTS RICH IN SLOWLY DIGESTIBLE STARCH FROM CASSAVA STARCH WITH ADDITION OF FATTY ACID

5.1 Abstract

The naturally occurring of amylose-lipid complexes (AMLs) shows the reduction of enzyme digestibility in many starches. The AMLs formation of cassava starch (CS) with the addition of glycerol, lauric acid (C12) and stearic acid (C18) at 5% (w/w) was investigated using extrusion cooking. The extrusion cooking was operated at 30 and 50% moisture content with the last zone barrel temperature of 120^{o}C and screw speed of 80 rpm. The C12 and C18 showed a higher capacity to form AMLs as the evidence of the high complexing index (0.9-1.0). The dissociation temperature of AMLs type I and II of extruded samples increased with the chain length of aliphatic fatty acid and the dissociation enthalpy tended to decrease as of the extrusion moisture increased. The increased slowly digestible starch (SDS) was observed in all extruded samples which were attributed to their rough surface and condensed structure with small porosity as monitored by SEM. The extruded samples were subjected to thermo-molding at a temperature of 90, 110, and 130^{o}C, and a pressure of 2 and 3 tons. The molded samples showed a densely packed or a compact

structure with a smooth surface, resulting in the increase of SDS yield. The AMLs type I could transform to type II during thermo-molding and its dissociation temperature was improved. The highest SDS content (69.8% SDS) was obtained by molding at 110°C with 2 tons pressure for 8 min and it showed thermal stability > 110°C. After steaming cooking at 70% moisture content, the cooked sample contained 29-30% SDS. This indicated that the extrusion cooking and thermo-molding are an alternative process to produce starchy products with the high SDS yield from cassava starch with addition of fatty acid.

Keywords: slowly digestible starch, extrusion cooking, thermo-molding, thermal properties, cooking stability

5.2 Introduction

The starch structure normally consists of two main components, amylose and amylopectin but the ratio varies regarding to the botanical sources of starch. Amylose can form helical inclusion complexes with a variety of ligands such as iodine, alcohols, aromas, and lipid. The formation of amylose-lipid complexes (AMLs) results in the significant changes of glucan properties, including a decrease in amylose solubility and swelling, an increased gelatinization temperature, retardation of retrogradation during storage, and a lower the starch digestibility, leading to increasing RS content. Thus, it has been included in the list of RS as RS type V (RS5) which is the inclusion complexes between lipids and starch (Bird & Topping, 2008). These complexes have two major polymorphic forms: an amorphous form (Type I) and a semi-crystalline form (Type II) depending on the dissociation temperature between lipid and amylose (Zhang, Huang, Luo, & Fu, 2012). The type II polymorphs were

divided into type II_a and II_b based on the degree of crystallinity and/or perfection of the ordered domains. The type II_b complexes have a slightly higher melting temperature than type II_a complexes but both are above 100°C (Seneviratne & Biliaderis, 1991). The dissociation temperature of AMLs type I is lower than type II (Zhang et al., 2015). The crystalline structure of AMLs showed V_h-type diffractograms (Godet, Bizot, & Buléon 1995). The formation of two types of AMLs was found to be dependent on the temperatures and duration of the heating, pre-heating of the complexes leads to the improvement of dissociation temperature of both types (Tufvesson, Wahlgren, & Eliasson, 2003a). The AMLs type I is less rigid and stable than type II, but it could be transformed to type II through annealing at an appropriate temperature. There are several factors affecting the formation of AMLs and its properties, e.g. amylose chain length, lipid structure (monoglyceride or free fatty acid), degree of lipid unsaturation, chain lengths of aliphatic compound, complexation temperature and duration time, water content, concentration of amylose and fatty acid, and processing methods. Previous studies revealed that the dissociation temperature of AMLs was increased with the chain length of the aliphatic chain of lipid and decreased with the degree of unsaturation (Kawai, Takato, Sasaki, & Kajiwara, 2012; Putseys, Derde, Lamberts, Goesaert, & Delcour, 2009; Zabar, Lesmes, Katz, Shimoni, & Bianco-Peled, 2009). Furthermore, AMLs complexes with fatty acids were more heat stable than those with monoglycerides (Tufvesson et al., 2003a; Tufvesson, Wahlgren, & Eliasson, 2003b). Many processing can be used to produce AMLs, especially thermal processing technologies, including steam-jet cooking (Fanta, Felker, & Shogren, 2002; Fanta, Kenar, & Felker, 2015), homogenization (Meng, Ma, Cui, & Sun, 2014), and extrusion cooking (De Pilli, Derossi, Talja, Jouppila, & Severini, 2011). Starch-lipid complexation during

extrusion cooking is very important reaction influencing the structure changes and the properties of extruded products. Thermal treatment, high pressure and shear forces of the extrusion destroyed the granular structure of starch, resulting in decline of RS content (or increased digestibility) (Vasanthan & Bhatty, 1998). However, an increase in RS content after extrusion was also found from extruded barley after frozen storage (Huth, Dongowski, Gebhardt, & Flamme, 2000). The extrusion conditions also influence the crystalline structure of the starch, an extreme condition of extrusion (35% moisture, 140°C) resulted in formation of some crystallinity of single helical V_h-type whereas mild condition of extrusion (50% moisture, 100°C) induced B-type crystalline structure formation (Chanvrier et al., 2007). The study of De Pilli et al. (2011) on the starch-lipid complexes in a model system and real food using extrusion cooking exhibited that the highest formation of starch-lipid complexes was obtained at the highest temperature (128°C) and water feed content (21%), which showed a highest dissociation enthalpy. Thus, the extrusion parameters and storage condition are important factors for producing extruded product with high SDS and RS yield. Nevertheless, the formation of SDS during extrusion cooking has never been reported. Consequently, the study on the formation of SDS and RS from starch with addition free fatty acid by extrusion cooking are interested for understand the mechanism and factors affecting the AMLs formation and its characteristics in terms of enzyme digestibility and thermal properties. The additional step after extrusion cooking for generating the densely packed matrices should be investigated in order to understand the relationship between the enzyme digestibility and structural characteristics such as surface morphology and crystalline structure.

5.3 Materials and methods

5.3.1 Materials

Cassava starch (10.4% moisture content) was provided by Sanguan Wongse Industries Co., Ltd. (Nakhon Ratchasima, Thailand). The glycerol and saturated fatty acid, including lauric acid (C12) and stearic acid (C18), PGO enzyme kits (P1179) and o-dianisidine (D3252) were purchased from Sigma-Aldrich (St. Louis, MO., USA). A resistant starch assay kits was purchased from Megazyme International (Ireland). Other chemicals were of analytical grade.

5.3.2 Preliminary study: effect of fatty acid concentration on the formation of amylose-lipid complexes

Two types of aliphatic fatty acid (lauric acid, C12 and stearic acid, C18) were used in this study. The AMLs was prepared according to the method of Ai, Hasjim, & Jane, (2013) with slight modification. The 8% cassava starch gel in deionized water was prepared by heating in a boiling water bath (99^{o}C) for 30 min. Then, each fatty acid at a concentration of 5 and 10% (w/w, dry starch basis) which was dissolved in hot 95% ethanol were added. The mixture was heated in a boiling water bath (99^{o}C) for 30 min followed by cool down to room temperature. The amylose-lipid complexes was recovered by centrifugation. The sediment was washed with 50% ethanol and dried at 40^{o}C overnight. The dried product was ground to fine powder for the complexing index (CI) analysis. The control sample was prepared from starch treated in the same manner, but without the fatty acid addition.

5.3.2.1 Complexing index (CI) analysis

The extent of complex formation between starch and fatty acid was determined based on the concept of complexing index (CI) using the method as described by Guraya, Kadan, & Champagne (1997) with slight modifications. A

sample (1 g) was mixed with 5 mL of distilled water. The mixture was stirred for 2 min by vortex mixer and centrifuged for 15 min at 3,000 rpm. The supernatant (500 μL) and distilled water (15 mL) were added to 2 mL of iodine solution (2.0% KI and 1.3% of I_2 in distilled water). The absorbance was measured at 690 nm through a UV-vis spectrophotometer. CI was calculated as follows:

$$CI = (Abs_{control} - Abs_{sample})/ Abs_{control}$$

where, $Abs_{control}$ is the absorbance of starch solution without added lipid and Abs_{sample} is the absorbance of the starch solution with added lipid.

5.3.3 Extrusion cooking

The feed material (cassava starch) was prepared by adding fatty acid at a concentration of 5% (w/w) (calculated on dry starch basis), which was dissolved in hot 95% ethanol, or adding glycerol at a concentration of 5% (w/w) (calculated on dry starch basis). The extrusion cooking was carried out using a co-rotating twin screw extruder (APV breaker MPF 19:25, Peterborough, English). The screw geometry was a diameter of 19 mm and a length of 475 mm (L/D= 25:1) and screw configuration used was illustrated in Table 5.1. The extruder was divided into four zones. For all experiments, the first two zones were set at 50 and 70°C respectively, whereas the last two zones were set at 120°C. The screw speed was 80 rpm. The dry feed rate was controlled at 0.48 $kg.h^{-1}$ whereas water feed rate was adjusted to obtain the moisture content of 30 and 50%. The die used was a retangular shape of the 3 mm length and width witm 1 mm. At the exit of the die, the extruded samples were manually cut into sticks (10 mm in length) using a knife, and then dried overnight at 50°C. The dried sample was ground into a powder using cryo-grinding and kept at -20°C for further characterization. All the ground samples were defatted in a Soxtec fat-extractor with

petroleum ether at 37°C for 155 min (De Pilli et al., 2011) to remove uncomplexed lipids before the samples were submitted for chemical analyses.

Table 5.1 Screw configuration used in extrusion experiment

Screw element type	No. of amount
1.5D Feed screw	2
1.0D Feed screw	2
60° Forward paddle	6
1.5D Feed screw	2
1.0D Feed screw	2
60° Forward paddle	5
1.5D Feed screw	1
1.0D Feed screw	1
60° Forward paddle	3
1.0D Single lead screw	2
60° Forward paddle	5
1.0D Single lead screw	3
60° Forward paddle	3
1.0D Single lead screw	1
1.0D Disch Single lead screw	1

5.3.4 Starch fractions determination

The starch fractions (RDS, SDS, and RS) of samples were measured according to the method of official AOAC method 2002.02 and Englyst et al. (1992) with slight modification. A sample (100 mg) was incubated with 4 mL of sodium maleate buffer (pH 6.0) containing pancreatic α-amylase (10 $mg.mL^{-1}$) and amyloglucosidase (3 $U.mL^{-1}$) in a shaking water bath with continuous shaking at 37°C for 16 h. During 20 min of incubation, an aliquot (0.4 mL) was taken and mixed well

with an equal volume of absolute ethanol, followed by adding two volumes of 50% ethanol (v/v). The volume was adjusted to 10 mL and the D-glucose content was measured using glucose oxidase/peroxidase reagent (GOPOD reagent) for used to calculate the SDS content. After 16 h of incubation, the reaction is terminated by the addition of an equal volume of absolute ethanol and the RS is recovered as a pellet on centrifugation. Then, the pellet was washed twice by suspension in 4 mL of 50% ethanol (v/v), followed by centrifugation. The supernatant was carefully decanted and collected. Then, the volume was adjusted to 10 mL and the D-glucose content was measured using GOPOD reagent for used to calculate the SDS content. The RS in the pellet was dissolved in 2 mL of 2 M potassium hydroxide and stirred in an ice bath for 20 min. The 1.2 M sodium acetate buffer pH 3.8 (8 mL) was added and followed by 0.1 mL of amyloglucosidase (3,300 U/mL). After that, it was incubated at 50°C in a shaking water bath for 30 min. The hydrolyzed sample was diluted with deionized water. The D-glucose content was determined using GOPOD reagent. The GOPOD enzyme reagent (3 ml) was added to 0. 1 mL of diluted sample, then it was incubated at 50°C for 20 min. The absorbance at 510 nm was measured against a reagent blank. The percentages of RDS, SDS, and RS were calculated as follows:

RDS (%) = glucose released at 20 min x 162/180 x 100

SDS (%) = glucose released at 16 h - glucose released at 20 min x 162/180 x 100

RS (%) = glucose content in the indigested starch at 16 h x 162/180 x 100

5.3.5 Crystalline structure

The crystalline structure was monitored using wide-angle X-ray diffraction (WAXD). The samples were prepared by adjusting the moisture content at 90% relative humidity for 10 days in desiccators under partial vacuum in the presence

of a saturated barium chloride solution. Approximately twenty mg sample was placed between two tape foils during experiment. The diffractograms were recorded on a BRUKER^{TM} (Karlsruhe, Germany) D8 Discover diffractrometer with Cu $K_{\alpha 1}$ radiation (λ=1.54Å). A two-dimension GADDS detector was used to collect the diffracted beam. The recording time for each data collection was 600 s. The sample to detector distance was 100 mm. X-ray spectral data were visualized and normalized using KaleidaGraph software. The Origin Pro 8 (OriginLab Corporation, Northampton, USA) were used to calculate the relative crystallinity of sample as the ratio of area of the crystalline sharp peak over the total diffractograms area (Frost, Karninski, Kirwan, Lascaris, & Shanks, 2009).

5.3.6 Thermal properties

Thermal properties were investigated using differential scanning calorimetry (DSC, a DSC Q100, TA Instruments Inc., Eschborn, Germany). The samples (10 mg) were weighted into a hermetic stainless steel pan and DI water (30 mg) was added. The sealed pan was operated by heating from 0 to 160°C at a rate of 3°Cmin^{-1}. Indium was used for the standard and empty stainless steel pan was used for a reference. The onset temperature (*To*), peak temperature (*Tp*), conclusion temperature (*Tc*) and enthalpy (ΔH) were used to define as the thermal transition of starch and calculated automatically by Universal Analysis 2000 V4.4 software (TA Instruments-Waters LLC).

5.3.7 Molecular mass and size distribution determined by high performance size exclusion chromatography coupled with multi-angle laser light scattering and differential refractive index (HPSEC-MALLS-DRI)

The native cassava starch and extruded native cassava starches with 30 and 50% moisture content were prepared as the method of Rolland-Sabaté et al. (2012) with a slight modification. The samples were dissolved in 95% dimethyl sulfoxide (50 mg mL^{-1}) for 3 days with agitation at room temperature. Then, the solution was precipitated with 95% ethanol at 4°C over night. The precipitates were recovered by centrifugation at 27,000x*g* for 10 min at 25°C. The sediments were rinsed with 99% ethanol followed by acetone, and then air-dried. The sample powder (10 mg) was dissolved in 20 mL of Millipore water, followed by carefully degassed with nitrogen gas. After that, the solution was heated in microwave 900 W for 40 sec followed by cool down in ice batch. The resulting solution was filtered through 0.5 µm syringe filter, and diluted before injected into SEC-MALLS-DRI system. The system was operated with Shodex KW-802.5 column (8 mm ID x 30 cm) from Showa Denko K.K. (Tokyo, Japan) together with KW-G guard column (6 mm ID x 5 cm) from Showa Denko K.K. The column and guard column were maintained at 30°C using a Crococil temperature control system from Cluzeau (Bordeaux, France). The eluant (Millipore water containing 0.02 g L^{-1} sodium azide in) was carefully degassed and filtered through Durapore GV (0.2 µm) membrane from Millipore before used and eluted at the flow rate 0.5 ml/min. The two online detectors consisted of a MALLS instrument (Wyatt Technology Corporation, Santa Barbara, CA) and an ERC-7515A refractometer (Erma, Tokyo, Japan).

5.3.8 Thermo-molding process

5.3.8.1 Preliminary study on thermo-molding process

The extruded cassava starch with and without added fatty acid or glycerol were ground into a powder by cryo-grinding. Then, powder sample (10% moisture content, 700 mg) was weighted into a rectangular stainless steel mold with size of 0.15 cm in thickness, 3 cm in length and 1 cm in width. Thereafter, it was placed in the molding machine (Carver Press, Model 1835 CB, Carver Inc., USA)and the temperature was programmed to 110^{o}C during a 15 min ramp. Then, the 2 tons pressure was applied for 8 min and then the temperature was cooled down to 20^{o}C in 10 min by cold water recirculation. The molded products were about 1.5 mm thickness. Some samples were then cut into the dimension size of 1.5 mm in thickness, 10 mm in length and 5 mm in width and the other samples were ground into a powder by cryo-grinding before analysis.

5.3.8.2 Effect of thermo-molding conditions on starch fractions, crystalline structure and thermal properties of extruded samples

In this study, the powder cassava starch (CS) extruded with C12 was used as starting material. The molded sample was prepared at molding temperature of 90^{o}C, 110^{o}C, and 130^{o}C and the pressure of 2 and 3 tons for 8 min. After molding finished, the molded products were cut into the same dimension size as section 5.3.8.1 and were used for starch fractions analysis, relative crystallinity, and thermal properties measurement according to the method described previously.

5.3.9 The microstructure of extruded and molded-extruded samples monitored by scanning electron microscopy (SEM)

The dried sample was placed on a double sided conducting adhesive and pasted onto a metallic stub. Then, it was coated with gold in a sputter coating unit for

8 min and observed in a JEOL JSM-6010LV electron microscope (Tokyo, Japan) and operated at an accelerating voltage of 5 kV.

5.3.10 Cooking stability test of the molded-extruded sample

The molded cassava starch, molded, C12 and C18 extrudateswere selected for cooking stability testing at 70% moisture content, which represents the high moisture food products. The molded samples were cut into the dimension size of 5 x 10 x 1.5 mm (width x length x thickness) and adjusted moisture content to 70% with distilled water. After that, it was sealed in a closed container, and steamed in the boiling steam for 30 min. After cooled down to room temperature, the cooked sample was determined the starch fractions according to method described previously.

5.3.11 Effect of storage on the SDS and RS content, thermal, and crystalline properties of molded-extruded samples

The molded-extruded CS, molded CS extruded with C12, and molded CS extruded with C18 were cut to the dimension size of 5 x 10 x 1.5 mm (width x length x thickness) and stored at 80% relative humidity in saturated salt solutions for 15 days (D15). Then, it was determined the starch fractions, crystalline, and thermal properties according to the method described previously.

5.3.12 Statistical analysis

All the experiments were conducted in two replications. Analysis of variance (ANOVA) was analyzed using SPSS version 13.0 (SPSS Institute Inc., Cary, NC, USA). The differences between mean values were established using Duncan's multiple-range test.

5.4 Results and discussion

5.4.1 Preliminary study: effect of fatty acid concentration on the formation of amylose-lipid complexes (AMLs)

The preliminary study on the AMLs formation was conducted using conventional method. Effect of fatty acid concentration on complexing index (CI) of the gelatinized cassava starch is shown in Figure 5.1. The CI values of the 5% fatty acid concentration did not differ from those of 10% fatty acid concentration (both C12 and C18) ($p>0.05$), indicating that fatty acid at 5% concentration may be enough to form complexes with amylose of cassava starch. Similar results were revealed by Kawai et al. (2012), the CI value of starch increased with an increase in the concentration of fatty acid and reached to a plateau at 0.5-1.0 mmol g.starch^{-1}. It has been reported that the amylose and fatty acid with weight ratio of 10:1 was an optimum for amylose-lipid complexes formation (Jovanovich & Maria, 1999; Jovanovich, Zamponi, Lupano, & Anon, 1992). Consequently, an optimum concentration of fatty acid to form complex with gelatinized cassava starch in this study was in the range of 5-10%.

5.4.2 Amylose-lipid complexes formation as induced by extrusion cooking

5.4.2.1 RS content and complexing index of the extruded samples

Before extrusion cooking, the DSC experiment was used to evaluate extrusion parameters, including temperature and moisture content ranges. The DSC results showed that the gelatinization temperature of cassava starch decreased with moisture content increased from 30% to 70% (data not shown). At 30% moisture content, the melting temperature of cassava starch was broadened in the range of 68-118^{o}C whereas the ranges of 69-86^{o}C were the gelatinization temperature

of 70% moisture content cassava starch. The previous results demonstrated that the dissociation

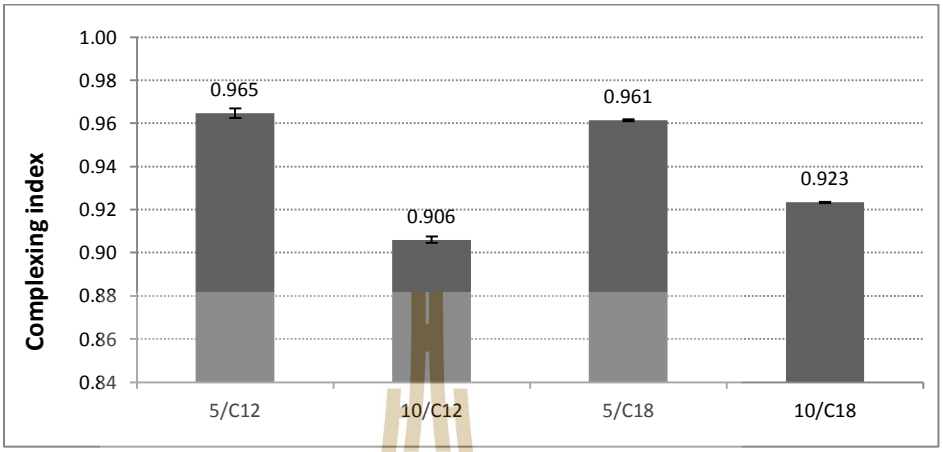

Figure 5.1 Complexing index of cassava starch complexed with C12 and C18 at the concentration of 5% and 10% (w/w).

temperature of AMLs tended to decrease at the high moisture content (>50%) (Le Bail et al., 1999). Therefore, the moisture content of 30, 50 and 70% were chosen for preliminary study on the AMLs formation of cassava starch with addition of C12 at a concentration of 5% by DSC technique. Similar results were obtained from this study, the dissociation temperature and the amount of AMLs formation decreased with increasing moisture content as observed by the reduction of the dissociation enthalpy (ΔH) (data not shown). Regarding the results of conventional method and DSC experiment, C12 and C18 at a concentration of 5% were chosen for study AMLs formation as induced by extrusion cooking at the temperature of 120^{o}C and the moisture content of 30 and 50% compared to glycerol.

After extrusion, the cassava starch extruded with glycerol, C12 and C18 at 30% moisture content showed a greater RS content than those 50%

moisture content (Table 5.2). In addition, they exhibited the CI value higher than 0.89 excepted for the CS extruded with glycerol. This was attributed to the steric hindrance of the glycerol molecules inside the internal helical section of amylose (Mercier, Charbonniere, Grebaut, & Gueriviere, 1980). These results implied that C12 and C18 had a capacity to form complex with the amylose of cassava starch by extrusion cooking similar to the conventional method and DSC technique. However, the CI values between C12 and C18 were not differ for both 30 and 50% moisture contents.

5.4.2.2 Crystalline structure of the extruded samples

The crystalline structure of all extruded samples determined by WAXD is shown in Table 5.2. The extruded CS and CS extruded with glycerol showed an amorphous structure but the CS extruded with C12 and C18 showed the V_h-type crystalline structure due to the characteristic diffraction peaks appeared at 2θ of 7.32, 13.06, and 20.03 (Gelders, Vanderstukken, Goesaert, & Delcour, 2004; Lopez-Rubio, Flanagan, Gilbert, & Gidley, 2008) and a minor A-type crystalline structure. This was in a good agreement with previous results (Zhang et al., 2012). However, the relative crystallinity of all extruded samples was reduced to 15-25% as compared with native CS (Table 5.2). This suggested that thermal, shearing and pressure during extrusion completely destroyed the A-type crystalline structure of CS in relation to the formation of an amorphous structure of extruded CS and CS extruded with glycerol as obtained from WAXD pattern. During extrusion, the high temperature and water which acts as a plasticizer, enhanced the starch gelatinization, leading to amylose leaching and form complexes with fatty acid (De Pilli et al., 2008).

5.4.2.3 Thermal properties of the extruded samples

DSC was used to study the loss of starch granular structures after

after extrusion and the AMLs formation of the extruded samples. DSC thermograms of all extruded samples in excess water illustrate in Table 5.3. The sample extruded with C12 at 30 and 50% moisture content showed four thermal transition temperature peaks. The first peak in the range of 40-49^{o}C was the melting temperature of the free C12 (the melting temperature of C12 = 41-58^{o}C, data not shown). The second peak in the range of 54-73^{o}C was considered to the melting temperature of the remained starch after extrusion. The third peak in the range of 75-101^{o}C was considered to the dissociation temperature of AMLs type I which was the form of amorphous structure and the fourth peak in the range of 108-132^{o}C was considered to be the dissociation temperature of AMLs type II which was the form of crystalline structure Generally, the crystalline form (AMLs type II, T_p = 115-125^{o}C) can melt at a higher temperature than an amorphous form (AMLs type I, T_p < 100^{o}C) (Tufvesson et al., 2003a, 2003b). For the cassava starch extruded with C18 at 30 and 50% moisture content, they showed only three thermal transition temperature peak. The first peak in the range of 56-76^{o}C was considered to the overlapping between the melting temperature of the remained starch and the free C18 (the melting temperature of C18 = 62-84^{o}C, data not shown). The second peak in the range of 90-109^{o}C was considered to the dissociation temperature of AMLs type I and the third peak in the range of 114-132^{o}C was considered to the dissociation temperature of AMLs type II. It was obvious that the dissociation temperature of both AMLs (type I and II) from C18 was higher than those for C12. It suggested that the longer hydrocarbon chains allowed more hydrophobic interactions with the interior of the helix in which requiring higher temperatures to break these bonds (Putseys et al., 2009). This was in agreement with previous results (Ai, et al., 2013, Kawai et al., 2012). However, the higher ΔH of AMLs type II (Peak 4,

Table 5.2 The RS content, complexing index (CI) and crystalline properties of extruded CS as prepared with various water contents and complexing agents

Sample	RS content (%)	Complexing index (CI)	Crystalline structure	Relative crystallinity (%)
CS	7.2 ± 0.5^{a}	-	A-type	45
CS+5% glycerol	8.2 ± 0.4^{a}	-	-	n.d.
CS+5% C12	8.5 ± 0.7^{a}	-	-	n.d.
CS+5% C18	8.3 ± 0.6^{a}	-	-	n.d.
Extruded 30%mc CS	1.0 ± 0.0^{c}	-	Amorphous	-
Extruded 30%mc CS + 5%Glycerol	1.3 ± 0.4^{c}	0.13^{c}	Amorphous	-
Extruded 30%mc CS + 5%C12	2.4 ± 0.2^{b}	0.95^{a}	V_h + A-type	15
Extruded 30%mc CS + 5%C18	2.1 ± 0.1^{b}	0.89^{a}	V_h + A-type	25
Extruded 50%mc CS	1.1 ± 0.0^{c}	-	Amorphous	-
Extruded 50%mc CS + 5%Glycerol	0.5 ± 0.5^{c}	0.43^{b}	V_h + A-type	15
Extruded 50%mc CS + 5%C12	0.5 ± 0.4^{c}	0.92^{a}	V_h + A-type	25
Extruded 50%mc CS + 5%C18	0.4 ± 0.2^{c}	0.95^{a}	V_h + A-type	15

Means values with different superscripts within each column are significantly different ($p < 0.05$). n.d. = not detemined, CS = cassava starch, C12 = lauric acid, C18= stearic acid, 30%mc = extruded at 30% moisture content, 50%mc = extruded at 50% moisture content, and 5% = fatty acid with concentration of 5%.

Table 5.3) was detected from cassava starch extruded with C12 compared with cassava starch extruded with C18. This implied that the higher amount of AMLs in the form of crystalline structure was formed when cassava starch extruded with C12. From the DSC results, it was noted that there are small remained starch in both cassava starch extruded with C12 and C18, which detected from the gelatinization peak in the range of 57-77^{o}C (Table 5.3) (the gelatinization temperature ranges of cassava starch was 62-89^{o}C, Table 5.6). This may be due to the reason that the fatty acid shows a lubricant effect on starch dough during extrusion. According to Hu (1992), the friction between dough and screw elements as well as between dough and barrel during extrusion were reduced due to the lubricant effect, leading to the decrease of the dough temperature. In addition, fatty acid may prevent the starch granules from severe mechanical breakdown by shear stress. Regarding 30% moisture extrusion, a slightly higher ΔH of AMLs type II (Peak 4, Table 5.3) was observed as compared to extruding at 50% moisture content. It suggested that the high formation of AMLs occurred under the operating conditions at 30% moisture content which was consistant with the higher RS content (Table 5.2). This behavior may be attributed to that the lower water content caused the higher friction between the viscous sample and the barrel, resulting in higher starch depolymerization which increase the ability to form complex with fatty acid. This evidence corresponded to the increase of torque from 12.5% (for 50% moisture content) to 20% (for 30% moisture content) (data not shown). These data are in agreement with De Pilli et al. (2011), who studied the formation of starch-lipid complexes during extrusion of model system (rice starch added oleic acid) at 16 and 21% moisture feed content.

Table 5.3 Thermal properties of cassava starch extruded with C12 and C18 at 30 and 50% moisture content

Sample	Peak 1				Peak 2			
	T_o (°C)	T_p (°C)	T_c (°C)	ΔH (Jg^{-1})	T_o (°C)	T_p (°C)	T_c (°C)	ΔH ($J.g^{-1}$)
Extruded 30%mc CS+5%C12	40.9	42.1	49.4	2.0	56.8^{b}	62.3^{b}	73.3^{a}	0.3^{c}
Extruded 50%mc CS+5%C12	40.9	42.1	48.0	2.0	54.3^{b}	60.3^{b}	66.1^{b}	0.2^{c}
Extruded 30%mc CS+5%C18	N.D.	N.D.	N.D.	N.D.	56.0^{b}	64.8^{a}	76.6^{a}	2.4^{b}
Extruded 50%mc CS+5%C18	N.D.	N.D.	N.D.	N.D.	62.8^{a}	66.8^{a}	74.9^{a}	3.7^{a}

Sample	Peak 3				Peak 4			
	T_o (°C)	T_p (°C)	T_c (°C)	ΔH (Jg^{-1})	T_o (°C)	T_p (°C)	T_c (°C)	ΔH ($J.g^{-1}$)
Extruded 30%mc CS+5%C12	91.0^{a}	95.1^{b}	101.4^{c}	0.1^{b}	108.4^{bc}	116.7^{b}	132.3^{a}	3.7^{a}
Extruded 50%mc CS+5%C12	77.5^{b}	82.6^{c}	90.2^{d}	0.2^{b}	110.4^{b}	116.9^{b}	129.5^{b}	3.4^{a}
Extruded 30%mc CS+5%C18	90.9^{a}	99.4^{a}	105.1^{b}	0.5^{a}	109.8^{b}	118.9^{a}	130.6^{b}	2.8^{b}
Extruded 50%mc CS+5%C18	92.2^{a}	98.5^{a}	109.8^{a}	0.4^{a}	114.0^{a}	120.6^{a}	132.5^{a}	2.3^{b}

Means values with different superscripts within each column are significantly different ($p < 0.05$). N.D. = not detected, CS = cassava starch, C12 = lauric acid, C18= stearic acid, 30%mc = extruded at 30% moisture content, and 50%mc = extruded at 50% moisture content.

5.4.2.4 The molecular characteristics of the extruded samples

In order to study the extrusion condition effect on molecular characteristics of cassava starch, the extruded cassava starch with 30 and 50% moisture content were chosen to characterize the molar mass and size distribution using HPSEC-MALL-DRI. The HPSEC chromatograms of all samples show in Figure 5.2., which exhibited a bimodal distribution. For 30% moisture extrudate, the sample peak eluted at higher elution volume compared to cassava starch and 50% moisture extrudate, indicating that the size of the molecules reduced, but the peak is broad and no distinction of amylose fraction is noticed, except for a shoulder (Figure 5.2). Its molar mass decreased from 2.16 x 10^8 g.mol^{-1} (for cassava starch) to 1.24 x 10^8 g.mol^{-1} (Table 5.4). The observed peak probably included branched fractions (which may come from amylopectin depolymerization) and linear fractions (corresponding to amylose). Therefore, no molecular size smaller than amylose were observed, indicating that amylose is not depolymerized. This is consistent with Zhang et al. (2015) in that a large reduction of amylopectin size was found in extruded high amylose maize starch as compared to normal starch. To analyze the size distributions, HPSEC chromatograms were transformed to size distributions using hydrodynamic radius (R_H) versus elution volume calibration curves (Rolland-Sabaté, Guilois, Jaillais, & Colonna, 2011). The size distributions of cassava starch displayed two populations were at R_H ~156 nm (corresponding to the major fraction of amylopectin) and at R_H ~71 nm (corresponding to amylose fraction)(Figure 5.3). They are in agreement with previous results (Rolland-Sabaté et al., 2012) for the R_H of amylopectin fraction from novel non waxy cassava starches (R_H ~120-176 nm) but the R_H obtained from amylose fraction was slightly differed. This could be due to the different in cassava cultivars.

For 50% moisture extrudate, its size distributions were similar to cassava starch. It showed two populations, the first peak (corresponding to the major fraction of amylopectin) was at R_H ~160 nm and amylose fraction was at R_H ~50 nm. The 30% moisture extrudate illustrated a single sharper peak at R_H ~125 nm and a shoulder peak at R_H ~70 nm (Figure 5.3), indicating that the molecular size of cassava starch was more reduced when extruding at 30% moisture content. For 50% moisture extrudate, amylopectin was eluted at the same elution volume as for cassava starch, implying that the size of the molecule is not modified. The molecular density of cassava starch gradually increased to 10.6 $g.mol^{-1}.nm^{-3}$ (for 30% moisture extrudate) and 9.7 $g.mol^{-1}.nm^{-3}$ (for 50% moisture extrudate) (Table 5.4), confirming that the densest structure was occurred after extrusion. Overall, amylopectin is not depolymerized by extruding at 50% moisture content, whereas it is by extruding with 30% moisture content (decrease of molecular mass and size). The mechanical/shear force during extrusion is believed to randomly cleave glycosidic bonds in branched of amylopectin and the degradation preferentially performs on the large molecular size and highly branched structure of amylopectin whereas whole amylose molecules could be largely retained (Li, Hasjim, Xie, Halley, & Gilbert, 2014; Liu, Halley, & Gilbert, 2010).

5.4.3 Effect of thermo-molding process on the extruded cassava starch with and without the addition of complexing agents

5.4.3.1 Preliminary study on thermo-molding process of the extruded samples

In the preliminary study, the extruded samples were ground to obtain a powder sample. After grinding, the decline of SDS fraction and the increase of RDS fractions were observed (Table 5.5). This indicated that SDS fraction which

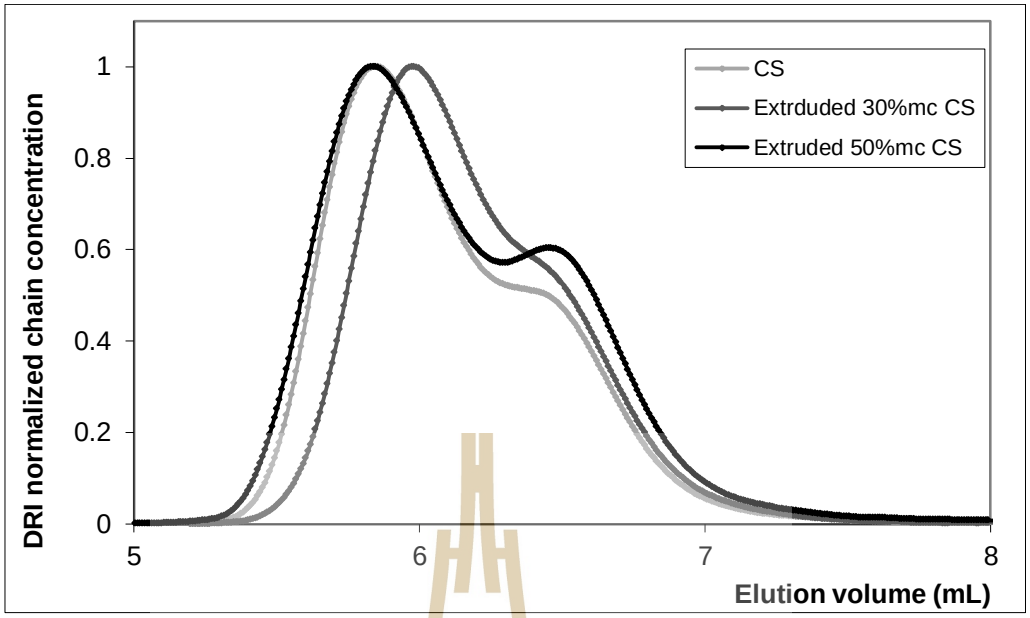

Figure 5.2 HPSEC chromatograms of native cassava starch (CS) and extruded CS as prepared at 30 and 50% moisture content.

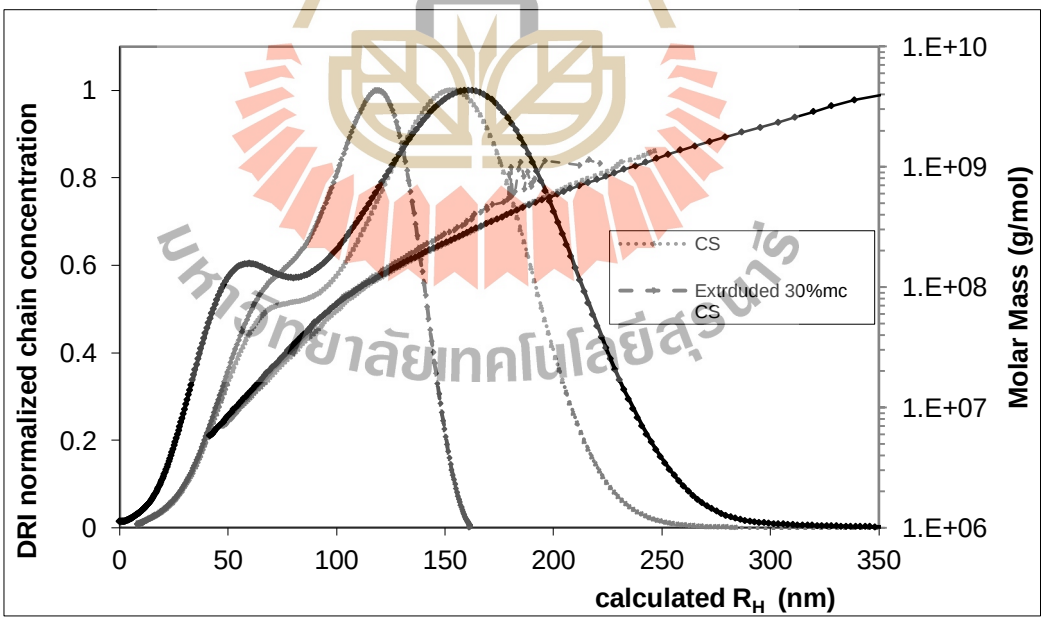

Figure 5.3 Size distributions and molar masses of native cassava starch (CS) and extruded CS as prepared at 30 and 50% moisture content obtained by HPSEC-MALLS-DRI.

Table 5.4 Macromolecular characteristics of extruded cassava starch (CS) and extruded CS as prepared at 30 and 50% moisture content determined by HPSEC-MALLS-DRI

Sample	$\overline{M}_w$ **x10^{-6}** **(g.mol^{-1})**	$\overline{M}_n$ **x10^{-6}** **(g.mol^{-1})**	$\overline{M}_w/\overline{M}_n$	**D_{gapp}** **(g.mol^{-1}.nm^{-3})**
CS	216.0	43.8	4.93	7.7
Extruded 30%mc CS	124.0	38.3	3.24	10.6
Extruded 50%mc CS	345.0	34.4	10.02	9.7

$\overline{M}_w$ = weight average molar mass, $\overline{M}_n$ = number average molar mass, $\overline{M}_w/\overline{M}_n$ = dispersity index, and D_{gapp} = molecular density for the amylopectin population.

was formed during extrusion was transformed to RDS by grinding process. Grinding might destroy the macromolecular structure and increase in the surface area (Silva, Couturier, Berrin, Buléon, & Rouau, 2012). An increase in the surface area favored more susceptible to diffusion and consequently enzymatic hydrolysis. The thermo-molding process was conducted using powder extruded samples, aiming to produce the compact starch in order to improve SDS and RS yield. After molding at 110^{o}C with 2 tons pressure for 8 min, the size of molded sample was reduced to obtain a dimension size of 5 x 10 x 1.5 (width x length x thickness, mm). All molded samples with rectangular shape showed the highest proportion of SDS as compared to powder samples which had a highest proportion of RDS (Table 5.5). However, the RS content of all extruded samples did not improve after thermo-molding. The increment of SDS content might be due to thermo-molding process promoted the formation of a densely packed non-ordered structure. This densely packed structure can be an effective structure for slow digestion rate/extent (Tufvesson, Skrabanja, Björck, Elmståhl, & Eliasson, 2001). The enzymatic susceptibility of amylose is ranked as follows:

amorphous amylose >amylose-lipid complex>retrograded amylose (Tufvesson et al., 2001). Comparable the complexing agents, molded sample extruded with glycerol and C12 showed a higher SDS content than those from molded sample extruded with C18. It

Table 5.5 Starch fractions and crystalline properties of molded CS extruded with various complexing agents after molded at 110°C with 2.0 tons pressure for 8 min

Sample	RDS (%)	SDS (%)	RS (%)	Crystalline structure
Molded_ CS	39.1 ± 0.1^{f}	60.5 ± 0.1^{d}	0.4 ± 0.1^{f}	Amorphous
Extruded CS*	53.6 ± 0.8^{d}	46.4 ± 0.7^{f}	0.0 ± 0.0^{h}	Amorphous
Powder extruded CS	97.0 ± 0.3^{a}	2.0 ± 0.3^{i}	1.0 ± 0.0^{e}	Amorphous
Molded_extruded CS	40.1 ± 0.2^{g}	59.6 ± 0.8^{d}	0.2 ± 0.0^{g}	Amorphous
Extruded CS+Glycerol	44.3 ± 1.1^{e}	55.6 ± 1.0^{e}	0.1 ± 0.1^{g}	Amorphous
Powder extruded CS+Glycerol	95.7 ± 1.6^{a}	3.1 ± 1.3^{h}	1.3 ± 0.4^{cd}	Amorphous
Molded_extruded CS+Glycerol	28.7 ± 0.5^{i}	69.7 ± 0.2^{a}	1.7 ± 0.7^{c}	Amorphous
Extruded CS+C12	36.0 ± 0.7^{g}	60.1 ± 0.9^{d}	3.9 ± 0.3^{a}	V_h+A-type
Powder extruded CS+C12	93.3 ± 0.4^{b}	4.2 ± 0.2^{h}	2.4 ± 0.2^{c}	V_h+A-type
Molded_extruded CS+C12	28.1 ± 0.2^{i}	69.8 ± 0.2^{a}	2.1 ± 0.1^{c}	V_h+A-type
Extruded CS+C18	35.6 ± 0.5^{g}	62.2 ± 0.3^{c}	2.2 ± 0.2^{c}	V_h+A-type
Powder extruded CS+C18	92.2 ± 0.3^{c}	5.8 ± 0.4^{g}	2.1 ± 0.1^{c}	V_h+A-type
Molded_extruded CS+C18	31.2 ± 0.4^{h}	66.0 ± 0.5^{b}	2.8 ± 0.1^{b}	V_h+A-type

* extruded samples were prepared by extrusion cooking at 30% moisture content, CS = cassava starch, C12 = lauric acid, and C18= stearic acid. Means values with different superscripts within each column are significantly different ($p < 0.05$).

indicated that thermo-molding for 8 min could induce high formation of a dense packing of non-crystalline starch polymers of molded CS extruded with glycerol and C12. The dense packing of non-crystalline starch polymers may also be an effective structure for slowing digestion (Zhang et al., 2015).

The crystalline structure of molded sample extruded with C12 and C18 exhibits in Table 5.5. They also showed V_h-type and A-type crystalline structure similar to the sample extruded with C12 and C18. For the molded-extruded sample without the addition of complexing agents and molded sample extruded with glycerol, they showed an amorphous structure similar to the extruded samples before thermo-molding. This result implied that thermo-molding process in this study did not change the crystalline structure of all extruded samples, but it could induce the transformation of AMLs type I into type II, which will be discussed later.

With respect to thermal properties, DSC thermograms of mold, C12 extrudate displayed two thermal transition temperature peaks (Table 5.6). The first peak in the range of 56-76^{o}C was attributed to the gelatinization temperature of the remained starch, whereas the second peak in the range of 113-133^{o}C was attributed to the dissociation temperature of AMLs type II. Similar to the molded sample extruded with C12, DSC thermograms of mold, C18 extrudate showed two thermal transition temperature peaks at 55-76^{o}C and 111-133^{o}C but the additional peak in the range of 90-106^{o}C was observed, which was attributed to the dissociation temperature of AMLs type I. The T_o and T_p of AMLs type II from mold, C12 extrudate was slightly shifted to a higher temperature as compared to mold, C18 extrudate. It indicated that thermo-molding process for a short time (8 min) may enhance the formation of a densely packed crystallized AMLs type II, leading to form AMLs type II_b which showed a slightly higher dissociation temperature than type II_a complexes (Seneviratne & Biliaderis,

1991). Moreover, thermo-molding process in this study can induce the transformation of AMLs type I that was generated during extrusion cooking to AMLs type II as indicated from the disappearance of the third peak for mold, C12 extrudate (Table 5.3). Normally, the less rigid and unstable of type I complexes can be converted to type II complexes of the crystalline form by annealing at temperature above T_p of type I complexes, but lower than T_p of type II complexes (T_p of type I complexes < T < T_p of type II complexes) (Karkalas, Ma, Morrison, & Pethrick, 1995; Tufvesson et al., 2003a, 2003b; Zabar et al., 2009).

The sample extruded with C12, powder sample extruded with C12, and mold, C12 extrudate were chosen to monitor the surface morphology using scanning electron microscopy (SEM). The SEM micrograph of CS extruded with C12 showed the rough and condensed surface with porosity (Figure 5.4a). On the other hand, the powder CS extruded with C12 exhibited the mixture of smooth and rough surface morphology with large amount of porosity (Figure 5.4b). For molded CS extruded with C12, its surface structure was dense and smooth in which some cracked structure appeared (Figure 5.4c). As a result of the higher surface area and the more porous structure of power samples, the reduction of SDS content was found. In addition, the increased SDS content after thermo-molding might be due to that most surface were dense and compact. This suggests that the locally dense non-crystalline structures could also decrease and/or prevent the accessibility of enzymes (Zhang et al., 2015). Moreover, sample surface with a large porous promoted the ability of enzyme to penetrate into the substrate and digest thereafter, leading to show a lower of SDS content as compared with starch sample with a smooth surface. Starch surface with less porosity and smoother area can resist the enzyme digestion, leading to increase the RS content (Lertwana watana, Frazier, & Niranjan, 2015).

Table 5.6 Thermal properties of extruded CS* and molded CS extruded with various complexing agents after molded at 110°C with 2.0 tons pressure for 8 min

Sample	Peak 1				Peak 2			
	T_o (°C)	T_p (°C)	T_c (°C)	ΔH (J.g^{-1})	T_o (°C)	T_p (°C)	T_c (°C)	ΔH (J.g^{-1})
CS	N.D.	N.D.	N.D.	N.D.	61.8^{a}	68.4^{a}	88.8^{a}	14.4^{a}
Molded_ CS	N.D.	N.D.	N.D.	N.D.	56.2^{b}	64.9^{b}	87.6^{a}	11.4^{b}
Extruded CS+C12	40.9	42.1	49.4	2.0	56.8^{b}	62.3^{b}	73.3^{c}	0.3^{d}
Molded_extruded CS+C12	N.D.	N.D.	N.D.	N.D.	56.2^{b}	67.7^{a}	76.3^{b}	2.6^{c}
Extruded CS+C18	N.D.	N.D.	N.D.	N.D.	56.0^{b}	64.8^{b}	76.6^{b}	2.4^{c}
Molded_extruded CS+C18	N.D.	N.D.	N.D.	N.D.	55.0^{b}	64.5^{b}	76.3^{b}	2.3^{c}

Sample	Peak 3				Peak 4			
	T_o (°C)	T_p (°C)	T_c (°C)	ΔH (J.g^{-1})	T_o (°C)	T_p (°C)	T_c (°C)	ΔH (J.g^{-1})
CS	N.D.	N.D.	N.D.	N.D.	N.D.	N.D.	N.D.	N.D.
Molded_ CS	N.D.	N.D.	N.D.	N.D.	N.D.	N.D.	N.D.	N.D.
Extruded CS+C12	91.0	95.1	101.4	0.1	108.4^{b}	116.7^{c}	132.3^{a}	3.2^{a}
Molded_extruded CS+C12	N.D.	N.D.	N.D.	N.D.	112.5^{a}	125.5^{a}	133.3^{a}	1.0^{b}
Extruded CS+C18	90.9	99.4	105.1	0.5	109.8^{ab}	118.9^{b}	130.6^{b}	2.8^{a}
Molded_extruded CS+C18	90.1	96.5	106.3	0.5	110.8^{a}	119.9^{b}	133.5^{a}	3.4^{a}

* extruded CS prepared by extrusion cooking at 30% water content, N.D. = not detected, CS = cassava starch, C12 = lauric acid, and C18= stearic acid. Means values with different superscripts within each column are significantly different ($p < 0.05$).

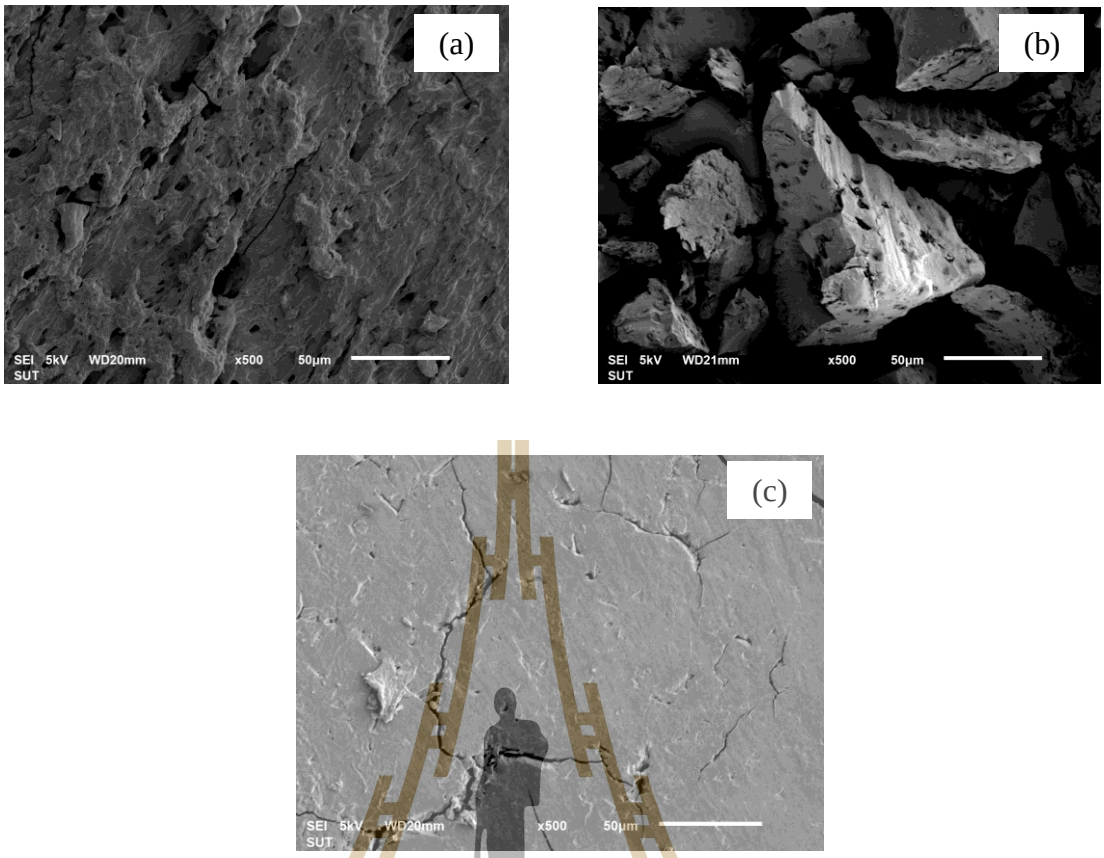

Figure 5.4 SEM micrographs of sample extruded with C12 as prepared by extrusion cooking at 30% moisture content (a), powder sample extruded with C12 (b), and mold, C12 extrudate which were molded at 110°C with 2 tons pressure for 8 min.

5.4.3.2 Effect of thermo-molding conditions on starch fractions, thermal and crystalline properties of the cassava starch extruded with C12

Since the mold, C12 extrudate at 30% moisture content showed the highest SDS content and high thermal stability, it was subjected to thermo-molding process at various conditions, aiming to improve SDS content, RS content, and thermal properties. The conditions of thermo-molding process included molding temperature from 90 to 130°C, molding pressure of 2 to 3 tons, and molding time for 8 min. The results in Table 5.7 showed that an increase in molding temperature from 90 to 110°C tended to improve the SDS yield. However, the SDS was declined when the molding temperature was increased to 130°C. It might be described that high molding temperature (130°C) can destroy the amorphous form of AMLs type I, which was noticed from the disappearance of the dissociation temperature peak of AMLs type I. In the mean time, some portion of AMLs type II was destroyed due to its T_p was less than 130°C (Table 5.6) as observed from the reduction of ΔH of type II complexes as compared with sample extruded with C12. Generally, AMLs type I can be transformed to AMLs type II by annealing at optimum temperature (T_p of type I complexes < T < T_p of type II complexes) (Karkalas et al., 1995; Tufvesson et al., 2003a, 2003b; Zabar et al., 2009). Furthermore, the interaction between molding temperature and pressure during molding process is another factor that may influence on the SDS formation of molded samples due to the high pressure resulted in the volume reduction of the system. This could promote the starch molecule closer together and generating more nuclei in the glassy state (Lertwanawatana et al., 2015) and the more densely packed and reduced porosity of non crystalline region. With respect to thermal properties, DSC thermograms of all mold, C12 extrudates illustrated two thermal transition temperature

peaks (Table 5.8). The first peak in the range of 50-77°C was considered to the gelatinization peak of the remained starch and the second peak in the range of 111-133°C was the dissociation peak of AMLs type II. Nevertheless, T_o, T_p, and T_c of all molded samples were similar to the extruded samples. The WAXD patterns of all molded samples showed a characteristic peak of V_h-type crystalline structure similar to extruded samples. Therefore, thermo-molding process in this study is an effective method to improve the SDS yield of extruded CS and CS extruded with a fatty acid. Overall, the optimum condition of thermo-molding process to produce a product rich in SDS content was the temperature of 110°C with 2 tons pressure for 8 min which gave the highest SDS content (70% SDS) and thermal stability higher than 110°C.

Table 5.7 Starch fractions of molded CS extruded with C12 as prepared at various thermo-molding conditions

Sample	RDS (%)	SDS (%)	RS (%)
Extruded CS+C12	36.0 ± 0.7^{c}	60.1 ± 0.9^{e}	3.9 ± 0.3^{a}
Molded_extruded CS+C12_90c2t	40.6 ± 0.5^{b}	59.2 ± 0.5^{e}	0.2 ± 0.0^{d}
Molded_extruded CS+C12_90c3t	44.1 ± 0.3^{a}	55.7 ± 0.4^{f}	0.2 ± 0.1^{d}
Molded_extruded CS+C12_110c2t	28.1 ± 0.2^{f}	69.8 ± 0.2^{a}	2.1 ± 0.1^{b}
Molded_extruded CS+C12_110c3t	31.6 ± 1.0^{e}	67.3 ± 1.0^{b}	1.1 ± 0.2^{c}
Molded_extruded CS+C12_130c2t	34.2 ± 0.1^{d}	65.6 ± 0.1^{d}	0.2 ± 0.0^{d}
Molded_extruded CS+C12_130c3t	32.1 ± 0.2^{e}	67.7 ± 0.2^{c}	0.2 ± 0.0^{d}

Mean values with different superscripts within each column are significantly different ($p < 0.05$). CS = cassava starch, C12 = lauric acid, 90c = molding temperature of 90°C, 110c = molding temperature of 110°C, 130c = molding temperature of 130°C, 2t = molding pressure of 2 tons, and 3t = molding pressure of 3 tons.

Table 5.8 Thermal properties of mold, C12 extrudates as prepared at various thermo-molding conditions

Sample	Peak 1				Peak 2			
	T_o (°C)	T_p (°C)	T_c (°C)	ΔH (J.g^{-1})	T_o (°C)	T_p (°C)	T_c (°C)	ΔH (J.g^{-1})
Molded_extruded CS+C12_90c2t	60.6^{a}	65.9^{b}	72.9^{b}	0.6^{b}	113.6^{a}	120.2^{b}	133.4^{a}	2.6^{b}
Molded_extruded CS+C12_90c3t	55.9^{b}	68.0^{a}	77.2^{a}	1.3^{b}	111.5^{b}	120.0^{b}	133.0^{a}	2.5^{b}
Molded_extruded CS+C12_110c2t	56.2^{b}	67.6^{a}	76.3^{a}	2.6^{a}	112.5^{a}	125.5^{a}	133.3^{a}	1.0^{c}
Molded_extruded CS+C12_110c3t	65.2^{a}	68.2^{a}	76.9^{a}	0.7^{b}	110.6^{bc}	120.2^{b}	132.9^{a}	2.1^{b}
Molded_extruded CS+C12_130c2t	50.0^{c}	65.5^{b}	72.8^{b}	1.9^{a}	113.4^{a}	121.3^{b}	132.4^{a}	3.0^{a}
Molded_extruded CS+C12_130c3t	63.5^{a}	68.2^{a}	77.1^{a}	0.9^{b}	112.6^{a}	117.8^{c}	125.1^{b}	0.5^{d}

Mean values with different superscripts within each column are significantly different ($p < 0.05$). N.D. = not detected, CS = cassava starch, C12 = lauric acid, 90c = molding temperature of 90°C, 110c = molding temperature of 110°C, 130c = molding temperature of 130°C, 2t = molding pressure of 2 tons, and 3t = molding pressure of 3 tons.

5.4.4 Cooking stability of the molded extruded starch

The three samples of molded extruded cassava starch (CS), molded CS extruded with C12, and molded CS extruded with C18 were selected to examine the cooking stability at 70% moisture content for 30 min. After cooking, the densely packed non-ordered structure of SDS and the ordered structure of RS in molded samples were destroyed to the loosely non-ordered structure, leading to show the higher RDS content (Figure 5.5). The SDS and RS content of both molded CS extruded with C12 and C18 decreased after cooking. The decreasing of RS in mold, C18 extrudate was less than mold, C12 extrudate, probably due to AMLs type II of mold, C18 extrudate had a higher dissociation temperature. For mold extruded CS, some fractions of SDS could be destroyed to RDS. These results implied that AMLs from C18 as induced by extrusion cooking and thermo-molding process are more heat stable than AMLs from C12 under this cooking condition. However, the SDS structure of all molded extruded products was transformed to RDS.

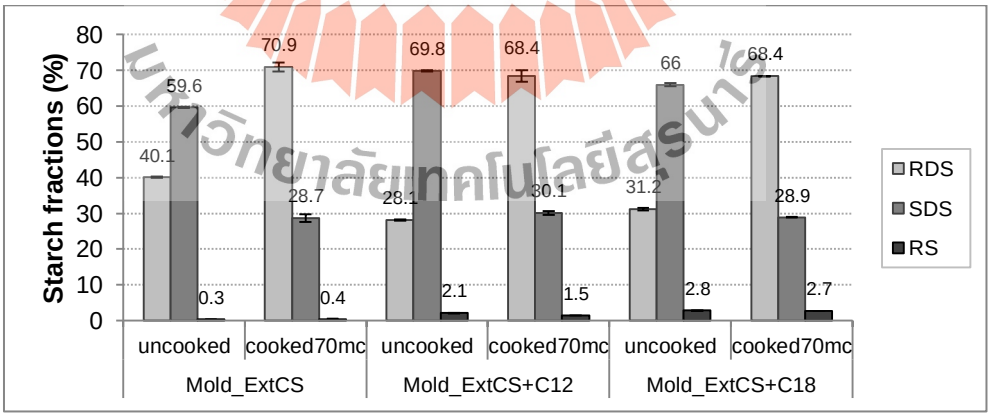

Figure 5.5 Starch fractions of molded extruded cassava starch (Molded_ExtCS), molded CS extruded with C12 (Molded_ExtCS+C12), and molded CS extruded with C18 (Molded_ExtCS+C18) before and after steam cooking at 70% moisture content for 30 min.

5.4.5 Effect of storage condition on SDS content, RS content, crystalline structure and thermal properties of the molded extruded starches

After thermo-molding at optimum conditions (the molding temperature of 110°C with 2 tons pressure for 8 min), mold, C12 and C18 extrudates were stored at 80% relative humidity for 15 days at room temperature compared to molded cassava starch, aiming to improve their RS yield and thermal stability. The storage did not improve the yield of RS but it enhanced the formation of SDS as noticed from the increasing of SDS content for all samples (Table 5.9). The highest yield of SDS content was found from mold, cassava starch extrudate (97% SDS), followed by mold, C18 (81% SDS) and mold, C12 extrudate (75% SDS), respectively. An increase in SDS content for 1.6 times was detected in molded cassava starch after storage. This was probably explained that a prolonged storage time with higher relative humidity promoted chain mobility and re-association of starch molecules, thereafter, leading to form imperfect crystalline structure of SDS (Niba, 2003). In the same time, some imperfect crystalline structure of molded cassava starch that formed by double helix aggregation of amylopectin were improved to more crystalline perfection as observed the shifted of DSC thermogram from 56-88°C (Table 5.6) to a higher temperature of 77-92°C (Table 5.10). Moreover, the transition temperature peaks at low melting temperature in the range 46-66°C were detected, which represented the melting temperature of retrograded amylopectin that was formed after storage at a long time (Table 5.10). This storage condition also changed the structure of molded cassava starch from an amorphous structure to B-type crystalline structure as evidenced the singlet peak at 2θ of 5.6° and 17° (Figure 5.6a). For both mold, C12 and C18 extrudates, an increase in SDS content only for 1.1-1.2 times were noticed after

storage, probably due to that the formation of AMLs during thermo-molding process retarded the starch re-crystallization. However, the re-association of starch molecules was also induced during storage, leading to form ordered structure of C-type crystalline structure which showed an additional singlet peak at 2θ of 5.6° which referred to B-type crystalline structure and the doublet peak at 2θ of 17° and 18° which referred to A-type crystalline structure (Figure 5.6a). After storage, the DSC thermograms of both mold, C12 and C18 extrudates illustrated two thermal transition temperature peaks (Table 5.10). The first peak in the range of 41-47°C was considered to the melting temperature of the free C12 whereas the temperature ranges of 58-70°C were the melting temperature of the free C18 overlapping with the melting temperature of retrograded amylopectin. The second peak for both samples was attributed the dissociation temperature of AMLs type II. The T_o and T_p of the stored-mold, C12 extrudate in the second peak were shifted to a lower temperature as compared with mold, C12 extrudate (T_o = 113°C and T_p = 126°C), but those of the stored-mold, C18 extrudate was similar to mold, C18 extrudate (T_o = 111°C and T_p = 120°C). Moreover, the AMLs type I of mold, C18 extrudate was transformed to AMLs type II after storage as observed the disappearance of DSC thermogram peak at a temperature of 90-106°C (Table 5.6).

Table 5.9 The SDS and RS content of molded samples after storage at 80% relative humidity for 15 days

Sample	SDS content (%)	RS content (%)
M_ CS	60.5 ± 0.1^{f}	0.4 ± 0.1^{d}
SM_ CS	96.7 ± 0.4^{a}	1.5 ± 0.0^{c}
M_extruded CS+ C12	69.8 ± 0.2^{d}	2.1 ± 0.1^{b}
SM_extruded CS+ C12	75.2 ± 0.8^{c}	2.0 ± 0.1^{b}
M_extruded CS + C18	66.0 ± 0.5^{e}	2.8 ± 0.1^{a}
SM_extruded CS + C18	81.4 ± 0.5^{b}	2.5 ± 0.3^{a}

CS = cassava starch, C12 = lauric acid, C18 = stearic acid, and SM = molded sample after storage at 80% relative humidity for 15 days at room temperature. Means values with different superscripts within each column are significantly different ($p < 0.05$).

Table 5.10 Thermal properties of molded CS and molded CS extruded with C12 and C18 after storage at 80% relative humidity for 15 days

Sample	Peak 1				Peak 2			
	T_o (°C)	T_p (°C)	T_c (°C)	ΔH (J.g^{-1})	T_o (°C)	T_p (°C)	T_c (°C)	ΔH (J.g^{-1})
SM_ CS	46.1	54.0	65.7	0.8	77.3^{b}	85.0^{b}	92.4^{a}	0.2^{b}
SM_ extruded CS+C12	41.2	42.4	47.4	0.4	109.5^{a}	120.7^{a}	138.8^{a}	3.9^{a}
SM_extruded CS +C18	58.4	63.7	70.0	0.3	110.3^{a}	120.0^{a}	132.2^{b}	3.4^{a}

Means values with different superscripts within each column are significantly different ($p < 0.05$).CS = cassava starch, C12 = lauric acid, C18 = stearic acid, and SM = molded sample after storage at 80% relative humidity for 15 days at room temperature.

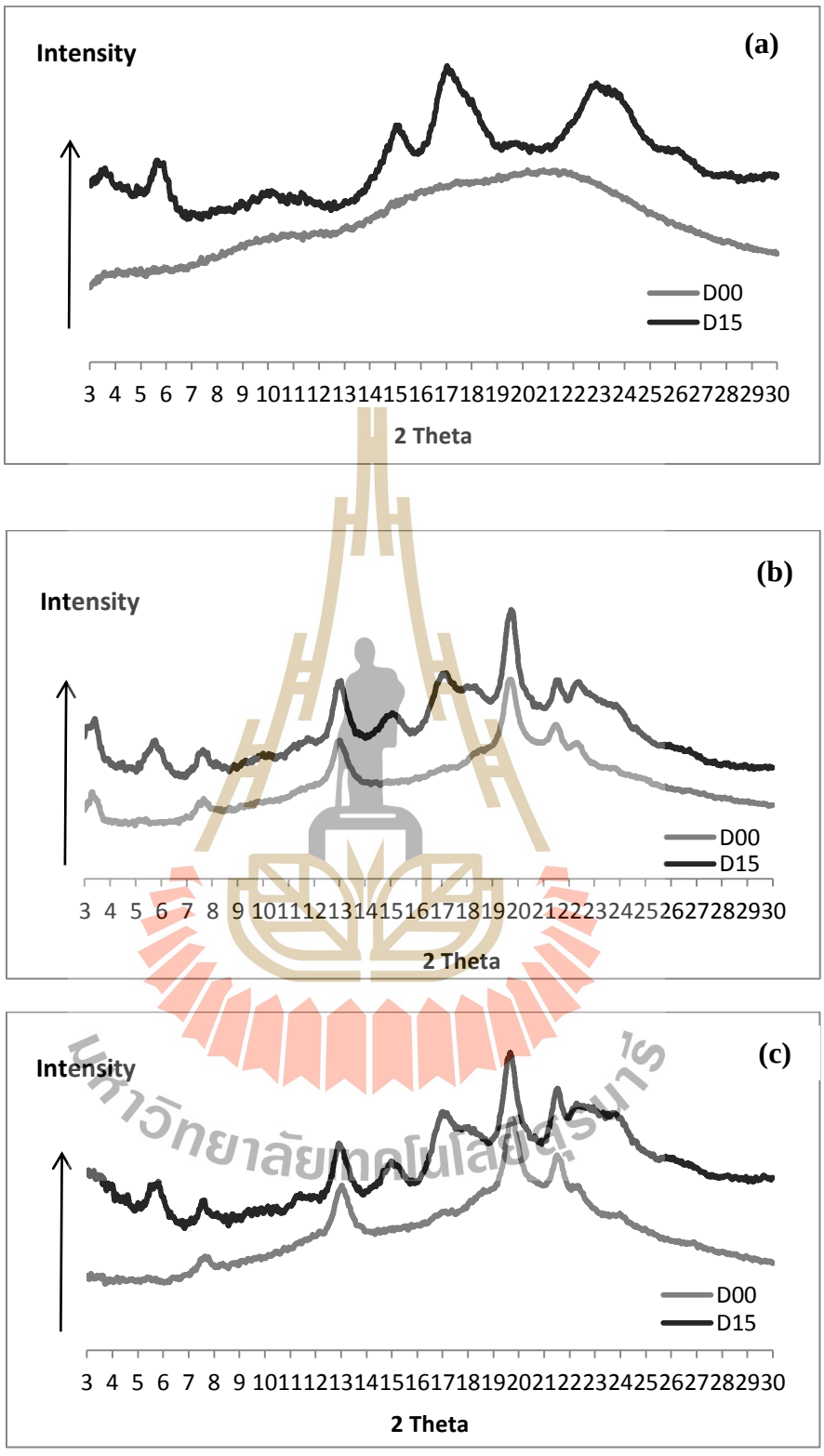

Figure 5.6 WAXD patterns of molded cassava starch extrudate (a), mold, C12 extrudate (b), and mold, C18 extrudate (c) before (D00) and after storage at 80% relative humidity for 15 days (D15).

5.5 Conclusion

The ability to form AMLs of cassava starch and its nutritional starch fractions and thermal properties depends on both fatty acid chain length and complexing conditions. The addition of fatty acid with aliphatic chain during extrusion can improve thermal properties of cassava starch. The dissociation temperature of AMLs type I and II extruded samples were increased with the chain length of aliphatic chains. The surface characteristics of material influence on enzyme digestibility. The rough and condensed surface with small porosity of the extruded products decreased the accessibility of enzyme, in contrast to the mixture of smooth and rough surface with large porosity and surface area of powder extruded products. Furthermore, a densely packed or a compact structure of material with smooth surface morphology as produced by thermo-molding process could also prevent the enzyme hydrolysis, leading to improve the SDS yield. The transformation of AMLs type I to type II of extruded cassava starch could enhance by thermo-molding process which provided higher SDS yield and thermal stability. After steaming cooking at high moisture content, the resulting product of this study contained about 29-30% SDS. This result suggested that the extrusion cooking and thermo-molding process could be used to produce starch-based novel biomaterials from starch inclusion complexes with fatty acid which are rich in SDS yield and high thermal stability. However, the cooking condition, structural and thermal properties of the molded product after cooking need to be further investigated to better understand the structural change and the nutritional starch fractions for application in many food products.

5.6 Acknowledgements

This work was financially supported by the Thailand Research Fund (TRF) through the Royal Golden Jubilee (RGJ) Ph.D. Program (Grant No. PHD/0090/2552) and the Embassy of France in Thailand. The authors are gratefully thank B. Pontoire, and M. de Carvalho, for the technical support.

5.7 References

Ai, Y., Hasjim, J., & Jane, J-L. (2013). Effects of lipids on enzymatic hydrolysis and physical properties of starch. **Carbohydrate Polymers,** 92, 120-127.

AOAC. (2002). **Official methods of analysis of AOAC international 17th ed.,** AOAC International, Gairhersburg, MD, USA.

Englyst, H. N., Kingman, S. M. & Cummings, J. H. (1992). Classification and measurement of nutritionally important starch fractions. **European Journal of Clinical Nutrition,** 46, S33-S50.

Bird, A. R. & Topping, D. L. (2008). Resistant starch as a prebiotic. In J. Versalovic and Wilson M. (eds.) **Therapectic microbiology: probiotica and related strategies.** ASM Press, Washington, pp. 159-173.

Chanvrier, H., Uthayakumaran, S., Appelqvist, I. A. M., Gidley, M. J., Gilbert, E. P., & Lopez-Rubio, A. (2007). Influence of storage conditions on the structure, thermal behavior, and formation of enzyme-resistant starch in extruded starches. **Journal of Agricultural and Food Chemistry,** 55, 9883-9890.

De Pilli, T., Derossi, A., Talja, R. A., Jouppila, K., & Severini, C. (2011). Study of starch-lipid complexes on model system and real food produced using

extrusion-cooking technology. **Innovative Food Science and Engineering Technologies,** 12, 610-616.

De Pilli, T., Jouppila, K., Ikonen, J., Kansikas, J., Derossi, A., & Severini, C. (2008). Study on formation of starch-lipid complexes during extrusion-cooking of almond flour. **Journal Food Engineering,** 87, 495–504.

Fanta, G. F., Felker, F. C., Shogren, R. L. (2002). Formation of crystalline aggregates in slowly-cooled starch solutions prepared by steam jet cooking. **Carbohydrate Polymers,** 48, 161–170.

Fanta, G. F., Kenar, J. A., Felker, F. C. (2015). Nanoparticle formation from amylose-fatty acid inclusion complexes prepared by steam jet cooking. **Industrial Crops and Products,** 74, 36-44.

Gelders, G. G., Vanderstukken, T. C., Goesaert, H., & Delcour, J. A. (2004). Amylose-lipid complexation: a new fractionation method. **Carbohydrate Polymers,** 56, 447-458.

Godet, M. C., Bizot, H., & Buléon, A. (1995). Crystallization of amylose-fatty acid complexes prepared with different amylose chain lengths. **Carbohydrate Polymers,** 27, 47-52.

Hu, L. (1992). **Food emulsifier effects on corn meal extrusion with dietary fiber.** Ph.D. Dissertation, Department of Agricultural Engineering, University of Missouri, Columbia.

Huth, M., Dongowski, G., Gebhardt, E., & Flamme, W. (2000). Functional properties of dietary fibre enriched extrudates from barley. **Journal of Cereal Science,** 32, 115-128.

Jovanovich, G., & Maria, C. A. (1999). Amylose–lipid complex dissociation, a study of the kinetic parameters. **Biopolymers,** 49, 81-89.

Jovanovich, G., Zamponi, R. A., Lupano, C. E., & Anon, M. C. (1992). Effect of water content on the formation and dissociation of the amylose–lipid complex in wheat flour. **Journal of Agricultural and Food Chemistry,** 40(10), 1789-1793.

Karkalas, J., Ma, S., Morrison, W. R., & Pethrick, R. A. (1995). Some factors determining the thermal-properties of amylose inclusion complexes with fatty-acids. **Carbohydrate Research,** 268, 233-247.

Kawai, K., Takato, S., Sasaki, T., & Kajiwara, K. (2012). Complex formation, thermal properties, and *in-vitro* digestibility of gelatinized potato starch-fatty acid mixtures. **Food Hydrocolloids,** 27, 228-234.

Le Bail, P., Bizot, H., Ollivon, M., Keller, G., Bourgaux, C., & Buléon, A. (1999). Monitoring the crystallization of amylose-lipid complexes during maize starch dissociation by synchrotron X-ray diffraction. **Biopolymer,** 50, 99-110.

Lertwanawatana, P., Frazier, R. A., & Niranjan, K. (2015). High pressure intensification of cassava resistant starch (RS3) yields. **Food Chemistry,** 181, 85-93.

Li, M., Hasjim, J., Xie, F. W., Halley, P. J., & Gilbert, R. G. (2014). Shear degradation of molecular, crystalline, and granular structures of starch during extrusion. **Starch-Stärke,** 66(7-8), 595-605.

Liu, W. C., Halley, P. J., & Gilbert, R. G. (2010). Mechanism of degradation of starch, ahighly branched polymer, during extrusion. **Macromolecules,** 43(6), 2855-2864.

Lopez-Rubio, A., Flanagan, B. M., Shrestha, A. K., Gidley, M. J., & Gilbert, E. P. (2008). Molecular rearrangement of starch during in vitro digestion: toward a better understanding of enzyme resistant starch formation in processed starches. **Biomacromolecules,** 9, 1951-1958.

Meng, S., Ma, Y., Cui, J., Sun, D. W. (2014). Preparation of cornstarch-fatty acid complexes by high-pressure homogenization. **Starch/Stärke,** 66, 809-817.

Mercier, C., Charbonniere, R., Grebaut, J., & Gueriviere, J. F. (1980). Formation of amylose-lipid complexes by twin-screw extrusion cooking of manioc starch. **Cereal Chemistry,** 57(1), 4-9.

Niba, L. L. (2003). Processing effects on susceptibility of starch to digestion in some dietary starch sources. **International Journal of Food Sciences and Nutrition,** 54, 97-109.

Putseys, J. A., Derde, L. J., Lamberts, L., Goesaert, H., & Delcour, J. A. (2009). Production of tailor made short chain amylose-lipid complexes using varying reaction conditions. **Carbohydrate Polymers,** 78, 854-861.

Rolland-Sabaté, A., Sánchez, T., Buléon, A., Colonna, P., Jaillais, B., Ceballos, H., & Dufour, D. (2012). Structural characterization of novel cassava starches with low and high-amylose contents in comparison with other commercial sources. **Food Hydrocolloids,** 27(1), 161-174.

Seneviratne, H. D., & Biliaderis, C. G. (1991). Action of a-amylases on amylose-lipid complex superstructures. **Journal of Cereal Science,** 13, 129-143.

Tufvesson, F., Skrabanja, V., Björck, I., Elmståhl, H. L., & Eliasson, A.-C. (2001). Digestibility of starch systems containing amyloseeglycerol monopalmitin complexes. **LWT-Food Science and Technology,** 34, 131-139.

Tufvesson, F., Wahlgren, M., & Eliasson, A. C. (2003a). Formation of amylose-lipid complexes and effects of temperature treatment. Part 1. Monoglycerides. **Starch-Stärke,** 55, 61-71.

Tufvesson, F., Wahlgren, M., & Eliasson, A. C. (2003b). Formation of amylose-lipid complexes and effects of temperature treatment. Part 2. Fatty acids. **Starch-Stärke,** 55, 138-149.

Vasanthan, T. & Bhatty, R. S. (1998). Enhancement of Resistant Starch (RS3) in Amylomaize, Barley, Field Pea, and Lentil Starches. **Starch/Stärke,** 50, 286-291.

Wolf, B. (2010). Polysaccharide functionality through extrusion cooking. **Current Opinion in Colloid and Interface Science,** 15, 50-54.

Zabar, S., Lesmes, U., Katz, I., Shimoni, E., & Bianco-Peled, H. (2009). Studying different dimensions of amylose-long chain fatty acid complexes: molecular, nano and micro level characteristics. **Food Hydrocolloids,** 23, 1918-1925.

Zhang, B., Dhital, S., Flanagan, B. M. Luckman, P., Halley, P. J., & Gidley, M. J. (2015). Extrusion induced low-order starch matrices: Enzymic hydrolysis and structure. **Carbohydrate Polymers,** 134, 485-496.

Zhang, B., Huang, Q., Luo, F., & Fu., X. (2012). Structural characterizations and digestibility of debranched high-amylose maize starch complexed with lauric acid. **Food Hydrocolloids,** 28, 174-181.

CHAPTER VI

SUMMARY

The RS yield of crystallized debranched cassava starch and its quality could be improved by several crystallization methods. The additional step of hydrothermal treatment with annealing or HMT could improve the RS formation and thermal stability of crystallized starch. Both annealing (ANN) and HMT induced the interaction of glucan chains to form double helix and more perfect crystalline structure, which enhanced RS formation. However, the high temperature during HMT can melt some imperfect crystallites and facilitated the new crystallites formation with different stability, leading to improvement the crystalline perfection and RS yield greater than ANN. The dual hydrothermal treatments of ANN and HMT could modify both structural and thermal properties. The sequence of ANN→HMT treatment showed higher thermal stability due to inducing the transformation of the crystalline structure to more crystalline perfection. An initial RS content and crystalline perfection of starchy products are an important factor that influenced the starch fractions after cooking. The product with a lower initial RS content and more crystalline perfection showed an improvement of RS content greater than the sample with a higher initial RS content and less crystalline perfection when cooking at intermediate moisture.

The modification of cassava starch structure by amylomaltase (AM) resulted in the broadening of chain length distribution. The action mode of AM on starch

structure depends on the reaction time. However, AM catalyzed the major disproportionation reaction, resulting in increasing the proportions of a long chain with DP 25-80. Chain length distribution of starch influenced the enzyme digestibility and thermal properties of debranched starch. The combination of AM and debranching enzyme could improve both RS yield and thermal properties of debranched cassava starches because of the action of AM to elongate the chain length of starch. An increase in the long chain proportions resulted in the higher melting temperature. Furthermore, when recrystallization by isothermal temperature incubation and HMT, the debranched starch with higher long chain proportion could form more double helix and ordered structure, which resist to enzyme susceptibility and has high thermal stability. The isothermal incubation yielded the higher RS content but HMT treatment showed a higher thermal stability as a resulted from the transformation of crystalline structure to more perfect structure. The surface morphology of starch is another factor influencing enzyme digestibility. Thermo-molding process enhanced the formation of a densely packed surface regions with a smooth surface, leading to improve the yields of SDS and RS. However, these yield depend on the thermo-molding conditions and its dimension size. The highest SDS and RS yield with showing higher thermal stability was produced at a high molding temperature and pressure. The molded sample with a larger dimension size showed a highest RS yield as a result of the lower accessibility of starch-acting enzymes. These results could apply for producing starchy product with enrich in SDS and RS content and high thermal stability by using AM combined with debranching enzyme. Furthermore, the physical modification of isothermal incubation, HMT, and the thermo-molding process can be further applied in order to achieve the starch product with higher SDS and RS content and thermal stability.

The addition of fatty acids (lauric acid or stearic acid) during extrusion cooking can improve thermal properties of cassava starch because of the formation of amylose-lipid complexes. The SDS and RS content of extruded products decreased after grinding into powder, which resulted from the larger surface area and the surface characteristics with the mixture of a smooth and a rough porosity surface. Furthermore, the formation a densely packed or a compact structure of material with a smooth surface as induced by thermo-molding could also prevent the enzyme hydrolysis, leading to improve the SDS yield. Thermo-molding process could enhance the transformation of amylose-lipid complexes from type I to type II, which provided higher SDS yield and thermal stability. This result suggested that the extrusion cooking and thermo-molding process could be used to produce starch-based biomaterials from starch inclusion complexes with fatty acid which are rich in SDS yield and high thermal stability.

APPENDICES

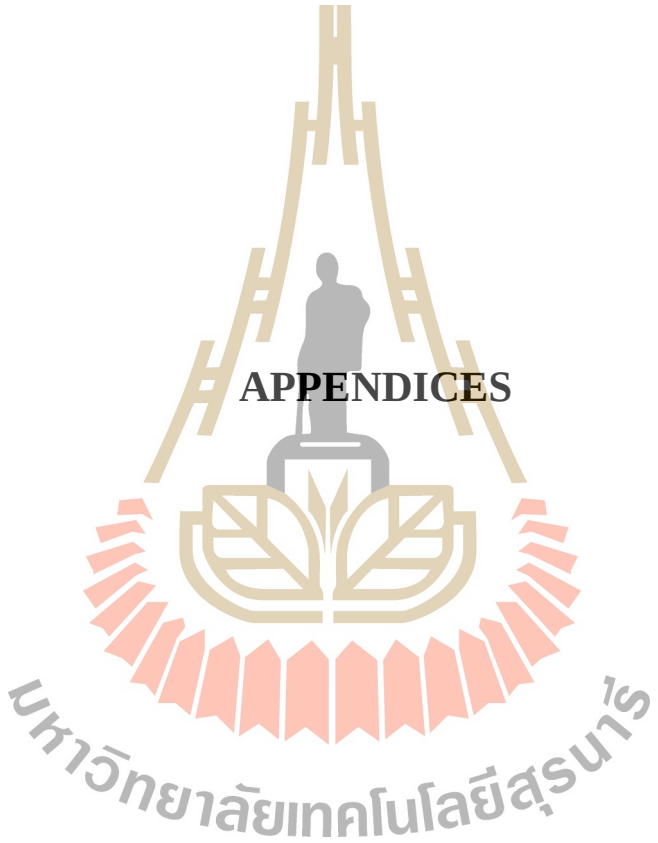

APPENDIX A

DETERMINATION OF AM ACTIVITY

1. The disproportionation activity of AM

The disproportionation activity of AM was assayed according to the method of Jung et al. (2011) with slight modification. Maltotriose was used as both substrate and acceptor molecules. A reaction mixture containing 1% maltotriose in 50 mM phosphate buffer (pH 6.0) and diluted enzyme was incubated at 70°C for 10 min. The reaction was stopped by adding 50 µL of 1 M hydrochloric acid. After neutralization with 50 µL of 1 M sodium hydroxide, the glucose content in the reaction mixture was measured using PGO enzymes reagent (containing glucose oxidase, peroxidase and o-dianisidine). The 2.5 mL of PGO enzyme reagent was added to the 0.25 mL of the diluted sample, then it was incubated at 37°C for 30 min. The absorbance was measured against a reagent blank using UV-vis spectrophotometer at 440 nm. One unit of enzyme was defined as the amount of the enzyme that produced 1 µmol of glucose per min.

APPENDIX B

SUPPLEMENTARY DATA

CHAPTER III

3.4.2 Effect of dual hydrothermal treatments on starch fractions and thermal properties

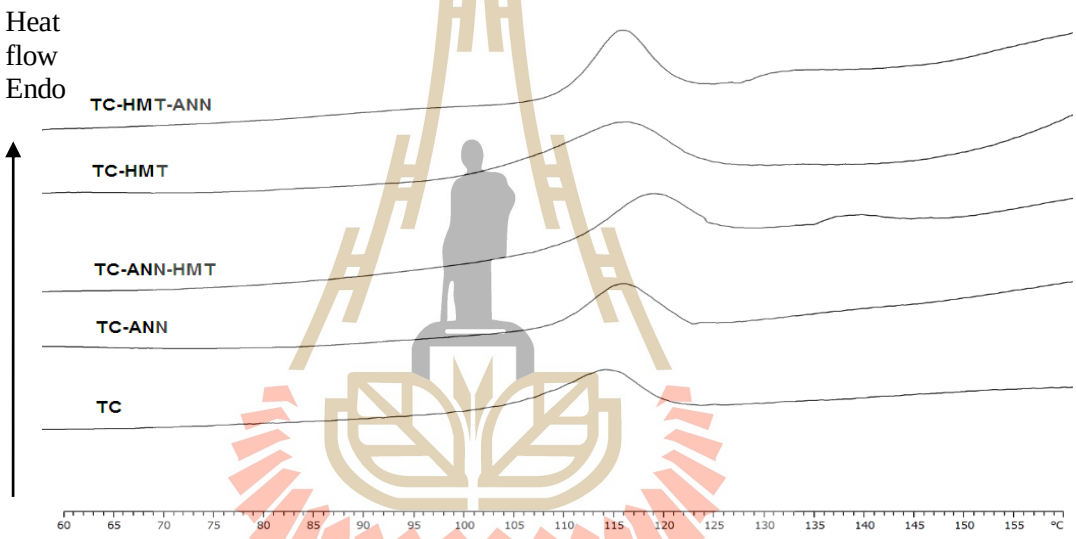

Figure 1B DSC thermograms of single and dual hydrothermal-treated temperature-cycled debranched starch. TC = temperature-cycled debranched starch, TC–ANN=temperature-cycled debranched starch subjected to annealing at 8^{o}C below *Tp* of TC sample for 48h, TC–HMT = temperature-cycled debranched starch subjected to heat-moisture treatment with 20% moisture content at 130^{o}C for 2 h, TC–ANN–HMT= temperature-cycled debranched starch subjected to annealing followed by heat-moisture treatment, and TC–HMT–ANN = temperature-cycled debranched starch subjected to heat-moisture treatment followed by annealing.

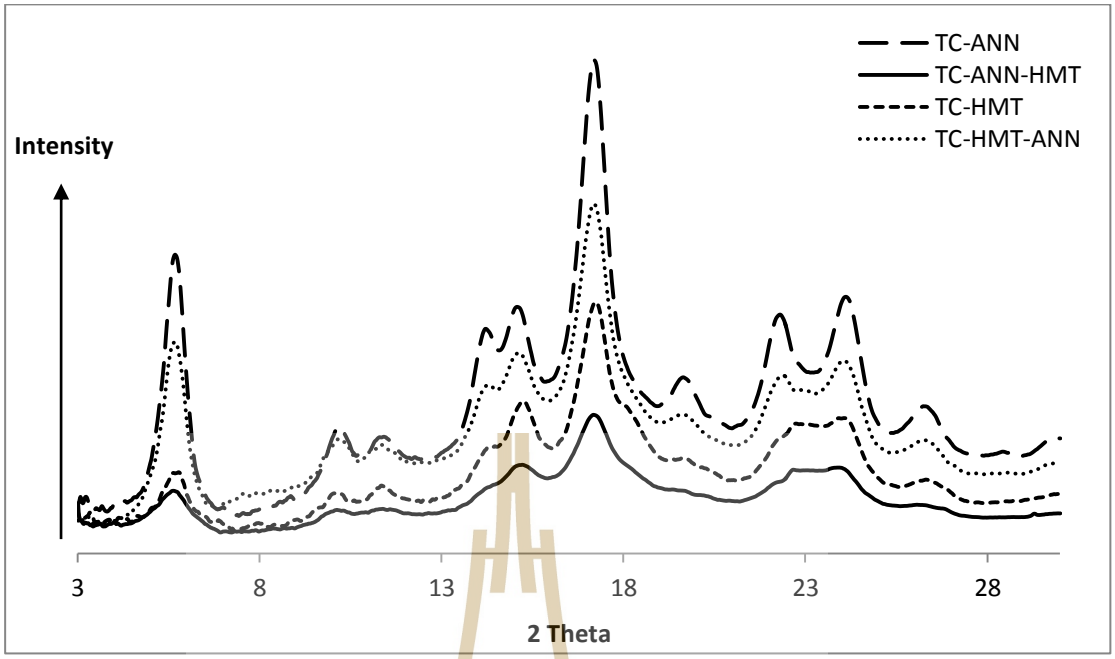

Figure 2B WAXS patterns of single and dual hydrothermal-treated temperature-cycled debranched starch. TC–ANN = temperature-cycled debranched starch subjected to annealing at 8°C below *Tp* of TC sample for 48h, TC–HMT = temperature-cycled debranched starch subjected to heat-moisture treatment with 20% moisture content at 130°C for 2 h, TC–ANN–HMT = temperature-cycled debranched starch subjected to annealing followed by heat-moisture treatment, and TC–HMT–ANN = temperature-cycled debranched starch subjected to heat-moisture treatment followed by annealing.

CHAPTER IV

4.4.3.2 Effect of recrystallization method on starch fractions, crystalline and thermal properties of debranched native and AM-treated starch

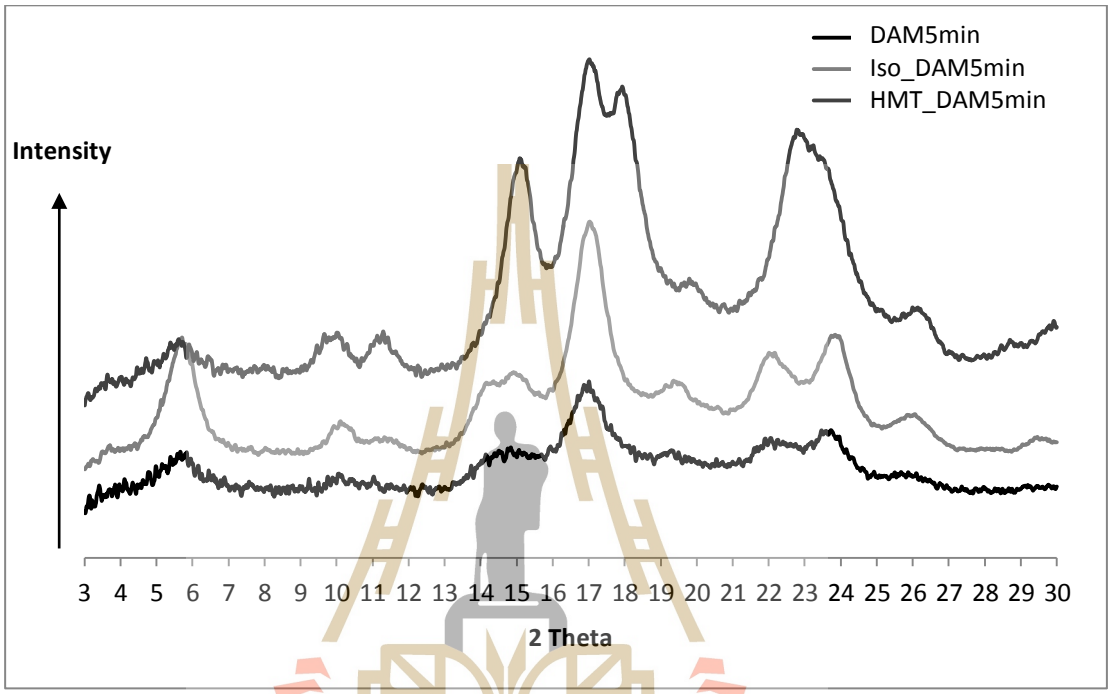

Figure 3B WAXD patterns of debranched native and AM-treated cassava starch with different CL distribution after subjected to recrystallization. DAM5min = debranched AM-treated cassava starch for 5 min, Iso = isothermal temperature incubation with 90% moisture content at 50°C for 3 days, HMT = heat- moisture treatment with 30% moisture content at 130°C for 3h.

4.4.4.2.2 Effect of thermo-molding conditions on starch fractions, crystallinity, and thermal properties of DAM5min

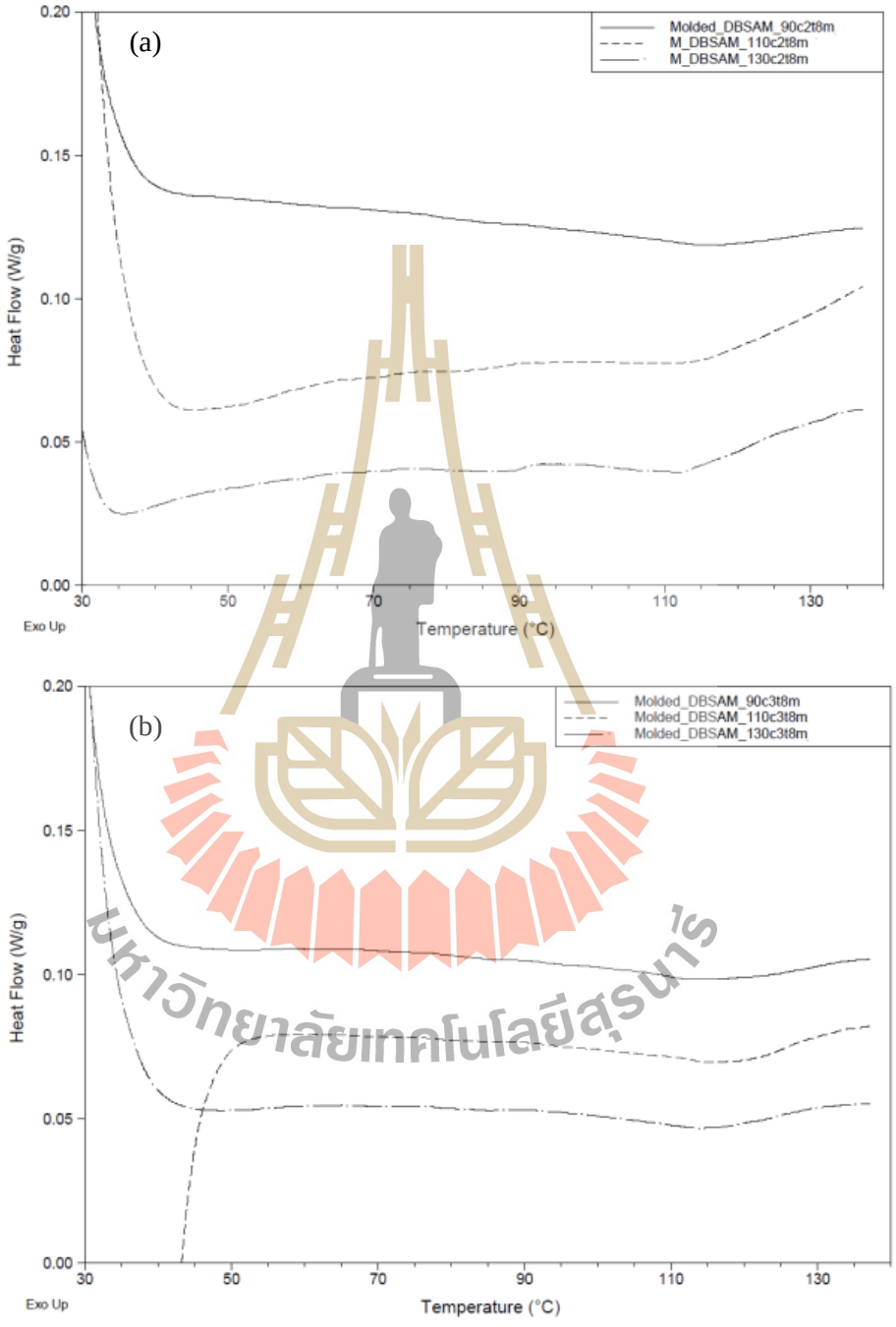

Figure 4B DSC thermograms of molded debranched AM-treated cassava starch which was molded at (a): the pressure of 2 tons and (b): the pressure of 3 tons for 8 min with different molding temperature.

CHAPTER V

5.4.2. 3 Thermal properties of the extruded samples

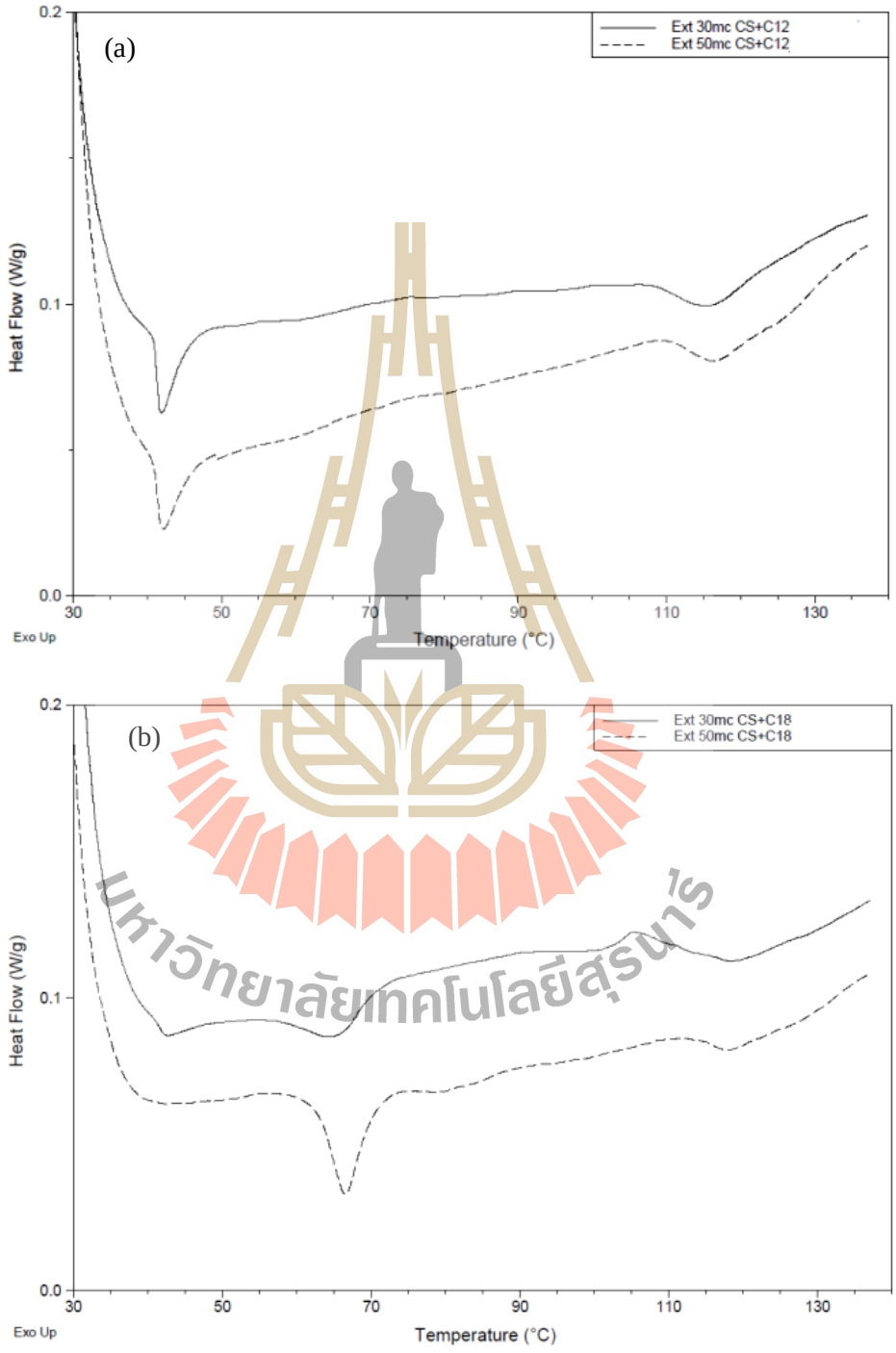

Figure 5B DSC thermograms of cassava starch extruded with (a): C12 and (b): C18 at 30 and 50% moisture content.

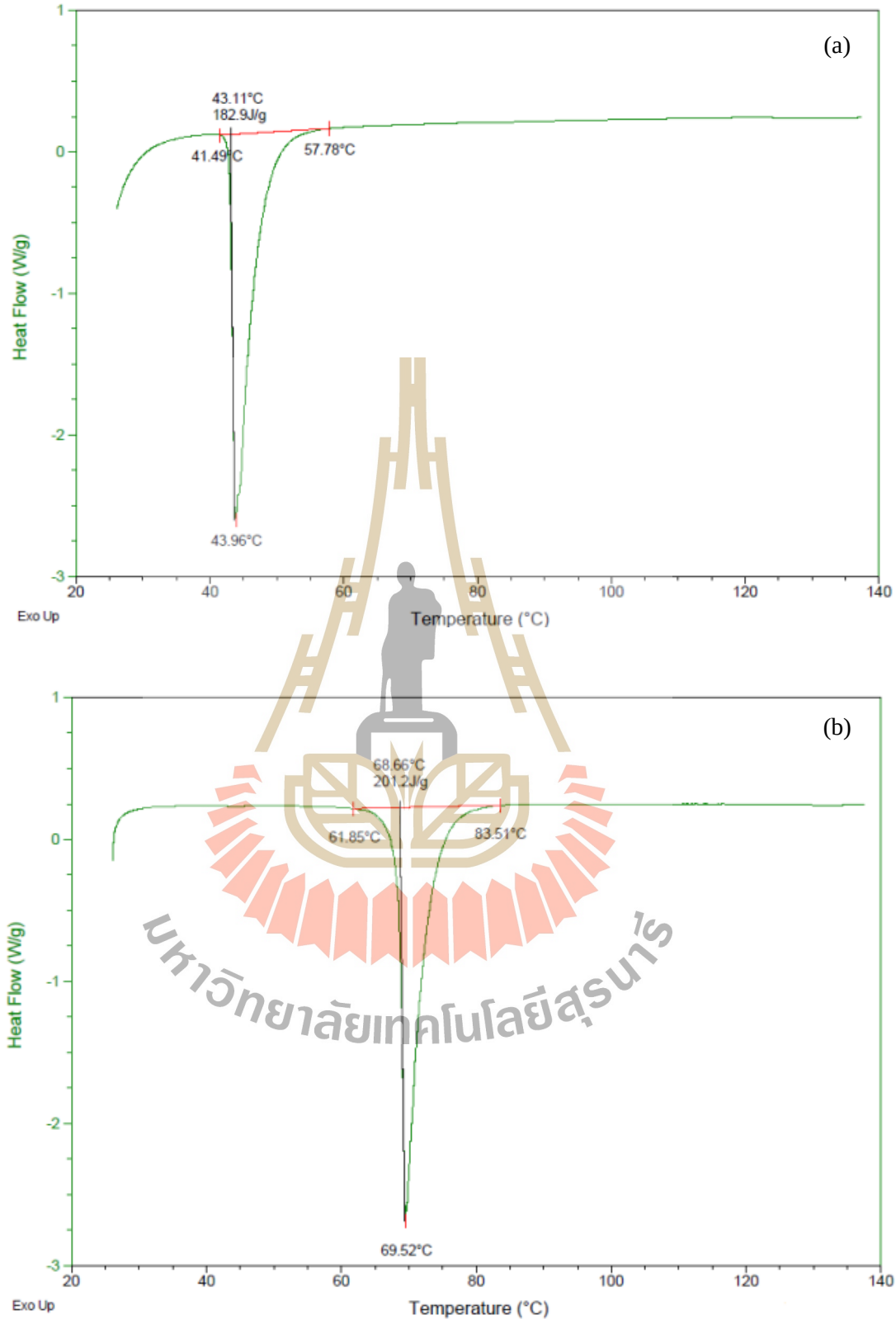

Figure 6B DSC thermograms of (a): lauric acid (C12) and (b): stearic acid (C18).

5.4.3 Effect of thermo-molding process on the extruded cassava starch with and without the addition of complexing agents

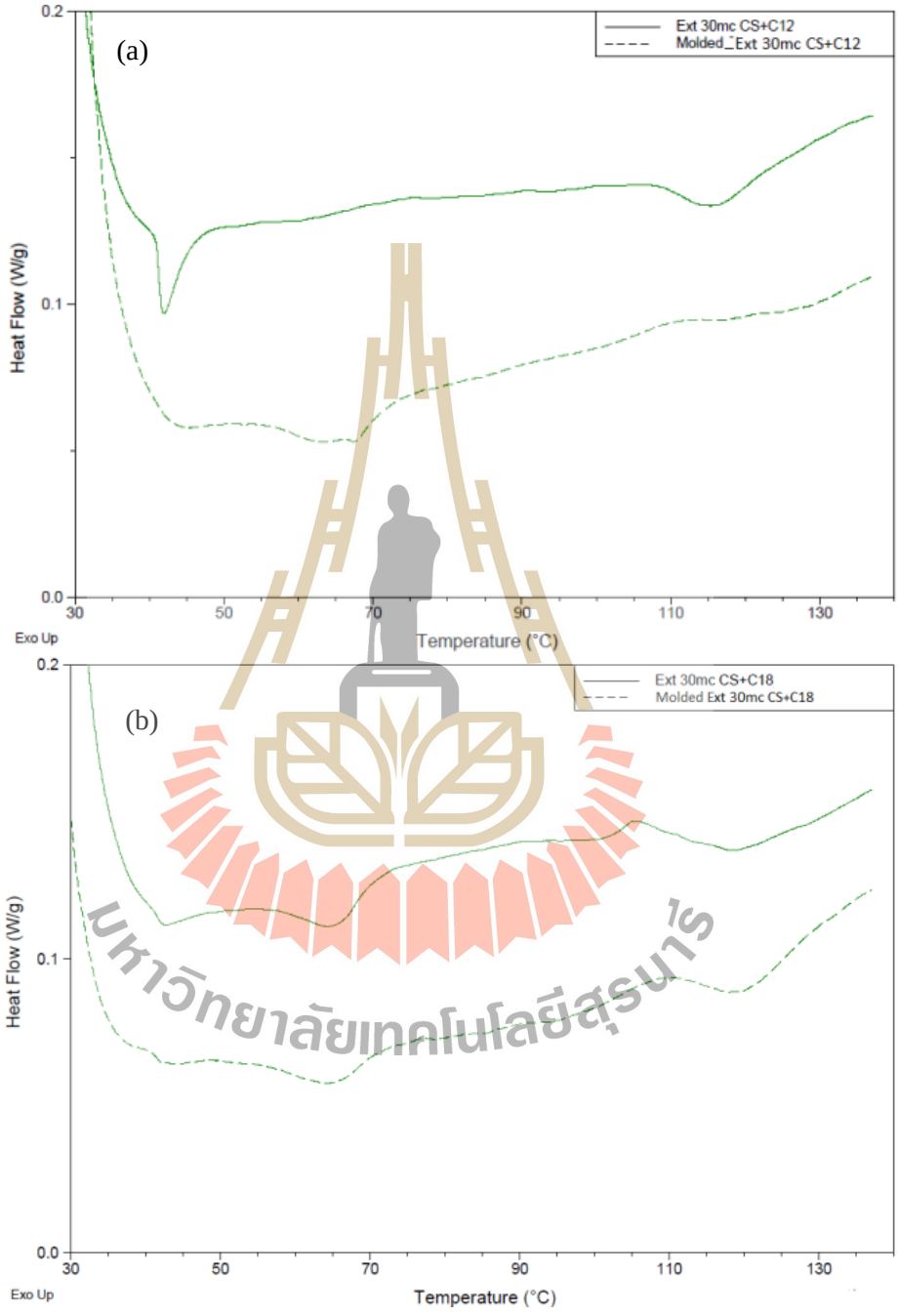

Figure 7B DSC thermograms of (a): cassava starch extruded with C12 and molded C12 extrudate and (b)**:** cassava starch extruded with C18 and molded C18 extrudate.

CURRICULUM VITAE

Sureeporn Boonna was born in November 12, 1981, at Chanthaburi, Thailand. She studied for her high school diploma at LaSalle Chanthaburi School (1995-1997) and Sriyanusorn School (1998-2000). In 2004, she received the degree of Bachelor of Science (Food Technology) from Suranaree University of Technology. In 2010, she received the degree of Master of Science (Food Technology) from Suranaree University of Technology and she also received OROG scholarship from Suranaree University of Technology to financially support during her study.

In 2011, she studied the doctoral degree at Suranaree University of Technology and also received Royal Golden Jubilee Ph.D. Scholarship (RGJ) granted by the Thailand Research Fund under the Office of the Prime Minister, the Royal Thai Government. During her Ph.D. study, she has presented a poster presentation, including: RGJ-Ph.D. Congress XIV 2013 **in** Thailand, The 3nd SUT International Agricultural Colloquium 2015 **in** Thailand, AACC International Annual Meeting 2015 in USA, The 4th SUT International Agricultural Colloquium 2016 **in** Thailand, RGJ Seminar Series No.116 2016 in Thailand, and Starch Round Table EU 2016 in France. She has also filed the petty patent entitled "กระบวนการผลิตแป้งที่มีค่าดัชนีน้ำตาลต่ำและทนต่อสภาวะการหุงต้มและผลิตภัณฑ์ที่ได้จากกรรมวิธีดังกล่าว" in Thailand in 2015.